Interactions of nerve growth factor and tumour necrosis factor alpha signalling in pain relevant cell types

Hammett, Kessia May

Awarding institution:
King's College London

KING'S COLLEGE LONDON

INTERACTIONS OF NERVE GROWTH FACTOR AND TUMOUR NECROSIS FACTOR ALPHA SIGNALLING IN PAIN RELEVANT CELL TYPES

Kessia May Hammett

Institute of Psychiatry, Psychology and Neuroscience

Thesis submitted for the degree of Doctor of Philosophy in Neuroscience

Awarded 1st May 2019

Abstract

Chronic pain occurs due to a maladaptive response of the nociceptive system. As a global health issue, the discovery of novel pain treatments is key to reducing the substantial economic burden associated with this condition, as well as the myriad of co-morbid diseases. Data from pre-clinical mouse models of chronic pain have shown a superior analgesic effect when using a bispecific blocker directed against both nerve growth factor (NGF) and tumour necrosis factor (TNFα) compared to targeting either one alone. Here, we tested the hypothesis that synergistic interactions exist between these two pain-relevant mediators. In primary neuronal cultures and a novel co-culture system, comprising mouse adult dorsal root ganglia (DRG) neurones with bone-marrow derived macrophages (BMDM), we quantified gene expression and functional cellular responses to NGF, TNFα or a combination of the two, assaying for additive or synergistic actions of these two mediators. We demonstrate robust responses of highly purified DRG neuronal cultures to NGF but fail to detect TNFα responsiveness. However, using our novel adult DRG neurone-macrophage co-culture system we highlight a role for NGF and TNFα in sensitising primary afferent CGRP release. We show a critical role for macrophages in delivering TNFα-driven sensitisation, which appears to summate with the direct NGF sensitisation of DRG neurones. In a mouse models of inflammatory chronic pain, we detect an increase in *Cd14* and *Itgam* mRNA within pain-relevant tissue (DRG and knee fat pad), indicative of myeloid cells (most likely macrophage) infiltration. Combined individual antagonism of NGF and TNFα does not prevent these increases in mRNA levels from occurring post intra-articular CFA (Complete Freund's Adjuvant) administration. We show that conditioned medium derived from TNFα-stimulated

BMDM enhances the expression of several pain-relevant transcripts in purified DRG cultures. These data suggest that the mechanism(s) by which the dual blockade (of NGF and TNFα) regulates analgesia is not simply by an inhibition of non-neuronal cell type infiltration into pain-relevant tissue types, but more likely to be dependent on a combined dampening of neuronal sensitisation evoked by the TNFα-induced macrophage secretome and the direct activity of NGF at nociceptors.

Acknowledgements

Firstly, I would like to extend my greatest gratitude to my two PhD supervisors: Professor Stephen McMahon and Dr Pete Thornton. Their guidance and advice throughout my PhD has been invaluable and has contributed to an unforgettable PhD experience. I also give my sincere thanks to The Biotechnology and Biological Sciences Research Council (BBSRC) and to MedImmune (AstraZeneca) for funding this project. I would like to thank all members of the 'Mac Lab', for always being there for help if needed, in particular Viv and Caroline for always being on hand! I would like to thank Jayne Kelleher, Federica La Russa, Damini Tewari and Franziska Denk for training me in various techniques at the start of my PhD and for continued guidance throughout. Additionally, I would like to thank Kim Chisholm and Martin Smith for always making time to share their knowledge with me and for proof-reading parts of this thesis.

I would like to thank MedImmune (AstraZeneca) for allowing me to spend a prolonged amount of time in their labs, allowing me access to world-class technology and new experiences within an industry setting. I would like to thank the whole Neuroscience Team for making me feel welcome and one of them. I would like to particularly thank Pete, who went out of his way to ensure that my time spent at MedImmune was worthwhile and productive, as well as proof-reading endless chapters of this thesis! A special thanks to Jon Hatcher who performed all surgeries and behavioural testing presented in the *in vivo* chapter of this thesis, without his knowledge and help this would not have been possible.

My PhD has been an unforgettable experience partly due to the amazing group of people I have been lucky enough to work with. The tough days would have been much harder to get

through without them. A special mention to Nik, Jayne, Kat, Kim, Natasha, Martin and Fede who could always put a smile on my face and will be life-long friends.

I would like to thank my family and friends for always believing in me and supporting me no matter what. To Dad, Mum, Rom, Matt, Mima and Rors; you are a constant source of inspiration and I couldn't be prouder to be part of the 'Hammett' clan! A special thanks to the love of my life, Ads, for the never-ending support, always putting a smile on my face and putting up with me for the last couple of months; without him I would not be the person I am today, and I am forever grateful.

Table of Contents

List of Figures and Tables

Introduction

Investigating the Individual and Combined Effect of NGF and TNFα on Sensory Neurones In Vitro

Investigating the Individual and Combined Effect of NGF and TNFα on Bone Marrow-Derived Macrophages (BMDM) In Vitro

Investigating the Individual and Combined Effects of NGF and TNFα in a Co-Culture System of Sensory Neurones and BMDM In Vitro

Investigating the Dual Antagonism of NGF and TNFα in an In Vivo Setting

Figure 64. DRG transcriptional changes 1-day or 7-day post-vehicle or test compound administration following PNL.

Table 13. List of mouse gene transcripts and the associated catalogue number used for L3, L4, L5 DRG tissue (following intra-articular CFA administration) at day 1 and day 7.

Table 14. List of mouse gene transcripts and the associated catalogue number used for knee fat pad samples (following intra-articular CFA administration) at day 1.

Table 15. List of mouse gene transcripts and the associated catalogue number used for knee fat pad samples (following intra-articular CFA administration) at day 7.

Table 16. List of mouse gene transcripts and the associated catalogue number used for L3, L4, L5 DRG samples (PNL model of neuropathic pain) at day 1 and day 7.

Table 17. ΔΔCt values of pain-relevant transcripts in the knee fat pad 1-day post-vehicle or test compound administration in the intra-articular CFA model of joint pain.

Abbreviation List

Abbreviation	Description
ADCYAP1	Adenylate Cyclase Activating Polypeptide 1
ADIPOQ	Adiponectin
AIF1/IBA1	Allograft Inflammatory Factor 1/Ionised Calcium-Binding Adapter Molecule 1
AMPAR	A-Amino-3-Hydroxy-5-Methyl-4-Isoazolepropionic Acid Receptor
ANOVA	Analysis of Variance
AREG	Amphiregulin
ARRIVE	Animal Research: Reporting of *In Vivo* Experiments
ATF3	Activating Transcription Factor 3
ATP	Adenosine Triphosphate
β2M	Beta-2-Microglobulin
BDNF	Brain-Derived Neurotrophic Factor
BMDM	Bone Marrow-Derived Macrophage
C3	Complement Component 3
C4b	Complement Component 4b
CACNA2D1	Calcium Voltage-Gated Channel Auxiliary Subunit Alpha 2 Delta 1
CALCA	Calcitonin-Related Polypeptide Alpha

CAMKII	Calmodulin-Dependent Protein Kinase II
CASPR2	Contactin-Associated Protein-Like 2
CCL1	Chemokine (C-C Motif) Ligand 1
CCL2	Chemokine (C-C Motif) Ligand 2
CCL3	Chemokine (C-C Motif) Ligand 3
CCL4	Chemokine (C-C Motif) Ligand 4
CCL5	Chemokine (C-C Motif) Ligand 5
CCL12	Chemokine (C-C Motif) Ligand 12
CCL20	Chemokine (C-C Motif) Ligand 20
CCL21	Chemokine (C-C Motif) Ligand 21
CCR2	C-C Motif Chemokine Receptor 2
CD14	Cluster of Differentiation 14
cDNA	Complementary Deoxyribonucleic Acid
CDH	Chronic Daily Headache
CFA	Complete Freund's Adjuvant
CGRP	Calcitonin Gene-Related Peptide
CM	Conditioned Medium
CNS	Central Nervous System
COX2	Cyclooxygenase 2

CREB	cAMP Response Element-Binding Protein
CRPS	Complex Regional Pain Syndrome
CSF	Cerebral Spinal Fluid
CSF1	Colony Stimulating Factor 1
CSF1R	Colony Stimulating Factor 1 Receptor
CSF2R	Colony Stimulating Factor 2 Receptor
CSF3	Colony Stimulating Factor 3
CST7	Cystatin F
CTSS	Cathepsin S
CXCL5	Chemokine (C-X-C Motif) Ligand 5
CXCL12	Chemokine (C-X-C Motif) Ligand 12
DIV	Days *In Vitro*
DMARD	Disease-Modifying Antirheumatic Drugs
DMEM	Dulbecco's Modified Eagle's Medium
DPBS	Dulbecco's Phosphate-Buffered Saline
DRG	Dorsal Root Ganglia
EAE	Experimental Autoimmune Encephalomyelitis
ECS	Extracellular Solution
EIA	Enzyme Immunometric Assay

EGFR	Epidermal Growth Factor Receptor
EREG	Epiregulin
ERK	Extracellular Receptor Kinase
ESCs	Endometriotic Stromal Cells
F2RL1/PAR2	Coagulation Factor II Receptor-Like 1/ Protease-Activated Receptor 2
FADD	Fas-Associated Protein with Death Domain
FBS	Fetal Bovine Serum
FCGR1	Fc-Gamma Receptor 1
FCGR2b	Fc-Gamma Receptor 2b
FCGR3	Fc-Gamma Receptor 3
FRET	Fluorescence Resonance Energy Transfer
GAL	Galanin
GAPDH	Glyceraldehyde 3-Phosphate Dehydrogenase
GCH1	GTP Cyclohydrolase 1
GDNF	Glial Cell-Derived Neurotrophic Factor
GFAP	Glial Fibrillary Acidic Protein
GMCSF	Granulocyte-Macrophage Colony-Stimulating Factor
GPCRs	G-Protein Coupled Receptors

GPR84	G-Protein Coupled Receptor 84
HBSS	Hank's Balanced Salt Solution
HIV	Human Immunodeficiency Virus
HSAN-IV	Hereditary Sensory and Autonomic Neuropathy Type IV
HTRF	Homogenous Time Resolved Fluorescence
IB4	Isolectin B4
ICC	Immunocytochemistry
IFNβ1	Interferon Beta 1
IFNγR1	Interferon Gamma Receptor 1
IFNγR2	Interferon Gamma Receptor 2
IL-1β	Interleukin 1 Beta
IL-3	Interleukin 3
IL-6	Interleukin 6
IL6RA	Interleukin 6 Receptor Subunit Alpha
IL10RA	Interleukin 10 Receptor Subunit Alpha
IL-11	Interleukin 11
IL-17A	Interleukin 17A
IL-18	Interleukin 18
ITGAM	Integrin Subunit Alpha M

JAK2	Janus Kinase 2
JNK	c-Jun N-Terminal Kinase
LDH	Lactate Dehydrogenase
LEP	Leptin
LIMMA	Linear Model for Micro Array Data
LLOQ	Lower Limits of Quantification
LPS	Lipopolysaccharide
LTP	Long-Term Potentiation
MACS	Magnetic-Activated Cell Sorting
MAPK	Mitogen-Activated Protein Kinase
MCSF	Macrophage Colony-Stimulating Factor
mTNFα	Membrane Tumour Necrosis Factor Alpha
NF-κB	Nuclear Factor Kappa-Light-Chain Enhancer of Activated B Cells
NGF	Nerve Growth Factor
NGFR	Nerve Growth Factor Receptor
NMDA	N-Methyl-D-Aspartate
NO	Nitric Oxide
NOS1	Nitric Oxide Synthase 1
NOS2	Nitric Oxide Synthase 2

NPY	Neuropeptide Y
NSAIDs	Non-Steroidal Anti-Inflammatory Drugs
NTRK1	Neurotrophic Receptor Tyrosine Kinase 1
NTRK2	Neurotrophic Receptor Tyrosine Kinase 2
NTRK3	Neurotrophic Receptor Tyrosine Kinase 3
NT3	Neurotrophin 3
NT4	Neurotrophin 4
NT5	Neurotrophin 5
OA	Osteoarthritis
OPRM1	Opioid Receptor Mu 1
P2X3R	P2X Purinoceptor 3
P2X4R	P2X Purinoceptor 4
P2Y12R	P2Y Purinoceptor 12
$P75^{NTR}$	Low-Affinity Nerve Growth Factor Receptor
PDL	Poly-D-Lysine
Pen/Strep	Penicillin-Streptomycin
PFA	Paraformaldehyde
PI3K-Akt	Phosphatidylinositol-3-Kinase and Protein Kinase B
PKC	Protein Kinase C

PLC	Phospholipase C
PNS	Peripheral Nervous System
PTGS2	Prostaglandin-Endoperoxide Synthase 2
RA	Rheumatoid Arthritis
RAC-1	Ras-Related C3 Botulinum Toxin Substrate 1
RIN	RNA Integrity Number
RLT	RNeasy Lysis Buffer
RW1 and RPE	RNeasy Wash Buffers
RPMI	Roswell Park Memorial Institute medium
RT	Room Temperature
RT-qPCR	Quantitative Reverse Transcription Polymerase Chain Reaction
SCN9A	Sodium Voltage-Gated Channel Alpha Subunit 9
SCN10A	Sodium Voltage-Gated Channel Alpha Subunit 10
SCN11A	Sodium Voltage-Gated Channel Alpha Subunit 11
SEM	Standard Error of the Mean
SLFN2	Schlafen 2
SLFN5	Schlafen 5
SNL	Spinal Nerve Ligation
SNP	Single Nucleotide Polymorphism

SODD	Silencer of Death Domains
SP	Substance P
Sp5C	Spinal Trigeminal Nucleus Caudalis
STAT1	Signal Transducer and Activator of Transcription 1
STAT3	Signal Transducer and Activator of Transcription 3
STAT6	Signal Transducer and Activator of Transcription 6
sTNFα	Soluble Tumour Necrosis Factor Alpha
TAC1	Tachykinin Precursor 1
TACE	Tumour Necrosis Factor Alpha Converting Enzyme
TLR4	Toll-Like Receptor 4
TNFα	Tumour Necrosis Factor Alpha
TNFR1	Tumour Necrosis Factor Receptor 1
TNFR2	Tumour Necrosis Factor Receptor 2
TRAF2	Tumour Necrosis Factor Receptor-Associated Factor 2
TrkA	Tropomyosin Receptor Kinase A
TRP	Transient Receptor Potential
TRPA1	Transient Receptor Potential Ankyrin 1
TRPV1	Transient Receptor Potential Vanilloid 1
TRADD	Tumour Necrosis Factor Receptor Type 1-Associated Death Domain

TTX-R	Tetrodotoxin-Resistant
VGF	VGF Nerve Growth Factor Inducible
VGSCs	Voltage- Gated Sodium Channels
WDR	Wide-Dynamic Range
YWHAZ	Tyrosine 3-Monooxygenase/Tryptophan 5-Monooxygenase Activation Protein
18S	18S Ribosomal RNA

1. General Introduction

1.1 Historical Perspective on Pain

Throughout history the definition of pain has been altered per the current beliefs at the time. The theories for the root cause of pain have ranged from an imbalance in the vital fluids of the human body (Sykiotis et al., 2005) to a punishment from God (Bial and Cope, 2011). The shift between pain being a spiritual experience to a physiological one was first described by René Descartes' *Treatise of Man* in 1662, where the potential link between sites in the periphery and centres in the brain was outlined. Since then several theories have been proposed, these include the Specificity Theory of Pain, whereby different noxious modalities are transmitted via distinct pathways to the central nervous system (CNS), and the Gate Control Theory of Pain, the idea that non-noxious stimuli are able to close the 'gate' to noxious stimuli and therefore able to suppress pain sensations (Melzack and Wall, 1966). It is the amalgamation of centuries of theories that have formed the basis of the current definition of pain given by the International Association of Pain (IASP); Pain is 'an unpleasant sensory and emotional experience associated with actual or potential tissue damage, or described in terms of such damage' (Bonica, 1979).

1.2 Non-Pathological Nociceptive Signalling

In healthy individuals, acute pain functions as a protective mechanism serving as a physiological warning to potentially tissue-damaging stimuli and promoting avoidance of those same stimuli in the future. The importance of this physiological drive to avoid danger is highlighted in individuals who suffer from a rare autosomal recessive condition; known as congenital insensitivity to pain (Nagasako, Oaklander and Dworkin, 2003). These patients cannot perceive when they are engaging with damaging stimuli and often suffer from extreme

injuries resulting in a substantially reduced life-span (Nagasako, Oaklander and Dworkin, 2003).

1.2.1 Transmission of Pain Signals from the Peripheral Nervous System to the Central Nervous System

Noxious mechanical, thermal and chemical stimuli are detected in the periphery by specialised nerve endings known as nociceptors; nociceptors are pseudounipolar sensory neurones. A single process originates from the cell body which then splits in two branches; one axon to innervate peripheral sensory organs (*e.g.* skin) and the other to synapse on second-order neurones in the dorsal horn of the spinal cord in the CNS (Dubin and Patapoutian, 2010).

These specialised sensory neurones are responsible for converting the above stimuli into electrical signals that are then sent to the higher brain centres, via the spinal cord, to illicit the appropriate response (Figure 1). The cell bodies of the above neurones are located in the dorsal root ganglia (DRG), where they modulate the expression of a number of regulatory proteins (Dubin and Patapoutian, 2010).

The DRG is a multicellular environment, with many other cell types being present in addition to the neuron cell bodies. One such cell type is satellite glial cells which wrap completely around the sensory neurones (Hanani, 2005). Given their close proximity to the neurones, it is perhaps not entirely surprising that this particular cell type has received growing interest in the context of pain. It has emerged that satellite glial cells play an active role in the initiation and maintenance of neuronal changes that underlie pain mechanisms (Ohara et al., 2009). For example, one study demonstrated that fractalkine/CX3CR1 signalling in satellite glial cells is a key component of the genesis of inflammatory pain, resulting in increased production and

release of TNFα, IL-1β and prostaglandin E_2 (Souza et al., 2013). Additionally, in a model of neuropathic pain, the continuous infusion of a glial metabolism inhibitor into the injured DRG, was able to significantly alleviate mechanical allodynia (Liu et al., 2012). These studies highlight the importance of changes occurring in non-neuronal cell types as well as the neurones themselves.

The signal generated in the periphery is transmitted predominantly to laminae I, II and V of the dorsal horn in the spinal cord, mainly via thinly myelinated Aδ fibres or unmyelinated C fibres (although some Aβ fibres have been described as being nociceptive (Djouhri and Lawson, 2004)), the characteristics of which are specified in Table 1.

The primary afferents terminate in the dorsal horn with a distribution pattern which is determined by two factors; their sensory modality and the region of the body that they innervate (Todd, 2010). It is at this point that the incoming information undergoes processing by complex circuits involving inhibitory (GABA or glycine as their main neurotransmitter) and excitatory (glutamate as their main neurotransmitter) interneurons, subsequent to being transmitted via projection neurones, to various areas of the brain (Todd, 2010). It is now widely accepted that changes in this region can contribute to chronic pain states, with the interneurons playing a particularly profound role (Todd, 2017). Under normal conditions, inhibitory interneurons continuously release GABA to control the excitability of lamina 1 projection neurones and modulate pain transmission. However, it is now known that a reduction in this inhibitory effect (as a result of trauma or injury) can lead to both hypersensitivity and allodynia (Yin, Yi and Kim, 2018).

The major ascending pathway associated with conveying information about pain is the spinothalamic tract (Treede, 2007). Tracing studies have demonstrated that primary

supraspinal targets for projection neurones (in the rat) include the caudal ventrolateral medulla (CVLM), the nucleus of solitary tract (NTS), the lateral parabrachial area (LPb), the periaqueductal grey matter (PAG) and certain nuclei in the thalamus (Gauriau and Bernard, 2003).

Neuronal activity in the dorsal horn is further regulated by descending modulatory pathways. In contrast to interneurons, the key neurotransmitters involved in the latter are noradrenaline and serotonin (Steeds, 2009). Under normal conditions, two important areas of the brainstem are involved in the reduction of pain; the PAG and the nucleus raphe magnus (NRM) (Steeds, 2009). However, there is growing evidence to support the hypothesis that dysregulation of descending pain modulation contributes to chronic pain states, for example, via diminished inhibitory influences (Ossipov, Morimura and Porreca, 2015).

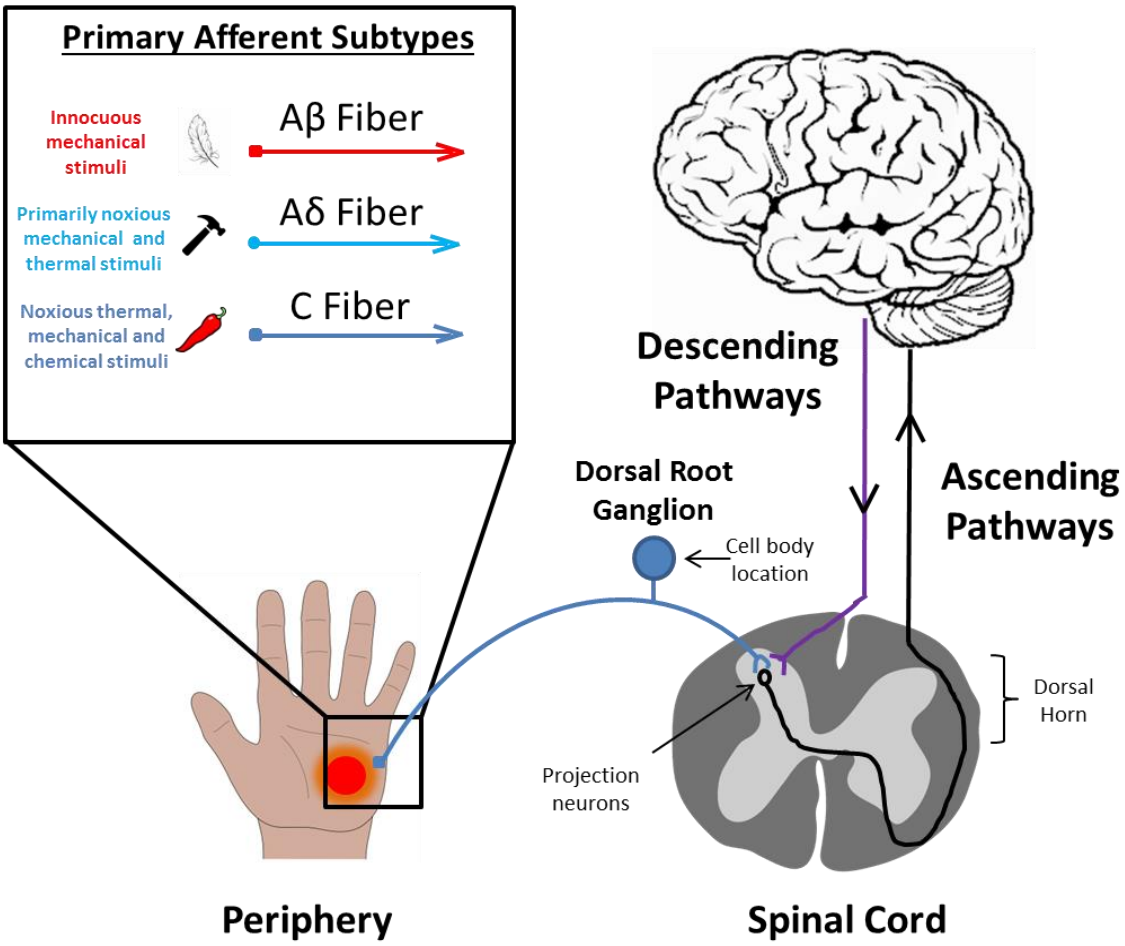

Figure 1. Nociceptive pathways from the peripheral tissues to the CNS. Schematic demonstrating the basic nociceptive pathway. Aδ and C fibres innervating peripheral tissues transduce and transmit pain signals initiated by noxious mechanical, thermal or chemical stimuli. These primary afferents terminate in the dorsal horn of the spinal cord where they synapse with projection neurones prior to being transmitted to the brain where an appropriate response is initiated. This pathway can be modulated at both the spinal cord level (involvement of interneurons) and descending pathways from the brain.

Abbreviations: CNS: central nervous system.

Despite often being over-simplified, the pain signalling pathway is highly dynamic, shaped by a number of integrative influences from both the peripheral and central nervous system, and therefore can be modulated and influenced at several points (Bolay and Moskowitz, 2002). In addition to the physiological aspect, pain is a highly subjective phenomenon influenced by sociological, psychological and genetic factors of the individual (Coghill, 2010). For instance, it has recently been suggested that neonates experiencing painful procedures, such as heel punctures, not only have a heightened pain response at the time due to the incomplete development of pain inhibition pathways, but also have increased pain responses later in life

(Beggs, 2015). The latter highlights how early life experiences can shape the nociceptive system in adulthood.

1.2.2 Classification of Nociceptors

Nociceptors form late during neurogenesis and are derived from neural crest stem cells migrated from the dorsal part of the neural tube (Anderson, 2000). This differs from larger-diameter sensory neurones, such as proprioceptors, that develop much earlier (Anderson, 2000). During neurogenesis all developing nociceptors in the DRG are known to express TrkA, the receptor for Nerve Growth Factor (NGF). However, during perinatal and postnatal periods, approximately 50 % will switch off their TrkA expression and start to express Ret (Golden et al., 2010), the receptor for glial cell-derived neurotrophic factor (GDNF)-family ligands. Following this pivotal change in receptor expression, the fate of these neurones diverges into either non-peptidergic or peptidergic nociceptors (Woolf and Ma, 2007). Classically, ret-expressing non-peptidergic nociceptors are isolectin B4 (IB4) positive, whereas TrkA-expressing peptidergic nociceptors are calcitonin gene-related peptide (CGRP) and substance P (SP) positive (Woolf and Ma, 2007). Recently, using single-cell RNA-sequencing and neurone size-based hierarchical clustering, it has been possible to further sub-classify the small-diameter neurones of the mouse DRG based on their transcriptome profile (Li et al., 2016a), allowing for more in depth study of the sensory mechanisms associated with pain. The authors showed that small diameter DRG neurones can be classified into one type of low-threshold mechanoreceptor and five types of mechanoheat nociceptors. In contrast, large diameter neurones are categorised into four separate groups. These distinct 'signatures' provide a more comprehensive manner in which somatosensory neurones may be characterised (Li et al., 2016a).

Table 1. Properties of Different Primary Afferent Fibers Types. Information regarding the different properties of different nerve fibers, including the type of information conveyed, location, whether the fibre is myelinated, the conduction velocity at which information is transmitted and the diameter of each fiber type.

Type of Nerve Fiber	Information Conveyed and Location	Myelination?	Conduction Velocity (m/s)	Fiber Diameter (μm)
Aβ	Touch, non-noxious, afferents from skin and joints, small receptive field	Myelinated	>40	6-12
Aδ	Fast pain, noxious mechanical and thermal stimuli, afferent sensory nerves, small receptive fields for precise localisation of pain	Thinly myelinated	5-40	2-5
C	Slow pain, noxious chemical, mechanical and thermal stimuli, afferent sensory nerves, large receptive fields with less precise localisation of pain	Non-myelinated	<5	<2

1.3 Chronic Pain

While acute pain serves a physiological function, chronic pain is the result of a maladaptive response of the nociceptive system, and therefore no longer serves a protective purpose. It has been estimated that up to eight million people in the UK live with chronic pain (Fayaz et al., 2016). These patients often experience a detrimental impact on their quality of life, with chronic pain affecting the ability to maintain employment, exercise, sleep, attendance at social activities, and even impacting the ability to maintain and develop healthy relationships (Breivik et al., 2006). Chronic pain is defined as pain which lasts longer than 3-6 months and persists despite the initial injury or trauma having healed (Treede et al., 2015). In addition to suffering from chronic pain, it is not uncommon for these patients to suffer from a range of co-morbid conditions, such as anxiety, depression and insomnia (Nicholson and Verma, 2004), further adding to the economic and personal burden of this disease.

1.3.1 Current Treatment for Chronic Pain Patients

Current treatment for chronic pain is often based upon the 'analgesic ladder', a treatment strategy originally used for patients suffering from cancer pain (Takeda, 1990, Jadad, 1995). The 'lowest rung' of the ladder involves oral administration of non-opioid based drugs such as paracetamol/aspirin, with or without an adjuvant, such as cyclooxygenase-2 (COX-2) inhibitors (Vargas-Schaffer, 2010). Following disease progression or lack of pain relief, the patient moves up the ladder where the use of weak (*e.g.* codeine) or strong (*e.g.* morphine) opioids is employed in addition to the use of non-opioid drugs and non-steroidal anti-inflammatory drugs (NSAIDs) (Vargas-Schaffer, 2010). The opioid dose is escalated until either the patient achieves adequate pain management, or the maximum dose is reached (Vargas-Schaffer, 2010). This system fails to acknowledge any individual differences and often results

in poor pain-management. The primary drawback of the above system is the extensive use of potent opioids, treatment of which can result in both psychological and physiological addiction, as well as extensive adverse effects (Benyamin et al., 2008) and the development of tolerance (Dumas and Pollack, 2008).

Although the above analgesic drugs account for 89 % of analgesic prescriptions (Mico et al., 2006), antidepressants and anticonvulsants are increasingly being viewed as legitimate treatment options, particularly for neuropathic pain patients (Ryder and Stannard, 2005). It is thought that the mechanisms involved in antidepressant-induced analgesia include enhanced availability of noradrenaline, activation of endogenous opioid receptors, and N-methyl-D-aspartate (NMDA) receptor inhibition, whereas anticonvulsant-induced analgesia results from blockade of both sodium and calcium channels in addition to the modulation of neurotransmitter release (Sarder et al., 2016). Although the above drugs are recognised as first-line treatments for several neuropathic pain conditions, these drugs are not themselves without extensive side effects (Maizels and McCarberg, 2005). These limitations highlight the need for the identification of novel and more effective pain targets and therapies.

1.3.2 Mechanisms of Chronic Pain

Chronic pain may be driven via both peripheral and CNS dependent mechanisms (Dray et al., 1999), often with components of one affecting the other, resulting in a heightened sensitivity in pain, a phenomenon referred to as hyperalgesia. This project will primarily focus on the peripheral aspect of pain; however, a brief overview of CNS-dependent mechanisms will be outlined below.

1.3.2.1 CNS-Dependent Mechanisms of Pain

Treating patients with chronic pain is a complex task partly due to the wide array of changes that occur in the CNS, both at a functional and structural level. These changes include molecular, synaptic, cellular and network level modifications (Kuner, 2010). Examples of these are highlighted below:

One of the key molecular changes contributing to the development of hyperalgesia (an enhanced sensitivity to pain) is the recruitment of GluR1 α-amino-3-hydroxy-5-methyl-4-isoxazolepropionic acid receptor (AMPAR) to neuronal plasma membranes at the spinal level (Galan et al., 2004). Studies have demonstrated that mice lacking the GluR1 subunit of the receptor display a loss of nociceptive plasticity *in vitro* and a reduction in acute inflammatory hyperalgesia *in vivo* (Hartmann et al., 2004).

At the synaptic level there is strong evidence to implicate long term potentiation (LTP) in the development of hyperalgesia. LTP is defined as the long-lasting, but not irreversible, increase in synaptic strength (Bliss and Collingridge, 1993). The induction of activity-dependent LTP and the subsequent rise in Ca^{2+} spinal cord lamina I neurones is well established (Sandkuhler and Gruber-Schoffnegger, 2012). The rise in intracellular Ca^{2+} is indeed known to initiate a myriad of signalling cascades, including protein kinase C (PKC), phospholipase C (PLC) and Ca^{2+}/calmodulin-dependent protein kinase II (CAMKII) activation, all of which are important for the development of hyperalgesia (Ikeda et al., 2006). As a consequence, spontaneous activity develops at the cellular level (Latremoliere and Woolf, 2009).

Despite the lack of nociceptive stimulus in the periphery, this spontaneous activity demonstrates the continued input into the central nervous system and subsequent signal amplification (Kuner, 2010). The consequences of unchecked nociceptive signalling include

modulation of neural networks; changes that can now be visualised in the brains of chronic pain patients. Individuals suffering from chronic back pain have been shown to display alterations in the spontaneous resting patterns and the brain default mode network during an attention task compared to control patients (Tagliazucchi et al., 2010).

The above examples are changes occurring at the functional level, but structural modifications also occur. It has been found that chronic pain patients show a reduction in brain gray matter, in a number of brain regions, compared to healthy age-matched controls (Apkarian et al., 2004, Schmidt-Wilcke et al., 2005, Kuchinad et al., 2007). This effect was seen to be reversed in patients who were pain free following total hip replacement, suggesting this structural change is a response to chronic nociceptive transmission rather than one of the underlying causes (Rodriguez-Raecke et al., 2009). Furthermore, alterations in dendritic spine morphology within the spinal cord have been observed. These include dendritic spine dysgenesis on wide-dynamic range (WDR) neurons in lamina IV – V (Tan et al., 2008), but also on lamina II neurones following spinal cord injury (Cao et al., 2017). The inhibition of Ras-related C3 botulinum toxin substrate 1 (Rac-1) activity, resulting in suppression of dendritic spine modifications, has been shown to be associated with the reversal of the neuropathic pain phenotype in rats (Zhao et al., 2016).

1.3.2.2 PNS-Dependent Mechanisms of Pain

Although the mechanisms produced centrally and peripherally are regularly treated as separate entities, often the modulation of signalling pathways in the periphery is a prelude to the subsequent changes in the CNS (Richards and McMahon, 2013).

When a tissue injury occurs in the periphery, resident as well as recruited immune cells secrete a vast array of inflammatory mediators including adenosine tri-phosphate (ATP), IL-

1β, histamine and bradykinin (Ji et al., 2014). One such immune cell is mast cells. A primary role of mast cells in inflammatory conditions is to enhance the local recruitment of neutrophils (Galli, Borregaard and Wynn, 2011). It has been shown that mast cells, which are optimally positioned in close proximity to the vasculature, initiate an early phase of neutrophil recruitment by releasing the chemoattractants CXCL1/CXCL2 (De Filippo et al., 2013). Blockade of either chemokine with monoclonal antibodies, or the depletion of mast cells, results in a significant depletion in neutrophil recruitment (De Filippo et al., 2013). This early immune response has been shown to be critical in the development of pain states, for example, mast cell stabilisation (using sodium cromoglicate to prevent the release of inflammatory mediators) reduces neutrophil infiltration and consequently suppresses both mechanical and thermal hypersensitivity development (Perkins and Tracey, 2000).

Additionally, the sensory nerve terminals themselves are known to release neuropeptides such as SP and CGRP, modulating nociceptive pathways at both peripheral and central sites via enhancing the immune response and directly sensitising sensory neurones (Molyva, 2010). Both SP and CGRP have been shown to be significantly upregulated in the synovium and synovial fluid in patients suffering from developmental dysplasia of the hip, a musculoskeletal disorder which has a strong pain component (Wang et al., 2015). In line with this, CGRP blockade via the use of peripherally acting antagonists can significantly reduce the mechanical hypersensitivity associated with joint pain in rat models of osteoarthritis (OA) (Walsh et al., 2015a).

Following the release of numerous inflammatory mediators in the tissue (e.g. ATP, IL-1β, histamine and bradykinin etc.), these substances act upon their respective receptors. The receptors may reside on the sensory neurone terminal (Grace et al., 2014), the axon itself

(Moalem et al., 2005) or on neighbouring uninjured afferents within the same vicinity (Ma et al., 2003).

Examples of the receptor types involved in chronic pain states include voltage-gated and voltage insensitive sodium channels, ligand-gated purinoceptor channels, transient receptor potential (TRP) channels and G-protein-coupled receptors (GPCRs). Following receptor activation, a myriad of second messenger signalling pathways may be activated (Kidd and Urban, 2001, Gangadharan and Kuner, 2013). The resulting change in the local chemical milieu has the net impact of increased neuronal excitability, resulting in the induction of peripheral sensitisation; a phenomenon whereby non-noxious stimuli are now perceived as noxious (allodynia) and there is a heightened sensitivity to noxious stimuli (hyperalgesia) (Ji et al., 2014).

A further consideration is the presence of “silent nociceptors” located in the periphery. Unlike other Aδ- and C-fibres, these nociceptors do not respond within the normal range of noxious stimulus intensities, instead only being active at the extreme ends of this scale. These nociceptors are often held responsible for spontaneous neural activity, thus increasing the input into the spinal cord and leading to central sensitisation (Schmidt et al., 1995, Gold and Gebhart, 2010).

The importance of the peripheral drive of pain is highlighted in cases where OA patients report a significant attenuation of their painful symptoms following removal of the diseased joint (Hawker et al., 1998). Furthermore, the use of biologics (therapeutics that lack a central-acting component) to target specific mediators in the periphery, have been shown to be successful in a number of painful conditions, including those of a neuropathic origin (Richards and McMahon, 2013). Individual inflammatory mediators have been shown to have a

profound effect on the excitability of primary sensory neurones, as well as altering the secretory profile of non-neuronal cells.

This PhD thesis will particularly focus on two peripheral inflammatory mediators; nerve growth factor (NGF) and tumour necrosis factor alpha (TNFα). The current evidence for their role in pathogenic nociceptive signalling is outlined below, along with an introduction to each mediator.

1.4 NGF Signalling

1.4.1 Biology of NGF

NGF was discovered over 50 years ago as the signalling molecule responsible for the survival of sympathetic and sensory neurones during development (Levi-Montalcini and Hamburger, 1951). NGF is a member of a group of signalling molecules known as the neurotrophins, with other members including brain-derived neurotrophic factor (BDNF), neurotrophin 3 (NT3) and neurotrophin 4/5 (NT4/5). This growth factor is a highly conserved molecule that is synthesised from a pro-NGF molecule, which undergoes processing via proteases located in the trans-golgi network to produce mature NGF (Fahnestock et al., 2004). Although the majority of research has focused on the mature form of NGF, there is evidence to indicate that pro-NGF itself has biological activity, with possible links to neurodegenerative conditions such as Alzheimer's disease (Fahnestock et al., 2001). The mature form of NGF exists as a dimer of a 13.2 kDa with a protomer structure consisting of three antiparallel pairs of beta strands (McDonald et al., 1991).

Within the central nervous system, NGF is crucial for the survival and function of cholinergic neurones of the basal forebrain complex, contributing to functions such as attention,

motivation and memory (Dreyfus, 1989). Additionally, NGF is known to modulate the hypothalamus-pituitary-adrenocortical axis, thus contributing to the response to stressful stimuli (Scaccianoce et al., 1993, Taglialatela et al., 1991). Within the periphery, sensory neurone release of neuropeptides, such as SP and CGRP, are known to be under NGF control (Mearowa and Kril, 1995). NGF levels within adult tissues correlate with peripheral neurone phenotypic features, including cell soma size, axonal sprouting and innervation density (Aloe et al., 2012). Additionally, NGF is thought to exert a profound effect on the immune system, suggesting NGF as a key regulator of the cross-talk between the immune and nervous systems (Minnone et al., 2017).

1.4.2 NGF Receptors

NGF signals via two receptors; the high affinity TrkA receptor, a Type 1 transmembrane protein, and the low affinity p75 receptor ($p75^{NTR}$), which belongs to the TNF receptor superfamily (Toni, Dua and van der Graaf, 2014). Signalling via the TrkA receptor is highly specific for NGF, the specificity of which has been shown to be augmented via $p75^{NTR}$ signalling (Barker and Shooter, 1994). One study has suggested that the means by which p75 can augment trkA signalling is via a specific 29-amino acid peptide derived from the intracellular domain fragment of p75 (Matusica et al., 2013). The authors show that this fragment interacts with, and potentiates binding of, NGF to trkA expressing cells via a conformational change within the extracellular domain of TrkA, resulting in enhanced neurite outgrowth in sympathetic neurones due to an increase in Erk1/2 and Akt signalling.

In contrast to TrkA, the $p75^{NTR}$ receptor is more promiscuous, binding to all four members of the neurotrophin family (Longo and Massa, 2013). In the adult nervous system, TrkA is expressed on approximately 40-45 % of DRG neurones (peptidergic C fibres) (Snider and

McMahon, 1998), sympathetic neurones (Fagan et al., 1996) and both cholinergic and non-cholinergic neurones in areas of the brain, including the basal forebrain and neostriatum, the paraventricular anterior, the rostrail and intermediate subnuclei of the interpenduncular nucleus and the area postrema (Holtzman et al., 1995). Following wide-spread expression in development, the $p75^{NTR}$ levels decrease significantly in adulthood (Firouzi, 2012). As well as being co-expressed with TrkA on sensory neurones, $p75^{NTR}$ is also expressed on a range of non-neuronal cells, including oligodendrocytes (Yoon et al., 1998) and astrocytes (Hutton et al., 1992).

1.4.3 Primary Signalling Pathways

The main signalling pathways associated with these two receptors are depicted in Figure 2. Following binding of NGF to the TrkA receptor, the TrkA receptor monomers dimerise and the intracellular component of the receptor is auto-phosphorylated (Pezet and McMahon, 2006), leading to activation of pathways primarily associated with cell survival. These include activation of Ras-mitogen activated protein kinase (MAPK), phosphatidylinositol 3-kinase-Akt (PI3K-Akt), ERK and protein kinase C (PKC) pathways (Klesse and Parada, 1999, Reichardt, 2006b). This promotion of cell survival is particularly important at the developmental stage. In line with this, mice lacking either the TrkA receptor, or the NGF molecule itself, survive birth but do not survive past 4 weeks of age (Klein, 1994).

The $p75^{NTR}$ receptor is also critical for this signalling and its activation positively regulates TrkA function, with cell survival depending on the ratio of receptor activation between these two receptors (Horton et al., 1997). It has been shown that embryonic sensory neurones deficient in $p75^{NTR}$ require a much higher concentration of NGF to promote cell survival compared to wild-type neurones (Davies et al., 1993). Post-developmentally, the $p75^{NTR}$ receptor has been

primarily associated with pro-apoptotic cell signalling, however, it is now known that the $p75^{NTR}$ receptor can also mediate anti-apoptotic pathways. Two of the major signalling pathways associated with apoptosis are the activation of the Jun kinase signalling cascade, which results in apoptosis via p53 activation, and secondly, the activation of the hydrolase enzyme sphingomyelinase, resulting in ceramide production and activation of caspase cascades (Reichardt, 2006b). However, an alternative protective role of $p75^{NTR}$ receptor signalling has been described (Mamidipudi and Wooten, 2002). A study by Roux et al., 2001, showed that $p75^{NTR}$ expression increased survival of TImp75-3 cells, derived from the MG87 fibroblast cell line, subjected to serum withdrawal, an effect thought to be due to $p75^{NTR}$-dependent phosphorylation of Akt.

Activation of both receptors can result in activation of the nuclear factor kappa-light-chain-enhancer of activated B cells (NF-κB); an important transcription factor (Lee and Burckart, 1998). This protein complex is important in the modulation of a number of cell survival processes and dysregulation is known to be present in a number of diseases, including cancer (Hoesel and Schmid, 2013) and autoimmune diseases (Aksentijevich and Zhou, 2017). It is known that antibodies that block binding of NGF to $p75^{NTR}$ prevented NF-κB activation and subsequently reduced the NGF survival response in developing sensory neurones (Hamanoue et al., 1999).

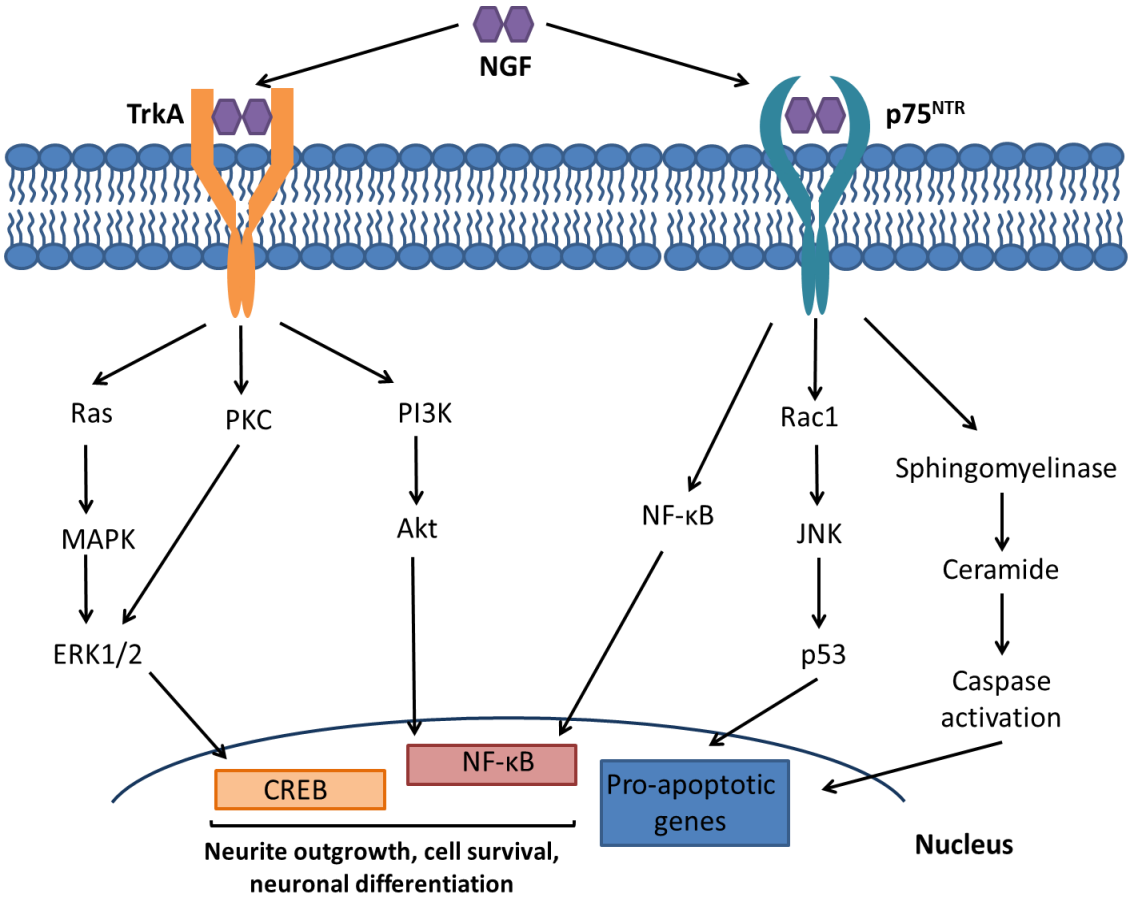

Figure 2. Primary signalling pathways associated with activation of TrkA and p75^{NTR} following NGF activation. NGF binding to its high affinity receptor, TrkA, results in phosphorylation of the receptor and activation of multiple signalling pathways (*e.g.* PI3K/Akt, Ras/MAPK/ERK1/2 or PKC signalling pathways). The activation of these signalling pathways results in a range of biological functions, including neurite outgrowth, cell survival, neuronal differentiation and transducer channel regulation. The binding of NGF to its low affinity receptor, p75^{NTR}, activates different signalling pathways depending on the cellular context. Activation of this receptor can result in both enhanced cell survival (through NF-κB signalling) as well as enhanced apoptotic signalling (via JNK/p53 signalling or caspase activation) (Wang et al., 2014).

Abbreviations: NGF: nerve growth factor; TrkA: tropomyosin receptor kinase A; PI3K: phosphoinositide 3-kinase; MAPK: mitogen-activated protein kinase; ERK: extracellular signal-regulated kinases; PKC: protein kinase C; p75^{NTR} : low affinity nerve growth factor receptor; NF-κB: nuclear factor kappa-light-chain-enhancer of activated B cells; JNK: c-Jun N-terminal kinase.

1.5 NGF in Pain

The role of NGF as an inflammatory mediator in acute and chronic pain states is well established. Interestingly, the sensitising effect of NGF seems to only occur in adult nociceptors, and not in embryonic nociceptors, suggesting a developmental switch, the nature of which is proving to be elusive (Zhu et al., 2004), in signal transduction cascades once

NGF has fulfilled its developmental role (Zhu et al., 2004). Evidence for the role of NGF in pain signalling, originating from pre-clinical studies and human studies, is outlined below:

1.5.1 Pre-Clinical Evidence for a Role of NGF in Pain

In addition to the location of its cognate receptors on nociceptors, NGF is also known to be significantly upregulated in inflamed tissue in a number of inflammatory models, including Complete Freund's Adjuvant (CFA) and carrageenan injection (McMahon, 1996). One of the earliest studies looking at the involvement of NGF in pain demonstrated that repeated application of exogenous NGF in the periphery, given to rats from birth, resulted in a profound mechanical and thermal hypersensitivity compared to age-matched controls (Lewin et al., 1993). This hypersensitivity was found to coincide with the upregulation of a number of pain related peptides, including substance P and CGRP, an effect that could be abolished with the application of an anti-NGF neutralising antibody (Woolf et al., 1994). The expression of TrkA alone has been shown to be sufficient to mediate the noxious effects of NGF (Bergmann et al., 1998), and the upregulation of TrkA expression in murine DRG, following a long-lasting inflammatory model, is linked to the maintenance rather than the development, of the inflammatory state (Pezet et al., 2001). However, it has also been observed that the induction of $p75^{NTR}$ in undamaged DRG neurones facilitates TrkA signalling (Obata et al., 2006), thus contributing to hyperalgesia indirectly. Furthermore, there is evidence to suggest that the binding of pro-NGF to $P75^{NTR}$ is required for CFA-induced hyperalgesia (Watanabe et al., 2008), suggesting the involvement of NGF signalling via $p75^{NTR}$ should not be underestimated.

1.5.2 Clinical Evidence for a Role of NGF in Pain

The role of NGF in pain is clearly illustrated in those individuals who have mutations in the gene encoding for the NGF molecule or the TrkA receptor. One such example is individuals

suffering from hereditary sensory and autonomic neuropathy type IV (HSAN-IV), also known as Congenital Insensitivity to Pain with Anhidrosis, which is a product of a mutation in the TrkA gene, NTRK1 (Indo et al., 1996). Patients suffering from HSAN-IV have a severe deficit in sensory perception but maintain a certain degree of vibration awareness (Axelrod and Gold-von Simson, 2007). Skin biopsies taken from HSAN-IV patients reveal a lack of C and Aδ fibres, thought to be caused by the absence of NGF-TrkA signalling (Nolano et al., 2000). Furthermore, it has been shown that the perinatal loss of sensory neurones in mice lacking the NGF gene, resulting in a failure to respond to noxious mechanical stimuli, cannot be rescued via the compensation of other neurotrophins (Crowley et al., 1994). The latter studies highlight the crucial role for NGF in pain signalling.

In humans, levels of NGF in cerebral spinal fluid (CSF) have been shown to be significantly higher in Chronic Daily Headache (CDH) patients compared to controls, an increase which is positively correlated with levels of SP and CGRP (Sarchielli et al., 2001), supporting the pre-clinical evidence. Increased levels of NGF and TrkA expression have been reported in pancreases of patients suffering from chronic pancreatitis (Friess et al., 1999), painful conditions of the urinary bladder (Lowe et al., 1997) and primary fibromyalgia syndrome (Sarchielli et al., 2007). The effect of administration of NGF has also been tested in healthy volunteers. In a double blinded, placebo-controlled study, injection of 5 µg of NGF into the masseter muscle resulted in significantly reduced pressure pain thresholds and tolerance thresholds which persisted for over 7 days (Svensson et al., 2003).

1.5.3 Molecular Changes Associated with NGF Induced Pain

The molecular changes associated with NGF administration are due to both local transcriptional-translational changes and post-translational modifications occurring at both

the distal axon and in the soma (Woolf and Costigan, 1999). The sub-population of nociceptors that are specific for TrkA also co-express the Transient Receptor Potential Vanilloid 1 (TRPV1) (Cavanaugh et al., 2011), an ion channel that responds to a range of stimuli, principally temperatures greater than 43 ˚C and capsaicin, and is associated with the development of hypersensitivity and allodynia (Szallasi et al., 2007). Indeed, mice lacking this ion channel do not develop thermal hypersensitivity following an inflammatory insult (Davis et al., 2000). One known mechanism for NGF sensitisation is the binding of NGF to the TrkA-expressing nociceptors, resulting in activation of PI3 kinase, allowing for phosphorylation of TRPV1 at a single tyrosine residue, Y200, and increased insertion of the TRPV1 ion channel into the membrane (Zhang et al., 2005b) (Figure 3). In addition, NGF-mediated activation of PLC is thought to reduce the threshold of TRPV1 channels via phosphatidylinositol 4,5-biphosphate (PIP2) hydrolysis (Chuang et al., 2001), thus leading to heightened thermal responses.

As well as local changes occurring in the distal axons, the NGF-TrkA complex can be internalised (Grimes et al., 1996) and transported to the cell soma, located in the DRG, where it drives transcriptional changes associated with increased synthesis of peptides, such as CGRP and SP (Zweifel et al., 2005), as well as ion channels, such as TRPV1 (Nicol and Vasko, 2007).

Following internalisation, it is thought that the NGF-TrkA complex undergoes endocytosis (Marlin and Li, 2015). The signalling endosome containing the complex and any associated signalling molecules are trafficked down the axon in a retrograde manner. The latter requires the association of motor protein along the microtubules, as well as the prevention of endosome maturation in order to prolong the liganded state of the NGF-TrkA complex (Marlin and Li, 2015).

Furthermore, the increase in TRPV1 translation, and subsequent increase in heat sensitivity of the sensory neurone terminal, has been shown to be dependent on phospho-p38, an effect which can be abolished using the molecule SB203580 (a specific inhibitor of the p38-MAPK pathway) (Ji et al., 2002). These two distinct mechanisms explain both the rapid sensitisation seen with NGF application and the secondary sustained effects of NGF.

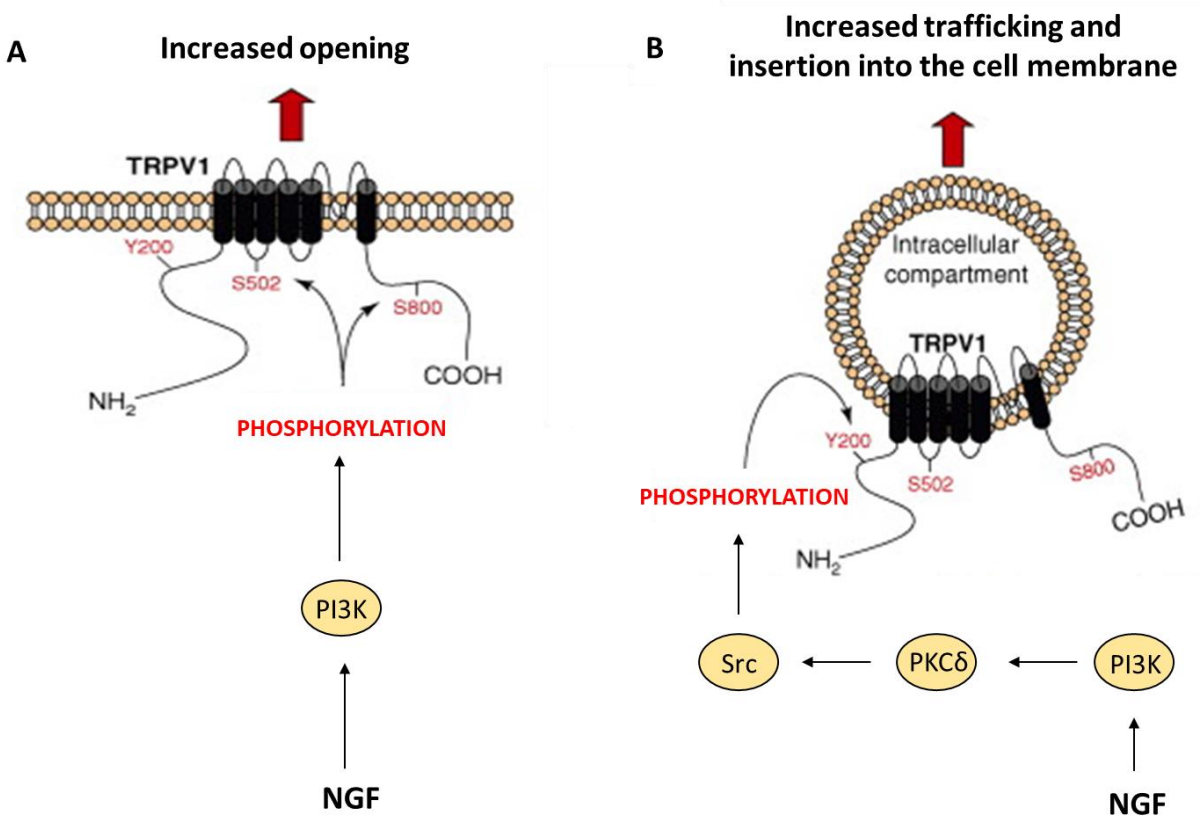

Figure 3. Schematic displaying the phosphorylation pathways associated with increased opening, increased trafficking and increased insertion of TRPV1 into the cell membrane following NGF activation. Following NGF activation, phosphorylation at the S502 and S800 residues results in an increased opening of the TRPV1 channel, whereas phosphorylation of the Y200 residue results in increased trafficking and insertion into the cell membrane. Adapted from Meents, Neeb and Reuter, 2010.

Abbreviations: TRPV1: transient receptor potential vanilloid 1; NGF: nerve growth factor; PI3K: phosphoinositide 3-kinase; PKCδ: protein kinase C gamma; Src: proto-oncogene tyrosine-protein kinase.

1.5.4 NGF Modulation of Sodium Channels

Voltage-gated sodium channels (VGSCs), such as $Na_V1.7$, 1.8 and 1.9 are key for translating external stimuli into the language of the nervous system; electrical impulses known as action potentials (Stuart et al., 1997). VGSCs are vital for both the initiation and propagation of

action potentials in neurones, a process initiated following depolarisation of the membrane potential to a threshold level (Stuart et al., 1997). For an action potential to be initiated it has been shown that a high density of VGSCs are required in a specialised region of the neurone, known as the axon hillock (Kole et al., 2008). Following a stimulus, a rapid opening in VGSCs occurs, depolarising the membrane potential via sodium influx into the cell. Following complete depolarisation of the membrane potential, sodium channels close at the same time as the opening of voltage gated potassium channels, resulting in hyperpolarisation (Kress and Mennerick, 2009). Subsequently, the resting membrane potential is re-established through potassium leak channels and the sodium-potassium pump before another action potential can be initiated (Vassalle, 1987, Cohen et al., 2009). Given the crucial role of VGSCs in neuronal activity, it is no surprise that sodium channels have been intricately implicated in pain states, evidence for which is presented below.

There is abundant evidence for the involvement of sodium channels in chronic pain conditions. Evidence for the role of sodium channels in the detection and conduction of pain signals in the periphery comes from patients presenting with “gain of function” mutations in the *SCN9A* gene encoding $Na_V1.7$. The *SCN9A* mutation is responsible for a number of familial human disorders, such as erythromelalgia and paroxysmal extreme pain disorder (Drenth and Waxman, 2007). The mutant gene results in channels that are either open more readily in response to depolarising stimuli or channels that are less affected by inactivation at resting membrane potentials. These properties lead to a significantly enhanced pain sensation to sub-threshold stimuli and a severely diminished quality of life for these patients (Levinson et al., 2012).

Sodium channels have been shown to be modulated by NGF in chronic pain models, with $Na_V1.7$, 1.8 and 1.9 expressed in a variety of pain conducting pathways (Strickland et al., 2008, Rogers et al., 2006). NGF produces a significant increase in guinea pig DRG neuronal spontaneous activity following an inflammatory insult, partly due to altered sodium channel expression, an effect that can be prevented with NGF depletion (Djouhri et al., 2001). Subcutaneous administration of NGF in rats resulted in a significant upregulation of sodium channels in the small diameter neurones of the DRG at 23 h, reaching maximal intensity at one week and persisting for up to 3 months. Furthermore, pre-treatment with an anti-NGF antibody prevented the accompanying hyperalgesia and reduced sodium channel labelling (visualised via immunocytochemistry techniques) within the DRG (Gould Iii et al., 2000), suggesting a crucial role of sodium channels in both the development and maintenance of pain. In mice that had a nociceptor specific knockout of the $Na_V1.7$ channel, NGF induced inflammatory responses were reduced (Nassar et al., 2004), as was the development of NGF induced thermal hyperalgesia in $Na_V1.8$ null mice (Kerr et al., 2001). The acid-sensing ion channel 3 (ASIC3), a sodium channel specifically expressed in sensory neurones, has been shown to be involved in modulating moderate- to high- intensity pain sensation (Chen et al., 2002). Furthermore, ASIC3 has increased expression in the presence of high levels of NGF during inflammation, an effect which correlates with neurone hyper-excitability and hyperalgesia (Mamet et al., 2003).

The above section has highlighted some specific examples, out of the myriad of proteins and secreted factors, associated with NGF-mediated sensitisation. Based on this pre-clinical evidence, NGF was considered a plausible and promising pain target for use in humans with chronic pain disorders; osteoarthritis (OA), rheumatoid arthritis (RA) and cancer pain to name

a few (Chang et al., 2016). The following section examines the success of NGF blockade in the clinic and the obstacles that have become apparent throughout this clinical testing process.

1.6 NGF in the Clinic

1.6.1 Biologics as Anti-NGF Molecules

One of the approaches used in the clinic to block NGF activity is the use of monoclonal antibodies (Cohen et al., 2016). Examples include tanezumab (the most advanced), fulranumab and fasinumab, all of which inhibit the binding of NGF to its cognate receptors, TrkA and $p75^{NTR}$ (Yeh et al., 2017). This biologic approach has been successful in a competitive market partly due to several advantages over the more traditional small molecule approaches. These include increased specificity, an improved safety profile due to a reduction in off-target effects and a longer duration of action leading to a higher rate of patient compliance (Mócsai et al., 2014). One of the difficulties in the case of NGF is the ability to specifically block the TrkA receptor with the small molecule approach (Su et al., 2017). This is in part due to the preferred target of the small molecule-the ATP binding pocket of the receptor kinase being identical in TrkA, TrkB and TrkC (Su et al., 2017). In line with this, despite reports of pain relief in animal models of cancer pain (Ghilardi et al., 2010) and bone fracture (Ghilardi et al., 2011) following the use of a pan-Trk inhibitor, the compound caused significant over-eating and consequential weight gain. The latter likely to be an effect of blocking BDNF/TrkB signalling (Unger et al., 2007).

It has been shown that administration of increasing doses of tanezumab in osteoarthritic patients resulted in a significant reduction in knee pain scores in these patients (Mantyh et al., 2011). In addition, this therapy showed no signs of adverse effects on normal nociceptor functioning (Mantyh et al., 2011). Tanezumab has also been shown to be efficacious in

significantly reducing pain in patients with interstitial cystitis (Evans et al., 2011) and chronic low back pain (Katz et al., 2011). Likewise, fulranumab has been suggested to produce a significantly superior pain relief in patients with moderate to severe chronic knee pain when compared to controlled-release oxycodone, but not when compared to the placebo group (Mayorga et al., 2016). In a 36-week clinical trial, fasinumab was found to produce a significant improvement compared to the placebo group regarding pain scores and associated functionality in patients with moderate to severe OA (Maloney et al., 2017). However, another study showed that the administration of fasinumab showed no significant differences in pain scores from the placebo group in patients with acute sciatic pain (Tiseo et al., 2014).

1.6.2 Side Effects Associated with Anti-NGF Molecules in the Clinical Setting

Despite impressive efficacy of anti-NGF molecules seen in some pain conditions, clinical trials had to be halted due to safety concerns. A number of patients receiving anti-NGF therapy, across a number of clinical trials at different pharmaceutical companies, experienced worsening of their arthritic condition, resulting in joint replacement and suggesting a possible class effect (Garber, 2011). Retrospective analysis of these trials revealed that these cases were highest in the patient cohorts taking anti-NGF therapy in combination with non-steroidal anti-inflammatory drugs (NSAIDs) (Seidel et al., 2013). To date, as far as we are aware, the mechanisms underlying the rapidly progressive OA seen in patients administered both anti-NGF and NSAIDS are yet to be elucidated. However, it has been postulated that NSAIDs may contribute to the latter condition via enhancing the risk of microvascular thrombotic events in bone and inhibiting the repair of subchondral microfractures (Enomoto et al., 2018).

At the time, a prevailing question was whether the higher rate of rapidly progressive arthritis was due to a direct action of the drug in question, or due to the analgesic property of the drug

resulting in overuse of the joint in patients that had a pre-existing condition (Garber, 2011). The lack of compelling evidence for a direct molecular mechanism linking anti-NGFs to joint destruction was key in reinitiating the anti-NGF molecule programme. In addition to the increased cases of joint degeneration, there have also been concerns about the effect of anti-NGF treatment on the autonomic system. Although the basis for these concerns has not been released in full, Pfizer have since revealed that their anti-NGF molecule, tanezumab, does not result in death or loss of neurones in the sympathetic nervous system. The Food and Drug Administration have since given approval for anti-NGF trials to continue, albeit with a number of changes to study protocol to address the raised safety concerns (Mullard, 2015). These changes include the exclusion of OA patients with pre-existing rapidly progressive OA, the removal of treatment groups involving the concomitant administration of NSAIDs, increased surveillance measures and a more thorough patient history prior to study inclusion (Holmes, 2012).

In conclusion, NGF is known to be a key regulator in pain states via the modulation of a number of signalling pathways, for example, TRPV1 phosphorylation and enhanced membrane insertion. Evidence has been presented for a role of NGF in several pain diseases, *e.g.* OA, and how the use of anti-NGF molecules has been an effective analgesic (albeit with challenges along the way). The following sections will now examine how TNFα signalling is implicated in pain states and how TNFα blockade may be beneficial in this instance.

1.7 TNFα Signalling

1.7.1 Biology of TNFα

TNFα was discovered in 1975 as a soluble cytokine capable of causing necrosis in neoplastic cell lines in response to activation by the immune system (Carswell et al., 1975). It is now

known that TNFα is a pleiotropic cytokine, primarily secreted from immune cells, and has a primary role in inflammatory processes (Baugh and Bucala, 2001). TNFα is one of 19 ligands which make up the TNF ligand superfamily, most of which are type II transmembrane proteins whose extracellular domains can be cleaved to produce the soluble form (Saha and Pahan, 2006). In the case of TNFα, the metalloprotease TNF alpha converting enzyme (TACE) induces proteolytic cleavage of the membrane integrated form (mTNFα) to produce the soluble form of TNFα (sTNFα), both of which are biologically active (Figure 4) (Saha and Pahan, 2006). This cleaved product exists as a homotrimer in solution, with a total molecular weight of 52-kDa (Saha and Pahan, 2006). Each monomer is composed of two antiparallel β-pleated sheets.

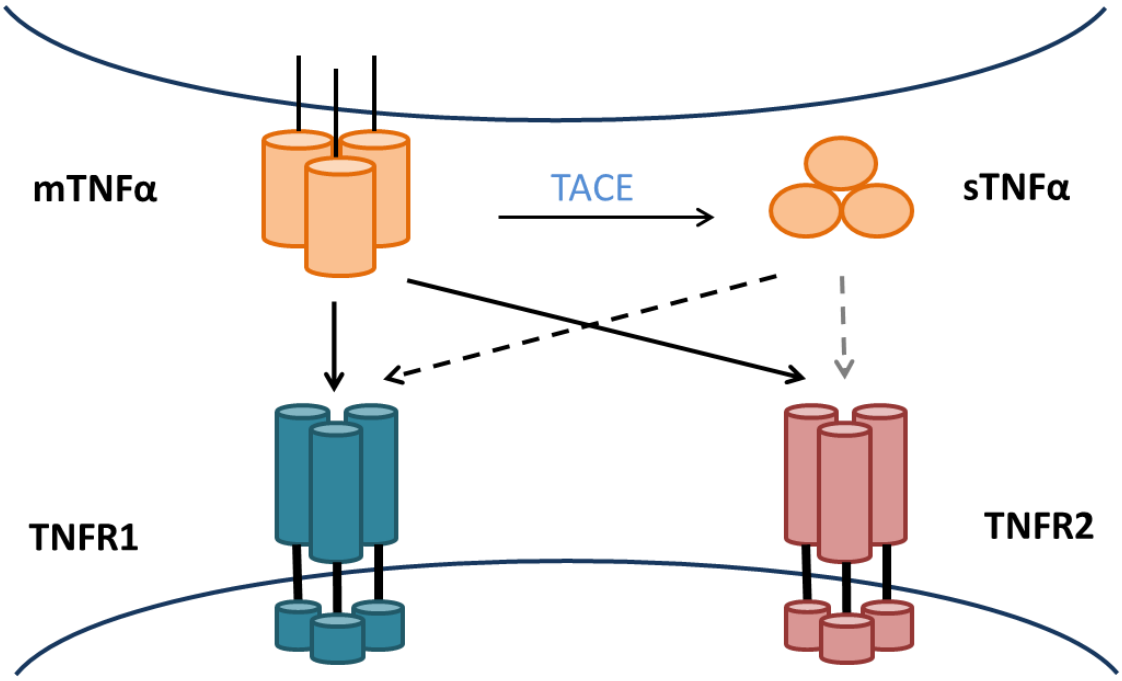

Figure 4. Interaction between the TNFα ligands and their cognate receptors. mTNFα, which can bind to both TNFR1 and TNFR2 with equal affinity, is cleaved via the metalloprotease TACE to produce the soluble form of TNFα. Although sTNFα is capable of binding to both receptors, it displays a greater affinity for the TNFR1. Image adapted from Saha and Pahan (2006).

Abbreviations: mTNFα: membrane tumour necrosis factor alpha, sTNFα: soluble tumour necrosis factor alpha, TNFR1: tumour necrosis factor receptor 1, TNFR2: tumour necrosis factor receptor 2, TACE: tumour necrosis factor alpha converting enzyme.

1.7.2 Physiological Role of TNFα

TNFα signalling is required for normal physiological cell signalling, with a particular important role in host defence against pathogens (Pfeffer, 2003). For example, mice deficient in TNFR1, or the TNF gene itself, have a severely impaired ability to successfully manage the fungal infection *Candida albicans* (Steinshamn et al., 1996) or the bacterial infection *Mycobacterium tuberculosis* (Bean et al., 1999). In line with TNFα being a crucial cytokine for inflammatory processes, it has been observed that mutations in the TNFR extracellular domains are responsible for the family of dominantly inherited auto-inflammatory syndromes, known as 'TNF-receptor associated periodic syndrome' (Aksentijevich et al., 2001). The latter results in patients experiencing fevers and unexplained bouts of inflammation (Hull et al., 2002). The possible reasons for these symptoms are wide-ranging; from aberrant folding and constitutive TNFR signalling to endoplasmic reticulum stress and increased levels of mitochondrial reactive oxygen species (Sedger and McDermott, 2014). TNFα has also been shown to be crucial in the recovery of muscle function following traumatic muscle injury (Warren et al., 2002) and TNFα signalling, via TNFR2, has been shown to be protective in neurodegeneration (Dong et al., 2016). However, due to the delicate balance of TNFα signalling (described above) it is no surprise that abnormal or overactive signalling has been associated with a number of diseases, including Crohn's disease, multiple sclerosis and pain (Van Deventer, 1997, Mikova et al., 2001, Zhang and An, 2007).

1.7.3 TNFα Receptors

To exert its wide range of biological functions TNFα binds to two receptors, the TNF receptor 1 (TNFR1) and the TNF receptor 2 (TNFR2), with molecular weights of 55- kDa and 75- kDa respectively (MacEwan, 2002). TNFR1 and TNFR2 display a high degree of homology between

their murine and human counterparts, whereas the homology between the two receptors is much lower (28 %) and confined to the extracellular ligand-binding domains (Goodwin et al., 1991).

TNFR1 is thought to be constitutively expressed in the majority of cells and has assumed responsibility for the majority of TNFα signalling outcomes (Fischer et al., 2015). In contrast, TNFR2 has restricted expression to immune cells and, compared to TNFR1, has not been well studied (Chu, 2013). One of the reasons for the latter was the previously made assumption that the soluble form of TNFα was an adequate activator of TNFR2. However, it has been demonstrated that the transmembrane form of TNFα is far superior in this respect (Grell et al., 1995) suggesting that the role of TNFR2 in TNFα signalling is potentially underestimated.

1.7.4 Primary Signalling Pathways

1.7.4.1 Forward Signalling

The binding of TNFα, to either receptor, results in a conformational change, recruiting adaptor proteins such as the Tumour Necrosis Factor Receptor Type 1-Asociated Death Domain (TRADD) (TNFR1-specific), Fas-Associated protein with Death Domain (FADD) and TNF Receptor-Associated Factor 2 (TRAF2). Subsequent intracellular cascades result in the activation of inflammatory or apoptotic pathways depending on the conditions. The main signalling pathways associated with both TNFR1 and TNFR2 are depicted in Figure 5.

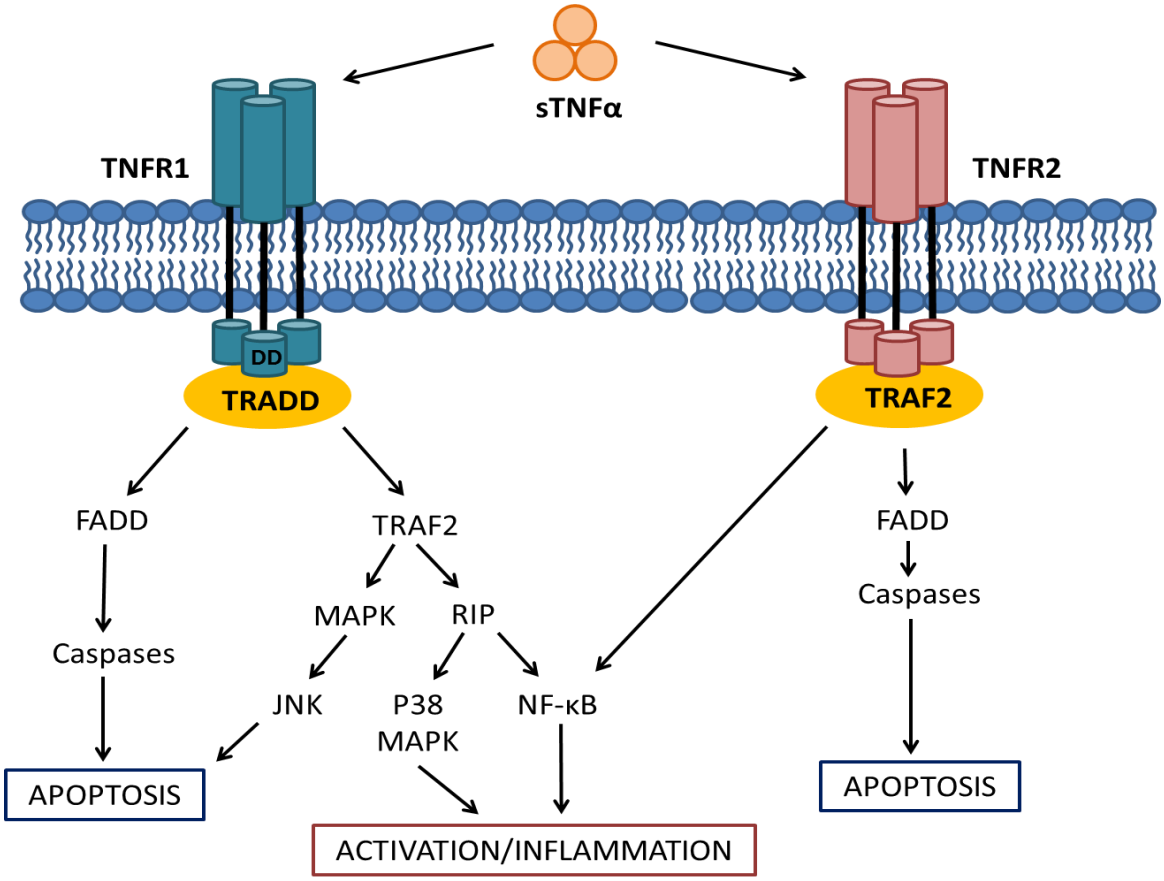

Figure 5. TNFα signalling pathways associated with binding to TNFR1 and TNFR2. TNFα activation triggers a conformational change in the receptors, allowing the recruitment of a number of adaptor proteins, such as TRADD, FADD and TRAF2, triggering signalling cascades associated with apoptosis or activation/inflammation.

Abbreviations: TRADD: TNFR1 associated death domain, FADD: Fas-associated death domain, TRAF2: TNF receptor associated factor 2.

One of the key differences between TNFR1 and TNFR2 is the presence of a death domain in TNFR1 (Jiang et al., 1999). In the absence of TNFα as a ligand, the death domain is kept inactive by the presence of a protein known as the Silencer of Death Domains (SODD). However, following activation, SODD disassociates and TRADD is recruited, acting as a platform for the recruitment of other crucial proteins (Jiang et al., 1999). Although TNFR2 does not contain a death domain itself, it is thought to contribute to apoptotic processes via a "ligand-passing" mechanism (MacEwan, 2002). Indeed, it has been shown that TNFR2 can regulate the rate of TNFα association with TNFR1, via increasing the local concentration of TNFα itself, thus enhancing death signalling indirectly (MacEwan, 2002).

There are several similarities between the signalling pathways activated via TNFα and NGF binding. These include activation of NF-κB, activation of the MAPK pathways and the induction of death signalling via activation of caspase cascades. Additionally, the same mechanism of rapid dissociation described above for TNFα has been proposed as a way that the $p75^{NTR}$ enhances NGF signalling via the TrkA receptor at the cell surface (Tartaglia et al., 1993).

1.7.4.2 Reverse Signalling

The above described pathways are as a result of TNFα forward signalling. However, it is also possible for the membrane form of TNFα to act as a receptor itself to cell types expressing TNFR2 (Qu et al., 2017); enabling reverse signalling pathways. Whereas soluble TNFα is often associated with apoptotic responses and a heightened inflammatory profile, the reverse signalling associated with the membrane form is thought to take on more of a protective role. For example, reverse signalling through mTNFα has been shown to confer resistance to lipopolysaccharide (LPS)-induced TNFα, IL-6 and IL-1 release in human monocytes and macrophages (Eissner et al., 2000). The above highlights how the outcomes of TNFα signalling are a result of a delicate balance between soluble and membrane bound TNFα-mediated effects, in addition to the distinct mechanisms of TNFR1 and TNFR2 activation.

1.8 TNFα in Pain

The role of TNFα as a pro-inflammatory cytokine has been well characterized, whereas its function as a pain mediator has been less well described. Although TNFα signalling principally modulates the immune system, there are reports suggesting TNFα can act directly upon the sensory neurons themselves, making TNFα an intriguing pain target. Evidence supporting the above is outlined below.

1.8.1 Genetic Evidence for a Role of TNFα in Pain

The intrigue surrounding the potential role of TNFα as a pain mediator comes in part from genetic studies in humans. One study looking at pain severity in lung cancer patients showed that patients with the TNFα-308GA single nucleotide polymorphism (SNP), resulting in increased TNFα production, was a strong predictor of pain (Reyes-Gibby et al., 2009). The above mutation has also been linked to an increased risk of developing migraines (Mazaheri et al., 2006, Yilmaz et al., 2010, Ates et al., 2011), in which pain is a defining feature, and the development of neuropathic pain following surgery (Kalliomäki et al., 2016). Furthermore, a polymorphism in the gene that codes for TNFR2 has recently been linked to high intensity pain severity in cancer patients experiencing severe cluster symptoms (two or more concurrent symptoms experienced by patients that are related and may or may not have a common cause) (Reyes-Gibby et al., 2013).

1.8.2 Pre-Clinical Evidence for a Role of TNFα in Pain

As with NGF, it has been shown that intraplantar injection of murine TNFα in adult male rats resulted in both mechanical and thermal hypersensitivity, possibly due to the subsequent upregulation of the pro-inflammatory cytokine IL-1β and NGF (Woolf et al., 1997). This is in line with studies showing that anti-TNF therapy can inhibit the production of pro-inflammatory cytokines in a variety of conditions, including rheumatoid arthritis and psoriasis (Schotte et al., 2004, Gottlieb et al., 2005). However, a study by Hakim and colleagues (Hakim et al., 2011), showed that TNFα-induced sensitisation of masseter muscle nociceptors can be partially reversed by the prostaglandin E2 (PGE2) inhibitor Diclofenac, whereas inhibition of NGF via a TrkA antibody did not alter the mechanical threshold of the nociceptors. Furthermore, TNFR1 and TNFR2 knockout mice were shown to have reduced thermal

hyperalgesia in response to injection of Complete Freund's Adjuvant (Zhang et al., 2011), and following nerve injury there is an up-regulation of TNFR1 in DRG neurones as well as TNFα secretion from surrounding glia (Ohtori et al., 2004). TNFα signalling has also been implicated in the development of neuropathic pain. Treatment of rats with the TNFα antagonist molecule, TNFRII-fc, 2 days prior to spinal nerve injury, can attenuate the mechanical hypersensitivity produced with administration of TNFα, an effect that has been shown to be dependent on activation of the MAP kinase p38 (Schäfers et al., 2003).

1.8.3 Human Studies as Evidence for a Role of TNFα in Pain

Patients suffering from neuropathic pain have been shown to have elevated levels of TNFα in both serum/plasma and cerebrospinal fluid (CSF) samples compared to healthy controls (Beckers et al., 2013). Furthermore, human nerve biopsies from patients with neuropathies showed an increase in TNFR1 in patients with centrally mediated mechanical allodynia, an effect which was seen alongside an up-regulation of TNFα expression in the Schwann cells from the same patients (Empl et al., 2001). A further study has demonstrated that patients suffering from chronic pain due to a lumbar disc hernia showed an increase in both mRNA levels and protein levels of TNFα and TNFR1 in muscle and the nucleus pulposus (the inner core of the vertebral disc), an effect which was positively correlated with pain severity (Andrade et al., 2011). A meta-analysis of 14 studies, looking at TNFα serum levels in the painful inflammatory condition rheumatoid arthritis, demonstrated a significant increase when comparing RA patients with healthy controls (Wei et al., 2015). This increase in TNFα levels is also seen in the synovial fluid of psoriatic arthritis patients (Partsch et al., 1997) and osteoarthritis (Larsson et al., 2015), an effect which is thought to be accompanied by an increase in self-reported pain scores (Orita et al., 2011).

1.8.4 Mechanisms of TNFα-Mediated Pain

Unlike NGF, the exact mechanisms involved in TNFα-mediated pain are still to be fully elucidated. Specifically, it remains unclear as to if TNFα can act *directly* on nociceptors or if its effects are due to an *indirect* action via non-neuronal cell types. TNFα is widely regarded as a "master cytokine" due to its ability to initiate the production of a range of pro-inflammatory cytokines, including IL-6 and IL-1β, both of which have been implicated in pathogenic pain (Cook et al., 2018b). The culmination of this signalling cascade is the release of prostanoids and catecholamines from sympathetic fibres (Poole et al., 1999), resulting in a maintained and enhanced inflammatory state. The prostanoid system has been shown to be an important element in the development of long-lasting sensitisation of primary afferent nociceptors in mice (Villarreal et al., 2013) and the levels of noradrenaline within the ventral striatum shown to be correlated with pain thresholds in a murine model of neuropathic pain (Taylor et al., 2014).

However, multiple lines of evidence point towards TNFα having an additional direct effect on the nociceptors themselves. Using electrophysiological techniques, the response of naïve, spinal nerve ligated (SNL)-injured or adjacent uninjured rat DRG to exogenous TNFα has previously been examined. It was found that *in vitro* perfusion of TNFα evoked short-lasting neuronal discharges in naïve DRG, whereas in SNL-injured and adjacent uninjured DRG, subthreshold concentrations of TNFα elicited high-frequency discharges of a much longer-lasting duration (Schafers et al., 2003a). One study used a CFA-induced inflammatory temporomandibular joint pain in mice to show an increase in immunofluorescence staining for TNFα. This was observed in both non-neuronal cells of the trigeminal ganglia and the spinal

trigeminal nucleus caudalis (Sp5C), but also enhanced expression in the Sp5C neurones themselves (Bai et al., 2018).

TNFα-mediated hyperalgesia is thought to be dependent on nociceptive TNFR1 activation (Hensellek et al., 2007a) triggering downstream activation of stress kinases and simultaneous mobilisation of calcium (Pollock et al., 2002), resulting in increased sensory neurone sensitivity via modulation of various channels. For example, it has been proposed that TNFα can enhance tetrodotoxin-resistant (TTX-R) sodium channel currents, via a phosphorylation mechanism that can be prevented by the use of the p38 MAPK inhibitor SB202109, in isolated (non-purified) mouse DRG neurones (Jin and Gereau, 2006). TTX-R sodium channel currents are thought to contribute to the membrane excitability of DRG sensory neurones, with inflammatory mediators capable of enhancing these currents and therefore contributing to neuronal hyperexcitability (Tan et al., 2014). Furthermore, TNFα is thought to contribute to thermal hypersensitivity via a similar mechanism to NGF signalling. It has been shown that TNFα application to both rat and mouse DRG cultures (non-purified) for 24/48 h, results in increased TRPV1 expression (Hensellek et al., 2007a). In TNFR1 knockout mice, but not in TNFR2 mice, this response was abolished, corroborating the importance of TNFR1 in the development and maintenance of chronic pain (Parada et al., 2003, Andrade et al., 2016, Zeng et al., 2014). In contrast to the apparent role of p38 in sodium channel mediated hypersensitivity, the increase in TRPV1 has been suggested to be dependent on activation of ERK (Hensellek et al., 2007a).

1.9 TNFα in the Clinic

1.9.1 Biologics as Anti-TNF Molecules

A common first-line treatment for RA patients is the use of Methotrexate, known as a disease-modifying anti-rheumatic drug (DMARD). The mechanisms by which Methotrexate is effective include suppression of lymphocyte proliferation and inhibition of pro-inflammatory cytokines (Li et al., 2017) via inhibition of folic acid reductase. Methotrexate is known to be effective even after prolonged use and is a low-cost option. However, there is a relatively high rate of adverse effects experienced with this drug, possibly associated with concomitant treatment with NSAIDs and corticosteroid treatment (El-Zorkany et al., 2013).

Once the gold standard for RA treatment, methotrexate has since been over-taken by the development of anti-TNF biologics. There are currently several effective biologics on the market; etanercept, adalimumab and infliximab to highlight a few.

Both infliximab and adalimumab are full IgG1 monoclonal antibodies: the latter is a fully humanized antibody whereas infliximab is a mouse/human chimeric. They work by binding to and deactivating the TNFα molecule, thus preventing its activation of either TNFR1 or TNFR2. Infliximab is often prescribed to patients with active on-going RA. It is thought that it primarily exerts its effect via down-regulation of a range of pro-inflammatory cytokines, such as IL-6, resulting in an improvement in the patients' symptoms. Furthermore, reduced expression of IL-8 and MCP-1 in the synovial tissue of patients results in reduced migration of leukocytes into the damaged joint (Taylor et al., 2000), a process known to be key in the pathology of RA. However, one study has suggested that in addition to the latter, TNFα administered peripherally could impact on brain responses. RA patients treated with infliximab showed reduced fMRI signals in brain areas associated with pain processing as early as 24 h, whereas

any significant anti-inflammatory effects were seen later in the treatment at day 14 (Hess et al., 2011). The rapid action of anti-TNF treatment seen in this study suggests that as well as having disease modifying effects, it may also act as an analgesic acutely.

Etanercept exerts its therapeutic benefit by acting as a decoy TNFα receptor, therefore also binding to lymphotoxin. It is a fusion protein made up of recombinant human TNFR2 monomer fused with the Fc domain of the IgG1, which can bind to TNFα and deactivate it (Weinblatt et al., 1999, Marotte and Cimaz, 2014). Not only has etanercept treatment alone been shown to be superior to methotrexate treatment in rheumatoid arthritis patients (Genovese et al., 2002), but combination treatment of methotrexate and etanercept results in significantly improved outcomes in terms of disease activity, functional disability and radiographic progression of the disease (Klareskog et al., 2004).

1.9.2 Issues with Anti-TNF Molecules in the Clinic Setting

As with anti-NGF treatment, there are a number of drawbacks associated with anti-TNF treatment. In line with this, one study showed that chronic treatment with either infliximab or adalimumab over 12 weeks resulted in an increased risk of serious infection and malignancies (Bongartz et al., 2006), adverse effects thought to be due to the interruption of the biological role of TNFα in host defence mechanisms and tumour growth regulation (Ehlers, 2003, Balkwill, 2006).

Furthermore, infliximab has been linked with between a two-fold to seven-fold greater risk for developing infections, such as tuberculosis, compared to etanercept (Wallis et al., 2004). One possible explanation for infliximab's increased risk of infection, in addition to the differing mechanism, is that peak blood levels are several times those of etanercept (Wallis, 2008).

Despite their impressive efficacy in a number of indications, it is also known that not all patients treated with anti-TNF treatment respond sufficiently. The latter suggests that there are alternative mechanisms of TNFα which we are currently unaware of and scope for the improvement of current mainstay therapies.

1.10 Neuroimmune Interactions

1.10.1 Overview of Neuroimmune Interactions

The focus on the interplay between the immune system and the nervous system has emerged as a crucial area of scientific research in the past decade. Previously, it had been assumed that immune cell types, *e.g.* microglia, only interacted with neurones following an inflammatory insult; whereas it is now evident that the communication between these two distinct cell types is also present in non-pathological states (Veiga-Fernandes and Pachnis, 2017, Fung et al., 2017, Prinz and Priller, 2017). The lines of communication between these two systems are bidirectional, with each capable of having a profound effect on the other (Steinman, 2004). Given the complexity of this bidirectional cross talk, it is no surprise that there is mounting evidence for the dysfunction of neuroimmune signalling in a range of disorders, including neurological, gastrointestinal and respiratory related diseases (Nockher and Renz, 2003, Di Filippo et al., 2008, Hughes et al., 2013). The following paragraphs will outline how these neuroimmune interactions are key in the initiation, development and maintenance of pain states.

1.11 Neuroimmune Interactions in Pain

There are several commonalities that exist between the immune and nociceptive system. Both cell types are widespread throughout the body, have a principal function to recognise

and acutely respond to a threat, and have the ability for long-term adaptation (McMahon et al., 2015). Therefore, it is no surprise that these systems are intricately interlinked, important pathways of which are highlighted in Figure 6. In the next paragraphs, the focus will explicitly be on how nociceptors and immune cells are known to influence each other in the context of pain.

1.11.1 Immune Modulation of the Nociceptive System

The immune system is known to primarily exert its effect on the nervous system via the production of soluble products, such as cytokines (Staud, 2015). Cytokines are known to act upon the neurones themselves, both in the peripheral nervous system (PNS) and the CNS, initiating downstream signalling cascades and, depending on the cytokine in question, exacerbating the inflammatory response (Zhang and An, 2007). The release of a range of soluble factors, secreted by both resident and recruited immune cells at the tissue site injury, triggers a number of changes in the peripheral sensory neurone. These changes include increased calcium mobilisation, increased voltage- or ligand- gated channel activation and increased neuropeptide transcription and release, to name a few (Ji et al., 2014). The net result of these changes is an increase in sensory neurone excitability and reduction in threshold activation leading to the hallmark signs of peripheral sensitisation; hyperalgesia and allodynia. The importance of these soluble factors is highlighted in diseases where targeting pro-inflammatory mediators, such as TNFα in RA, have produced favourable clinical outcomes in regard to pain-related endpoints (Seymour et al., 2001).

Recently there has been growing evidence for the role of autoantibodies (antibodies produced by the immune system that react with self-antigens (Elkon and Casali, 2008)) in pathological pain (Dawes and Vincent, 2016). It has been known in a number of disease states,

such as RA and systemic lupus erythematosus, that autoantibodies contribute to pain via enhancing inflammatory processes (Aletaha and Blüml, 2016, Dema and Charles, 2016). Pain can arise from an increase in neuronal excitability, or from structural damage, caused by the binding of the autoantibody to its complement Fc-region, causing the release of inflammatory mediators and the subsequent excitation of nearby nociceptors, or from the direct binding of autoantibodies to the nociceptor itself (Goebel, 2016). Autoantibodies have been shown to be involved in pain processing in a number of diseases, including complex regional pain syndrome (CRPS) and neuromyelitis optica (Dawes and Vincent, 2016). One study demonstrated that CPRS patients who received plasma exchange therapy experienced a significant reduction in pain compared to pain levels experienced pre-treatment (Aradillas et al., 2015). Furthermore, it has been shown that neuropathic pain patient-derived Contactin-associated protein-like 2 (CASPR2) antibodies induce neuropathic pain in previously healthy mice via a direct action on primary afferent cell bodies (Dawes et al., 2018).

Immune modulation of the nociceptive system occurs in the CNS as well as in the PNS. There has been a growing body of evidence that outline a crucial role for glia, and in particular microglia, in the development and maintenance of chronic pain states (Vallejo et al., 2010, Ji et al., 2013, Gosselin et al., 2010). Microglia constitute 5-10% of all glia within the CNS (Tsuda et al., 2005) and are conventionally known as the resident macrophages of the CNS. Microglia can be broadly classified into two forms within the CNS; resting and activated, with differing morphologies. The activated forms have a hypertrophied soma, retracted processes and increased proliferation (Inoue and Tsuda, 2009) compared to the resting phenotype which takes a ramified form. Following activation, they release a number of molecules, including pro- and anti-inflammatory cytokines, such as IL-1ß and IL-10 respectively. Although their

primary function is to protect against invading foreign material, they are thought to have a significant role in neuropathic pain (Inoue and Tsuda, 2018). Additionally, it has been shown in female rats, in the collagen-induced arthritis model, that the use of microglia inhibitors can prevent mechanical hypersensitivity, reduce microgliosis and attenuate the microglial-mediated release of IL-1ß in the spinal cord, highlighting the role of this cell type in painful conditions such as RA (Nieto et al., 2016).

The precise triggers which activate microglia and drive their cytokine secretion, in response to tissue damage or injury, are not completely understood. However, there is evidence to suggest that pattern- and damage-associated molecular patterns, such as LPS, are key contributing stimuli in the activation of microglia (Qin et al., 2005a). A number of these molecules have been shown to up-regulate ion channels on the cell surface membrane of microglia.

One such ion channel is the P2X4 receptor. P2X4 receptors are cell surface purinoceptors activated by extracellular ATP, often co-expressed alongside P2X7, and reside on the plasma membrane as well as intracellular vesicular compartments in both central and peripheral neurons, endothelial cells and microglia (Suurväli et al., 2017). Experiments that have selectively antagonised the P2X receptor family, using the molecule TNP-ATP, are suggested to be effective in alleviating allodynia and hypersensitivity following a peripheral nerve injury (Tsuda et al., 2003). Following nerve injury, expression of P2X4R is thought to be upregulated in microglia and a crucial step for the development of chronic pain. This pathway has since been well defined by those working in this area. The P2X4 receptor is thought to drive microglial phospho-p38 activation, resulting in BDNF synthesis and release. BDNF in turn is claimed to bind to the TrkB receptor on the Lamina 1 projection neurones and down-regulates

neuronal potassium-chloride transporter member 5 (KCC2), which is vital for chloride extrusion. This results in neuronal Cl^- concentrations rising, impairing the inhibitory effect on gamma-Aminobutyric acid (GABA) and ultimately leading to neuronal hyperexcitability (Beggs and Salter, 2010). Once activated, microglia can activate adjacent microglia and astrocytes by paracrine mechanisms allowing maintenance of the pain state (Ji and Wen, 2006).

1.11.2 Neural Modulation of the Immune System

Similar to immune cells, nociceptors themselves have been shown to produce and release a range of small proteinaceous molecules, known as neuropeptides, in response to an inflammatory insult (Levine et al., 1993). These neuropeptides are key in contributing to "neurogenic inflammation", a concept first introduced by Goltz in 1874 and by Bayliss in 1901 (Bayliss, 1901). These early experiments demonstrated, via electrically stimulating dorsal roots, that vasodilation of the skin (and the associated inflammation) could be induced independently of the immune system (Chiu et al., 2012). Two key neuropeptides involved in neurogenic inflammation are SP and CGRP, both of which can have a direct effect on the surrounding vasculature, via increased capillary permeability and vasodilation respectively (Pinho-Ribeiro et al., 2017b). In line with this, it has been shown that using antibodies to neutralise the effect of SP and CGRP, the symptoms associated with neurogenic inflammation have been significantly reduced (Louis et al., 1989, Amann et al., 1995, Zeller et al., 2008). The above process is the best example of how neurones can affect the immune response, details of which are discussed in the below paragraphs.

In addition to the above neuropeptides, it has been reported that upon activation, nociceptors can release numerous mediators; growth factors, cytokines, chemokines and purines to highlight a few (Pinho-Ribeiro et al., 2017a). The above signalling molecules are

potentially capable of not only activating neighbouring neurones but also modulating a range of immune cell types, including dendritic cells, neutrophils, macrophages, mast cells and T cells (Pinho-Ribeiro et al., 2017a).

In addition to contributing to neurogenic inflammation, both SP and CGRP are capable of regulating a range of immune cell phenotypes (Chavan et al., 2017). For example, SP causes mast cell accumulation, activation and degranulation following a hindlimb injury in rats (Li et al., 2012), enhanced lymphocyte proliferation (Lambrecht et al., 1999) and increased activation of NF-κB (known to regulate numerous pro-inflammatory cytokines) in murine macrophages and dendritic cells (Marriott et al., 2000). Likewise, CGRP can modulate dendritic cell phenotype, skewing T cell priming and thus affecting downstream adaptive immune responses (Hosoi et al., 1993). Of note, there is evidence to suggest that mediators of neuronal origin are capable of working in cohort with immune cells to resolve inflammation and restore tissue homeostasis (Pradhan et al., 2009).

Neurones can also affect the activation state of microglia. There are various different signals which neurones can use to modulate microglia activation (Biber et al., 2007). Broadly, these are classified into two categories, the 'off' signals which keep microglia in their resting state and the 'on' signals which are inducible and include the production of purines, chemokines and glutamate (Biber et al., 2007). This further highlights the bidirectional relationship between the immune system and the nervous system. In line with this, it has previously been shown that neuronal conditioned medium can modulate the levels of activated microglia (Polazzi and Contestabile, 2003).

The importance of these neuromediators, and their subsequent action on immune cell types, are highlighted in a number of disease models. For example, the use of SP and CGRP

antagonists in a mouse model of psoriasis, showed a reduction in skin lesions, leukocyte infiltration and skin inflammation (Ostrowski et al., 2011). On the other hand, the intranasal administration of SP in a murine model of allergic airway inflammation resulted in an increase in leukocyte infiltration, as well as an increase in the number of TNF+ and IFNγ+ T cells in lymph nodes (Joachim et al., 2006). In line with the involvement of neuroimmune involvement in the resolution phase of inflammation, the exogenous application of CGRP in a murine model of experimental sepsis, shows a reduction in neutrophil recruitment, decreased levels of pro-inflammatory cytokines (*e.g.* TNFα) and an increase in anti-inflammatory cytokines (*e.g.* IL-10) (Gomes et al., 2005).

Furthermore, trigeminal nociceptors have been found to express both the toll-like receptor 4 (TLR4) and cluster differentiation 14 (CD14) receptors, enabling a direct activation from bacterial substances such as LPS (Wadachi and Hargreaves, 2006), resulting in neuronal sensitisation and subsequent activation of a range of immune cells. Woolf and colleagues (Chiu et al., 2013) demonstrated that both mechanical and thermal hyperalgesia in mice is correlated with live bacterial load as opposed to tissue swelling or immune activation of T cells, B cells, neutrophils and monocytes. The authors illustrate an induction of calcium in nociceptor-specific neurones following bacterial infection and an inhibition of bacteria-induced pain in neurones lacking the sodium channel $Na_v1.8$ ((Chiu et al., 2013). Additionally, it has been shown that the fungal infection *Candida albicans* can directly activate nociceptors, leading to CGRP release and increased production of IL-23 from $CD301b^+$ dermal dendritic cells (Kashem et al., 2015).

In conclusion, the above sections have highlighted the intricate relationship between sensory neurones and immune cell types. Evidence has been presented to highlight how this

interaction may be relevant in inflammation and therefore contribute to pain signalling. The next section will focus particularly on the role of macrophages in the above process.

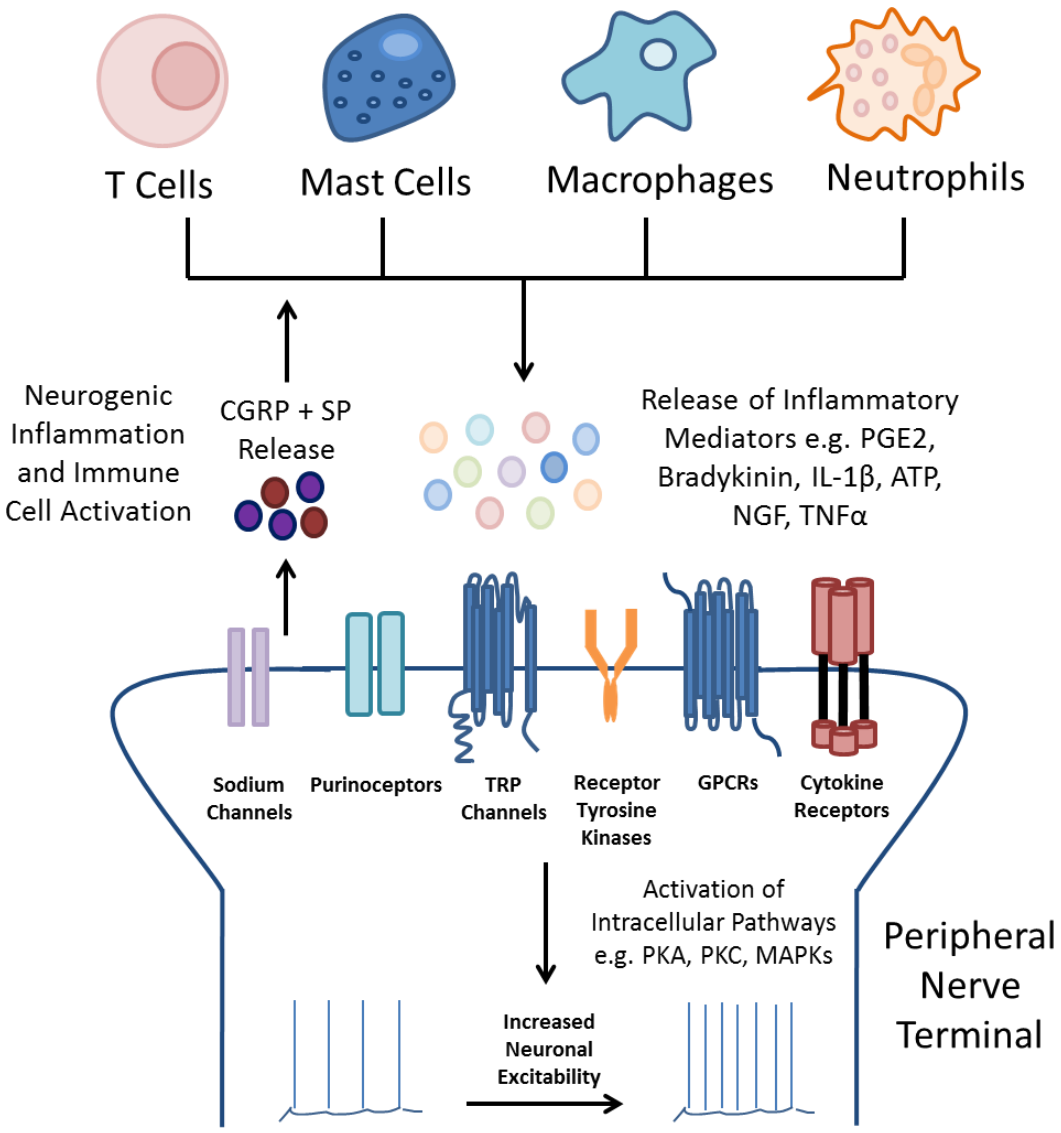

Figure 6. Neuroimmune interactions following tissue injury in the periphery. A number of immune cells release a range of inflammatory mediators that act upon their respective receptors on the peripheral nerve terminal. Intracellular signalling pathways are activated and have the net result of an increase in neuronal excitability. In turn, the sensory neurone can release neuropeptides, such as CGRP and SP, which contribute to neurogenic inflammation and immune cell activation.

Abbreviations: CGRP: calcitonin gene-related peptide; SP: substance P; TRP: transient receptor potential; GPCRs: G protein-coupled receptors; PKA: protein kinase A; PKC: protein kinase C; MAPKs: mitogen-activated protein kinases; PGE2: prostaglandin E2; IL-1β: interleukin-1β; ATP: adenosine triphosphate; NGF: nerve growth factor; TNFα: tumour necrosis factor alpha.

1.12 Role of Macrophages in Pain

Although there is abundant evidence for a range of immune cell types in both the development and maintenance of chronic pain states, this PhD project will focus on the interaction between nociceptors and one immune cell type; the macrophage. Therefore, this introductory section will give a brief overview of the biological function of macrophages, their importance in the inflammatory response and how they can modulate nociceptor function.

1.12.1 Biological Function of Macrophages

Macrophages are bone-marrow derived leukocytes, present in all vertebrate tissues, whose principal role is to promote homeostasis in response to internal and external changes by identifying foreign bodies and destroying them via phagocytosis (Gordon and Plüddemann, 2017). This specialised cell type is divided into subpopulations based on their anatomical location and functional phenotype, *e.g.* osteoclasts (bone), Kupffer cells (liver) and alveolar macrophages (lung) (Murray and Wynn, 2011). Macrophages are critical in immune surveillance function and are amongst the first cell type on the scene following an injury or infection (Gordon, 2016, Wynn et al., 2013). To prevent mistaken identity of healthy cells, macrophages recognise foreign material or dead/dying cells through pattern recognition receptors, such as toll-like receptors and C-type lectin receptors (Takeuchi and Akira, 2010).

Their influence over a wide-range of cell types can be demonstrated by their ability to secrete over 100 different substances, depending on their activation state and surrounding environment (Arango Duque and Descoteaux, 2014, Laskin and Pendino, 1995). For example, the macrophage-driven secretion of pro-inflammatory cytokines, such as IL-1β and IL-6, results in recruitment of neutrophils, monocytes and T cells to the site of infection or injury (Arango Duque and Descoteaux, 2014). These recruited monocytes can then themselves

differentiate into macrophages, further contributing to the inflammatory environment (Italiani and Boraschi, 2014). The production of macrophage-derived IL-12 and IL-23 is important in the differentiation and expansion of anti-microbial T cells, a process needed to drive inflammatory responses forward (Sica and Mantovani, 2012). Macrophages are also known to play a role in the resolution phase of inflammation, via the production of anti-inflammatory cytokines, such as IL-10 (Ortega-Gómez et al., 2013). Additionally, macrophages have been shown to be critical for wound-healing processes; clearing apoptotic cells and producing factors that stimulate angiogenesis and fibroplasia (Koh and DiPietro, 2011).

A common model used to describe macrophage activation states is that of the M1/M2 paradigm. In this model macrophages are said to have two opposing activated states, either classically activated, referred to as M1 macrophages (with a pro-inflammatory phenotype), or alternatively activated (with an anti-inflammatory phenotype), referred to as M2 macrophages (Mills, 2015). However, recent research has suggested that a 'spectrum model' may be more suitable to due to the multiple and diverse macrophage activation states that can exist (Nahrendorf and Swirski, 2016, Martinez and Gordon, 2014). For example, the proposed conditions associated with chronic inflammation involve TNFα, PGE2 and P3C (Xue et al., 2014). The above model highlights the broad range of macrophage activation states and by extension, the wide-reaching biological functions of macrophage signalling.

The inflammatory responses triggered via macrophage activation are initially considered beneficial, with the aim of restoring and maintaining the microenvironment. However, if left unresolved this continued inflammatory environment can lead to considerable tissue damage (Nathan and Ding, 2010). In line with this, macrophage signalling has been implicated in a number of chronic inflammatory and autoimmune diseases, including atherosclerosis,

inflammatory bowel disease and fibrosis (Wynn et al., 2013). Given the focus of this PhD thesis, the potential role of macrophage signalling in pain mechanisms is outlined below.

1.12.2 Evidence for a Role of Macrophage Signalling in Pain

As described above, activated tissue-resident and recruited macrophages from the blood are drawn to the site of injury as a first line response. In the context of both inflammatory and neuropathic models of pain, it has been proposed that macrophages not only infiltrate the DRG but also surround the affected sensory neurone terminal (Segond von Banchet et al., 2009, Peters et al., 2007). The infiltration of activated macrophages has been demonstrated in humans with symptomatic OA, with the quantity of knee-related macrophages being significantly associated with pain severity (Kraus et al., 2016) and the macrophage biomarker CD14 (Daghestani et al., 2015). Mice injected with acidic injections into the gastrocnemius muscle displayed an increase in the number of local muscle macrophages, whilst the depletion of these macrophages (via the use of clodronate liposomes prior to acid injection) attenuated the associated hyperalgesia produced (Gong et al., 2016).

1.12.2.1 Macrophage Modulation of Nociceptors

Following macrophage infiltration (in addition to a number of other cell types) into the affected area, a range of mediators are released into the microenvironment, including TNFα, NGF, prostanoids and nitric oxide (NO). The role of these macrophage-derived mediators is highlighted in a number of studies. A recent study used macrophage specific COX2 knock-out mice to show that the mechanical and thermal hypersensitivity associated with CFA-evoked hind paw inflammation was significantly decreased, most likely due to a reduction in inflammatory cell infiltration alongside PGE2, IL-1β and TNFα levels (Chen et al., 2017b). Another study demonstrated that enhancing the number of peritoneal macrophages (via the

use of thioglycolate) in mice resulted in an increased number of nociceptive writhing responses to zymosan and acetic acid (Ribeiro et al., 2000). Similarly, intraperitoneal injection of the supernatant from LPS-stimulated macrophages into mice promoted nociceptive behaviour, an effect which was partially prevented using antisera directed against TNFα, IL-1 or IL-8 (Thomazzi et al., 1997). These cytokines subsequently may act directly upon the sensory neurone terminal itself, or indirectly via other non-neuronal cell types, to lower the neuronal threshold for activation and increase action potential firing (as previously discussed in section 1.3.2.2)(Ji et al., 2014). An additional mechanism for macrophage-mediated pain has been proposed by Shutov and colleagues (Shutov et al., 2016). The authors suggest a crucial role for the complement system; a collection of soluble and membrane-bound proteins that are important in both the recognition and clearance of foreign molecules. The authors specifically suggest that the complement component 5a induces thermal hyperalgesia by activating macrophage-driven signalling, initiating the mobilisation of NGF and subsequent sensitisation of TRPV1 in sensory neurones (Shutov et al., 2016). Finally, a recent study demonstrated that pain hypersensitivity in male and female mice (induced via angiotensin II (Ang II) injection into the hind paw) is mediated via activation of the Ang II receptor (AT2R) and the ion-channel TRPA1 (Shepherd et al., 2018). Crucially, the authors demonstrate that activation of AT2R occurs on peripheral/skin macrophages, triggering the production of reactive oxygen/nitrogen species, which in turn trans-activate TRPA1 on mouse and human DRG sensory neurones via cysteine modification of the channel (Shepherd et al., 2018). The latter study highlights how the relationship between non-neuronal cell types and sensory neurones can be crucial when trying to understand the mechanisms associated with chronic pain.

1.12.2.2 Macrophage Modulation of Immune Cells

Macrophage released mediators can also act upon other immune cells, further increasing the release of pro-inflammatory cytokines and contributing to the 'inflammatory soup' and sensitisation of surrounding nociceptors (Lama Tamang et al., 2012). It has been shown that through the glucocorticoid-induced tumour necrosis factor ligand system, the interaction between macrophages and T cells can mediate neuropathic pain states (Kobayashi et al., 2015). In addition, released mediators may also act upon the macrophage itself in an autocrine fashion. For example, TNFα signalling in macrophages mediates the further invasion of macrophages to the injured area by causing the up-regulation of adhesion molecules and the release of proteases (Scholz and Woolf, 2007). NGF has also been shown to have this chemotactic effect *in vitro* on murine macrophages (Kobayashi and Mizisin, 2001). Furthermore, TNFα can activate an interferon-β autocrine loop in macrophages that sustains the expression of inflammatory genes such as IRF7 and STAT1, thus exacerbating the inflammatory environment (Yarilina et al., 2008a).

The above section has highlighted the critical role for macrophage signalling in host defence and the biological mechanisms by which this is achieved, *e.g.* cytokine production and immune cell recruitment. Evidence for the dysregulation of macrophage signalling in the context of pain has also been presented. This thesis aims to dissect further mechanisms by which macrophages could be contributing to pain states and their possible contribution to both NGF and TNFα-induced nociceptive signalling.

2. Aim of PhD

The above introduction has outlined the crucial role of inflammatory mediators in pain states. Evidence has been presented for the involvement of two mediators; NGF and TNFα, and how they affect the excitability of nociceptors, via both direct and indirect mechanisms. However, *in vivo*, these mediators are not secreted in isolation but rather as part of a complex array of molecules. While the individual actions of these molecules on primary sensory neurones are important, the interactions between these mediators, in addition to cross-talk between nociceptors and non-neuronal cells, are likely to be critical in the transition to chronic pain states and therefore crucial to improving pain management.

Drugs which modulate NGF and TNFα have been developed and are having some degree of success as analgesics, yet safety concerns still exist around their usage. Investigating the relationship between NGF and TNFα could unearth new pain targets that have reduced adverse effects compared to targeting individual mediators.

The above is further reinforced by several *in vivo* studies performed in-house at AstraZeneca. The use of a bispecific blocker, directed against NGF and TNFα simultaneously, in rodent models of both inflammatory and neuropathic pain, exhibits a superior analgesic effect compared to the blockade of either factor in isolation. Furthermore, this apparent synergistic analgesia is seen at doses at which the individual components are inactive, which could improve the risk to benefit ratio for patients (if translatable in the clinic). Although the *in vivo* data is striking, it remains largely unknown as to the biological mechanism(s) behind these results. This project explores the pathogenic contribution of NGF and TNFα in the development and maintenance of chronic pain.

The primary aims of this PhD thesis are to test the hypotheses that:

1. TNFα (and NGF) produce pain-relevant responses via direct actions on sensory neurones. Specifically, primary cultures of purified sensory DRG neurones and bone-marrow derived macrophages will be stimulated with NGF or TNFα to assess their influence on a number of pain-relevant endpoints. These endpoints include changes at both the molecular and cellular level.
2. NGF and TNFα act in a synergistic manner to drive pain-relevant responses *in vitro*. The effect of stimulating purified DRG neuronal cultures, macrophages or a co-culture system with a combination of NGF/TNFα (compared to either one alone), on molecular and cellular readouts, will be deduced.
3. Combined individual antagonism of NGF and TNFα *in vivo*, (which elicits superior analgesic efficacy), is associated with changes in the expression of pro-nociceptive genes and circulating cytokines in both the CFA model of inflammatory pain and the Seltzer model of neuropathic pain.

3. Investigating the Individual and Combined Effect of NGF and TNFα on Sensory Neurones *In Vitro*

3.1 Introduction

The primary purpose of this chapter is to discern both the individual and combined effect of NGF and TNFα on sensory neurones *in vitro*. This chapter will present data from the neuronal PC12 pheochromocytoma cell line, purified adult mouse DRG neuronal cultures and mixed adult mouse DRG neuronal/glia cultures.

3.1.1 NGF Effect on DRG Sensory Neurones

The profound effect of NGF on DRG sensory neurones has been extensively examined and therefore a large body of literature around this topic exists (Denk et al., 2017, Delcroix et al., 2003, McMahon et al., 1995, Winter et al., 1988, Yip and Johnson, 1984). The mechanisms by which NGF contributes to a chronic pain state are well understood and have been outlined in section 1.5 of this thesis. Therefore, the purpose of including NGF as an experimental treatment group within this chapter are three-fold; firstly, to confirm those effects described within the literature, secondly, to act as a positive control to compare the effect of TNFα against and thirdly, to assess if NGF can synergise with TNFα.

3.1.2 TNFα Effect on DRG Sensory Neurones

It is less clear whether DRG sensory neurones are a cellular target for the cytokine TNFα. Due to its widespread effects, via multiple cell types, and its role as a master pro-inflammatory cytokine, dissecting the mechanisms by which TNFα can contribute to chronic pain conditions is considerably harder to establish. One of the main pieces of evidence suggesting a possible direct activation of the nociceptive system by TNFα comes from patients suffering from chronic inflammatory conditions, such as rheumatoid arthritis and osteoarthritis. Patients receiving therapeutic intervention which blocked the effects of TNFα found that there was a

significant reduction in their pain (Walsh and McWilliams, 2012, Mobasheri, 2013). However, the intriguing element of the above comes from the timescale on which this effect has been observed. The reduction in pain following anti-TNFα infusion has been shown to be apparent as early as 24 h, despite markers of inflammation being unaffected at this early time point (Hess et al., 2011). This suggests a direct action of TNFα on the nociceptive system, rather than an indirect effect via resolution of the inflammatory response, a process that would take considerably longer. The direct effect of TNFα on neurones is made more plausible by reports of TNFα receptor expression on sensory neurones (Li et al., 2004), expression levels (of both TNFR1 and TNFR2) have been reported to further increase in a number of pain models (Schafers et al., 2003b, Ma et al., 2009, Dubový et al., 2006). However, which TNFα receptor is present, on what cell type and to what extent, is still a controversial topic. For example, contrary to the above studies, Inglis and colleagues have reoorted that the increase in TNFR2 expression is exclusively present in non-neuronal cell types (Inglis et al., 2005b). Another study reported that within the DRG TNFR1 co-localised with nociceptive markers >99 % of the time whereas TNFR2 was found to be completely absent (Wheeler et al., 2014).

A number of studies have been conducted demonstrating that TNFα can have a profound effect *in vivo* by increasing responsiveness of C-fibers to mechanical stimulation, an effect which can be prevented via the blockade of TNFα (Sorkin et al., 1997, Richter et al., 2010). There is evidence to suggest a link between TNFα and the development of heat hyperalgesia. Studies have shown that acute application of TNFα to rat cutaneous nociceptors *in vitro* resulted in an enhanced heat-evoked release of CGRP (Bowen et al., 2006b, Oprée and Kress, 2000), an effect possibly explained by a reported increase in TRPV1 expression in cultured DRG sensory neurones following 24-48 h exposure to TNFα (Hensellek et al., 2007a).

However, an element which all the above studies fail to consider/address is the involvement of non-neuronal cell types in all the preparations used, whether *in vivo* or *in vitro*. This PhD thesis is unique in that, as far as we are aware, this is the first time that the direct effect of TNFα on nociceptive neurones has been examined in a system where the presence of non-neuronal cell types has been removed. The advantages and disadvantages of using this method are briefly outlined below.

3.1.3 Purified Neuronal Cultures from MACS Sorting

The magnetic-activated cell sorting (MACS) technique allows for the generation of 95 % pure neuronal populations, the characteristics of which are unchanged when compared with unsorted DRG cultures (Thakur et al., 2014). This technique allows the experimenter to use a substantially more controlled system to address fundamental biological questions. This method has been utilised in this PhD project to ascertain, with a high degree of certainty, if a particular treatment group has a direct effect upon the neurones themselves or whether any effects occur through an indirect mechanism, for example, via non-neuronal cell types. Although the characteristics of individual neurones passed through the magnetic columns are unchanged, a substantial reduction in neuronal yield occurs due to the entrapment of larger diameter neurones in the column. This limitation will be considered when drawing conclusions from the data presented. Nevertheless, the enrichment of small and medium diameter neurones in this pain-focussed project could be beneficial (Thakur et al., 2014). However, this reduction in neuronal yield also poses a technical challenge, particularly in experiments which require large quantities of neurones to yield sufficient assay signal. Therefore, throughout this project there are instances where it was deemed more

appropriate to use a mixed DRG glial-neuronal culture (following the use of a percoll gradient to remove debris) to obtain sufficient cell numbers.

3.2 Aims and Experimental Strategy

The aims of this chapter are:

- to determine whether TNFα can directly signal and activate DRG sensory neurones
- to determine whether the direct effects of TNFα, on sensory neurones, can summate with or synergise with the known actions of NGF

Where possible, the data presented in this chapter is conducted on purified DRG sensory neurones in order to negate any potential indirect effects of TNFα via non-neuronal cell types located in the culture.

To assay the effect on DRG sensory neurones, four primary read-outs have been selected to achieve a broad assessment of sensory neurone function. Specifically, modulation of neurite outgrowth, nociceptive gene expression, cellular signalling (*e.g.* phospho-p38 induction and cytosolic calcium) and release of the neurotransmitter CGRP.

Throughout all following data chapters, three different culture types have been used and will be referred to as follows;

1. Purified DRG neuronal cultures (MACS sorted)
2. Mixed DRG neuronal/glia cultures (percoll gradient to remove debris)
3. Mixed DRG neuronal/glia + BMDM co-culture (percoll gradient to remove debris)

3.3 Methods

All animals were obtained from Charles River and housed in a designated facility and maintained in accordance with the United Kingdom Home Office Animals (Scientific Procedures) Act (1986) and Home Office regulations. Animals were kept in a 12 h light dark cycle and fed *ad libitum*. All animals were sacrificed using schedule 1.

3.3.1 Primary Cell Culture of DRG Cultures

Adult C57BL/6 mice aged approximately 7-10 weeks were used to obtain primary sensory neurones. DRGs were collected from all levels of the spinal column. To access the DRGs, spinal columns were dissected out from the surrounding tissue and any extraneous muscle, fat and excess tissue removed. Using a scalpel, a longitudinal cut along the midline of the dorsal aspect of the spinal column was made to produce two equal halves. The spinal cord was then carefully removed in a rostral to caudal direction to reveal the DRGs. To remove the DRGs, the meninges were peeled back and the DRG was cut at its root prior to carefully being pulled out and transferred to ice-cold 1X Hank's Balanced Salt Solution (HBSS) (Life Technologies, 14175-053) in a 60 mm low bind petri dish (Corning, CLS3261). DRGs were incubated for 1 h at 37 ºC in an enzymatic mix made up of 3 mg/mL dispase (Life Technologies, 17105 041) and 0.1 % collagenase (Type 1) (Life Technologies, 17100 017). Following incubation, DRGs were carefully triturated in the enzyme mix up to 40 times before filtering through a 100 µM cell strainer (Corning, 352360) and basal F12 medium (Life Technologies, 21765-069), with fetal bovine serum (FBS) (Life Technologies 10500-064), added to inactivate the enzyme mix. Cells were centrifuged at 111 *g* for 5 min (ALC Centrifuge PK110) before being re-suspended in 1mL basal F12 and layered on top of a percoll gradient to remove any myelin and nerve debris from the resulting culture. The percoll gradient consisted of a 12.5 % mix layered on top of a

28 % mix to form a gradient interface. Mixes were made by diluting percoll (GE Healthcare, 17-0891-01) in basal F12. Cells were spun for a further 10 min at 1300 *g* with the deceleration set to 6 (Hettich Zentrifugen). The debris and percoll gradient were removed prior to the cell pellet being re-suspended in the desired medium.

3.3.1.1 Mixed DRG Neuronal/Glia Cultures

For the mixed DRG neuronal/glia cultures, neurones were re-suspended in BS medium (basal F12, 1X N2 supplement (ThermoFisher Scientific, 17502048), FBS and Penicillin-Streptomycin (Pen/Strep) (Sigma Aldrich, P4333)) and plated at the desired density.

3.3.1.2 Purified DRG Neuronal Cultures

For purified DRG neuronal cultures, dissociated DRGs, following debris removal, proceeded to be purified using the MACS sorting technology and the Miltenyi Neuron Isolation Kit (Miltenyi, 130-098-752). Following removal of the percoll gradient the cell pellet was re-suspended in 160 µL ice-cold MACS buffer (Miltenyi autoMACS HBSS-based washing solution with 0.5 % bovine serum albumin (Sigma Aldrich, A9418)), followed by the addition of 40 µL of non-neuronal antibody cocktail (including antibodies against astrocytes, oligodendrocytes, microglia, endothelial cells and fibroblasts) and a 5 min incubation at 4 °C. Subsequently, 440 µL of MACS buffer and 160 µL anti-biotin microbeads were added. The cell solution was incubated for 10 min at 4 °C using an over-end mixer to ensure thorough mixing. The cell solution was passed through pre-washed LD exclusion columns (Miltenyi Biotech, 130 042 901). This process retains ~95 % of non-neuronal biotin bound cells within the column, and only allows antibody free cells to pass through, resulting in a purified neuronal elute. The columns were rinsed through with MACS buffer and spun down at 400 *g* for 5 min (ALC Centrifuge PK110). The cell pellet was re-suspended in B27 media (Ham's F12 with L-

Glutamine, 2 % B27 (Life Technologies, 17504 044), 1 % 100X Pen/Strep) and the cells plated at the desired density. The specific densities were dependent on the experimental design, details of which are given below. If cultures were kept for a prolonged period of time, cultures were fed with the above media every 2-3 days.

3.3.2 Culture of the Rat PC12 Neuronal Cell Line

For experiments requiring the use of the rat PC12 pheochromocytoma neuronal cell line, a sub clone of the PC12 culture, Neuroscreen-1 cells were purchased from ThermoScientific. PC12 cells were plated in 100 µL fresh Roswell Park Memorial Institute medium (RPMI) (ThermoFisher Scientific, 11875093) supplement with 15 % FBS, 1 % 100X Pen/Strep and L-glutamine) at 75K cells/well on Poly-D-Lysine-coated 96-well plates (Greiner).

3.3.3 Neurite Outgrowth Experiments

Following the culture and purification of adult mouse DRG neurones, purified neuronal cultures were plated on Poly-L-lysine (Sigma Aldrich, P4707) coated 13 mm coverslips (Academy, 400-04-17) placed in a 4-well plate (Thermo Scientific, 176740) incubated with growth-factor reduced matrigel (BD Bioscience, 356230) diluted 1:10 in pre-cooled F12 at room temperature (RT) for at least 1 h. Neurones were plated at a density of between 2-3K cells/well. Neurones were allowed to settle for 1 h, prior to being stimulated with NGF (Cambridge Bioscience, GFM11-1000), TNFα (Peprotech, 315-01A) or a combination of the two, see Table 2 for specific concentrations. Following a 24 h stimulation period, neurones were fixed in pre-warmed 2 % (w/v) paraformaldehyde (PFA) for 20 min at 37 °C. Prior warming of the PFA in these sets of experiments prevented the breakdown of the matrigel and therefore the loss of cells. Following fixation, neurones were blocked in normal goat serum (ThermoFisher Scientific, 31873) made up in 0.2 % PBS Triton-X (Sigma Aldrich, T8787-

50ML) for 30 min at RT to prevent non-specific binding. Following the removal of the blocking solution, the cells were incubated in the primary antibody solution mouse anti-β III tubulin (Promega, G712A), at a concentration of 1:1000 in 0.2 % PBS Triton X for 30 min at RT. Cells were then washed three times in 1X Dulbecco's Phosphate-Buffered Saline (DPBS) before being incubated with the secondary antibody Alexa Fluor® 488 donkey anti-mouse IgG (H+L) (Life Technologies, A21202), at a concentration of 1:1000 in 0.2 % PBS Triton X for 30 min at RT. The cells were then washed for a final three times before the coverslips were mounted onto slides using Prolong® Gold Anti-fade Mountant with DAPI (LifeTechnologies, P-36931). Fluorescence was visualised using Carl Zeiss Axioplan2 microscope and Axiovision software.

3.3.3.1 Data Analysis for Neurite Outgrowth Experiments

Neurite outgrowth was analysed using ImageJ. The following measures were analysed: the average neurite length per cell and the percentage of cells with neurite outgrowth. Neurones were considered to have outgrowth if any neurite was longer than the width of the cell soma.

Table 2. List of stimulations and concentrations of NGF and TNFα used throughout the neurite outgrowth experiments.

NGF	TNFα	Combinations
NGF 1 ng/mL	TNFα 1 ng/mL	NGF 1 ng/mL + TNFα 1 ng/mL
NGF 10 ng/mL	TNFα 10 ng/mL	NGF 10 ng/mL + TNFα 1 ng/mL
	TNFα 50 ng/mL	NGF 1 ng/mL + TNFα 10 ng/mL
	TNFα 100 ng/mL	NGF 10 ng/mL + TNFα 10 ng/mL

3.3.4 Gene Expression Analysis of Adult Mouse DRG Neurones

For gene expression analysis of both purified DRG neuronal cultures and mixed DRG neuronal/glia cultures, neurones were plated at 8-10K cells/well in pre-coated poly-D-lysine coated Greiner 96-well plates (Greiner Bio-One, 655946) incubated with laminin (Sigma Aldrich, L2020) diluted 1:50 in basal F12 for 2 h at 37 °C. Both types of neuronal cultures were left overnight to settle prior to stimulation with varying concentrations of NGF, TNFα or a combination of the two. See Table 3 for details.

Table 3. List of stimulations and concentrations of NGF and TNFα used throughout the gene expression experiments.

Condition	NGF	TNFα	Combinations
1	NGF 10 ng/mL	TNFα 10 ng/mL	NGF 10 ng/mL + TNFα 10 ng/mL
2	NGF 100 ng/mL	TNFα 100 ng/mL	NGF 100 ng/mL + TNFα 100 ng/mL

3.3.4.1 RNA Extraction and cDNA Synthesis

RNA was isolated using the RNeasy plus micro kit (Qiagen, 74034) according to the manufacturer's instructions: following stimulation, the supernatant was removed, and the remaining cells lysed via the addition of 75 µL RLT (RNeasy lysis buffer) Plus (Qiagen, 1053393). RLT Plus buffer was supplemented with β-mercaptoethanol (Sigma Aldrich, M6250), at a ratio of 1:100 (10 µL to every 1 mL of buffer). The homogenised lysate was transferred to a gDNA Eliminator Spin Column and centrifuged for 30 secs at 8000 *g* (Eppendorf centrifuge 5424). The column was discarded and the flow through saved. An equal volume of 70 % ethanol was added to the saved flow through and mixed thoroughly prior to being transferred to a RNeasy MinElute Spin Column and centrifuged for 15 secs at 8000 *g* (Eppendorf centrifuge 5424). At each of the following steps the flow through was discarded. The column was washed with 700 µL RW1 (RNeasy wash buffer), centrifuged for 15 secs at 8000 *g*, (Eppendorf centrifuge 5424) followed by 500 µL RPE (RNeasy wash buffer) and centrifuged once more (same settings). Subsequently, 500 µL 80 % ethanol was added to the column and centrifuged for 2 min at 8000 *g* (Eppendorf centrifuge 5424) to further wash the

membrane. At this point the column was transferred to a new collection tube and centrifuged at full speed for 5 min (Eppendorf centrifuge 5424) with the lid open in order to fully air dry the membrane. Finally, the column was placed in a new 1.5 mL collection tube and 14 µL RNase-free water added directly to the centre of the membrane. To elute the RNA, the column was spun for a final time at full speed for 1 min (Eppendorf centrifuge 5424).

Resulting RNA was quantified using the Agilent 2100 Bioanalyzer instrument. Samples were run using the Agilent RNA 6000 Pico Kit (Agilent, 5067-1513). This assay is based on traditional gel electrophoresis that have been transferred to a chip format, allowing for accurate quantification and integrity evaluation. Only samples with a RNA integrity number (RIN) < than 7 were taken forward for further analysis. Based on this quantification 15 ng of RNA was reverse transcribed using the Life Tech Vilo mastermix (Life Technologies, 11755050) following sample dilution with RNase free water. Total RT reaction consisted of 24 µL sample and 6 µL Vilo mastermix. The following RT cycling conditions were utilised; 25 °C for 10 min, 42 °C for 60 min and 85 °C for 5 min. Samples were diluted 3.5-fold in order to have enough sample for subsequent analysis and kept at 4 °C until ready for use.

3.3.4.2 RT-qPCR

To obtain the relative quantification of the desired transcripts, samples were run in duplicate (unless otherwise stated) on the QuantStudio 12-FLEX Real-Time PCR system (Applied Biosystems) using TaqMan® Gene Expression Assays (Applied Biosystems). The use of TaqMan probes exploits the 5'-3' nuclease activity of the *Taq* polymerase to detect and quantify specific PCR products. The target-specific TaqMan probe is conjugated with a reporter and quencher fluorochrome. Only in the presence of the target sequence is the probe degraded by the *Taq* polymerase, resulting in separation of the reporter and quencher dye.

Consequently, the fluorescence signal originating from the reporter dye is detected and increases during following PCR signals (van der Velden et al., 2001).

Reaction mixtures were prepared on ice and contained: 5 µL TaqMan® Fast Universal PCR Master Mix 2X (Applied Biosystems, 4366073), 0.5 µL Eukaryotic 18S rRNA Endogenous Control, VIC®/MGB Probe (Life Technologies, 4319413E), 0.5 µL primer/probe (see Table 4 for complete list of mouse gene transcripts examined), 2.5 µL of sample and 1.5 µL of ddH_2O, giving a final reaction volume of 10 µL. A blank sample of water was used as a negative control in all experiments. The following cycling conditions were utilised; 25 °C for 10 min, 42 °C for 60 min and 85 °C for 5 min.

3.3.4.3 Data Analysis for Gene Expression Experiments

mRNA transcripts were normalised to the expression of the housekeeping gene 18S using the ΔΔCt method (Schmittgen and Livak, 2008) and data expressed as ΔΔCt changes from the basal condition.

Table 4. List of gene transcripts examined and associated catalogue number.

Gene Transcript	Applied Biosystems Catalogue Number
Ntrk1 Neurotrophic Receptor Tyrosine Kinase 1	Mm01219406_m1
Ngfr Nerve Growth Factor Receptor	Mm01219406_m1
Scn9a Sodium Voltage-Gated Channel Alpha Subunit 9	Mm00450762_s1
Scn10a Sodium Voltage-Gated Channel Alpha Subunit 10a	Mm00501467_m1
Scn11a Sodium Voltage-Gated Channel Alpha Subunit 11a	Mm00449367_m1
Trpv1 Transient Receptor Potential Vanilloid 1	Mm01246300_m1

F2rl1 Protease-Activated Receptor 2	Mm00433160_m1
Calca Calcitonin Related Polypeptide Alpha	Mm00801462_m1
Tac1 Tachykinin Precursor 1	Mm01166996_m1
Ptgs2 Prostaglandin-Endoperoxide Synthase 2	Mm00478374_m1
Tnfrsf1a Tumour Necrosis Factor Receptor 1	Mm00441875_m1

3.3.5 CGRP Release Enzyme Immunometric Assay

Levels of CGRP in culture supernatants from mixed DRG neuronal/glia cultures were examined using SPI Bio's Rat CGRP EIA kit (SPI Bio/Bertin Pharma, A05482). All reagents were made up according to the manufacturer's instructions. The principle of the assay is based on a double-antibody sandwich technique (Frobert et al., 1999). The CGRP antibody coated on the bottom of the plate binds to any CGRP from the sample, while the addition of an AChE (acetylcholinesterase)-Fab' conjugate also binds selectively to a different epitope on the CGRP

molecule, creating an immobilised sandwich. The concentration of CGRP is measured using Ellman's Reagent to detect the enzymatic activity of the AChE (Grassi and Pradelles, 1991). The intensity of the yellow colour formed is proportional to the amount of CGRP present in that sample (Mitchell, 2006).

The above cultures were prepared as previously described in section 3.3.1.1. At the point of stimulation, performed in either duplicate or triplicate, 50 µL of culture supernatant was removed (leaving 100 µL of supernatant) and the desired concentration of stimulators (NGF 0.1 ng/mL, 1 ng/mL, 10 ng/mL or 100 ng/mL, TNFα 10 ng/mL) added at a 6X stock in a volume of 20 µL BS medium. Cultures were allowed to respond to the above stimulations for 48 h. Following stimulations, CGRP release was evoked by challenging cultures with 100 µL 25 mM potassium (K^+) solution, followed by a 30 min incubation at 37 ºC. Control wells were stimulated with 'normal' extracellular solution as a negative control for CGRP release. Normal extracellular control solution consisted of the following: 1L dH_2O, NaCl (140 mM), KCl (2 mM), $CaCl_2$ (2 mM), $MgCl_2$ (1 mM) and HEPES (10 mM). The 40 mM stock of high K^+ buffer solution consisted of the following: 1L dH_2O, NaCl (102 mM), KCl (40 mM), $MgCl_2$ (1 mM), $CaCl_2$ (2 mM) and HEPES (10 mM). Both solutions were made to a pH of 7.4 and an osmolarity of 293 mOsm. To make the working solution of 25 mM K^+ solution, 25 mL of the 40 mM high K^+ buffer solution was added to 15 mL of normal extracellular solution. The resulting supernatant was diluted in an equal volume of EIA buffer and diluted further as necessary. 100 µL of either sample or standard was added to the provided pre-washed CGRP pre-coated 96-well strip plate. Non-specific binding wells (100 µL EIA buffer) and blank wells were also incorporated in the plate layout. The anti-CGRP AChE tracer was made up in EIA buffer and 100 µL added to each well (except blank wells). The plate was sealed with a plastic film and incubated for

72 h at 4 ºC. Following the incubation period, the plate was washed six times with 180 µL wash buffer for 2 min on the orbital shaker before the addition of 200 µL/well of Ellman's Reagent. The plate was incubated in the dark for 45 min at RT using an orbital shaker for optimal development.

3.3.5.1 Data Analysis for CGRP Release Experiments

The absorbance was read at 405 nm on an EnVision Multimode Plate Reader (Perkin Elmer). The absorbance values of the standards were used to plot a standard curve, from which absorbance values of experimental samples were interpolated to determine their concentrations.

3.3.6 Calcium Imaging

For all calcium imaging experiments in this chapter, purified DRG neuronal cultures were utilised. Following the culture and purification of DRG sensory neurones, purified neurones were plated on Poly-L-lysine coated 13 mm coverslips placed in a 4 well plate incubated with growth-factor reduced matrigel as previously described in section 3.3.1.2. Neurones were plated at a density of approximately 1.5K cells/well in B27 medium and imaged 24 h later.

Calcium imaging experiments were performed using a physiological extracellular solution (ECS); NaCl (8.176 g), KCl (0.373 g), glucose (1.801 g), HEPES (2.383 g), $CaCl_2.6H_2O$ (0.294 g) and $MgCl_2.6H_2O$ (0.203 g) was added to 1 litre of distilled H_20 and the pH adjusted to 7.4 via the addition of hydrochloric acid or sodium hydroxide solutions. Neurones were loaded with Fura-2 AM, a ratiometric calcium indicator dye which has its emission peak at 505 nM and changes its excitation peak from 340 nm to 380 nm in response to calcium binding (Barreto-Chang and Dolmetsch, 2009). A stock concentration of 2.5 µM Fura-2 AM (Invitrogen, 1881420), with 0.01 % Pluronic Acid (Invitrogen, 1899021), was diluted to 1:1000 in the above

ECS and 1 mM Probenecid (Sigma Aldrich, P8761) added to prevent the extrusion of the dye from the cell via its action as an anion transporter inhibitor, and kept protected from the light for the duration of the experiment. To load the neurone-plated coverslips, the culture media was gently removed and 500 µL of the above Fura-2 AM solution added. Cover slips were incubated at 37 °C for an hour prior to imaging commencing.

For all experiments conducted, a perfusion system was utilised whereby the neurones were exposed to either a continuous flow of the above ECS or the physiological solution containing a desired concentration of the experimental stimulus. Each coverslip received a minimum of 3 min perfusion with the ECS to establish a robust baseline. KCl was always applied at the end of the experimental procedure to identify neurones and confirm their viability. Imaging was conducted using the NIKON ECLIPSE TE200 microscope, the ORCA Flash 4.0 camera and the Easy Ratio Pro Software.

3.3.6.1 Direct Activation on Purified DRG Neuronal Cultures with TNFα

To determine if TNFα could trigger calcium transients directly a simple protocol was used (Figure 7). Both TNFα and KCl solutions were made up in the above ECS and were perfused over the coverslip for 2 min.

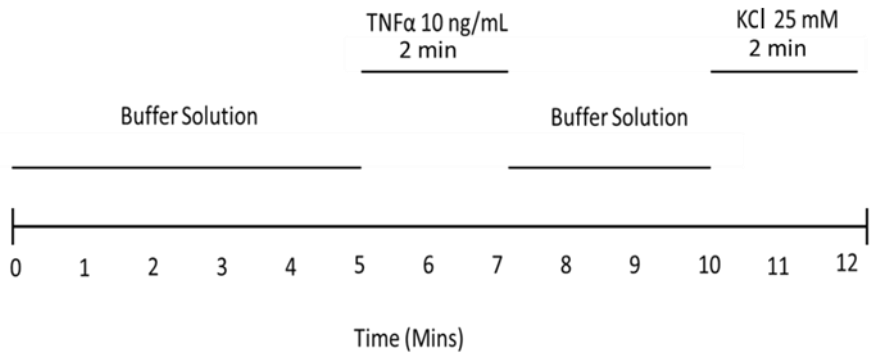

Figure 7. Schematic of timeline for calcium imaging experiments involving direct application of TNFα.

3.3.6.2 Determining Purified DRG Neuron Response to Capsaicin

To determine an appropriate dose of capsaicin to use, to produce a robust, sub-maximal response, a series of capsaicin concentrations were applied to purified DRG neurones as in the protocol summarised below (Figure 8). Both capsaicin and KCl solutions were made up in the above ECS. Capsaicin was perfused over the coverslip for 3 min and KCl for 1.5 min.

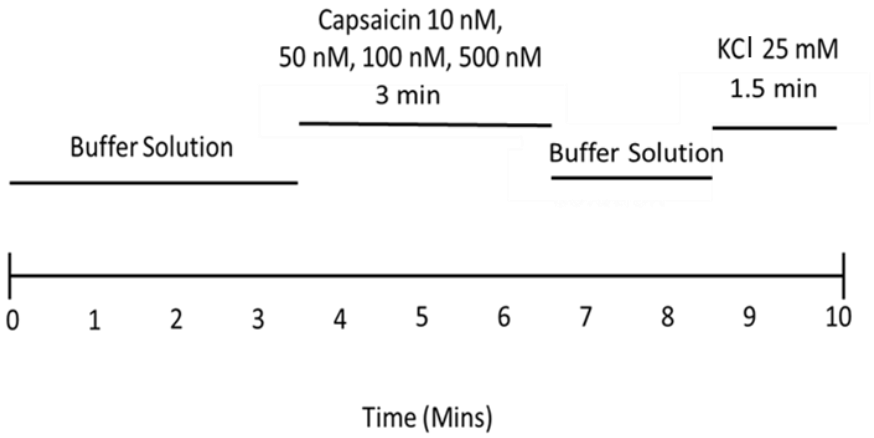

Figure 8. Schematic of timeline for calcium imaging experiments determining appropriate capsaicin dose.

3.3.6.3 TNFα as a Sensitisation Agent on Purified DRG Neuronal Cultures

To determine if TNFα could act as a sensitising agent and therefore increase the response of the neurones to capsaicin, coverslips were cultured for 24 h prior to calcium imaging in either B27 medium or TNFα 10 ng/mL (in B27 medium). A simple protocol was used to determine the response of purified neurones to a capsaicin concentration of 50 nM (Figure 9). Both capsaicin and KCl solutions were made up in the above ECS. Capsaicin was perfused over the coverslip 3 min and KCl for 1.5 min.

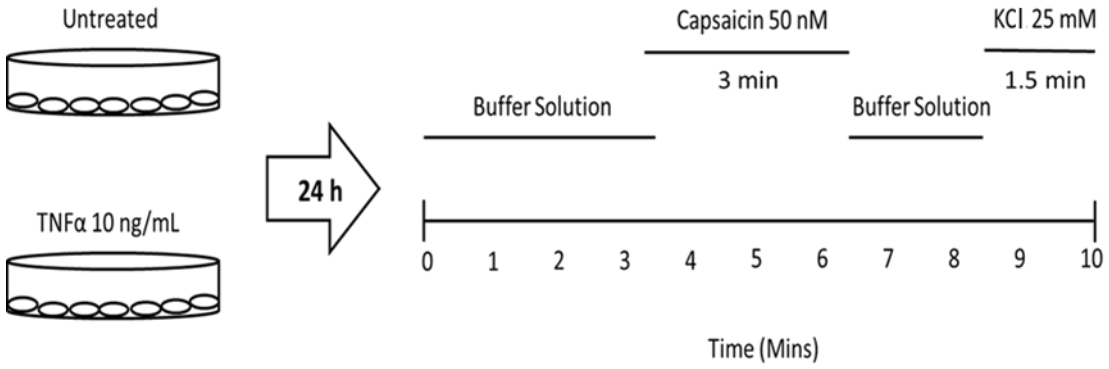

Figure 9. Schematic showing the experimental set-up and timeline for calcium imaging experiments regarding TNFα sensitisation capability.

3.3.6.4 Data Analysis for Calcium Imaging Experiments

Images were extracted from the Easy Ratio Pro software as Tiff files and further image processing was undertaken using ImageJ Version 1.8. Subsequent data evaluation, graphing and statistical analysis was achieved using Microsoft Excel and GraphPad software (version 7.04). Statistical analysis included either two-tailed t-tests or One-Way ANOVA followed by multiple comparison post-hoc tests. A P value <0.05 was considered significant.

In order to generate traces of calcium signals from time lapse images, cell bodies of neurons were circled using the oval selection tool in ImageJ. Cell bodies were circled with minimal

overlap where possible. To generate normalised data (as neurons show differences in their baseline fluorescence), the baseline period (at least 3 min) of fluorescence for each cell and changes from this baseline fluorescence were calculated as ΔF/F.

$$\frac{\Delta F}{F} = \frac{Ft - F0}{F0}$$

Where F_t is the fluorescence at time t and F_0 is the fluorescence average over a baseline period.

3.3.7 Homogenous Time Resolved Fluorescence Assay

As both TNFα and NGF signalling initiate the activation of a variety of MAP kinases, a phospho-p38 homogenous time resolved fluorescence (HTRF) assay (Jia et al., 2006) was employed to determine if any synergistic actions could be identified in this pathway. In order for p38 to be in an active form it must be phosphorylated on Thr180 and Tyr182 amino acid residues (Wilson et al., 1996). Following lysis of the cells, these phosphorylated forms can be detected using the following two monoclonal antibodies: the anti-phospho-p38 antibody conjugated to the donor molecule Eu^{3+}-cryptate and the anti-p38 antibody conjugated to the acceptor molecule d2. Only when p38 has been phosphorylated, and therefore the acceptor and donor molecules are in close proximity, will there be a transfer of energy resulting in a fluorescent signal (on excitation of the $Eu^{3+)}$. The fluorescence produced is proportional to the amount of phospho-p38 present.

Cisbio's phospho-p38 kit (Cisbio, 64P38PEG) was used according to the manufacturers' instructions. This assay was performed on the PC12 neuronal cell line and purified DRG neuronal cultures. Both cell types were stimulated with NGF, TNFα, a combination of the two or 100 µM anisomycin (Sigma Aldrich, A5862-0.5M), which acted as a positive control for p38

activation, for 5 or 20 min, for further details see Table 5. At the end of the specified time course the media was removed and 50 µL of lysis buffer from the Cisbio p38 kit was added. Subsequently, cells were placed on a shaker at 400 rpm at RT for 20 min. Following lysis, 16 µL of each lysate was transferred to a parallel HTRF white 384-well plate (Cisbio, 66PL384025) for the Cisbio HTRF reaction. A 4 µL mix of diluted d2-labelled anti-phospho IgG and Europium labelled anti-p38 IgG was added to each lysate sample. A number of controls were used; control lysate (as a positive control), blank control (used to check the cryptate signal at 620 nm) and a negative control (to check the non-specific signal). The plate was incubated with the antibody mix for 3 h at RT before being read on an EnVision Multilabel Plate reader equipped with a Xenon lamp. Upon the excitation of the donor (337 nm), the energy is transferred from the donor (620 nm emission) to the acceptor molecule (665 nm emission) if the two are in close proximity. This fluorescence resonance energy transfer (FRET) signal is proportional to the amount of phospho-p38 present in the samples.

Table 5. Information regarding details of cell type, concentrations and stimulation times for the HTRF assay.

Cell Type	Density of Cells	Concentration of NGF	Concentration of TNFα	Concentration of Anisomycin	Stimulation Time
PC12 Neuronal Cell Line	75K/well	100 ng/mL	100 ng/mL	100 µM	20 min
Purified DRG neuronal cultures	10K/well	10 ng/mL	10 ng/mL	100 µM	5 min/20 min

3.3.8 Immunocytochemistry-Phospho-p38 Staining of Purified DRG Neuronal Cultures

Levels of phospho-p38 were also measured using immunocytochemistry (ICC) techniques. Timings and stimulations were the same as previously described for the set-up of HTRF experiments (section 3.3.7) conducted with purified DRG neuronal cultures. Cultures were plated in pre-coated poly-D-lysine Greiner 96 well plates. DRG neurones were plated at 5K cells/well in 100 µL BS medium.

Following the stimulation of neuronal cultures for 5 or 20 min, the supernatant was removed, and the cells fixed in 300 µL 4 % formaldehyde/PBS methanol-free (w/v) (Pierce™, 28906) for 10 min at RT. Following aspiration of the fixative agent, cells were washed 3X with 1X PBS prior to being blocked in serum (1X PBS/ 5 % normal serum/ 0.3 % Triton™ X-100) for 1 h at RT. During this incubation period the primary antibody was prepared. Neuronal cultures were stained with a phospho-p38 MAPK 9Thr180/Tyr182 (D3F9) XP® Rabbit monoclonal antibody (Cell Signalling, 4511) diluted at a concentration of 1:1600 in the antibody dilution buffer (1X PBS/ 1 % BSA/ 0.3 % Triton™ X-100). The blocking solution was removed and 300 µL/well of primary antibody solution added overnight at 4 °C. The following day the cells were washed 3X in 1X PBS for 5 min each wash before being incubated with the secondary antibody Alexa Fluor® 488 donkey anti-rabbit IgG (H+L) (Life Technologies, A21202), at a concentration of 1:1000 in 0.2 % PBS Triton X for 2 h at RT. After the addition of secondary antibody, cells were protected from the light. The cells were again washed 3X in 1X PBS as before, after which cells were exposed to a Hoechst® (ThermoFisher Scientific, H1399) staining solution, diluted 1:2000 in 1X PBS, in order to counterstain the nuclei. Cells were incubated in this solution for 10 min, after which a final 3X wash with 1X PBS was performed. Neuronal cultures were visualised on the Olympus IX81 fluorescence microscope.

3.3.8.1 Data Analysis for Immunocytochemistry Experiments

CellSens Dimension 1.11 (Olympus) imaging software was used for fluorescent image analysis of phospho-p38 staining intensity. Within cellSens, the 'Count and Measure' toolbar was activated and a suitable threshold for detecting FITC positive regions in the image was evaluated and set at 8,500 RFU counts. The images were then segmented and regions of the image which showed FITC fluorescence above this threshold were detected and areas calculated using cellSens. Mean intensity values for each detected object were also determined. Excel exports of these collated values were created and graphed in GraphPad.

3.3.9 Statistical Analysis

All statistical analysis was performed using GraphPad software (version 7.04). Prior to any statistical analysis taking place, the data were tested for normality using the Shapiro-Wilk normality test. Within this chapter, all experimental conditions were compared to the control untreated group and analysed using the following statistical tests; unpaired two-tailed t-test, One-Way ANOVA or Two-Way ANOVA followed by *post-hoc* correction tests for multiple comparisons. In all instances, data are displayed as Mean ± SEM and n numbers and specific *post-hoc* correction tests used reported within the figure legend. A P value <0.05 was considered to be significant.

3.4 Results

3.4.1 Effect of Purifying Neuronal Cultures Using a Percoll Gradient In Vitro

In standard DRG cell culture protocols that do not include a percoll gradient (or similar method), debris can remain (Figure 10G). The presence of debris could obscure cells of interest or alter the properties of the neurones themselves. Therefore, throughout this PhD thesis all neuronal cultures underwent a debris removal step via the use of a percoll gradient. The addition of the percoll gradient successfully removed debris and resulted in clearer visualisation of cells (Figure 10G and H). Within the DRG there are multiple cell types present in addition to the sensory neurones. A MACS sorting technique has been employed to remove non-neuronal cells and obtain purified DRG neuronal cultures. One of the limitations of the purification method is the reduction in neuronal yield (Thakur et al., 2014) (Figure 10C, F and I), therefore assays which required higher number of neurones (to improve reliability of said assay) were performed on percoll-treated mixed DRG neuronal/glia cultures.

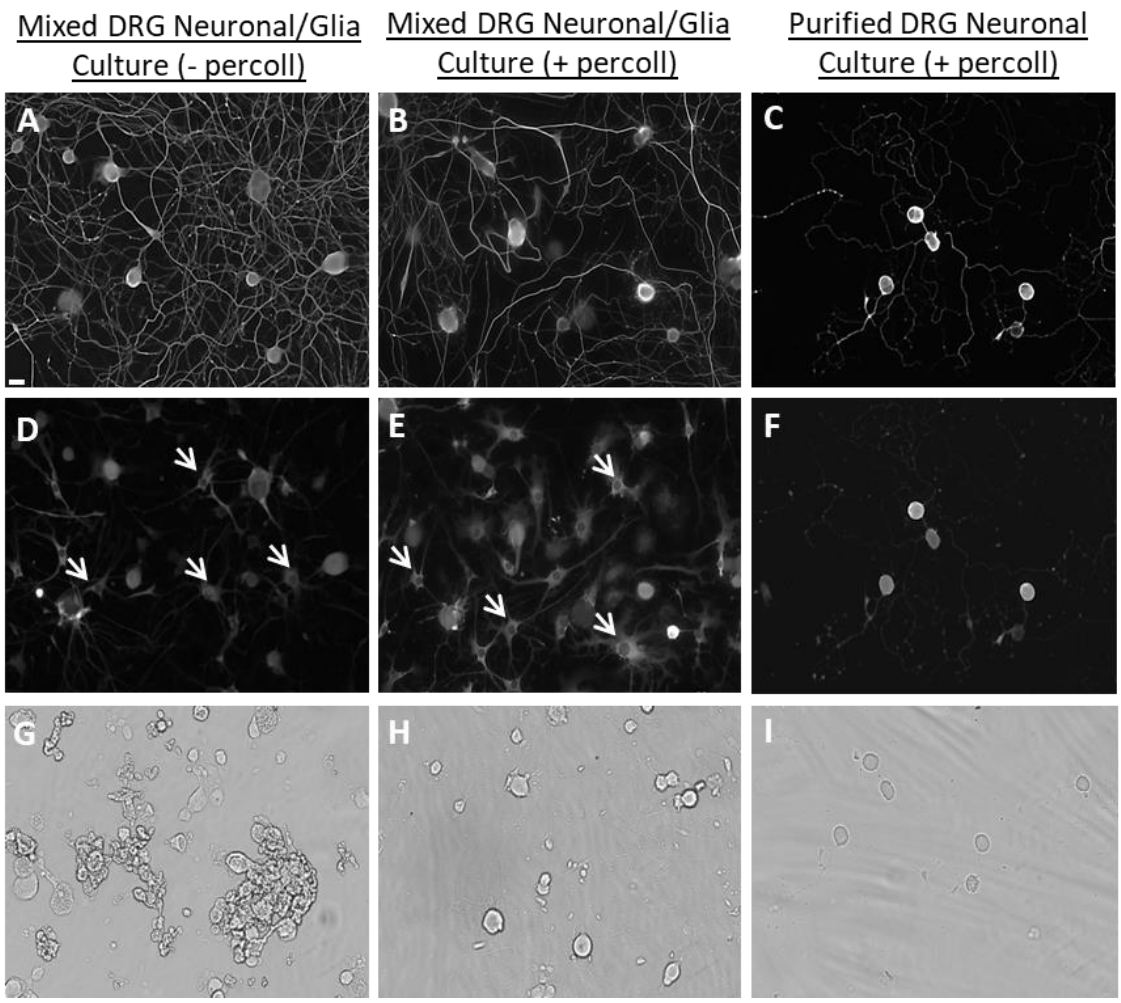

Figure 10. The effects of percoll gradient on the composition of plated cells in mixed and pure DRG neuronal cultures from adult mouse DRG. A-C) Images of neurones in a mixed DRG neuronal/glia culture minus a percoll gradient, mixed DRG neuronal/glia culture plus a percoll gradient and a purified DRG neuronal culture plus a percoll gradient. Cultures were stained with the neuronal marker βIII-tubulin. D-F) Images of the presence of non-neuronal cell types (highlighted with arrows) within the same cultures. Cultures were stained with the satellite glial cell marker glutamine synthetase. G-I) Images displaying the level of debris between the three different types of culture. Scale bar represents 20 µM.

Abbreviations: DRG: dorsal root ganglia.

3.4.2 TNFα has No Significant Effect on Neurite Outgrowth

A neurite outgrowth assay was used as a measure of the general sensitivity of the neurons to a range of TNFα concentrations. Purified DRG neuronal cultures were used to remove any involvement from non-neuronal cell types. Following a 24 h stimulation period, cultures were fixed, stained and visualised on the microscope. Two read-outs were performed; the average neurite outgrowth per cell and the % of cells with neurite outgrowth.

It was found, as shown previously (Wong et al., 2015), that treating purified neuronal cultures with NGF (10 ng/mL) resulted in a significant increase in average neurite outgrowth per cell (Figure 11A), with treated cells (average neurite outgrowth of 571.3 ± 76.99 µm, n=5 biological replicates, One-Way ANOVA; $F(5,24)=22.31$, $P<0.0001$) showing approximately 16 times more neurite outgrowth, compared to untreated cells (average neurite length of 34.88 ± 12.05 µm, n=5 biological replicates) (Figure 11D). The presence of NGF (10 ng/mL) did not affect the average % of cells with neurite outgrowth (Figure 11B).

Following the confirmation of NGF as a relevant positive control, a range of TNFα concentrations (ng/mL) were examined: 1, 10, 50 and 100. Neither average neurite outgrowth per cell nor % of cells with neurite outgrowth displayed any significant changes with TNFα at any concentration (Figure 12).

Since no effect of TNFα alone was observed, two concentrations of TNFα were chosen, 1 ng/mL and 10 ng/mL, and their effect on neurite outgrowth evaluated in combination with that of NGF (10 ng/mL) (Figure 12). Regarding average neurite outgrowth per cell, both combination groups (TNFα 1 ng/mL or 10 ng/mL in combination with NGF 10 ng/mL) produced a significant increase compared to both the untreated group and the individual TNFα treatment group (Figure 13A and B). The combination treatments showed no significant

difference to the NGF alone treatment group (Figure 13A and B). No significant changes were detected in relation to the % of cells with neurite outgrowth (Figure 13C and D).

To ensure that the use of NGF at 10 ng/mL was not a saturating concentration, and therefore able to mask any synergistic effect with TNFα in the combination treatment groups, the concentration of NGF was lowered to 1 ng/mL. Compared to the untreated group, NGF at 1 ng/mL induced a significant increase in the average neurite outgrowth per cell (211.9 ± 48.01 µm to 1032 ± 434 µm, n=3 biological replicates, One-Way ANOVA; $F(7,16)=3.38$, $P=0.0206$). No significant changes were seen in neurite outgrowth between the untreated group and the range of individual TNFα groups or the combination groups (Figure 14A). No significant changes were detected in the % of cells with neurite outgrowth in any groups (Figure 14B).

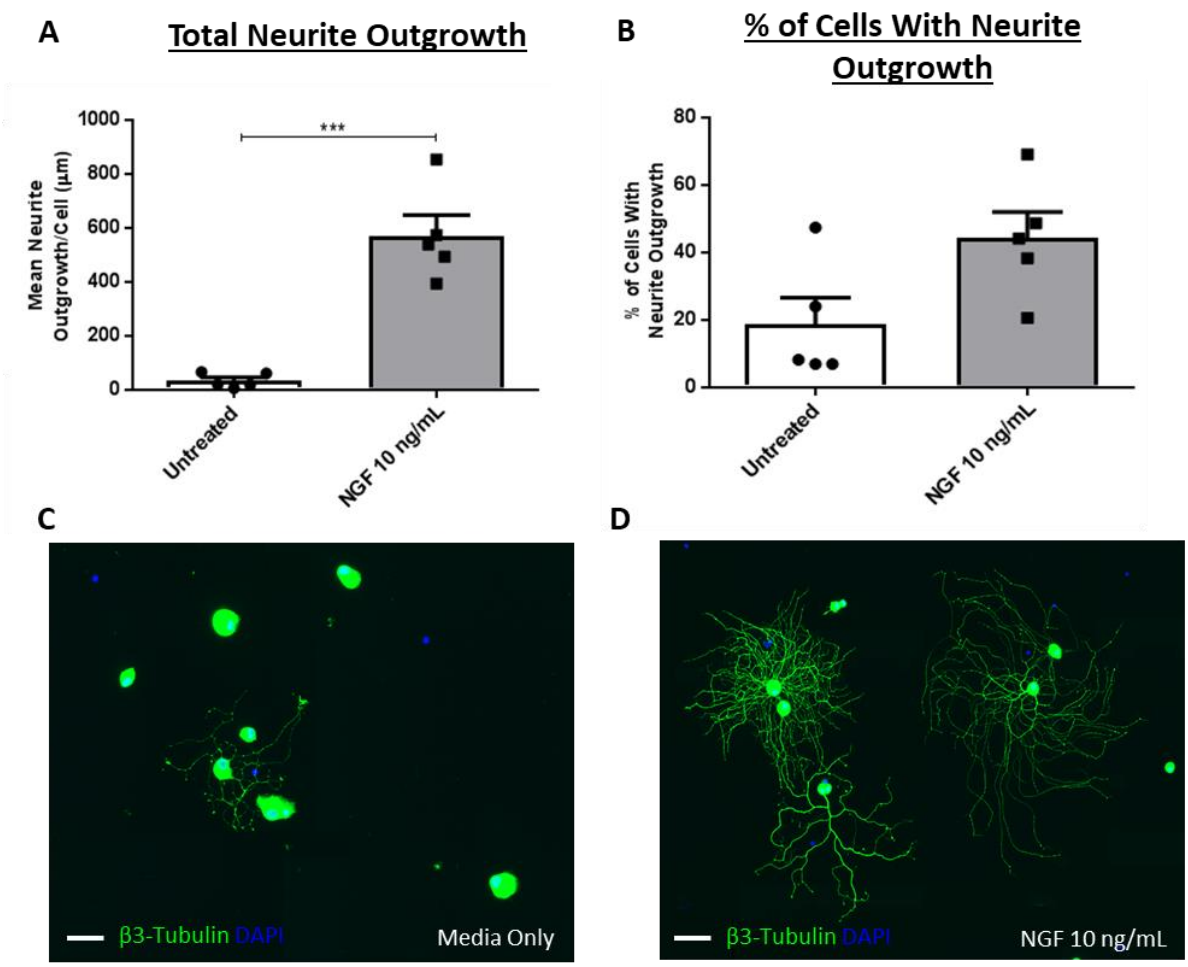

Figure 11. Neurite outgrowth of purified DRG neuronal cultures in response to NGF (10 ng/mL). A) The mean neurite outgrowth or B) the % of neurones with neurite outgrowth following 24 h treatment with NGF (10 ng/mL). C-D) Representative fluorescent micrographs following immunostaining for the neuronal marker βIII-tubulin, and the nuclear stain DAPI, in purified DRG neuronal cultures which were untreated or treated with NGF (10 ng/mL, 24 h). Data displayed as Mean ± SEM, n=5 biological replicates (displayed as individual data points). Data were analysed using One-Way ANOVA followed by Tukey's multiple comparisons test. *** P<0.001. Scale bar represents 50 µM.

Abbreviations: NGF: nerve growth factor; DAPI: 4',6-diamidino-2-phenylindole; DRG: dorsal root ganglia.

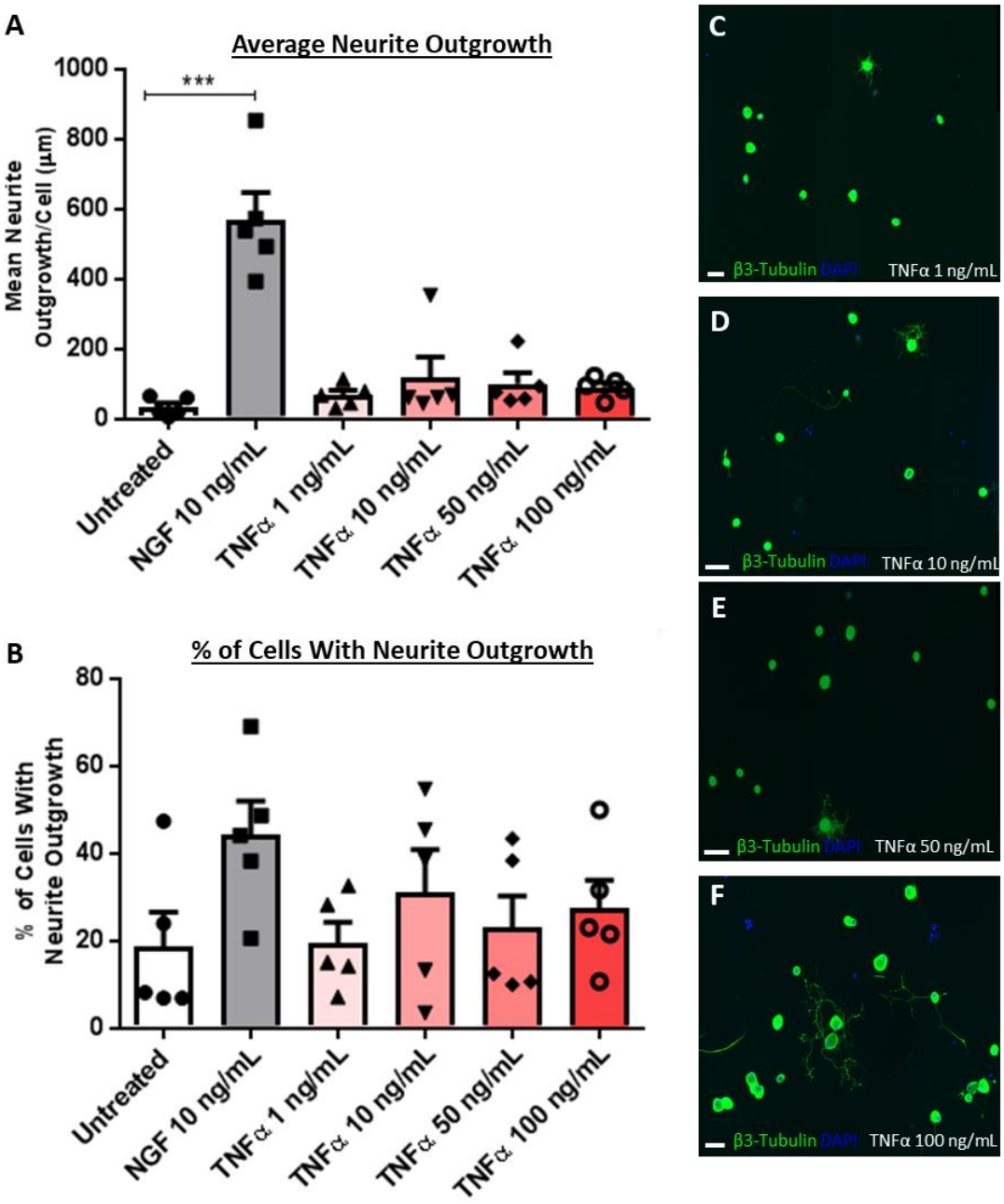

Figure 12. Neurite outgrowth of purified DRG neuronal cultures in response to a range of TNFα concentrations. A) The mean neurite outgrowth or B) the % of neurones with neurite outgrowth following 24 h treatment with TNFα (1, 10, 50 or 100 ng/mL). C-F) Representative fluorescent micrographs following immunostaining for the neuronal marker βIII-tubulin, and the nuclear stain DAPI, in purified DRG neuronal cultures which were untreated or treated with TNFα. Data displayed as Mean ± SEM, n=5 biological replicates (displayed as individual data points). Data were analysed using One-Way ANOVA followed by Tukey's multiple comparisons test. *** P<0.001. Scale bar represents 50 µM.

Abbreviations: TNFα: tumour necrosis factor alpha; DAPI: 4',6-diamidino-2-phenylindole; DRG: dorsal root ganglia.

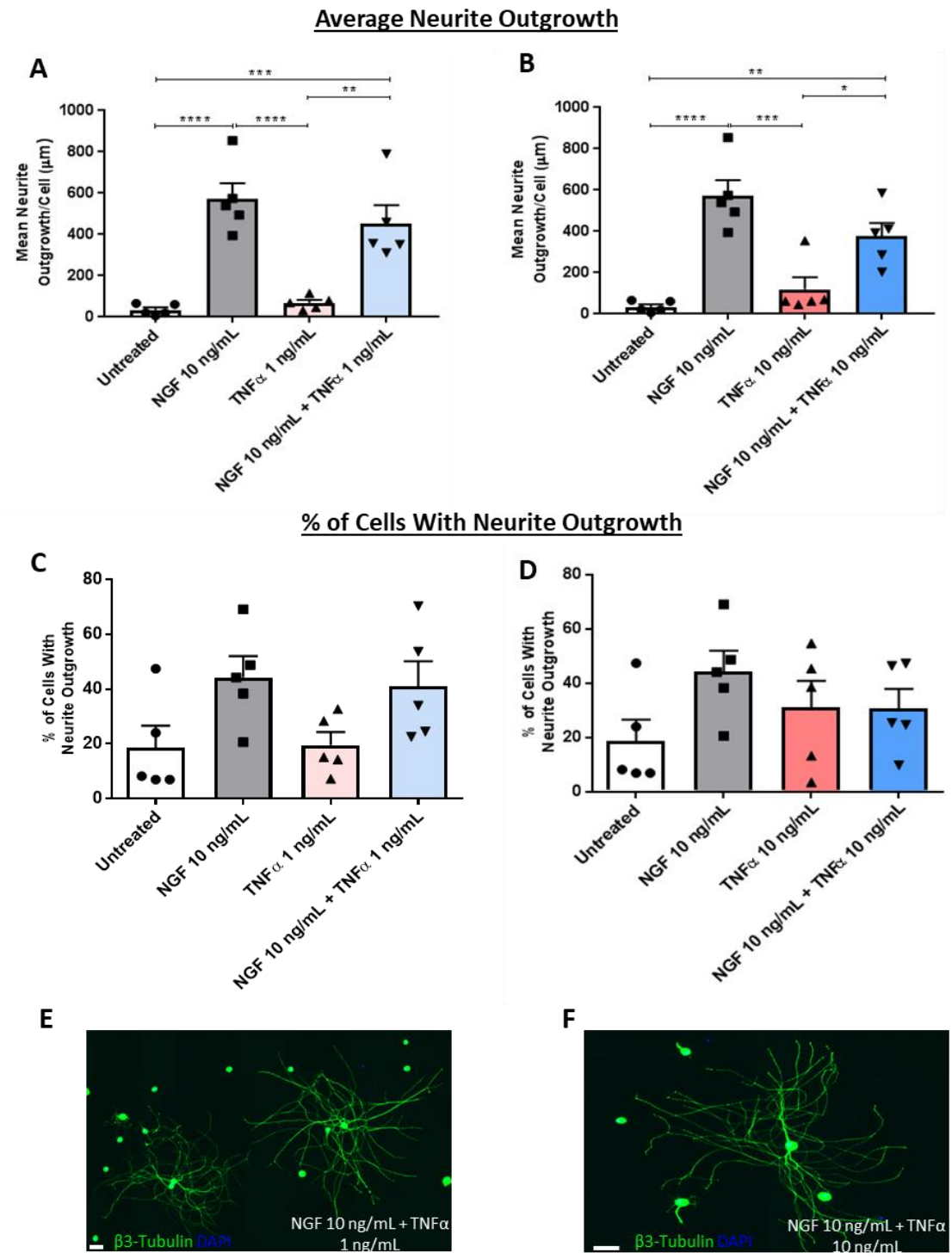

Figure 13. Neurite outgrowth of purified DRG neuronal cultures in response to the combination treatment of NGF and TNFα. A-B) The mean neurite outgrowth or C-D) the % of neurones with neurite outgrowth following 24 h treatment with NGF 10 ng/mL + TNFα 1 ng/mL or NGF 10 ng/mL + TNFα 10 ng/mL. E-F) Representative fluorescent micrographs following immunostaining for the neuronal marker βIII-tubulin, and the nuclear stain DAPI, in purified DRG neuronal cultures treated with the combination treatments. Data displayed as Mean ± SEM, n=5 biological replicates (displayed as individual data points). Data were analysed using One-Way ANOVA followed by Tukey's multiple comparisons test. * P<0.05, ** P<0.01, *** P<0.001, **** P<0.0001. Scale bar represents 50 µM.

Abbreviations: NGF: nerve growth factor; TNFα: tumour necrosis factor alpha; DAPI: 4',6-diamidino-2-phenylindole; DRG: dorsal root ganglia.

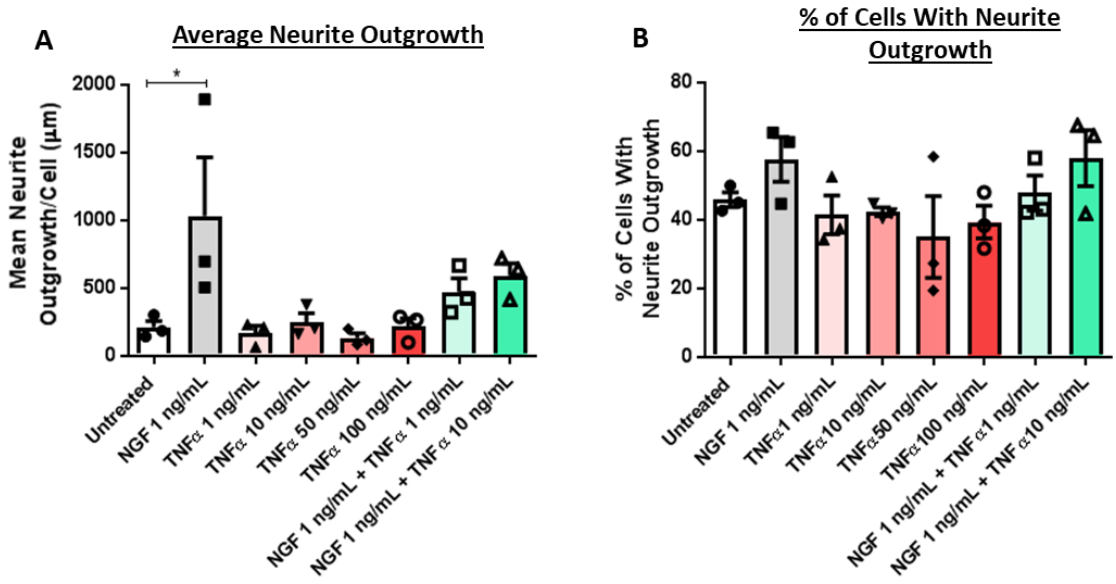

Figure 14. Neurite outgrowth of purified DRG neuronal cultures in response to low dose NGF (1 ng/mL). A) The mean neurite outgrowth or B) the % of neurones with neurite outgrowth following 24 h treatment with NGF 1 ng/mL, TNFα 1, 10, 50 or 100 ng/mL. Data displayed as Mean ± SEM, n=3 biological replicates (displayed as individual data points). Data were analysed using One-Way ANOVA followed by Tukey's multiple comparisons test. * P<0.05.

Abbreviations: NGF: nerve growth factor; TNFα: tumour necrosis factor alpha; DRG: dorsal root ganglia.

3.4.3 TNFα Showed no Regulation of Pain-Relevant Genes Within Purified DRG Neuronal Cultures

The ability of the NGF-TrkA complex to be internalised and retrogradely transported to the cell body, where it can drive extensive transcriptional changes relating to increased pain sensitivity, have been well documented (Costigan and Woolf, 2000) and discussed previously in this thesis (section 1.5.3). Therefore, the possible effect of TNFα at the transcriptional level, on both a mixed and purified culture, on a panel of pain-related genes were investigated. In support of this line of research, it has previously been shown, in a neuropathic model of pain in mice, that the upregulation of a number of gene transcripts (*Atf3, Npy and Il-6*) in the L5 DRG could be significantly suppressed following lentiviral-mediated silencing of TNFα in the DRG (Ogawa et al., 2014).

In the first instance, the basal level of receptor expression for both NGF and TNFα was determined. *Ntrk1, Ngfr* and *Tnfrsf1a* were all detectable in both purified DRG neuronal cultures and mixed DRG neuronal/glia cultures (Figure 15). Levels of *Ntrk1* and *Ngfr* were found to be similar in purified DRG neuronal cultures, with an average Ct value of 29.97 ± 0.46 (Ct) and 28.58 ± 0.25 (Ct) respectively (n=3 biological replicates). However, the Ct value of *Tnfrsf1a* was found to be slightly higher with an average Ct value of 31.71 ± 0.55 (Ct) (n=3 biological replicates) (Figure 15). In mixed DRG neuronal/glia cultures, the average Ct values were found to be lower across all three receptors, with Ct values of 27.61 ± 0.48 (Ct), 25.89 ± 0.45 (Ct) and 30.4 ± 0.56 (Ct) (n=3 biological replicates) for *Ntrk1*, *Ngfr* and *Tnfrsf1a* respectively (Figure 15).

Following confirmation of all mRNA receptor transcripts in both culture types, the transcriptional effect of a 72 h stimulation with either NGF, TNFα or a combination of the two,

on a number of pain-related genes was examined. Experiments were performed at concentrations of both 10 ng/mL and 100 ng/mL.

In purified DRG neuronal cultures, the effect of NGF, TNFα and a combination of the two on gene expression was tested using a Two-Way ANOVA; a significant treatment effect was observed ($F(3,108)=17.79$, $P<0.0001$). It was found that NGF (10 ng/mL) produced a significant increase in *Trpv1* expression (2.49 ± 0.91 ΔΔCt, n=4 biological replicates) compared to the baseline untreated group and a trend for an increase in the expression of all other genes (Figure 16A). No significant changes in the expression of *Ntrk1, Ngfr, Scn10a, Scn11a, Trpv1, Calca, Ptgs2, F2rl1* or *Tac1* were detected when cultures were stimulated with TNFα alone or with TNFα in combination with NGF (Figure 16A).

Interestingly, in mixed DRG neuronal/glia cultures, treated in the exact same manner, the NGF effect was much less prominent, with no genes being significantly upregulated (Figure 16B). In mixed DRG neuronal/glia cultures, the effect of NGF, TNFα and a combination of the two on gene expression was tested using a Two-Way ANOVA; a significant treatment effect was observed ($F(3,108)=12.6$, $P<0.0001$). In these mixed DRG neuronal/glia cultures, the effect of TNFα was still minimal in the majority of genes examined but a prominent and significant increase was detected in both the expression of *Ptgs2* (prostaglandin-endoperoxidase synthase 2) *and F2rl1* (protease activated receptor 2) (an increase of 1.09 ± 0.39 ΔΔCt and 1.10 ± 0.58 ΔΔCt respectively, n=4 biological replicates) (Figure 16B). These genes also changed significantly in the combination group (Figure 15B) with increases of 1.06 ± 0.39 ΔΔCt and 1.70 ± 0.34 ΔΔCt (n=4 biological replicates) observed from the baseline untreated group regarding *Ptgs2* and *F2rl1* expression (Figure 16B).

On increasing the concentration of NGF to 100 ng/mL, a much more prominent effect, in both purified DRG neuronal cultures and mixed DRG neuronal/glia cultures on the expression of the pain-relevant genes (*Ntrk1, Ngfr, Scn10a, Scn11a, Trpv1, Calca, Ptgs2, F2rl1, Tac1, Tnfrsf1a, Scn9a*) was detected (Figure 17A and B). In the purified DRG neuronal cultures, the effect of NGF, TNFα and a combination of the two on gene expression was tested using a Two-Way ANOVA; a significant treatment effect was observed ($F(3,77)=23.68$, $P<0.0001$). NGF (100 ng/mL) produced significant increases in the expression of *Ntrk1, Ngfr, Scn10a, Scn11a, Trpv1* and *Calca* (Figure 17A) (increases of 1.74 ± 0.79 ΔΔCt, 2.05 ± 0.43 ΔΔCt, 1.93 ± 0.84 ΔΔCt, 1.65 ± 0.88 ΔΔCt, 2.44 ± 0.01 ΔΔCt and 1.65 ± 0.94 ΔΔCt respectively, n=3 biological replicates) from the baseline untreated group. In the mixed DRG neuronal/glia cultures, a significant treatment effect was also observed ($F(3,88)=17.37$, $P<0.0001$). NGF produced significant increases in the expression of similar genes (*Ngfr, Scn10a, Scn11a, Trpv1, Calca* as well as *Tac1)* (increases of 1.15 ± 0.32 ΔΔCt, 1.04 ± 0.48 ΔΔCt, 1.03 ± 0.42 ΔΔCt, 1.18 ± 0.19 ΔΔCt, 1.04 ± 0.56 ΔΔCt and 1.59 ± 0.32 ΔΔCt respectively, n=3 biological replicates). Interestingly, NGF-mediated enhancement of *Tac1* gene expression (encodes for substance P) was significantly dampened by the addition of TNFα (Figure 17B). The only detectable TNFα-driven change detected in this series of experiments were an increase in the mRNA expression levels of *Ptgs2* and *F2rl1* (Figure 16B and 17B). The TNFα-driven increases in *Ptgs2* and *F2rl1* (increases of 1.67 ± 0.23 ΔΔCt and 2.45 ± 0.53 ΔΔCt respectively, n=3 biological replicates), were only present in mixed DRG neuronal/glia cultures and not purified DRG neuronal cultures (Figure 16 and 17). The magnitude of the TNFα induced changes in mRNA for *Ptgs2* and *F2rl1* was unaffected by the co-administration of NGF treatment (Figure 17B).

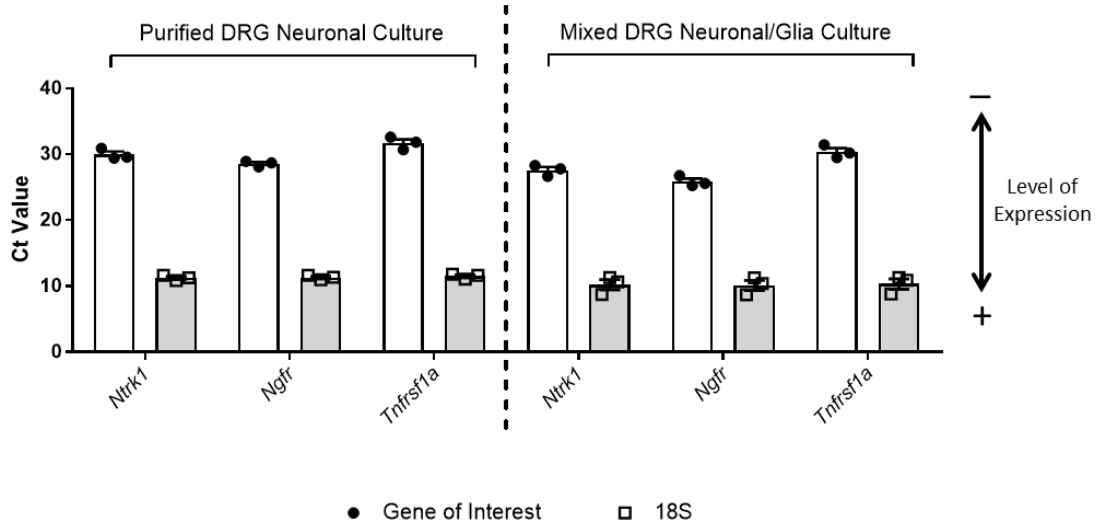

Figure 15. Expression levels of NGF and TNFα receptor mRNA in purified DRG neuronal cultures or mixed DRG neuronal/glia cultures. The graphs shown display the basal Ct values of *Ntrk1*, *Ngfr* and *Tnfrsf1α* as well as the housekeeping gene 18S. Data displayed as Mean ± SEM, n=3 biological replicates (displayed as individual data points).

Abbreviations: NGF: nerve growth factor; TNFα: tumour necrosis factor alpha; *Ntrk1*: neurotrophic receptor tyrosine kinase; *Ngfr:* nerve growth factor receptor; *Tnfrsf1α*: tumour necrosis factor receptor superfamily 1a.

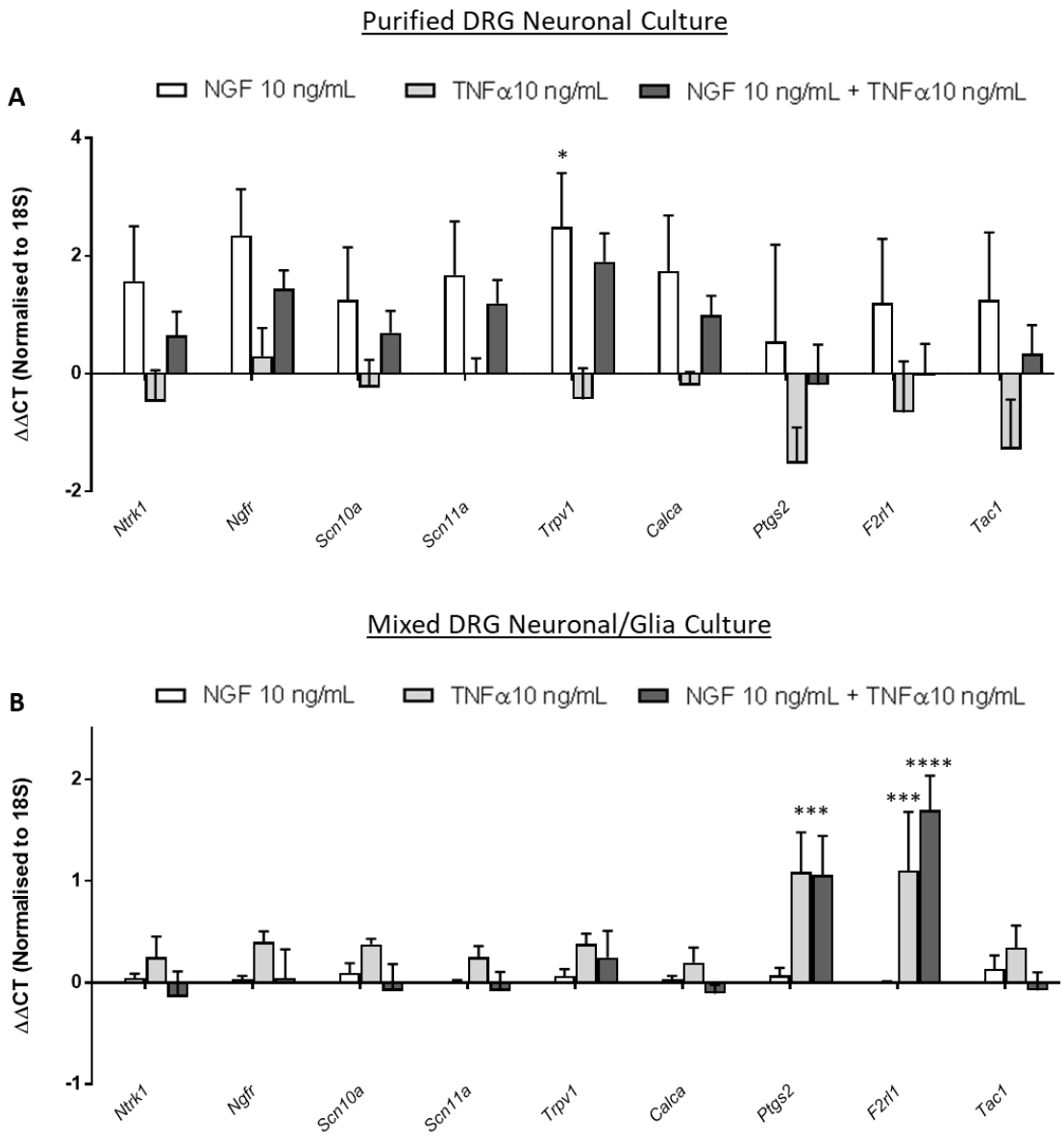

Figure 16. Comparison of transcriptional changes at the mRNA level in pain-relevant genes in either purified DRG neuronal cultures or mixed DRG neuronal/glia cultures (10 ng/mL). ΔΔCt values in A) purified DRG neuronal cultures or B) mixed DRG neuronal/glia cultures following treatment with NGF 10 ng/mL, TNFα 10 ng/mL or a combination of the two for 72 h. Data displayed as Mean ± SEM, n=4 biological replicates. Data were analysed using Two-Way ANOVA followed by Tukey's multiple comparisons test. * P<0.05, *** P<0.001, **** P<0.0001, significance displayed represents changes from the normalised baseline 'untreated' group.

Abbreviations: NGF: nerve growth factor; TNFα: tumour necrosis factor alpha; *Ntrk1*: neurotrophic receptor tyrosine kinase; *Ngfr:* nerve growth factor receptor; Scn10a: sodium voltage-gated channel alpha subunit 10; Scn11a; sodium voltage-gated channel alpha subunit 11; Trpv1: transient receptor potential vanilloid 1; Calca: calcitonin related polypeptide alpha; Ptgs2: prostaglandin-endoperoxide synthase; F2rl1: proteinase-activated receptor 2; Tac1: tachykinin precursor 1.

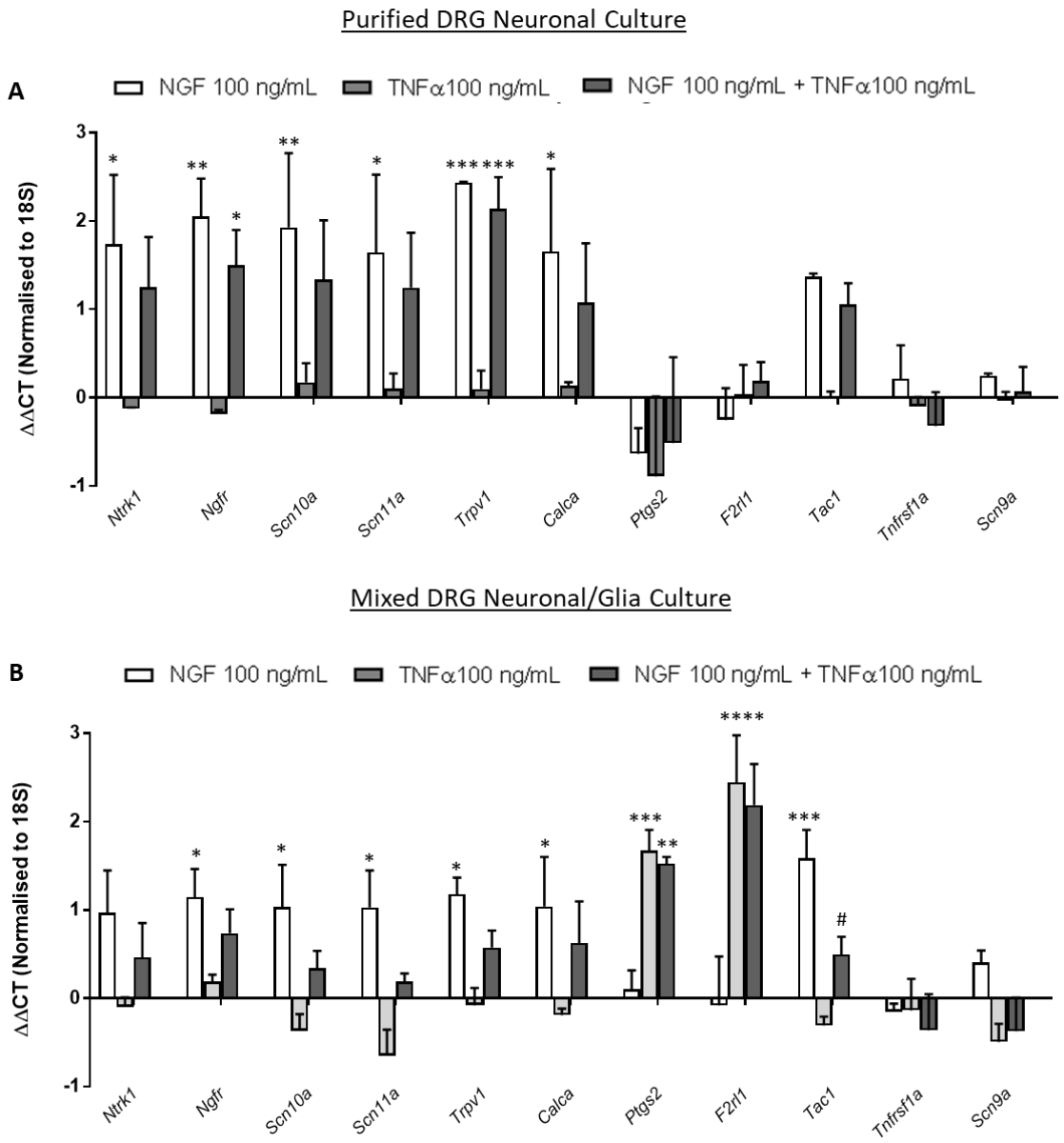

Figure 17. Comparison of transcriptional changes at the mRNA level in pain-relevant genes in either purified DRG neuronal cultures or mixed DRG neuronal/glia cultures (100 ng/mL). ΔΔCt values in A) purified DRG neuronal cultures or B) mixed DRG neuronal/glia cultures following treatment with NGF 100 ng/mL, TNFα 100 ng/mL or a combination of the two for 72 h. Data displayed as Mean ± SEM, n=3 biological replicates. Data were analysed using Two-Way ANOVA followed by Tukey's multiple comparisons test. * P<0.05, ** P<0.01, *** P<0.001, **** P<0.0001, significance displayed represents changes from the normalised baseline 'untreated' group. # P< 0.01, significance displayed represents changes from the NGF alone group compared to the combination group.

Abbreviations: NGF: nerve growth factor; TNFα: tumour necrosis factor alpha; *Ntrk1*: neurotrophic receptor tyrosine kinase; *Ngfr:* nerve growth factor receptor; Scn10a: sodium voltage-gated channel alpha subunit 10; Scn11a; sodium voltage-gated channel alpha subunit 11; Trpv1: transient receptor potential vanilloid 1; Calca: calcitonin related polypeptide alpha; Ptgs2: prostaglandin-endoperoxide synthase; F2rl1: proteinase-activated receptor 2; Tac1: tachykinin precursor 1; *Tnfrsf1a*: tumour necrosis factor receptor superfamily 1a; Scn9a: sodium voltage-gated channel alpha subunit 9.

3.4.4 K^+ Evoked CGRP Release is Sensitised by NGF, but not TNFα Treatment in Mixed DRG Neuronal/Glia Cultures

The release of CGRP, following K^+ stimulation, was used as a pain-relevant read-out to assess whether TNFα could modulate sensory neuronal activity. NGF increased K^+ induced CGRP release in a concentration-dependent manner (Figure 18A), with the top concentration of NGF (100 ng/mL) inducing CGRP release to a level of 3233 ± 349.7 pg/mL (n=at least 4 biological replicates) compared to the untreated treatment group (720.1 ± 72.81 pg/mL, n=at least 4 biological replicates) (Figure 18A). To avoid saturation, the effect of a 10 ng/mL dose of NGF was compared to the same dose of TNFα. Despite the lower dose, NGF (10 ng/mL) induced a significant increase in K^+ induced CGRP release (an increase ~176 %) when compared to the untreated control cultures (720.1 ± 72.81 pg/mL to 1988 ± 218.3 pg/mL, One-Way ANOVA; ($F(2,39)=37.35$, $P<0.0001$) n= at least 4 biological replicates) (Figure 18B). However, TNFα treatment showed no difference compared to the untreated control cultures (720.1 ± 72.81 pg/mL and 732.7 ± 65.63 pg/mL respectively, n=at least 4 biological replicates) (Figure 18B).

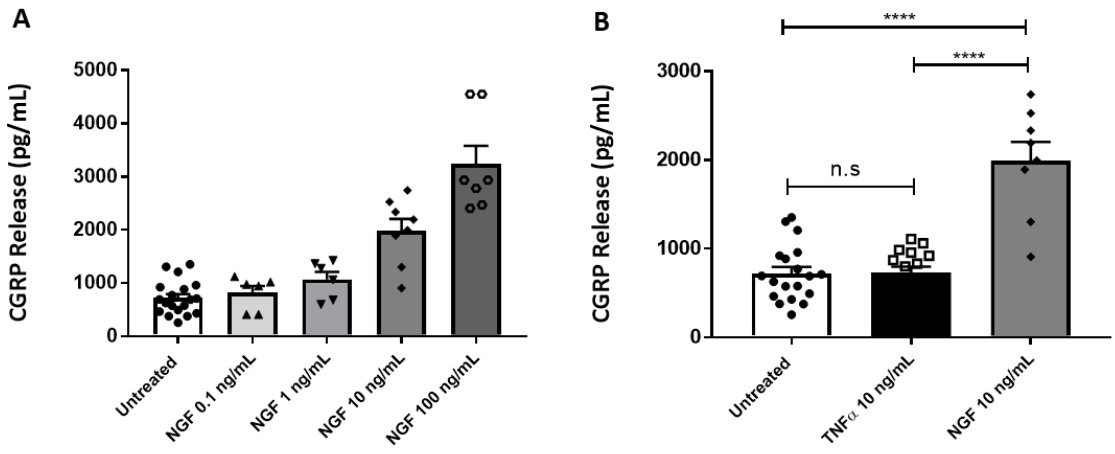

Figure 18. CGRP release following K^+ stimulation in a mixed DRG neuronal/glia culture. A) 25 mM K^+-evoked CGRP release in mixed DRG neuronal/glia cultures pre-treated (48 h) with varying NGF concentrations; 0.1 ng/mL (black triangle), 1 ng/mL (black upside-down triangles), 10 ng/mL (black diamonds) and 100 ng/mL (hollow hexagon). B) 25 mM K^+-evoked CGRP release in mixed DRG neuronal/cultures pre-treated with TNFα (10 ng/mL, 48 h, hollow squares) or NGF (10 ng/mL, 48 h, black diamonds). Data displayed as Mean ± SEM, data points represent data collected from at least 4 biological replicates. Data were analysed using One-Way ANOVA followed by Tukey's multiple comparisons test. **** P<0.0001.

Abbreviations: CGRP: calcitonin gene-related peptide; DRG: dorsal root ganglia; NGF: nerve growth factor; TNFα: tumour necrosis factor alpha.

3.4.5 Direct Application of TNFα Does Not Sensitise Calcium Responses in Purified DRG Neuronal Cultures

To further examine the possible action of TNFα using a functional read-out, calcium imaging was utilised to assess any modulation of neuronal activity. Both the ability of TNFα to directly activate neurones, or to sensitise them, was assessed.

In the first instance, the possible direct effect of TNFα was examined via the perfusion of a TNFα (10 ng/mL) solution directly over purified DRG neuronal cultures. Purified neurones showed no detectable response to TNFα stimulation (Figure 19A). However, strong and consistent responses to a positive control (KCl 25 mM) were seen, with 93.81 ± 2.3 % (n=848 neurones across 3 mice) of neurones responding (Figure 19B), suggesting that the lack of response seen in the TNFα condition is not due to the death/poor health of the neurones.

Next, the level of sensitisation of purified neurones cultured in TNFα (10 ng/mL in BS medium) was examined via the application of capsaicin.

To determine an appropriate dose of capsaicin to use in subsequent experiments, a pilot experiment was performed. Four concentrations of capsaicin were tested; 10 nM, 50 nM, 100 nM and 500 nM. Three read-outs were examined: the % of cells responding to capsaicin, the difference between the maximum capsaicin response and the baseline, to establish the magnitude of the response, and the % of cells responding to KCl (25 mM). It was found that very few neurones responded directly to 10 nM capsaicin (0.67 ± 0.07 % responding neurones, n=607 neurones across 2 mice), whilst more responded to 50 nM capsaicin (12.66 ± 1.69 % responding neurones, n=406 neurones across 2 mice). However, once the capsaicin concentration reached 100 nM, resulting in 18.7 ± 1.71 % recruitment of neurones (n=446 across 2 mice), a further increase to 500 nM did not increase the percentage of responding

neurones (18.13 ± 0.62 % responding neurones, n=361 neurones across 2 mice) (Figure 20A). Different concentrations of capsaicin did not significantly alter the magnitude of the responses to capsaicin (as measured by the difference between the maximum capsaicin response and the baseline) or the % of cells responding to KCl (Figure 20B and C). Based on the above data, a dose of 50 nM capsaicin was deemed a suitable concentration to deliver a robust, but not saturated, response during the imaging sessions. This would allow for the detection of changes in either the number or magnitude of responses to capsaicin in a putative sensitised state.

Following 24 h incubation of purified DRG neuronal cultures with either untreated or TNFα containing media, the response of the neurones to capsaicin (50 nM) was determined. It was found that there were no significant differences between the two groups in the % of cells responding to capsaicin. In the untreated group, 14.61 ± 1.81 % (n=1343 neurones across 3 mice) neurones responded to capsaicin compared to 14.26 ± 2.7 % (n=1177 neurones across 3 mice) neurones responding in the TNFα 10 ng/mL treatment group (Figure 21A-C). Likewise, there was no difference between the groups in the magnitude of the response to capsaicin (50 nM) (0.5 ± 0.09 ΔF/F in the untreated group (n=1343 neurones across 3 mice) compared to 0.49 ± 0.06 ΔF/F in the TNFα (10 ng/mL) treatment group (n=1177 neurones across 3 mice)) (Figure 21E) or KCl (25 mM) (0.54 ± 0.06 ΔF/F in the untreated group (n=1343 neurones across 3 mice) compared to 0.54 ± 0.06 ΔF/F in the TNFα (10 ng/mL) treatment group (n=1177 neurones across 3 mice)) (Figure 21F). The majority of neurones were responsive to KCl, 95.42 ± 1.79 % in the untreated group (n=1343 neurones across 3 mice) and 94.61 ± 1.44 % in the TNFα 10 ng/mL treatment group (n=1177 neurones across 3 mice) (Figure 21A, B and D), suggesting that the mere addition of TNFα is not significantly detrimental to the neurones.

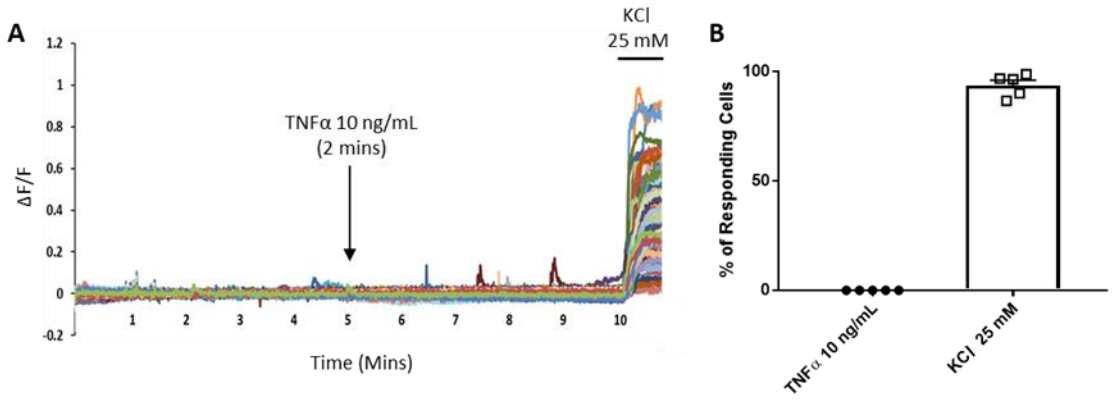

Figure 19. Calcium transients in purified DRG neuronal cultures following direct application of either TNFα (10 ng/mL) or KCl (25 mM). A) Representative trace from a coverslip displaying ΔF/F versus time. TNFα (10 ng/mL) was applied for 2 min followed by a wash-out period and a final KCl (25 mM) stimulus to ensure cell viability. B) Quantification of % of responding cells to both TNFα (10 ng/mL) or KCl (25 mM). Data displayed as Mean ± SEM, n=848 neurones across 3 mice. Data points on graphs represent individual cover slips.

Abbreviations: DRG: dorsal root ganglia; TNFα: tumour necrosis factor alpha; KCl: potassium chloride.

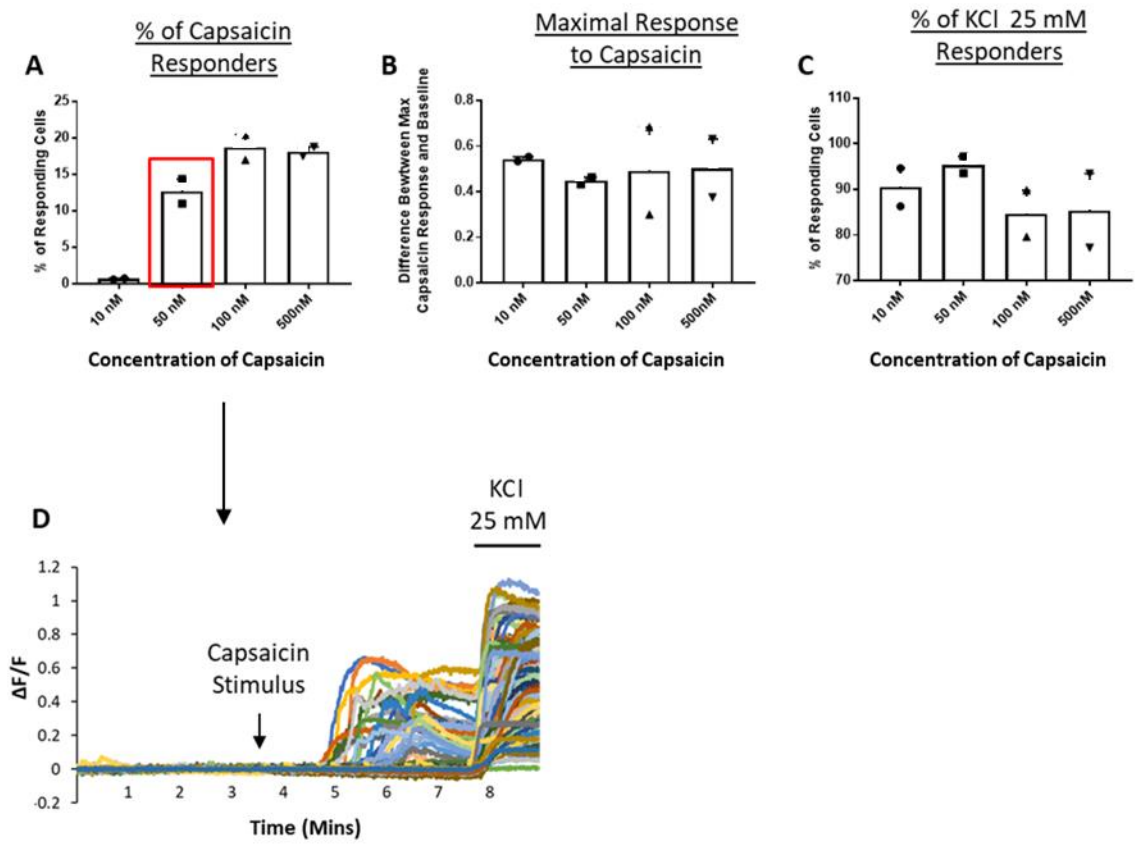

Figure 20. Calcium transients in purified DRG neuronal cultures following direct application of a range of capsaicin concentrations (10 nM, 50 nM, 100 nM or 500 nM) or KCl (25 mM). A) % of cells responding to each concentration of capsaicin. B) The maximum response after exposure to different capsaicin concentrations (calculated by taking the difference between the maximum capsaicin response recorded and the average intensity of ten frames pre-capsaicin stimulus.) C) % of cells responding to KCl (25 mM). D) Representative neuronal calcium displaying ΔF/F versus time. Capsaicin stimulus represents 50 nM capsaicin. Data displayed as Mean ± SEM, n=1820 neurones across cultures from 2 independent mice (1 coverslip/condition for each mouse). Capsaicin 10 nM (607 neurones), 50 nM (406 neurones), 100 nM (446 neurones), 500 nM (361 neurones).

Abbreviations: DRG: dorsal root ganglia; KCl: potassium chloride.

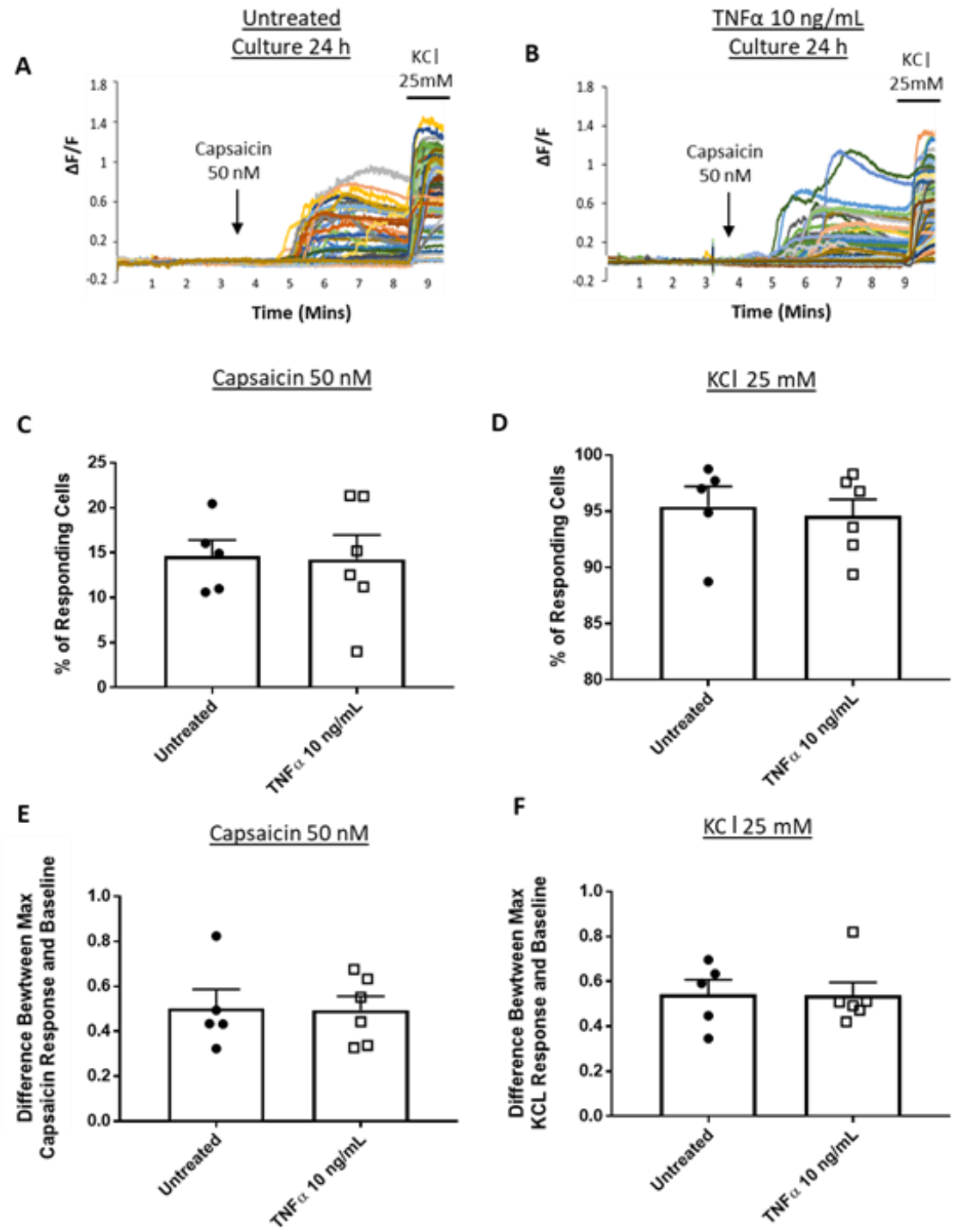

Figure 21. Calcium transients in purified DRG neuronal cultures following 24 h in untreated medium or medium treated with TNFα (10 ng/mL). A-B) Representative neuronal calcium transients displaying ΔF/F versus time. Capsaicin (50 nM) was applied for 3 min followed by a wash-out period and a final KCl (25 mM) stimulus to ensure cell viability. C-D) Quantification of % of responding cells to both capsaicin (50 nM) or KCl (25 mM). E-F) The maximum response seen after capsaicin (50 nM) or KCl (25 mM) application (calculated by taking the difference between the maximum capsaicin/KCl response recorded and the average intensity of ten frames pre-capsaicin/KCl stimulus.) Data displayed as Mean ± SEM, n=2520 neurones across cultures from 3 independent mice. Untreated (1343 neurones), TNFα 10 ng/mL (1177 neurones). Data were analysed using unpaired two-tailed t-test. Data points on graphs represent individual cover slips.

Abbreviations: DRG: dorsal root ganglia; TNFα: tumour necrosis factor alpha; KCl: potassium chloride.

3.4.6 TNFα does not Stimulate the Activation of the p-38 Pathway in Purified DRG Neuronal Cultures

It is well documented that both NGF and TNFα can activate MAP kinase signalling pathways in different cell types (Sabio and Davis, 2014, Reichardt, 2006a). Therefore, the induction of phospho-p38 was assessed, initially in the PC12 neuronal cell line and then subsequently in purified DRG neuronal cultures, in response to NGF, TNFα or a combination of the two. In contrast to the previous experiments outlined in this chapter, the time of stimulations (5 min and 20 min) was substantially shorter due to the more acute effects of MAP kinases (Pearson et al., 2001). In the following experiments anisomycin was used as a positive control as it is a known activator of stress-activated protein kinases, including phospho-p38 (Torocsik and Szeberenyi, 2000).

In the PC12 cell line, both NGF (100 ng/mL) and TNFα (25 ng/mL) could induce p-38 activation by 1.39 ± 0.14-fold over basal (n=3 biological replicates) and 1.32 ± 0.04-fold over basal (n=3 biological replicates) respectively. (Figure 22A). When the cell line was stimulated with a combination of the two, an additive response of the two individual inflammatory mediators was observed at 20 min (1.92 ± 0.19-fold over basal, n=3 biological replicates), a response similar to that of the positive control, anisomycin (2.14 ± 0.24-fold over basal, n=3 biological replicates) (Figure 22A). Although the PC12 cell line has been extensively used in neuronal differentiation studies (Greene, 1978b, Satoh et al., 1988, Greene, 1978a, Morooka and Nishida, 1998), it is a *neuronal-like* cell type and therefore has a number of limitations (as summarised in the discussion). Therefore, the same experiment was repeated in the primary cell purified DRG neuronal cultures.

In contrast to the PC12 cell line, the purified DRG neuronal cultures showed no differences from the untreated group when examining phospho-p38 induction in response to NGF, TNFα or a combination of the two (10 ng/mL). This was also true when examining the response to the positive control anisomycin, where only a difference in fold-over basal from 1 (untreated group) to 1.1 was observed (Figure 22B).

Levels of phospho-p38 in both the cell line and the primary cells were determined using HTRF technology. Due to the lack of a detectable response in the purified DRG neuronal cultures (when assayed using the phospho-p38 HTRF assay, Figure 22B) an alternative method of measuring phospho-p38 was explored, namely immunocytochemical detection. Therefore, immunocytochemistry techniques were employed. Figure 23A and B display the immunostaining for phospho-p38 following stimulation with NGF, TNFα or a combination of the two (10 ng/mL) for either 5 min or 20 min. These representative images show no clear differences in any of the groups, corroborating the data collected from the HTRF assay.

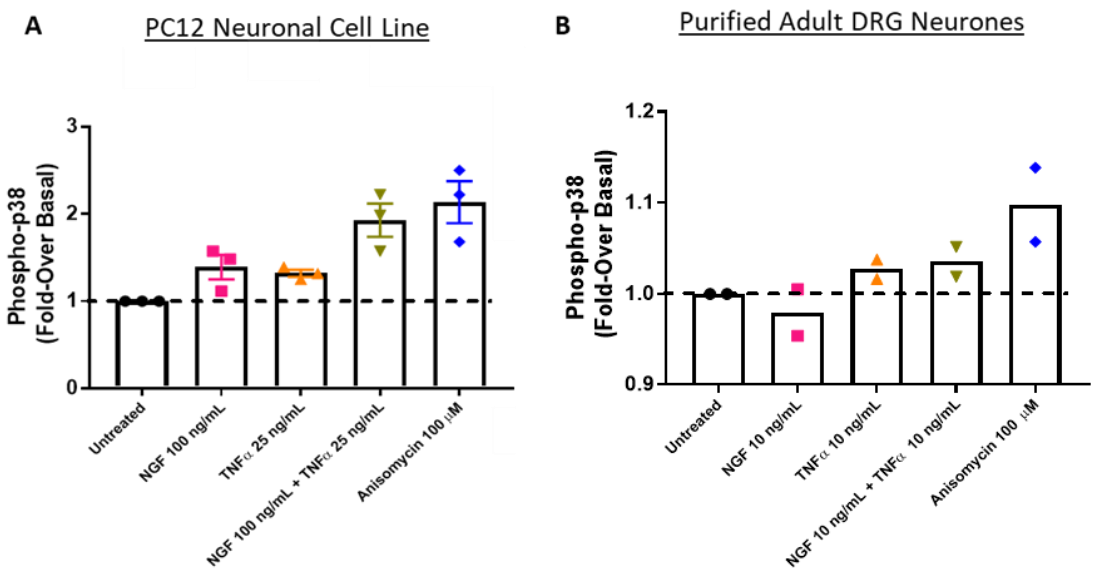

Figure 22. Induction of phospho-p38 in the PC12 neuronal cell line and purified DRG neuronal cultures. A) Levels of phospho-p38 induction in the PC12 neuronal cell line following treatment with NGF (100 ng/mL, 20 min), TNFα (25 ng/mL, 20 min), a combination of the two (20 min) or with the positive control anisomycin (100 µM, 20 min) as assessed by HTRF assay. B) Levels of phospho-p38 induction in purified DRG neuronal cultures following treatment with NGF (10 ng/mL, 20 min), TNFα (10 ng/mL, 20 min), a combination of the two (20 min) or with the positive control anisomycin (100 µM, 20 min) as assessed by HTRF assay. Data displayed as Mean ± SEM, n=3 biological replicates (A) and n=2 biological replicates (B) (displayed as individual data points).

Abbreviations: PC12: pheochromocytoma; NGF: nerve growth factor; TNFα: tumour necrosis factor alpha; HTRF: homogenous time-resolved fluorescence.

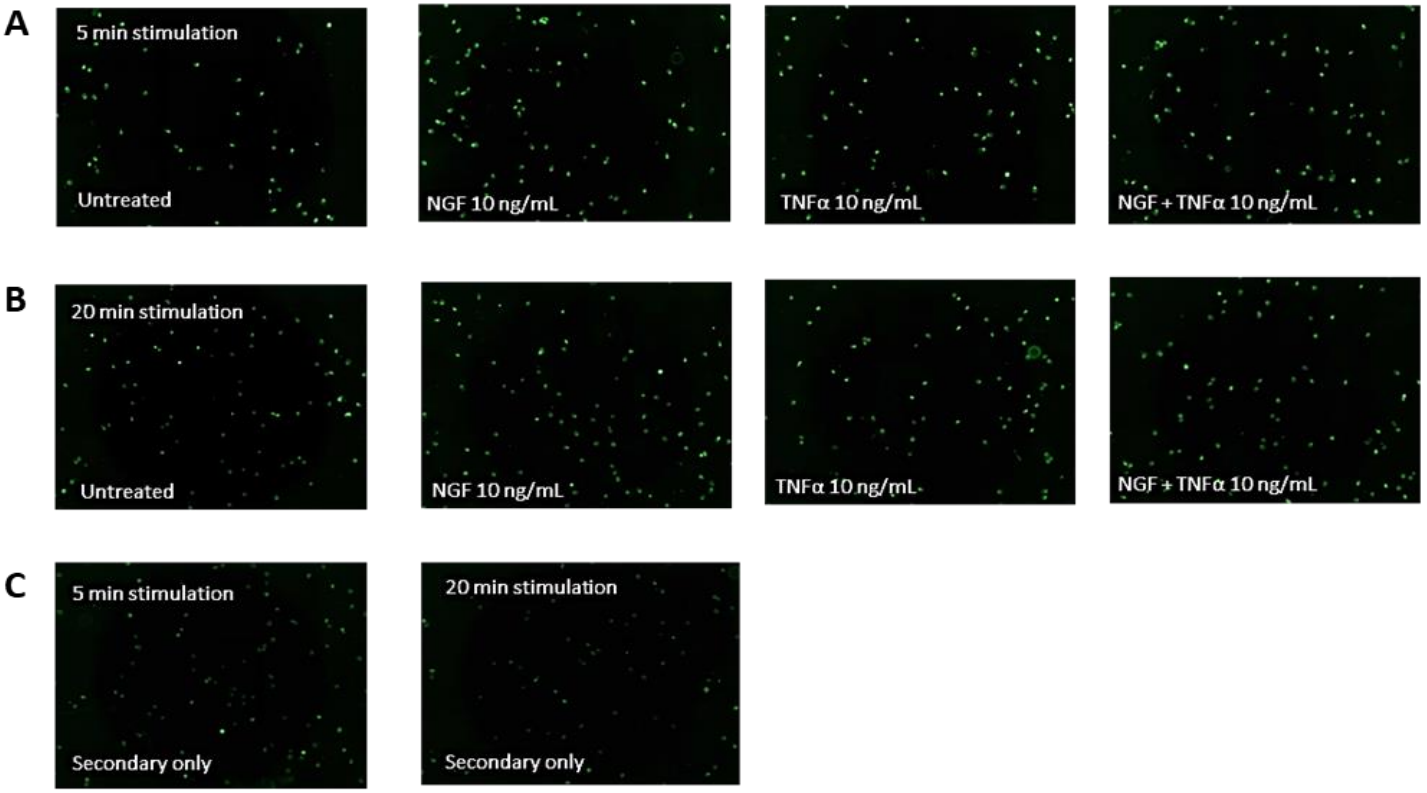

Figure 23. Visual representation of phospho-p38 induction in the PC12 neuronal cell line and purified DRG neuronal cultures. A-B) Representative fluorescent micrographs following immunostaining for phospho-p38 following treatments at (A) 5 min (B) 20 min with NGF (10ng/mL) or TNFα (10 ng/mL) and (C) the secondary stain only condition.

Abbreviations: PC12: pheochromocytoma; NGF: nerve growth factor; TNFα: tumour necrosis factor alpha; HTRF: homogenous time-resolved fluorescence.

3.5 Discussion

There is growing evidence within the literature to suggest that TNFα may contribute to both the generation and maintenance of pain states via multiple mechanisms, such as direct activation of primary nociceptors (as reviewed by (Pinho-Ribeiro et al., 2017a)) or via an indirect orchestration of inflammatory responses (as reviewed by (Kress, 2010)). Within this chapter we utilised a MACS sorting technique, enabling the isolation of purified DRG neurones from adult mice. This technique circumvents the limitations of previous studies (Sorkin et al., 1997, Richter et al., 2010, Bowen et al., 2006b, Hensellek et al., 2007a), conclusions from which may have been inadvertently affected by the presence of non-neuronal cell types.

One of the assays used to assess any changes in neuronal function in response to TNFα was the degree to which it could stimulate neurite outgrowth. Neurite outgrowth *in vitro* is a valuable tool commonly utilised as a proxy for the development and health of neurones in response to a range of compounds (Radio and Mundy, 2008). Therefore, any significant effects seen in this assay would be a good indicator of neuronal responsiveness to TNFα. Furthermore, previous work has indicated that TNFα can drive neurite outgrowth, albeit in hypothermic conditions (Schmitt et al., 2010).

Although a trend was apparent for an increase in neurite outgrowth at the lower concentration of NGF (1 ng/mL), this change was not significant. Instead, NGF (10 ng/mL) drove significant neurite outgrowth in purified DRG neuronal cultures when compared to the untreated cultures. This finding is consistent with studies within the literature (Liu et al., 2007). Indeed, it has been well established that NGF can stimulate neurite outgrowth in both sensory and sympathetic neurons (Levi-Montalcini and Angeletti, 1968), a property that is considered to be crucial for its role in stimulating neuronal connections in early development.

From work conducted in the PC12 cell line, it is thought that NGF induces neurite outgrowth via the assembly of microtubule proteins such as tau and MAP1 (Drubin et al., 1985). Additionally, research conducted in cultured adult DRG neurones showed that Src and FAK are key early signalling intermediates required for NGF-driven neurite outgrowth (Tucker et al., 2008).

When examining the effect of TNFα in this assay it was found that over a range of concentrations there was no significant increase or decrease in neurite outgrowth. Although no significant differences were found in our hands, one previous study showed that TNFα can inhibit neurite outgrowth and branching via a Rho-dependent mechanism (Neumann et al., 2002). However, this study was conducted in a mixed cell population and therefore the changes observed could be driven via a non-neuronal mechanism. In agreement with the above study, it has been demonstrated that rats which have undergone a peripheral nerve injury and subsequent treatment with an anti-TNFα drug, have an enhanced rate of axonal regeneration (Kato et al., 2010), suggesting a role for TNFα in the inhibition of neurite outgrowth. Again, the role of neuronal vs non-neuronal cells was not considered.

When examining the effect of the combination of NGF and TNFα on neurite outgrowth, only a significant increase from the untreated group was found. However, contrary to our findings, there is evidence in the literature to suggest that TNFα may be able to inhibit the effects of NGF. A study by Wheeler and colleagues (Wheeler et al., 2014) showed that TrkA-positive peptidergic nociceptors require TNFα-TNFR1 forward signalling to suppress NGF-induced outgrowth during development.

In addition to looking at anatomical markers of neuronal activation, transcriptional changes in a range of pain-relevant genes were examined. Although the gene expression studies

conducted within this chapter suggest that all three receptor types are present (*Ntrk1, Ngfr and Tnfrsf1a)* in both purified and mixed cultures, it is important to note that this does not necessarily translate into the expression of the receptor protein, or indeed the cell surface expression of the receptor protein.

The genes studied were selected due to evidence suggesting a strong link to either the generation or maintenance of pain states (Levinson et al., 2012, Iyengar et al., 2017, Levine and Alessandri-Haber, 2007, Tillu et al., 2015, Lee et al., 2004, Zhang and An, 2007). The effect of the treatment groups (NGF, TNFα, or a combination of the two) was examined in both purified DRG neuronal and mixed DRG neuronal/glia cultures. By studying expression changes in both a purified and a mixed culture, it was possible to evaluate *direct* vs *indirect* effects of these cytokines on sensory neurones.

Interestingly, one of the main things that became apparent from this dataset was that purified DRG neuronal cultures seemed to have an enhanced response to NGF, at both concentrations of 10 ng/mL and 100 ng/mL, in comparison to the mixed DRG neuronal/glia preparations. The effect was particularly noticeable at the lower concentration of NGF (10 ng/mL). One explanation for this observation could be non-neuronal cells provide a source of NGF, therefore increasing the basal level of NGF signalling in these cultures (Hanani, 2005). Indeed, it has been shown that enteric glia release a number of neurotrophic factors, including NGF, which enhances neurite outgrowth in DRG neurones (Hansebout et al., 2012). This would mean that any exogenously applied NGF will have a smaller window to exert an effect.

In the majority of pain-relevant genes examined it was found that NGF induced an increase in expression whereas TNFα exerted no effect. The combination treatment in most cases

seemed to produce a response similar to that of NGF alone, with the exception of a significant reduction in *Tac1* expression compared to the NGF alone treatment group.

Although TNFα was found not to influence *Trpv1* expression in either purified DRG neuronal or mixed DRG neuronal/glia cultures in our hands, there are conflicting reports within the literature regarding this finding. A recent study suggests that TNFα, induced by the application of vincristine, upregulates the expression of TRPV1 in DRG nociceptive neurones and consequently contributes to both mechanical and thermal hyperalgesia in this pain model (Wang et al., 2018). Furthermore, another study showed that cultured DRG neurones treated with TNFα for a prolonged period of time (24-48 h) significantly enhanced the proportion of neurones expressing TRPV1 via the TNFR1 receptor (Hensellek et al., 2007b). This latter finding could explain enhanced heat-evoked release of CGRP from sensory nerve terminals in rat skin following TNFα application (Opree and Kress, 2000).

Within this chapter, and a subsequent chapter, the levels of CGRP release have been used as a pain-relevant read-out. CGRP is a 37 amino acid neuropeptide which has diverse biological functions in both the peripheral and central nervous systems (as reviewed by (Russell et al., 2014)). The role of CGRP in migraine pain has been well established, with possible mechanisms including dilation of cerebral and dural blood vessels, release of inflammatory mediators from mast cells and transmission of nociceptive information from intracranial blood vessels to the nervous system (Durham, 2006). A recent clinical trial has shown the potential of CGRP as a therapeutic target. Here, an anti-CGRP migraine drug resulted in a significantly greater percentage of patients achieving pain relief together with a reduction in unpleasant migraine-associated symptoms (PharmaTimes online, 2018). Interestingly, TNFα has been implicated in the above pathophysiology, with studies showing that in rat trigeminal

ganglion neurones, TNFα stimulation can result in an increase in CGRP expression and secretion (Bowen et al., 2006a).

CGRP is not only implicated in migraine but rather a wide range of painful conditions. Indeed, CGRP is widely distributed throughout nociceptive pathways and can contribute significantly to both inflammatory and neuropathic pain conditions (Iyengar et al., 2017). For example, one study has demonstrated that CGRP is upregulated in arthritic joints, leading to peripheral sensitisation and activation of cell types that are crucial in the inflammation process (Walsh et al., 2015b). Likewise, it has been shown that CGRP can promote MAP kinase mediated glial activation, resulting in CCL5 production and an increase in behavioural hypersensitivity following a spinal nerve transection (Malon and Cao, 2014). This suggests that CGRP release is an important factor in multiple pain conditions and may provide a useful proxy for the effects of NGF and TNFα in pain pathways. However, when we examined the effect of TNFα on CGRP release (following depolarising of the cells), we found no change in CGRP levels compared to the control group.

Similarly, there are numerous reports in the literature of TNFα mediated modulation of sodium channels. Jin and Gereau (2006) suggest that TNFα application, in mouse DRG neurones (non-purified), results in a p38-dependent modulation of TTX-resistant Na^+ channels, leading to acute peripheral sensitisation. However, in the data presented above, we found no modulation in the expression of *Scn9a*, *Scn10a* or *Scn11a,* the latter two of which have been shown to be TTX-resistant (Lee and Ruben, 2008).

The major difference between the above studies and the data presented within this chapter is our utilisation of purified DRG neuronal cultures. The combination of our findings with those

in the literature, strongly support the hypothesis that the effect of TNFα on sensory neurons is most likely via a non-neuronal cell type.

One of the most striking differences in the gene expression patterns between purified DRG neuronal cultures and mixed DRG neuronal/glia cultures was that of TNFα-induced modulation of *Pgst2* and *F2rl1*. In the mixed DRG neuronal/glia cultures, TNFα strongly upregulated *Pgst2* and *F2rl1* mRNA levels, an effect which was absent in purified DRG neuronal cultures, despite reports that TNFα stimulates the expression of *Pgst2* in DRG sensory neurone cultures (Fehrenbacher et al., 2005). Taken together, this suggests that the TNFα effects seen in the mixed cultures are most likely mediated via non-neuronal cell types. In line with this, Zhang et al., 2010 showed that mast cells incubated with TNFα exhibited a 2.4-fold increase in expression of PAR2. Likewise, TNFα induced COX2 expression in spinal endothelial cells (Kanda et al., 2017) and enhanced COX2 expression in synovial fibroblasts from patients suffering from joint pain (Ke et al., 2007).

As expected, the use of NGF 100 ng/mL exerted a stronger response at the transcriptional level (compared to NGF 10 ng/mL). However, in further experiments lower concentrations of NGF were used to avoid ceiling effects. Indeed, to detect synergistic properties of NGF and TNFα, the relative concentrations of each factor should be significantly less than their respective EC100 (the maximal effective concentration), enabling an increased effect to be detected when the two factors are co-administered in the culture system (Foucquier and Guedj, 2015).

The use of calcium imaging is particularly useful in the field of neuroscience as calcium transients in a cell are indicative of neuronal activation. This method therefore allows for visualisation of neuronal activity and how this may be affected by the application of a variety

of different stimuli (Grienberger and Konnerth, 2012). Furthermore, increased calcium transients in sensory neurones have been shown to be indicative of neuronal sensitisation in a surgical mouse model of osteoarthritis (Miller et al., 2018). Studies from the literature have demonstrated that NGF can act as a sensitising agent and therefore increases the neuronal response to other pain-related agents, such as capsaicin (Bonnington and McNaughton, 2003, Zhang et al., 2005c, Zhu and Oxford, 2007).

The primary aims of the calcium imaging experiments within this chapter were to ascertain 1) if TNFα was capable of directly producing calcium transients in purified neurons and 2) if TNFα could act as a sensitising agent in a similar manner to NGF.

It was found that the application of TNFα, directly to purified DRG neuronal cultures in a perfusion set-up, did not produce a response. However, in contrast to NGF, it was also found that culturing purified neurones in TNFα for 24 h prior to calcium imaging did not alter the response of the neurones to capsaicin. This would suggest that the previous findings showing TNFα-induced upregulation in *Trpv1* expression (Kochukov et al., 2009, Wang et al., 2018, Rozas et al., 2016) did not occur because of direct activation of neurones in culture.

Although no response was seen to TNFα, either as direct activation or as sensitisation, almost all neurones responded to an application of KCl. This suggests that the application of TNFα did not alter the response of the neurones to a known activator and that TNFα application is not detrimentally toxic to these purified DRG neuronal cultures, either acutely or in a more chronic stimulation situation.

Both NGF and TNFα activate a range of secondary messenger signalling pathways that culminate in a myriad of cellular effects, ranging from pro-survival processes to apoptotic ones depending on the cellular environment. A crucial signalling pathway is that of the MAP

kinases, as previously described (Wu et al., 2016, Taves et al., 2016, Santulli et al., 2015, Edelmayer et al., 2014).

Due to the strong links between phospho-p38 and pain (as described above), the ability of NGF and TNFα to induce phospho-p38 was examined. Specifically, we wanted to address if TNFα can activate this pathway in neurones. Experiments were conducted in the PC12 neuronal cell line using HTRF technology in the first instance. In these experiments it was found that both NGF and TNFα were capable of activating p38, with TNFα producing a much more sustained activation compared to NGF (data not shown). When the combination treatment of both NGF and TNFα was used in this assay, an additive effect was observed. Following this intriguing result, the same experiment was performed in primary purified DRG neuronal cultures. However, we were unable to detect an effect of NGF, TNFα, a combination of the two or the positive control on phospho-p38 levels. This may have been due to a high basal level of phospho-p38 in the untreated group, making further modulation of p38 activation following stimulation difficult to detect or due to the low n number, consequently,the above experiment should be repeated. Additionally, it should be noted that PC12 cells were plated at 75K/well, whereas due to cell yield issues during the purification process (as discussed in the introduction of this chapter) it was only possible to plate 10K/well of purified neurones. Therefore, the density of neurones plated may not have been sufficient to detect changes with this assay. Finally, when using purified neurones, the concentration of cytokines was reduced to 10 ng/mL to enable a larger effect size window, which may have affected the results. However, the lack of response seen in the positive control condition, suggests that the negative results seen with NGF and/or TNFα were not due to this lowered concentration.

It is possible that the difference observed between PC12 cells and purified neuronal cultures were a function of the cells themselves. Although the use of cell lines has many advantages (including high cell yield and ease of use), there are also numerous disadvantages, including the fact that PC12 cells are not themselves neurones. As a result, numerous studies have described profound differences between PC12 cells and neurones. For example, one study showed that PC12 cells lacked functional NMDA receptors (Edwards et al., 2007). Therefore, there is no guarantee that the effects seen in this cell line can be reproduced in primary neuronal cultures.

3.6 Summary of Chapter

In summary, the data presented in this chapter have focussed on the individual and combined effects of NGF and TNFα on mouse adult DRG neurones. Within the suite of assays utilised to understand cellular responsiveness, we have demonstrated that the sensory neurone itself displays a distinct lack of TNFα sensitivity whether alone or in combination with NGF. In contrast, we provide further evidence of the profound effect of NGF on sensory neurones, including effects on neurite outgrowth, modulation at the transcriptional level, CGRP release. Furthermore, we demonstrate that at the level of the sensory neurone, the lack of synergistic effects (of NGF and TNFα) would argue against the sensory neurone as being the only sight of action for these two mediators in delivering the superior analgesic efficacy observed with the use of a bispecific blocker (Appendix Figure 1).

4. Investigating the Individual and Combined Effect of NGF and TNFα on Bone-Marrow Derived Macrophages *In Vitro*

4.1 Introduction

In the previous chapter, we assayed functional responses of adult mouse sensory DRG neurones to NGF, TNFα or a combination of the two. However, it has been well established that the generation and maintenance of pain states is not solely due to changes in sensory neurones (Ji et al., 2016a). As outlined in the main introduction of this thesis (section 1.11), the role of non-neuronal cell types in chronic pain states is both crucial and extensive. The following chapter will present data relating to the role of BMDM in this process.

4.1.1 The Effect of TNFα on Macrophage Signalling

Macrophages and monocytes are major sources of TNFα synthesis and release *in vivo* (Idriss and Naismith, 2000). Additionally, TNFα is known to act on macrophages themselves, affecting their physiology (Parameswaran and Patial, 2010). The pro-inflammatory actions of TNFα signalling in macrophages is thought to be primarily through the TNFR1 receptor, rather than through the potential regenerative actions of signalling via the TNFR2 receptor (Tseng et al., 2018). Exogenous application of TNFα stimulates well-established inflammatory pathways in macrophages *in vitro* (Parameswaran and Patial, 2010), including NGF signalling. Indeed, one study demonstrated that TNFα can upregulate NGF expression in both synovial fibroblasts and macrophages in osteoarthritic mice (Takano and Uchida, 2016). A further study confirmed that depleting levels of macrophages in an animal model of osteoarthritis, resulted in a significant reduction of TNFα, as well as NGF and IL-1β (Takano and Uchida, 2017), confirming that macrophages are a possible source of TNFα in this model. The same study also demonstrated that treatment of human synovial macrophages from osteoarthritic knee joints with either IL-1β or TNFα induced an increase in the levels of NGF mRNA and subsequent protein levels (Takano and Uchida, 2017) (Takano et al., 2016). It seems however,

that macrophage-produced TNFα does not only influence expression of cytokines in macrophages themselves but instead can induce expression of inflammatory cytokines in other cell types. This was suggested by Bondeson and colleagues (Bondeson et al., 2006) via the use of a model of osteoarthritis synovitis. In this model the removal of synovial macrophages not only depleted levels of TNFα but also resulted in a significant reduction in several other cytokines, including IL-6 and IL-8, which are predominantly produced by synovial fibroblasts in this model. The above highlights the crucial role of TNFα in the production of downstream pro-inflammatory cytokines, which can be released both by macrophages themselves as well as other cell types.

4.1.2 The Effect of NGF on Macrophage Signalling

Macrophages have been shown to express both the NGF receptors, TrkA and $p75^{NTR}$ (Ricci et al., 2004, Garaci et al., 1999, Williams et al., 2015). Various effects of NGF have been observed with respect to macrophage function. NGF treatment in mouse macrophages markedly increases the production of TNFα via MAP kinases as well as the secretion of nitric oxide, suggesting an important role in inflammatory responses (Barouch et al., 2001). It has been shown that NGF could act as an activator of macrophages *in vivo*, with increasing concentrations of NGF enhancing murine macrophage phagocytic ability of microspheres and leading to a significant increase in IL-1β release (Susaki et al., 1996). Human immunodeficiency virus (HIV) resistance in macrophages may be partly due to autocrine production and secretion of NGF (Balestra et al., 2001). Furthermore, treatment of macrophages with an anti-TrkA antibody prevents NGF-induced chemotaxis (Kobayashi and Mizisin, 2001). The above studies highlight how NGF may be a key modulator in macrophage behaviour.

In summary, the literature would suggest that NGF and TNFα are both capable of signalling via BMDM. The interaction between the two mediators, at the level of the macrophage, may facilitate a heightened pain state.

4.2 Aims and Experimental Strategy

The aims of this chapter were to test the following hypotheses:

- TNFα signalling in macrophages drives pain-relevant responses
- NGF can directly signal and activate pain-relevant signalling pathways in BMDM
- The direct effects of TNFα can summate with, or synergize with that of NGF, to produce a heightened pain state

The data within this chapter aims to clarify the basal expression of NGF and TNFα receptors in macrophages. Subsequently, any changes occurring at either the transcriptional or cellular level are investigated.

4.3 Methods

All animals were obtained from Charles River and housed in a designated facility and maintained in accordance with the United Kingdom Home Office Animals (Scientific Procedures) Act (1986) and Home Office regulations. Animals were kept in a 12 h light dark cycle and fed *ad libitum*. All animals were sacrificed using schedule 1. Experiments which involved intraperitoneal injections to the abdomen of mice where performed under the appropriate Home Office Licence.

4.3.1 Primary Cell Culture of Different Macrophage Types

Macrophage cultures were generated from adult C57BL/6 mice aged 7-10 weeks.

4.3.1.1 Bone-Marrow Derived Macrophages

To obtain BMDM, a protocol adapted from Trouplin et al., 2013 was used. The bone cavities of the tibia and femur from each hind limb were flushed through with pre-cooled 1X DPBS, until the cavity appeared white. The eluent was then centrifuged for 7 min at 850 *g* (Hettich Zentrifugen). The resulting cell pellet was re-suspended in 3 mL of pre-warmed Dulbecco's Modified Eagle Medium + Glutamax™ (Gibco®, 32430027) supplemented with 10 % FBS, 1 % Pen/Strep and 25 ng/mL recombinant macrophage colony stimulating factor (MCSF) and filtered through a 40 µM cell strainer (Corning, 352340). MCSF induces the proliferation and differentiation of myeloid progenitors into cells of the macrophage/monocyte lineage (Weischenfeldt and Porse, 2008a). In a number of experiments, NGF 10 ng/mL was also added into the above differentiation process. The cell suspension was made up to the desired volume with the supplemented medium, 25 mL cell suspension was plated per petri dish

(VWR International, 391-1502) and the progenitor cells allowed to differentiate for 7 days at 37 °C, 5 % CO_2. No media change was required during this incubation period.

Following the incubation period, culture supernatants were discarded. The remaining adherent cells were washed with 10 mL pre-warmed 1X DPBS, followed by 15 mL pre-warmed non-enzymatic cell dissociation solution (Millipore, S-014-B). Afterward, cells were incubated for 10 min at 37 °C, 5 % CO_2. To aid cell detachment a cell scraper was used to lift the adherent cells from each petri dish. Cells were pooled into a 50 mL conical tube, washed with pre-cooled 1X DPBS and centrifuged for 7 min at 478 *g* (Hettich Zentrifugen) at 4 °C. Cells were re-suspended in an appropriate volume of Dulbecco's Modified Eagle's Medium (DMEM) (+MCSF supplement) and plated at the desired density for 24 h prior to any experimental stimulations taking place.

4.3.1.2 Resident Peritoneal Macrophages

To obtain resident peritoneal macrophages, the culled mouse torso was sterilised with 70 % ethanol, the abdominal skin retracted, and the peritoneal wall exposed. 10 mL of sterile 1X HBSS was injected into the peritoneal cavity using a 23 g needle (BD Microlance, 300800), taking care not to puncture any internal organs. The peritoneal cavity was gently massaged to dislodge any cells of interest from linings within the cavity. Using a syringe and a 23 g needle, the peritoneal fluid was retrieved and spun at 212 *g* for 10 min at RT (Hettich Zentrifugen) to obtain a cell pellet. The pellet was re-suspended in 1 mL pre-warmed DMEM + 10 % FBS + 1 % Pen/Strep and plated at the desired density. Approximately 2 h post-plating, the cells were washed with 1X HBSS and the medium replaced to remove any unspecific cells. The cells were ready to use 24 h post-plating.

4.3.1.3 Activated Peritoneal Macrophages

To allow time for an appropriate inflammatory response, 4 days prior to the collection and culture of peritoneal macrophages (see section 4.3.1.2), 1 mL of Bio-Gel P-100 2 % polyacrylamide beads (Bio-Rad, 1504174) was delivered via intraperitoneal injection to the mice, being careful to avoid the bladder upon injection. The Bio-Gel beads (2 g) were washed twice in 20 mL DPBS and subsequently centrifuged at 400 *g* for 5 min prior to being resuspended in 100 mL PBS to give a 2 % solution ready for administration into the peritoneal cavity. A 26-gage needle was used to administer the injection (at an angle of 45 ° to the skin) into the lower right quadrant of the abdomen to avoid any vital organs. Following the incubation period of 4 days, the procedure followed the same process outlined above (see section 4.3.1.2) for the culture of resident peritoneal macrophages.

4.3.2 Viability Assessment of BMDM

To confirm that cultured macrophages were viable after stimulation with either NGF, TNFα or a combination of the two, both an alamarBlue™ assay and FACS analysis were employed.

4.3.2.1 AlamarBlue™ Assay

AlamarBlue™ contains a permeable, non-fluorescent molecule which is converted to a highly fluorescent compound in healthy cells. The change in supernatant colour acts as an indicator of cell health and subsequent viability.

BMDM were plated in a 96-well plate format and allowed to adhere prior to being treated with NGF 10 ng/mL, TNFα 10 ng/mL, a combination of the two or LPS 1 mg/mL as a positive control (Enzo, ALX-581-008-L002) for 24 h. Following the treatment period, $1/10^{th}$ volume of alamarBlue™ reagent (Invitrogen, DAL1025) was added directly to the cells in culture medium

and incubated for 5 h at 37 °C, 5 % CO_2. The absorbance was read at 570 nm, using 600 nm as a reference/normalisation wavelength.

4.3.2.2 Flow cytometry

Following 24 h stimulation with the same treatments as described above (section 4.3.2.1), BMDMs were washed with cold 1X PBS and gently dislodged following a 10 min incubation period with non-enzymatic dissociation buffer. Cells were centrifuged for 7 min, 688 *g* at 4 °C (Hettich Zentrifugen), and subsequently re-suspended in 200 µL FACS buffer and transferred to FACS tubes for staining. Macrophages were stained with Amcyan-conjugated viability dye for 30 min on ice in the dark. The latter is a cell membrane impermeable amine-reactive dye. The dye can enter dead cells that have compromised membrane integrity and subsequently bind to intracellular proteins. On live cells, the dye can interact with cell surface proteins but the resulting staining is significantly lower to dead cells (Biotium, 2018). Cells were then washed with complete FACS buffer and fixed in 3.8 % PFA for 5 min. Fixed samples were washed and resuspended in FACS buffer until ready to analyse.

4.3.2.3 Flow Cytometry Data Analysis

Flow cytometry was performed on a BD FACS Fortessa (BD Pharmingen) and data analysed using FlowJo software (Treestar). Cell discrimination was achieved by applying the following gating strategy: 1) BMDMs were identified based on forward scatter (FSC) and side scatter properties 2) live cells were gated as negative for live/dead staining and 3) cells negative for the viability dye were used to quantify percentage of positive cells.

4.3.3 HTRF (Homogenous Time Resolved Fluorescence) Assay

Cisbio's phospho-p38 kit (Cisbio, 64P38PEG) was used according to the manufacturers' instructions as previously described in section 3.3.7. In this instance, the assay was performed on BMDM plated at 50K/well. BMDM were stimulated with NGF, TNFα, a combination of the two or anisomycin (Sigma, A5862), for 5 or 20 min.

4.3.4 MSD® U-PLEX Platform as a Cytokine Secretion Measure

In U-PLEX immunoassays, the biotinylated capture antibody is coupled to U-PLEX linkers, which self-assemble onto unique spots on the assay plate. Following sample addition, analytes bind to the capture antibody. To complete the immunoassay, a detection antibody conjugated with an electro-chemiluminescent label (SULFO-TAG) binds to the analytes. Applying a voltage to the plate causes the captured label to emit light; the intensity of the emitted light is proportional to the amount of analyte present in the sample.

A custom-made kit (MSD, K15069L-1) was utilised to measure the levels of the GM-CSF, IL-10, IL-6, TNFα, IL-1β, KC/GRO, MCP1, MIP1α, MIP-3α or NGF in the supernatant of BMDM, stimulated with NGF 10 ng/mL, TNFα 10 ng/mL or a combination of the two, for 24 h. For TNFα secretion, BMDM were stimulated with LPS 100 ng/mL for 24 h as a positive control. For NGF secretion, the cynom-K1 keratinocyte cell line was used as a positive control. Cynom-K1 cells were obtained from the European Collection of Authenticated Cell Cultures. Cynom-K1 cells were seeded at 15K/well on 96 well PDL plates supplemented with DMEM 10 % FCS and 1 % pen/strep and collected following the 24 h stimulation period.

The assay was performed according to manufacturer's instructions. All reagents were bought to RT prior to use. For each biotinylated antibody, one per cytokine (provided in the kit), 200 µL was added to 300 µL of the assigned linker and vortexed prior to being incubated at RT for

30 min. Following the addition of 200 µL of Stop Solution, the mix was vortexed and incubated for a further 30 min at RT. To prepare the multiplex coating solution, 600 µL of each U-PLEX-coupled antibody solution was combined into a single tube and vortexed. The solution was made up to 6 mL with Stop Solution to result in a final 1X concentration and vortexed a further time. To coat the U-PLEX plate, 50 µL of the multiplex coating solution was added to each well. The plate was sealed with an adhesive plate seal and incubated with shaking at 4 ˚C overnight. The following morning the plate was washed 3X with 150 µL/well of 1X DPBS + 0.05 % Tween-20.

Following plate preparation, 25 µL of Diluent 41 (diluent containing protein, blockers and preservatives) was added to each well followed by 25 µL of calibrator (prepared in Diluent 41) or sample, the plate was sealed with an adhesive plate seal and incubated at RT with shaking for 1 h. Following this incubation period, the plate was washed 3X with 150 µL/well of 1X DPBS + 0.05 % Tween-20 and subsequently 50 µL of 1X detecting antibody solution was added to each well. The plate was once more sealed and incubated at RT with shaking for 1 h. The plate was washed 3X with 150 µL/well of 1X DPBS + 0.05 % Tween-20 and finally 150 µL of 2X Read Buffer T was added to each well. The plate was read on a SECTOR Imager 6000 (MSD).

4.3.5 Gene Expression Analysis of BMDM Using Custom TaqMan Array Microfluidic Cards or SYBR Green Technology

For the TaqMan Array cards, BMDM were collected as previously described (section 4.3.1.1) and plated at $1x10^6$ cells/well in a 6-well plate (Thermo Scientific, 140675) with DMEM + 10 % FBS + 1 % Pen/Strep + 25 ng/mL M-CSF (2 mL/well). 24 h later, the medium was removed, and the cells were washed in 1 mL 1X DPBS. Following this wash step, the cells were exposed to various stimulations (2 mL/well) made up in DMEM + 10 % + 1 % Pen/Strep for 24 h. The

treatment groups were as follows: Untreated, NGF 10 ng/mL, TNFα 10 ng/mL, NGF 10 ng/mL + TNFα 10 ng/mL or LPS 100 ng/mL (Enzo, ALX-581-008-L002) as a positive control. No M-CSF was added to the medium at this stage.

To assess the expression levels of NGF/TNFα receptors (*Tnfrsf1a, Ntrk1* and *Ngfr*), SYBR green technology was used. Following isolation, BMDM, peritoneal and induced peritoneal macrophages were collected as previously described (section 4.3.1) and plated at $1x10^6$ cells/well in a 6-well plate with DMEM + 10 % FBS + 1 % Pen/Strep + 25 ng/mL M-CSF (2 mL/well). Cells were allowed to settle for 24 h before the medium was removed and the cells were washed in 1 mL 1X DPBS. Following this wash step, the cells were exposed to either fresh DMEM + 10 % + 1 % Pen/Strep or LPS 100 ng/mL (2 mL/well) for 24 h. No M-CSF was added to the medium at this stage.

4.3.5.1 RNA Extraction and cDNA Synthesis

Following the stimulation period, RNA was extracted as previously described (section 3.3.4.1) using the RNeasy Micro Kit (Qiagen, 74004) with the following exceptions; cell lysates were collected in 1 mL RLT buffer + β-mercaptoethanol and genomic DNA was removed via a 15 min incubation at RT with 80 µL DNase I and RDD buffer solution using an RNase-Free DNase Set (Qiagen, 79254).

Resulting RNA was immediately quantified and tested for purity on the NanoDrop ND-100 Spectrophotometer (Thermo Fisher Scientific) prior to cDNA synthesis. Based on this quantification, 200 ng of RNA was reverse transcribed using the SuperScript® III First-Strand Synthesis Supermix kit (Invitrogen, 11752-050). For cDNA synthesis, samples were diluted as required using RNase-free water to make a solution of 12 µL in qPCR tubes (STARLAB, A1402-3800). To this solution, 1 µL of dNTPs (1:10 dilution from 100 mM stock (Promega, U1240) in

RNase-free water and 1 µL of random primers (100 µg/mL) (Promega, C1181) were added. Samples were run on the PCR machine at 65 °C for 4 min, followed by 1 min on wet ice. To make up the final volume to 20 µL, 6 µL of a second mix was added. Per reaction, this mastermix consisted of: 4 µL 5X first strand buffer, 1 µL DTT (0.1 M) and 1 µL Superscript® III Reverse Transcriptase. The following RT cycling conditions were used: 25 °C for 5 min, 50 °C for 60 min, 70 °C for 15 min, samples were held at 4 °C until collection and kept at -20 °C until ready for use.

4.3.5.2 RT-qPCR for TaqMan Array Microfluidic Cards

Custom made TaqMan 384-well PCR array microfluidic cards (Applied Biosystems) were used to analyse the effects of NGF, TNFα or a combination of the two on 48 gene transcripts simultaneously, including three housekeeping genes; *18S* ribosomal RNA (*18s*), β2-Microglobulin (*β2m*) and glyceraldehyde 3-phosphate dehydrogenase (*Gapdh)*. See Table 6 for full list of gene transcripts quantified. Sample cDNA was diluted to 2 ng/mL in 50 µL molecular grade water before a TaqMan universal PCR master mix (Applied Biosystems, 4304437) was added at a 1:1 ratio to give a final volume of 100 µL. Each custom card held eight cDNA samples and was allowed to acclimatise to RT prior to loading. Once thoroughly mixed, 95 µL of the sample mix was loaded into the corresponding channel and centrifuged at 158 *g* for 1 min (Sorvall ST 40 Centrifuge), twice. The card was sealed, and entry wells removed prior to the card being run on the ABI 7900HT Real Time PCR instrument (Applied Biosystems, serial number: 201276). The following cycling conditions were used: 25 °C for 10 min, 42 °C for 60 min and 85 °C for 5 min.

4.3.5.3 RT-qPCR for SYBR Green Technology

To obtain the relative quantification of the desired transcripts, real time qPCR was performed in triplicate on a LightCycler 480 (Roche) using SYBR Green Real-Time PCR Master Mix (Roche, 04 887 352 001). cDNA samples were diluted to 5 ng/µL in RNase-free water. Reaction mixtures were prepared on ice and contained the following per reaction; 5 µL 2X SYBR green master mix, 0.5 µL primer pair mix at 10 µM, 3.5 µL ddH_2O and 1 µL of cDNA sample, giving a final reaction volume of 10 µL. See Table 7 for transcripts quantified and primer pair details. A blank sample of water was used as a negative control in all experiments. The completed 384-well PCR plate (Roche, 04 729 749 001) was centrifuged for 20 secs to ensure collection of sample mix at the bottom of the well before being run on the machine. The following cycling conditions were utilised; 25 °C for 10 min, 42 °C for 60 min and 85 °C for 5 min.

4.3.5.4 Data Analysis

mRNA transcripts were normalised to the expression of the housekeeping genes (TaqMan Array Microfluidic Cards: average of *18s*, *β2m* and *Gapdh* expression*;* SYBR green method: *β2m* expression) using the ΔΔCt method and data expressed as ΔΔCt changes from the basal condition.

Table 6. List of gene transcripts included on the PCR TaqMan card (housekeeping genes are identified in bold font)

Gene Transcripts						
Aif1	*Ccl5*	*Fcgr1*	*Ifnyr1*	*Jak2*	*P2x4r*	*Stat6*
Atf3	*Ccr2*	*Fcgr2b*	*Ifnyr2*	*Ngf*	*P2y12r*	*Tlr4*
Bdnf	*Ccr5*	*Fcgr3*	*Il10ra*	*Ngfr*	*Ptgs2*	*Tnf*
C3	*Cd63*	*Gfap*	*Il-18*	*Ntrk1*	*Slfn2*	***18s***
C4b	*Csf1r*	*Gm2002*	*Il-1ß*	*Ntrk2*	*Slfn5*	***ß2m***
Ccl12	*Cst7*	*Gpr84*	*Il-6*	*Ntrk3*	*Stat1*	***Gapdh***
Ccl2	*Ctss*	*Ifnb1*	*Il6ra*	*Oprm1*	*Stat3*	

Table 7. List of gene transcripts and the corresponding primer pairs

Gene Transcript	Primer Pairs (oligo sequence 5'-3')
Ntrk1 Neurotrophic Receptor Tyrosine Kinase	Fwd: GCAGTATTGCAGGTGTCCCA Rev: AGGACCAAGGCTCTCACAAC
Ngfr Nerve Growth Factor Receptor	Fwd: AGACACCTCCAGTACAGAGTCAA Rev: CCCTTCTCCAGGTCTCATTCC
Tnfrsf1a Tumour Necrosis Factor Receptor 1	Fwd: TTTACGGGTTCCCAGAATTACCT Rev: ATCTCCACCTGGGACATTTCTTT
ß2m Beta-2-Microglobulin	Fwd: TTCTGGTGCTTGTCTCACTGA Rev: CAGTATGTTCGGCTTCCCATTC

4.3.6 Statistical Analysis

All statistical analysis was performed using GraphPad software (version 7.04). Prior to any statistical analysis taking place, the data were tested for normality using the Shapiro-Wilk normality test. Within this chapter, all data were analysed using the following statistical tests; One-Way ANOVA, Two-Way ANOVA or Linear Models for Microarray (LIMMA) (for the TaqMan card data) followed by *post-hoc* correction tests for multiple comparisons. In all instances, data are displayed as Mean ± SEM, n numbers and specific *post-hoc* correction tests used are reported within the figure legend. A P value <0.05 was considered to be significant.

4.4 Results

4.4.1 Diverse Macrophage Cultures Express Similar Levels of NGF and TNFα Receptors

Three types of macrophages are commonly used *in vitro*; BMDM, peritoneal macrophages and activated peritoneal macrophages. One of the first things we explored was if the expression of the receptors for NGF and TNFα (*Ntrk1, Ngfr* and *Tnfrsf1a*) differed between macrophage types.

Across all three macrophage cell types similar results were found. *Tnfrsf1a* was expressed highly in all three, with a Ct value of 24.9 ± 0.61 in BMDM (n=3 biological replicates), 23.91 ± 0.54 in peritoneal macrophages (n=3 biological replicates) and 25.66 ± 1.65 in induced peritoneal macrophages (n=3 biological replicates) (Figure 24A-C), corroborating the extensive literature surrounding the significant role of TNFα signalling in immune cell types (Horiuchi et al., 2010, Ji et al., 2016b, Bradley, 2008).

NGF receptor levels were also similar between all three macrophage cell types, with *Ntrk1* displaying a Ct value of 38.83 ± 1.17 in BMDM (n=3 biological replicates), 38.67 ± 1.33 in peritoneal macrophages (n=3 biological replicates) and 35.95 ± 2.03 in activated peritoneal macrophages (n=3 biological replicates) (Figure 24A-C). *Ngfr* displayed a Ct value of 37.22 ± 1.39 in BMDM (n=3 biological replicates), with slightly higher levels of expression in the peritoneal and activated peritoneal macrophage types, with Ct values of 31.62 ± 0.32 (n=3 biological replicates) and 31.83 ± 0.46 (n=3 biological replicates) respectively (Figure 24A-C). Relative to *Tnfrsf1a* expression, *Ntrk1* expression displayed a fold change of 0.00025 (-13.93 ± 1.75 ΔΔCt, n=3 biological replicates), 0.00008 (-14.76 ± 1.35 ΔΔCt, n=3 biological replicates) and 0.02520 (-10.29 ± 3.36 ΔΔCt, n=3 biological replicates) in unstimulated BMDM, unstimulated peritoneal macrophages and unstimulated activated peritoneal macrophages

respectively (Figure 24G). *Ngfr* expression displayed a fold change of 0.00048 (-12.32 ± 1.61 ΔΔCt, n=3 biological replicates), 0.00677 (-7.71 ± 0.86 ΔΔCt, n=3 biological replicates) and 0.03065 (-6.16 ± 1.27 ΔΔCt, n=3 biological replicates) in unstimulated BMDM, unstimulated peritoneal macrophages and unstimulated peritoneal macrophages respectively (Figure 24G). No significant differences were observed.

To establish if introducing a pre-stimulus would alter the responsiveness of these cell types to NGF or TNFα, all three types were stimulated with LPS 100 ng/mL and the expression levels of the receptors re-examined. Following stimulation with LPS 100 ng/mL it was found that the expression levels were unchanged in all three cell types compared to their unstimulated state (Figure 24D-F). Relative to *Tnfrsf1a* expression, *Ntrk1* expression displayed a fold change of 0.00005 (-14.65 ± 0.81 ΔΔCt, n=3 biological replicates), 0.00005 (-15.16 ± 1.16 ΔΔCt, n=3 biological replicates) and 0.00254 (-10.66 ± 1.78 ΔΔCt, n=3 biological replicates) in LPS-stimulated BMDM, LPS-stimulated peritoneal macrophages and LPS-stimulated activated peritoneal macrophages respectively (Figure 24H). *Ngfr* expression displayed a fold change of 0.00015 (-13.3 ± 1.11 ΔΔCt, n=3 biological replicates), 0.00038 (-11.66 ± 0.71 ΔΔCt, n=3 biological replicates) and 0.00186 (-9.83 ± 1.07 ΔΔCt, n=3 biological replicates) in LPS-stimulated BMDM, LPS-stimulated peritoneal macrophages and LPS-stimulated peritoneal macrophages respectively (Figure 24H). No significant differences were observed.

In our subsequent studies evaluating NGF and TNFα effects on macrophages, it was decided that BMDM would be utilised. One major advantage of utilising BMDM (over peritoneal macrophages) is that they exist in a quiescent form and therefore represent a suitable system to detect even subtle changes in their behaviour following stimulation (Weischenfeldt and Porse, 2008b). The use of peritoneal and activated peritoneal macrophages could instead

introduce significant variation into the culture system due fluctuating levels of pre-activation (Zhang et al., 2008).

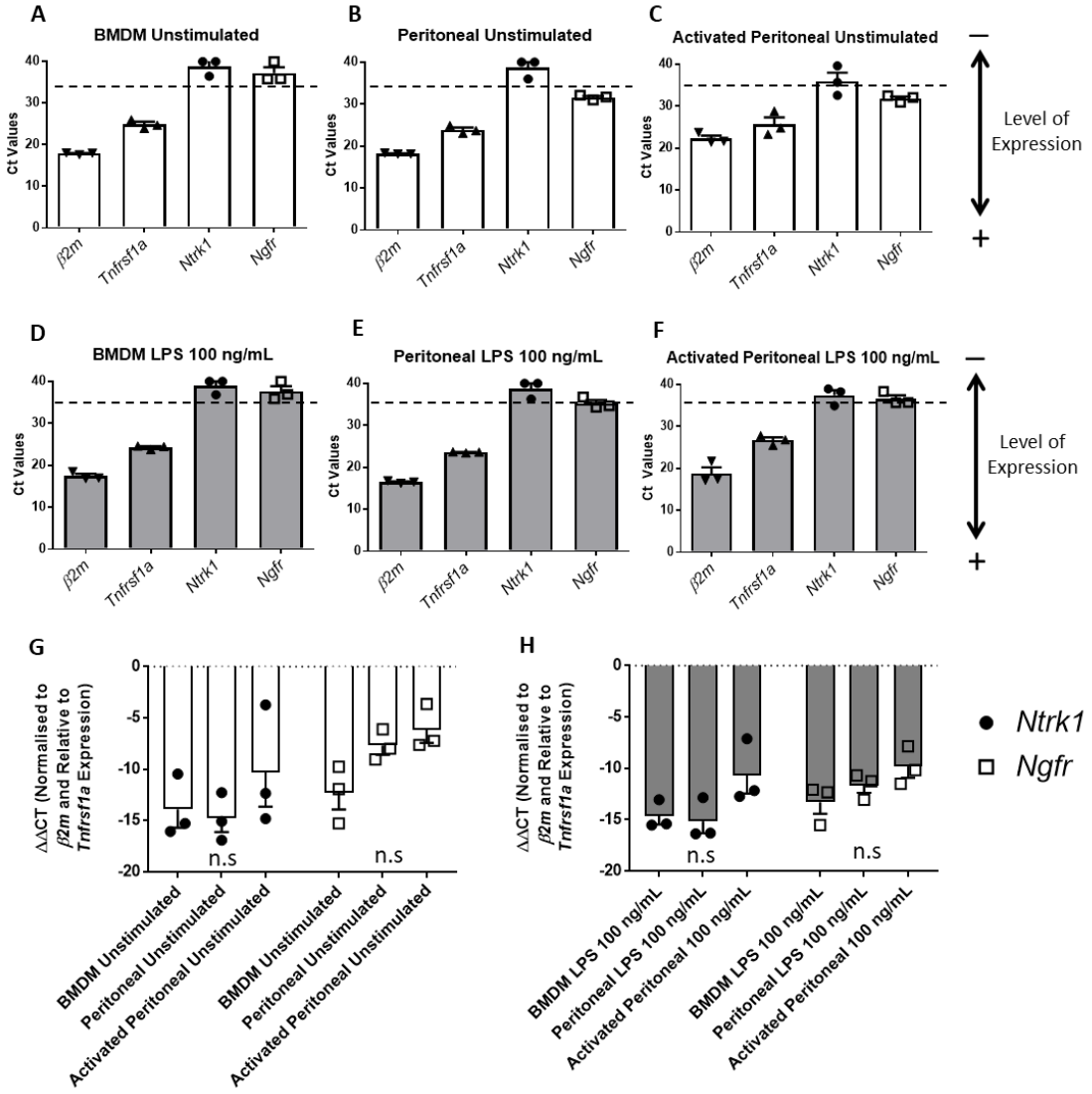

Figure 24. Expression levels of TNFα and NGF receptors (*Tnfrsf1a, Ntrk1, Ngfr*) in different activation states of macrophages. A-C) Graphs displaying the Ct values of *Tnfrsf1a* (black triangles, white bars), *Ntrk1* (black circles, white bars), *Ngfr* (hollow squares, white bars) and the housekeeping gene *β2m* (black upside-down triangles, white bars) in unstimulated BMDM, peritoneal macrophages and activated peritoneal macrophages. D-F) Graphs displaying the Ct values of *Tnfrsf1a* (black triangles, shaded bars), *Ntrk1* (black circles, shaded bars), *Ngfr* (hollow squares, shaded bars) and the housekeeping gene *β2m* (black upside-down triangles, shaded bars) in LPS-(100 ng/mL) stimulated BMDM, peritoneal macrophages and activated peritoneal macrophages. G-H) Expression levels of *Ntrk1* (black circles) and *Ngfr* (hollow squares) relative to *Tnfrsf1a* expression (normalised to *β2m* expression) in (G) unstimulated BMDM, peritoneal or activated peritoneal macrophages or (H) LPS-stimulated (100 ng/mL) BMDM, peritoneal or activated peritoneal macrophages. Data displayed as Mean ± SEM, n=3 biological replicates (displayed as individual data points). Data were analysed using Two-Way ANOVA followed by Tukey's multiple comparisons test.

Abbreviations: NGF: nerve growth factor; TNFα: tumour necrosis factor alpha; BMDM: bone marrow-derived macrophages; *Ntrk1*: neurotrophic receptor tyrosine kinase; *Ngfr:* nerve growth factor receptor; *Tnfrsf1a*: tumour necrosis factor receptor superfamily 1a; *β2m*: beta 2-microglobulin; n.s: not significant.

4.4.2 Addition of NGF in the Differentiation Process does not Alter NGF or TNFα Receptor Expression in BMDM

The culture of BMDM includes a 7-day period in which they are cultured in the presence of MCSF, a growth factor which is essential to stimulate the bone-marrow derived progenitors to differentiate into a macrophage lineage cell. Previous work has highlighted a role for NGF in regulating human macrophage phenotype (Williams et al., 2015). To address whether NGF-driven modulation of macrophage differentiation was indeed possible, and regulated via receptors such as *Ntrk1* and *Ngfr*, we assessed the effect on receptor expression, following addition of NGF into the differentiation period. It was found that adding NGF 10 ng/mL into the culture system for the full 7-day period of bone marrow differentiation (in addition to the presence of MCSF) had no significant effect on the expression levels of all three receptor types (*Ntrk1, Ngfr* and *Tnfrsf1a*) (Figure 25A-C).

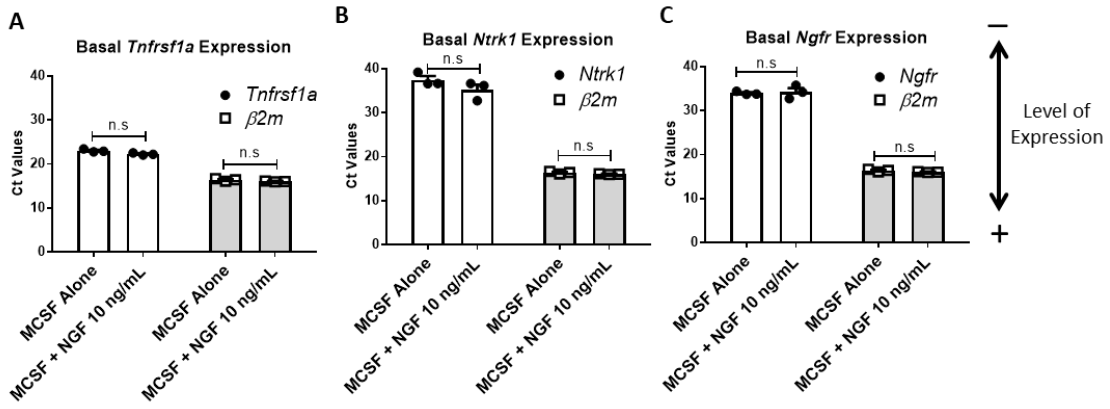

Figure 25. Expression levels of TNFα and NGF receptors in BMDM following NGF treatment in the differentiation process. A-C) Graphs displaying the Ct values of *Tnfrsf1a, Ntrk1, Ngfr* and the housekeeping gene *β2m* in BMDM grown in either MCSF alone or MCSF with NGF (10 ng/mL) throughout the 7-day differentiation process. Data displayed as Mean ± SEM, n=3 biological replicates (displayed as individual data points). Data analysed using Two-Way ANOVA followed by Tukey's multiple comparisons test.

Abbreviations: NGF: nerve growth factor; TNFα: tumour necrosis factor alpha; BMDM: bone marrow-derived macrophages; *Ntrk1*: neurotrophic receptor tyrosine kinase; *Ngfr:* nerve growth factor receptor; *Tnfrsf1a*: tumour necrosis factor receptor superfamily 1a; *β2m*: beta 2-microglobulin; n.s: not significant.

4.4.3 BMDM Viability was Unaffected by NGF or TNFα Treatment

To assess BMDM viability following stimulation, both an alamarBlue™ assay and flow cytometry analysis was employed. BMDM viability (as assessed by both assays) was unaffected by treatment with NGF (10 ng/mL, 24 h), TNFα (10 ng/mL, 24 h) or a combination of the two factors (10 ng/mL, 24 h) (Figure 26). Indeed, no significant changes (in response to either factor) were detectable from the untreated group in the alamarBlue™ assay (Figure 26A). Furthermore, flow cytometry analysis revealed that the % of live BMDM did not decrease, relative to the untreated group level, in any of the stimulation groups (Figure 26B). The untreated group displayed 80.25 ± 0.05 % (n=2 biological replicates) of live BMDM, compared to 81.35 ± 1.75 % (n=2 biological replicates) of live BMDM in the NGF (10 ng/mL) group, 87.95 ± 0.95 % (n=2 biological replicates) of live BMDM in the TNFα (10 ng/mL) and 84.55 ± 0.35 % (n=2 biological replicates) of live BMDM in the combination group. Due to the number of replicates in the FACS data set, statistical analysis was not performed.

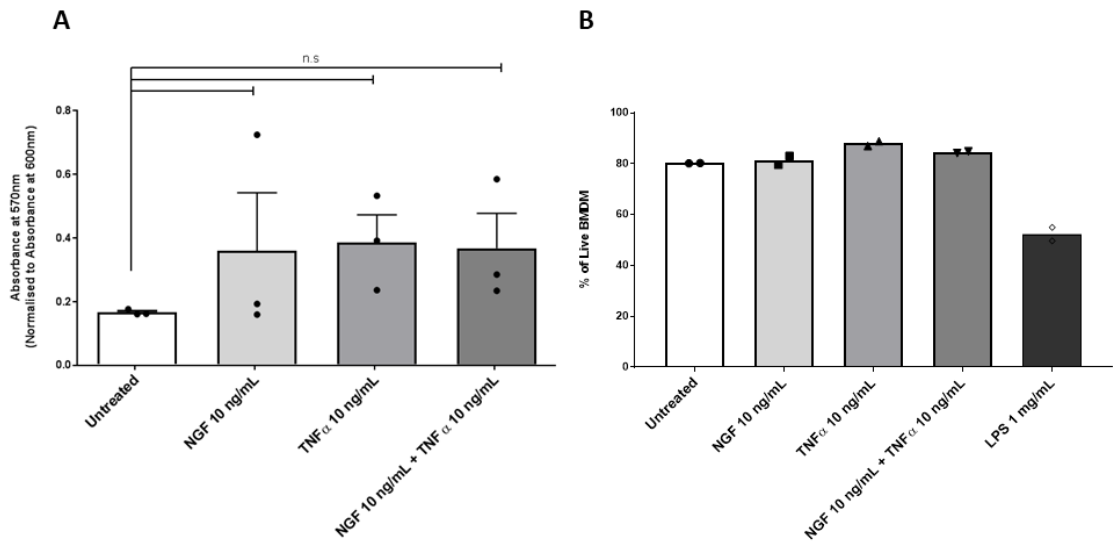

Figure 26. Confirming BMDM viability following treatment with NGF, TNFα or a combination of the two for 24 h. A) % of BMDM viability (normalised to the untreated group) determined using the alamarBlue® assay and B) % of live BMDM determined via flow cytometry analysis across the different conditions; untreated (black circles), NGF (10 ng/mL, 24 h, black squares), TNFα (10 ng/mL, 24 h, black triangles), NGF + TNFα (both at 10 ng/mL, 24 h, black upside-down triangles) or LPS as a positive control (1 mg/mL, 24 h, hollow diamonds). Data displayed as Mean ± SEM, for A) n=3 biological replicates (displayed as individual data points). Data were analysed using One-Way ANOVA followed by Tukey's multiple comparisons test. For B) n=2 biological replicates (displayed as individual data points), therefore statistics were not performed.

Abbreviations: NGF: nerve growth factor; TNFα: tumour necrosis factor alpha; BMDM: bone marrow-derived macrophages; LPS: lipopolysaccharide; n.s: not significant.

4.4.4 TNFα (not NGF) Activates p38 Signalling in BMDM

To further characterise the response of BMDM to both NGF and TNFα, induction of phospho-p38 was investigated, using both methods described in sections 3.3.7 and 3.3.8 (HTRF and immunocytochemistry).

Representative images of the ICC from each group (Figure 27A and B) and the corresponding quantification (Figure 28A and B) show a clear effect of TNFα (10 ng/mL) on phospho-p38 induction, with an overall fluorescence increase of 2461 ± 192.5 % (n=2 biological replicates) at 5 min (Figure 28A) and 3710 ± 1674 % (n=2 biological replicates) at 20 min (Figure 28B), from the untreated group. No effect of NGF (10 ng/mL) was observed from the untreated group and the combination group (NGF + TNFα) saw the same effect as TNFα alone (Figure 27 and 28). At both time points, levels of phospho-p38 induction in response to TNFα alone and the combination treatment (NGF/TNFα) reached the levels of induction seen with the positive control, anisomycin (Figure 28A and B). Statistical analysis was not performed on this data set due to a low n number of 2 biological replicates.

BMDM induction of phospho-p38 following stimulation with NGF, TNFα or a combination of the two was also determined using the HTRF approach. Using this technique, the above findings (as measured using ICC) were replicated. NGF treatment of BMDM was found to have no significant effect, whereas both the TNFα alone and combination group displayed a 3-fold significant increase over basal levels (One-Way ANOVA; $F(4,10)=689.3$, $P<0.0001$) (Figure 29A). Anisomycin treatment of BMDM was found to induce an approximately 8-fold increase over basal phospho-p38 levels (One-Way ANOVA; $F(4,10)=689.3$, $P<0.0001$) (Figure 29A), a stronger response than what we previously saw from the immunocytochemistry data. This

result suggests that the HTRF assay is a more sensitive technique compared to immunocytochemistry.

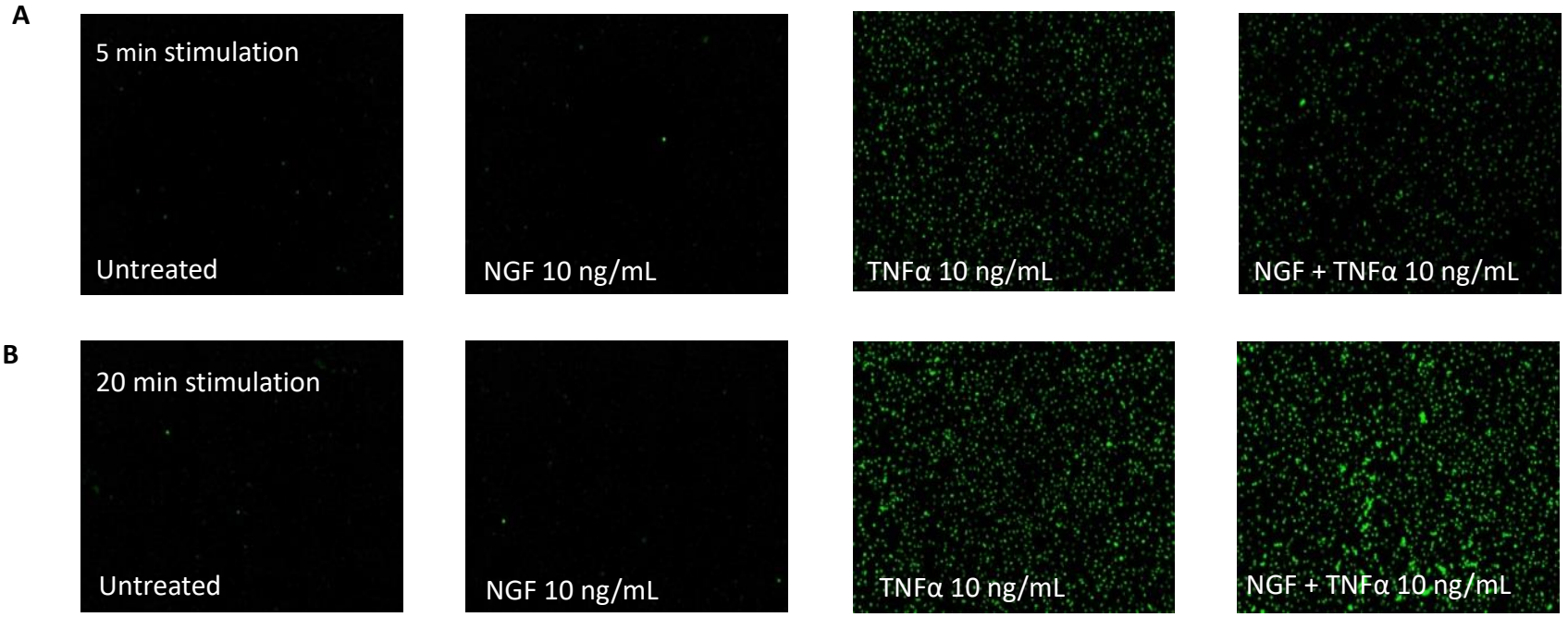

Figure 27. Visual representation of phospho-p38 induction in BMDM following treatment with NGF, TNFα or a combination of the two (10 ng/mL as measured by ICC. A) Representative ICC images of phospho-p38 staining following treatments for 5 min or B) 20 min.

Abbreviations: NGF: nerve growth factor; TNFα: tumour necrosis factor alpha; BMDM: bone marrow-derived macrophages; ICC: immunocytochemistry.

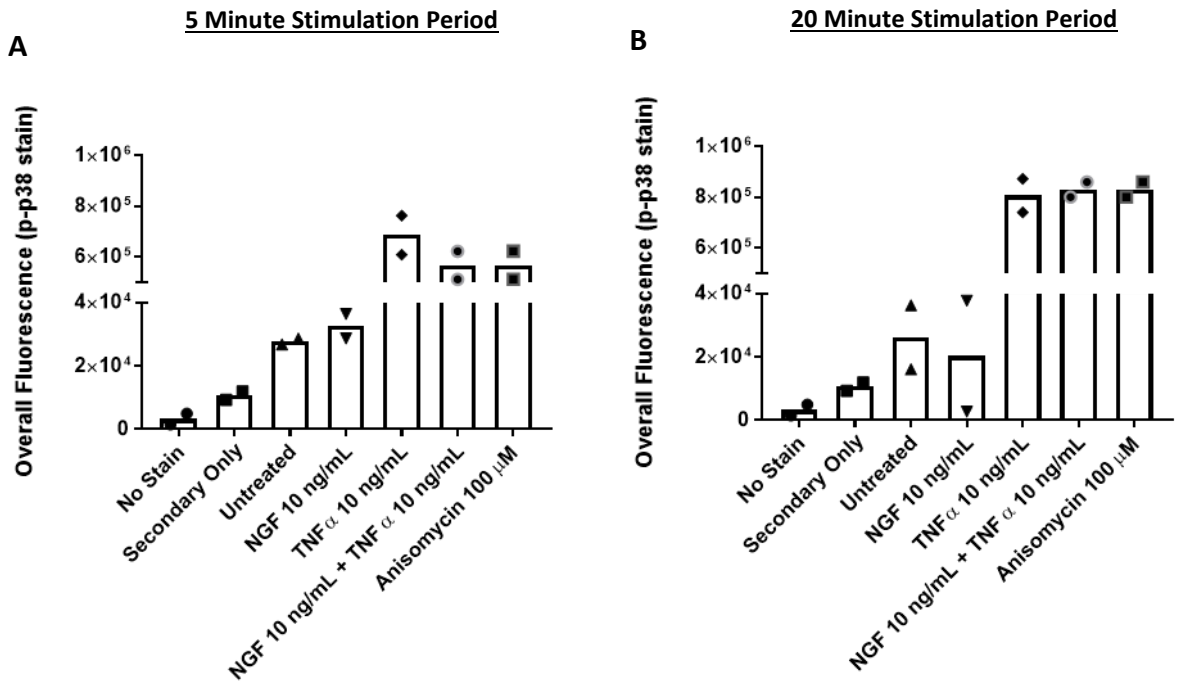

Figure 28. Quantification of levels of phospho-p38 in BMDM following treatment with NGF, TNFα or a combination of the two (10 ng/mL) as measured by ICC. A-B) Quantification of overall fluorescence following immunocytochemistry with a phospho-p38 antibody following a 5 min stimulation period C) or a 20 min stimulation period D) Data displayed as Mean ± SEM, n=2 biological replicates (displayed as individual data points).

Abbreviations: NGF: nerve growth factor; TNFα: tumour necrosis factor alpha; BMDM: bone marrow-derived macrophages; ICC: immunocytochemistry.

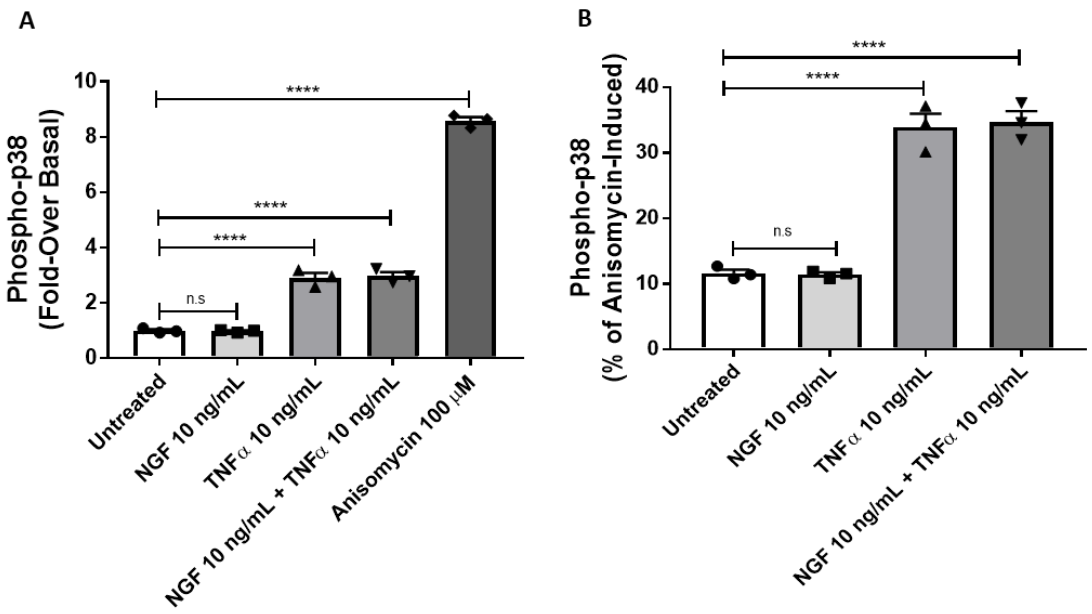

Figure 29. Levels of phospho-p38 in BMDM in response to NGF, TNFα or a combination of the two (10 ng/mL) as measured by HTRF assay. A-B) Levels of BMDM phospho-p38 in response to NGF (10 ng/mL, 20 min, black squares), TNFα (10 ng/mL 20 min, black triangles), NGF + TNFα (10 ng/mL, 20 min, black upside-down triangles) or Anisomycin (100 µM, 20 min, black diamonds) displayed as fold-over basal (A) or displayed as % of anisomycin-induced (B) following a 20-minute stimulation period. Data displayed as Mean ± SEM, n=3 biological replicates (displayed as individual data points). Data were analysed using One-Way ANOVA followed by Tukey's multiple comparisons test. **** P<0.0001.

Abbreviations: NGF: nerve growth factor; TNFα: tumour necrosis factor alpha; BMDM: bone marrow-derived macrophages; HTRF: homogenous time resolved fluorescence; n.s: not significant.

4.4.5 NGF and TNFα do not Stimulate the Release of Each Other from BMDM In Vitro

One theory that we wanted to explore was the presence of a possible feedback mechanism whereby NGF or TNFα may drive the release of each other, leading to a heightened pain state (Figure 30). However, it was found that BMDM cultures stimulated with NGF (10 ng/mL) did not secrete any detectable TNFα (Figure 31A) and likewise, BMDM cultures stimulated with TNFα (10 ng/mL) did not secrete any detectable NGF (Figure 31B). Significant increases in secreted NGF or TNFα were however detectable in the following positive controls (used in the ELISA/MSD assay) (Figure 31A and B). For TNFα secretion, LPS 100 ng/mL was used as a positive control (One-Way ANOVA; $F(2, 6)=197.6$, $P<0.0001$) (van der Bruggen et al., 1999). For NGF secretion, the cynom-K1 cell line was used as a positive control (One-Way ANOVA; $F(2,9)=497.1$, $P<0.0001$)(Di Marco et al., 1991).

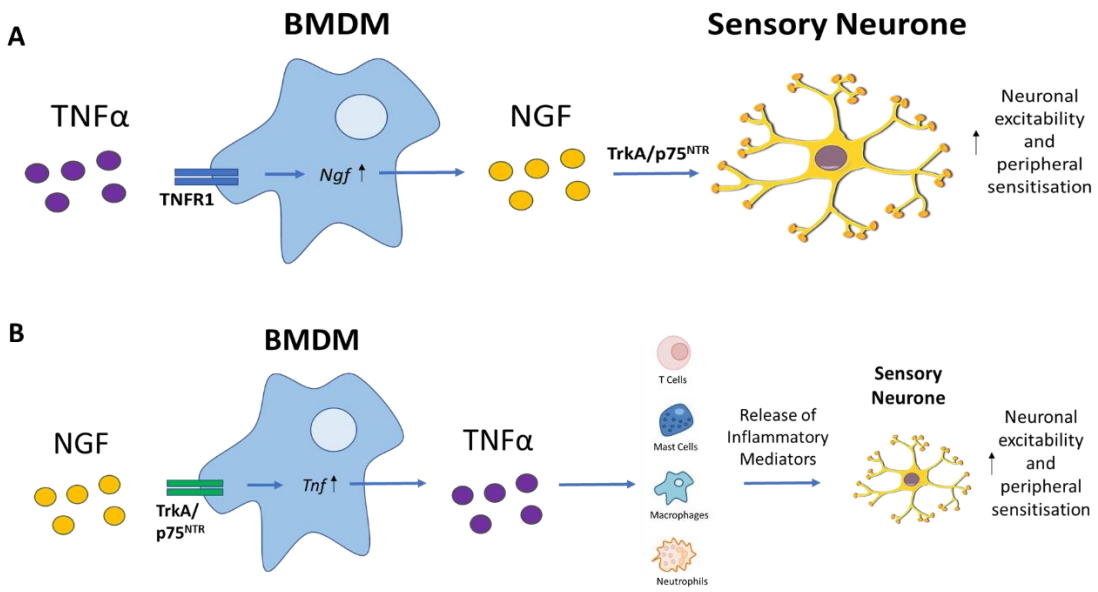

Figure 30. Schematic showing possible signalling pathways initiated by NGF/TNFα in BMDM leading to heightened pain states. A) TNFα causes a possible increase in *Ngf* expression and NGF secretion in BMDM (Takano and Uchida, 2017), the release of which may then act directly on the sensory neurone resulting in increased neuronal activity and contributing to pain states. B) NGF may cause a possible increase in *Tnf* expression and TNFα secretion in BMDM (Rina et al., 2001), the release of which may act on a variety of immune cell types causing the release of a range of inflammatory mediators which may act directly on the sensory neurone resulting in increased neuronal activity and contributing to pain states (Ji et al., 2014).

Abbreviations: NGF: nerve growth factor; TNFα: tumour necrosis factor alpha; BMDM: bone marrow-derived macrophages.

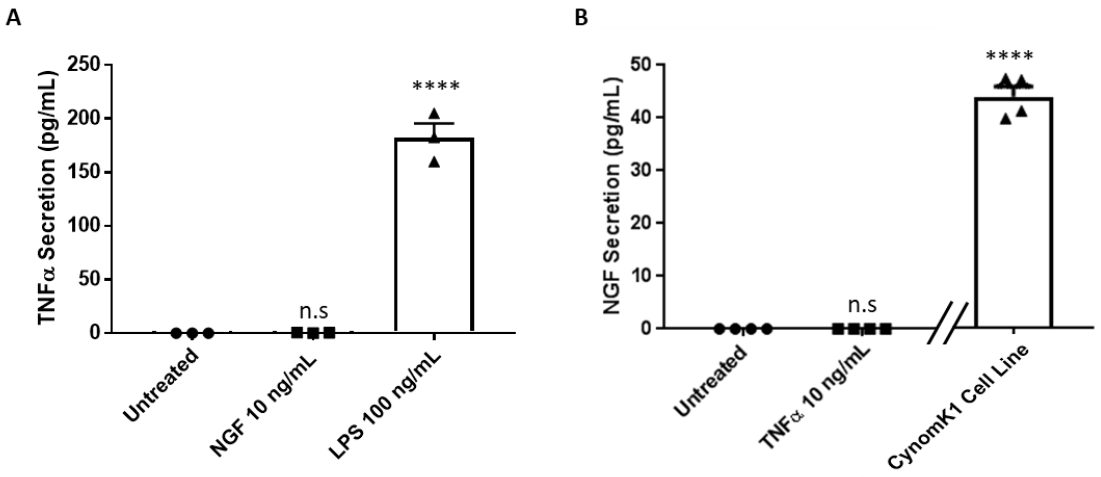

Figure 31. Levels of NGF or TNFα Secretion in cell culture supernatants of BMDM. A) Levels of TNFα secretion from BMDM in response to NGF (10 ng/mL, 24 h) and B) levels of NGF secretion from BMDM in response to TNFα (10 ng/mL, 24 h). Data displayed as Mean ± SEM, n=3-4 biological replicates (displayed as individual data points). Data were analysed using One-Way ANOVA followed by Tukey's multiple comparisons test. **** P<0.0001. Significance represents a change from the 'untreated' group.

Abbreviations: NGF: nerve growth factor; TNFα: tumour necrosis factor alpha; BMDM: bone marrow-derived macrophages; n.s: not significant.

4.4.6 TNFα (not NGF) Enhances Cytokine Secretion from BMDM in vitro

Diverse inflammatory mediators (other than NGF and TNFα) have been implicated in pain states, including IL-1β (as reviewed by (Ren and Torres, 2009)), KC/GRO (also known as CXCL1) (as reviewed by (Silva et al., 2017)) and IL-10 (as reviewed by (Ouyang et al., 2011)). Thus, we also determined whether macrophage release of these factors in response to NGF and TNFα treatment (24 h) could be observed. Due to the low n number, statistics were not performed in this instance, but there was a clear trend for TNFα to induce the secretion of IL-10, IL-1β and KC/GRO compared to the untreated group (increases of 6.03 pg/mL (fold change of 2.8), 8.26 pg/mL (fold change of 4.2) and 22.6 pg/mL (fold change of 4.1) respectively) (Figure 32A-C). This trend was also observed in the combination group. Consistent with the previous data presented, NGF at 10 ng/mL was found to have no detectable effect (Figure 32A-C). Levels of GM-CSF, TNFα, IL-6, MCP-1, MIP-1α and MIP-3α were also examined but were below detection levels (data not shown).

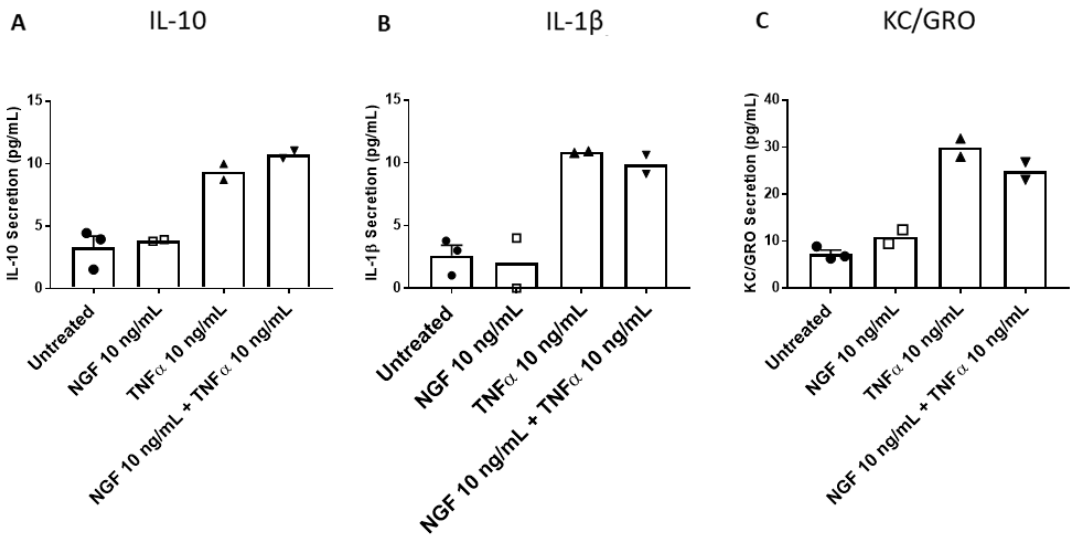

Figure 32. Modulation of BMDM cytokine release in response to NGF and TNFα. Levels of A) IL-10 secretion, B) IL-1β secretion and c) KC/GRO secretion from BMDM in response to NGF (10 ng/mL, 24 h, hollow squares) TNFα (10 ng/mL, 24 h, black triangles) or a combination of the two (10 ng/mL, 24 h, black upside-down triangles). Data displayed as Mean ± SEM, n=3 biological replicates for untreated group and n=2 biological replicates for all other treatment groups (displayed as individual data points). Lower limits of quantification (LLOQ) for these assays were 3.8 pg/mL (IL-10), 3.1 pg/mL (IL-1β) and 0.43 pg/mL (KC/GRO).

Abbreviations: NGF: nerve growth factor; TNFα: tumour necrosis factor alpha; BMDM: bone marrow-derived macrophages; IL-10: interleukin-10; IL-1β: interleukin-1β; KC/GRO: keratinocyte chemoattractant/growth-regulated oncogene.

4.4.7 TNFα Drives the Expression of a Number of Pain-Relevant Genes in BMDM

Since we observed only modest differences in a small panel of cytokines, we decided to study the effects of NGF, TNFα or a combination of the two (10 ng/mL) on a wide range of genes and examine BMDM modulation at the transcriptional level. To enable a broad analysis, a TaqMan array card with 45 known inflammatory genes (and 3 control housekeeping genes; *18s*, *β2m* and *Gapdh*) was employed. Figure 33 displays a heat map showing the relative overall expression levels of each gene in response to treatments. TNFα alone, or in combination with NGF, drove the upregulation of a number of genes, whereas NGF alone showed no effect on the expression of genes in this panel (Figure 33). The gene expression upregulation with TNFα was similar to that of TNFα in combination with NGF (Figure 33). Statistical analysis revealed a number of genes which were significantly upregulated following TNFα alone (or in combination with NGF) (Figure 34A); *Aif1, C3, Ccl12, Gpr84, Il-1β, Slfn2* and *Tnf* itself. The highest regulated gene was *C3* with an increase in ΔΔCt value of 8.88 ± 2.25 (n=4 biological replicates) from the baseline untreated group (Figure 34B), followed by *GPR84* with an increase in ΔΔCt value of 7.19 ± 0.61 (n=4 biological replicates) (Figure 34B), equating to a fold change of 470.8 and 146.4 respectively.

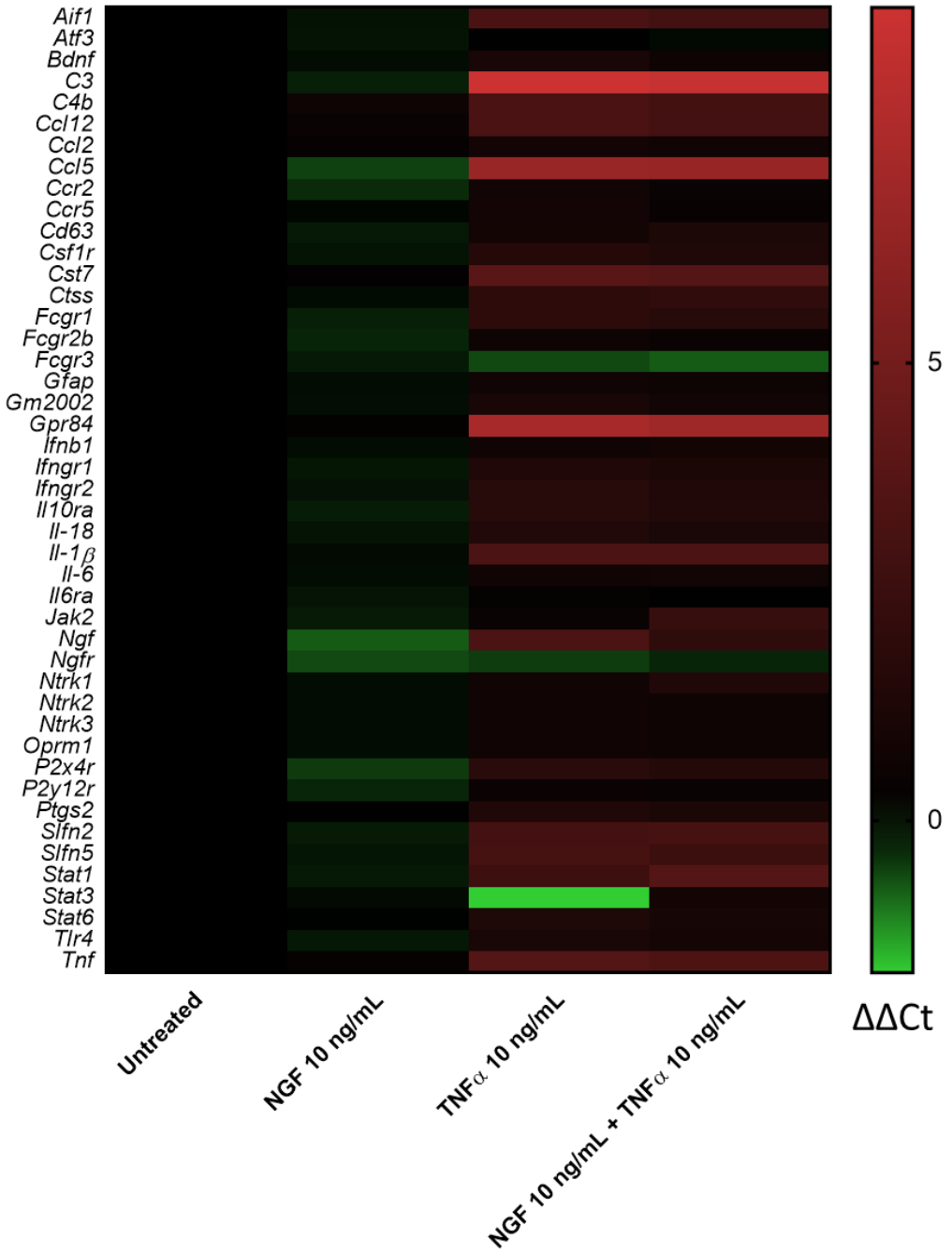

Figure 33. Heat map demonstrating the differential expression of mRNA transcripts in BMDM following 24 h treatment with NGF (10 ng/mL), TNFα (10 ng/mL) or NGF (10 ng/mL) + TNFα (10 ng/mL). Each row represents a different gene and each column represents a different treatment group. Data represents the average ΔΔCt value of 4 biological replicates. Red represents an upregulation in gene expression whereas green represents a downregulation in gene expression.

Abbreviations: NGF: nerve growth factor; TNFα: tumour necrosis factor alpha; BMDM: bone marrow-derived macrophages; further details of all genes examined can be found in the abbreviation list.

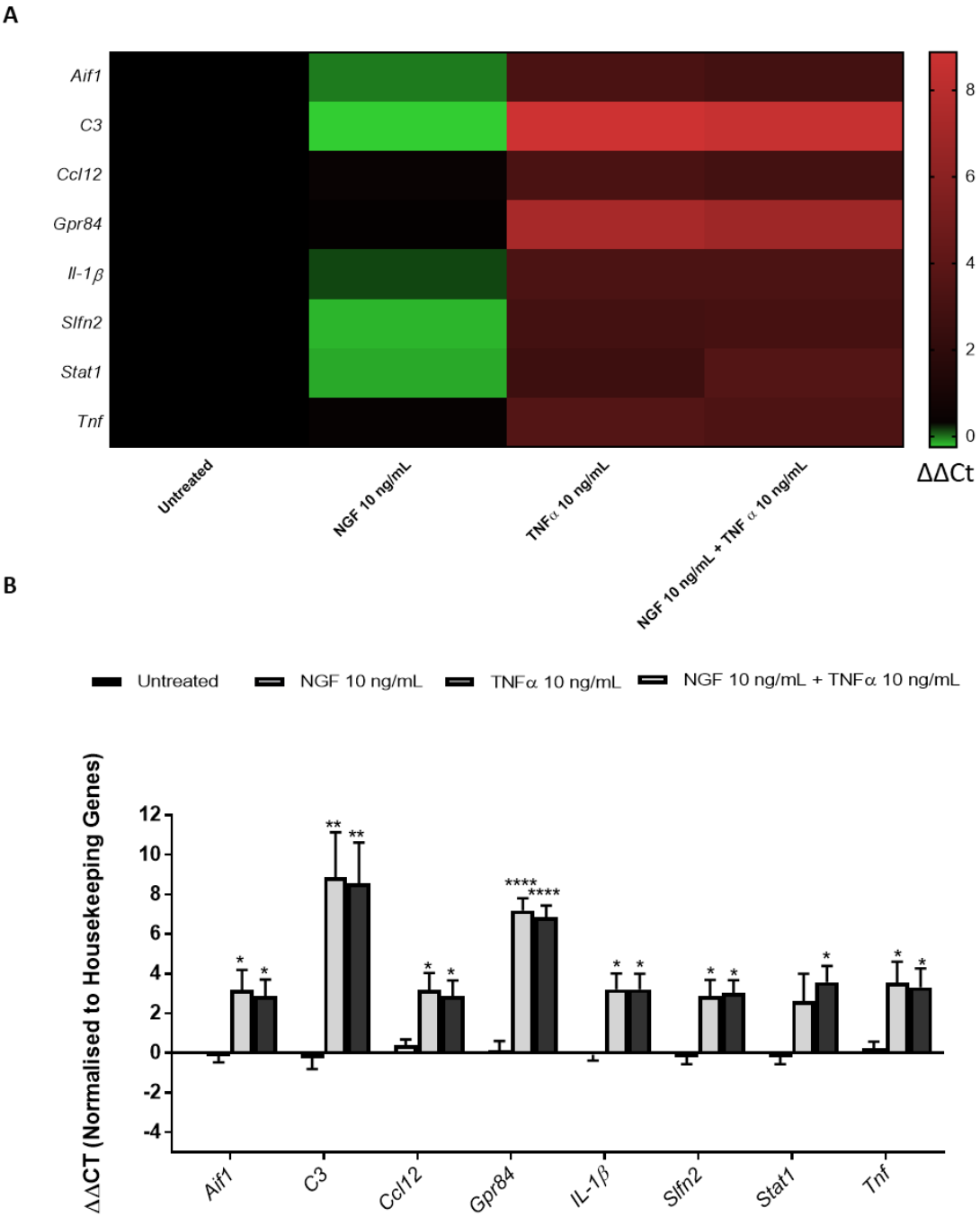

Figure 34. Genes significantly regulated by TNFα treatment. A) Heat map demonstrating the differential expression of mRNA transcripts in BMDM in genes that reached statistical significance. Each row represents a different gene and each column represents a different treatment group. B) Quantification of data in the above heat map. Data represents the average ΔΔCt value of 4 biological replicates displayed as Mean ± SEM. Data were analysed using LIMMA and adjusted for multiple comparisons. ****P<0.0001, **P<0.01, *P<0.05. Asterisks signify significance from the untreated group.

Abbreviations: NGF: nerve growth factor; TNFα: tumour necrosis factor alpha; BMDM: bone marrow-derived macrophages; *Aif1*: allograft inflammatory factor 1; *C3*: complement component 3; *Ccl12*: chemokine (C-C motif) ligand 12; *Gpr84*: G-protein coupled receptor 84; *IL-1β*: interleukin-1β; *Slfn2*: schlafen 2; *Stat1*: signal transducer and activator of transcription 1; *Tnf*: tumour necrosis factor; LIMMA: linear models for microarray data.

4.5 Discussion

Evidence in the literature (outlined in the introduction of this chapter) suggested that macrophages are a potential target for both NGF and TNFα and could be important in chronic pain states. Although we saw a convincing effect of TNFα on a number of pain-relevant read-outs in macrophages, this was not the case following macrophage stimulation with NGF. Furthermore, we saw no evidence that NGF could augment TNFα-driven responses of the macrophages.

In a range of culture models of adult murine macrophages (BMDM, peritoneal or activated peritoneal) the expression of *Ntrk1* was undetectable, and the presence of *Ngfr* only detectable at very low levels. Furthermore, despite reports demonstrating that the use of a pre-stimulus, such as LPS, could increase human macrophage *NTRK1* expression (Caroleo et al., 2001, Rina et al., 2001), we found that this was not the case in our hands. However, gene transcription is not directly correlated to the level of receptor protein expression, and therefore no firm conclusions may be drawn regarding the protein receptor expression level.

In line with this absence of receptor expression, no macrophage response to NGF was detected at either the transcriptional or protein level. This finding contrasted with the reported modulatory effect of NGF and TNFα on one another in this cell type (summarised in section 4.1). The viability assays performed also suggest that the lack of response seen from NGF treatment was not due to the deterioration of the health of the BMDMs. A recent study showed that although an increase in NGF expression was detected in injured intervertebral discs from C57Bl/6J mice, this was not reduced following macrophage depletion (Miyagi et al., 2018). This suggests that the changes observed in NGF expression were not mediated by macrophages in this instance.

One possible explanation for a lack of NGF effect seen could be that the *in vitro* model we have been utilising is too simplified. *In vivo*, macrophages will receive signals coming from multiple different cell types, which could modify their behaviour and modulate their receptor expression levels (Sica and Mantovani, 2012). Our *in vitro* model may be lacking a component which is critical for such a response.

Despite the lack of NGF effect observed, TNFα stimulation resulted in a range of pain-relevant changes, which the combination treatment mimicked closely. It was found that BMDMs stimulated with TNFα showed an increase in the release of KC/GRO, IL-1β and IL-10, an effect which is in line with the literature (Zhang and An, 2007).

KC/GRO is known to be involved in neutrophil chemotaxis (De Filippo et al., 2013) and has numerous links to pain (Zhang et al., 2013). It has been shown that both spinal nerve ligation and inflammation in the periphery induced a significant upregulation of KC/GRO in the DRG itself (Li et al., 2007, Xie et al., 2006). Furthermore, KC/GRO has been shown to directly modulate sensory neurone activity via increasing sodium current activity (Wang et al., 2008), inducing an increase in TRPV1 activity measured via patch clamp methods (Dong et al., 2012) and increasing NMDA receptor activity along with COX2 expression in spinal cord neurones via activation of CXCR2 (Cao et al., 2014). However, despite the above studies demonstrating a pro-nociceptive effect of KC/GRO, one study has demonstrated a potential anti-nociceptive role for this chemokine. It was found that a spinal nerve ligation induced a significant increase in KC/GRO only in CD40 knock-out mice, and injection of KC/GRO in wild-type mice significantly reduced the mechanical hypersensitivity usually seen in this model of neuropathic pain (Malon and Cao, 2016). The above demonstrates that regulation of KC/GRO

through TNFα may be a crucial component in the pathway that allows intricate communication between non-neuronal cell types and neurones in pain states.

The pro-inflammatory actions of IL-1β have been extensively described in a number of therapeutic areas (Dinarello, 2011). TNFα is known to stimulate the production of IL-1β, as confirmed in this dataset (at mRNA and protein level), and together they recruit and activate a number of non-neuronal cell types, including macrophages (Nadeau et al., 2011), further potentiating the inflammatory cascade. Injection of IL-1β itself results in both thermal and mechanical hyperalgesia (Fukuoka et al., 1994) and models of inflammatory pain, such as the use of CFA, are associated with a significant increase of IL-1β (Safieh-Garabedian et al., 1995). Interestingly, the latter study demonstrated a crucial role for IL-1β in the upregulation of NGF and associated hypersensitivity in these inflammatory states, an effect which could be prevented via the use of an IL-1 receptor antagonist. This suggests an alternative way in which TNFα may be able to modulate NGF signalling. Disrupting IL-1β signalling has been shown to be an effective method in the clinic to improve a number of inflammatory conditions (Dinarello et al., 2012). Currently, a number of methods are employed; an IL-1 receptor antagonist (anakinra) (Arend, 2002), a soluble decoy receptor (rilonacept) (Hoffman et al., 2008) and a neutralising monoclonal antibody directed again IL-1β (canakinumab) (Dhimolea, 2010). It has been shown that patients with rheumatoid arthritis have a reduced intimal layer macrophage accumulation following treatment with anakinra, an effect associated with the halt of progressive joint damage (Cunnane et al., 2001). Furthermore, these patients report a significant improvement in their pain scores (visual analogue scale), disease activity and number of swollen/tender joints (Bresnihan et al., 1998). Patients suffering from Schnitzler syndrome, a systemic inflammatory disease, benefit greatly from treatment with both

anakinra and canakiumab (Szturz et al., 2011). Additionally, the blockade of IL-1β signalling in auto-inflammatory diseases has shown a significant improvement in patients reported pain, in conjunction with a marked reduction in levels of pro-inflammatory markers (Jesus and Goldbach-Mansky, 2014).

In contrast to IL-1β and KC/GRO, IL-10 is traditionally considered an anti-inflammatory cytokine that is produced in response to inflammatory insults to try and bring the system back into balance where possible. It has previously been shown that IL-10 application, to a macrophage cell line as well as peritoneal macrophages, results in a reduction in both secretion and expression of TNFα (Fiorentino et al., 1991). Additionally, IL-10 has been shown to be significantly upregulated following chronic constriction injury (Okamoto et al., 2001) as well as in the CFA model of inflammatory pain (Chen et al., 2010). Our data supports the upregulation of IL-10 following an insult (in our case TNFα stimulation).

At the transcriptional level, TNFα significantly upregulated several pain-relevant genes, the involvement in pain states are briefly described below:

Aif1 is also known as ionised calcium-binding adapter molecule 1 (*Iba1*) and encodes for a protein that is specifically expressed in macrophage and microglia. Aif1 is upregulated following activation in pain models, such as peripheral nerve injury (PNI) and chronic constriction injury (CCI) (Romero-Sandoval et al., 2008, Li et al., 2013, Patro et al., 2010). These studies highlight the importance of TNFα in this activation pathway and in the subsequent production of a pro-inflammatory feedback loop which could be crucial in maintaining a painful state.

C3 is a gene that encodes for the complement component 3 protein. This plays a crucial role in the activation of the complement system which is vital in contributing to innate immunity

(Ricklin et al., 2010). It has previously been described that abnormal activation of this protein, in the spinal dorsal horn of the spinal cord in rats which had undergone PNI, leads to a cascade reaction of other complements that are involved in the development of hyperalgesia (Nie et al., 2013). Additionally, mice lacking *C3* demonstrated a 2-fold increase in sensory axon regeneration within the spinal cord, following a peripheral conditioning lesion, compared to wildtype mice (Peterson et al., 2017). The administration of C3a into the cerebral ventricles of mice resulted in the inhibition of morphine induced analgesia (Jinsmaa et al., 2000). It has been shown that mice infected with Ross River Virus (RRV), leading to severe inflammation of bones, joints and skeletal muscle tissue, develop considerably less severe symptoms when deficient in C3 (Morrison et al., 2007). Furthermore, it has previously been shown that both C3a and C5a (an additional complement component protein) upregulates expression of NGF mRNA in rat astrocytes (Jauneau et al., 2006), once more highlighting the important role of non-neuronal cell types.

Although in our work the expression levels of *C5a* were not examined, recent work outlines a possible mechanism for C5a induced thermal hyperalgesia (Shutov and Warwick, 2016). The authors suggest that C5a can produce thermal hyperalgesia via macrophage-dependent NGF mobilisation which then allows the subsequent NGF-dependent sensitisation of TRPV1. Based on the above study, the secretion of C5a protein was examined via ELISA following TNFα treatment of BMDM (data not shown), however no presence of C5a was detectable.

The *Ccl12* gene encodes for a cytokine that belongs to the chemokine family within mice and has many similarities with the human chemokine MCP-1. In agreement with our data, it has been shown to be significantly upregulated at the mRNA level in activated macrophages where it may act as a potent chemoattractant for peripheral blood monocytes (Sarafi et al.,

1997). The expression of *Ccl12* has previously been identified as being significantly upregulated in rat cartilage of the knee joint in the monosodium iodoacetate (MIA) chronic pain model (Dawes et al., 2013). Its human analogue, MCP1, has been implicated in the pathophysiology of fibromyalgia (Ang et al., 2011) and in the maintenance of chronic pain states in a murine urinary tract infection model (Rosen et al., 2018).

The *Gpr84* gene encodes an orphan receptor, known to be upregulated in inflammatory conditions (Suzuki et al., 2013, Bouchard et al., 2007, Oh and Lagakos, 2011). The exact physiological function of GPR84 has remained elusive but its role in pain mechanisms has recently been dissected. It has been found that GPR84 knock-out mice exhibited normal pain behaviours in response to acute stimuli, but were unable to develop either mechanical or thermal hypersensitivity in response to partial sciatic nerve ligation (PNL) (Nicol et al., 2015). The authors concluded that the GPR84 receptor contributes to nociceptive signalling via the modulation of macrophages, with GPR84 knockout mice resulting in an impaired pro-inflammatory response from macrophages. In line with the above, a recent study has demonstrated that activation of the GRP84 receptor in murine macrophages results in enhanced levels of several inflammatory mediators, including TNFα, IL-6, IL-12B, CCL2, CCL5 and CXCL1 (Recio et al., 2018). TNFα stimulated macrophages could therefore be contributing to a pain state via the GPR84 driven pro-inflammatory response.

The SLFN2 protein has been implicated in a number of functions, including cell growth, differentiation and contributing to the immune response (Mavrommatis et al., 2013). A recent study has demonstrated a crucial role for SLFN2 in modulation of T cell quiescence via regulation of cholesterol levels and endoplasmic reticulum stress (Williams et al., 2015). In line with above, mice with *Slfn2* mutations have fewer naïve T cells, reduced responsiveness

to IL-7 (a crucial regulator of T cells (Bradley et al., 2005)) and increased apoptotic signals (Sprent and Surh, 2011). These results are corroborated by data suggesting that mice with a mutation encoding SLFN2 are more susceptible to both viral and bacterial infections (Berger et al., 2010). SLFN2 protein has also recently been demonstrated to be involved in the control of IFN-stimulated genes and the subsequent regulation of IFN-mediated biological responses via modulation of the NFκB pathway (Fischietti et al., 2018). It has been shown that ablating IFNγ receptors significantly impairs nerve injury induced microglia activation and the associated tactile allodynia (Tsuda et al., 2009), suggesting a potential link between *Slfn2* and pain behaviours.

Stat1 is a gene that encodes a transcription factor which plays an important role in both IFNα and IFNγ signalling (Schindler et al., 2007). Macrophages lacking STAT1, display an attenuation of the TLR-induced production of inflammatory cytokines, such as TNFα (Kim et al., 2015). TNFα itself can activate an IRF1-dependent autocrine loop leading to a sustained expression of chemokines and STAT1-dependent type 1 interferon response genes (Yarilina et al., 2008b) Furthermore, levels of both STAT1 mRNA and protein have been shown to be upregulated in isolated microglia following spinal nerve injury in mice (Denk et al., 2016). The above studies therefore suggest a potential crucial role of STAT1 in the generation and maintenance of pain states.

It is well known that TNFα can result in an increased expression of itself (Parameswaran and Patial, 2010), an effect that we also see in our data set. However, the increase in TNFα production may also be due to the upregulation of a number of other pro-inflammatory cytokines, as described above, leading to a sustained inflammatory environment.

Although the effect of NGF treatment was below the detection threshold in our macrophage cultures, the reported effects of TNFα in this chapter strongly suggest a crucial role for both TNFα and macrophages in pain signalling. Furthermore, given the lack of an effect of TNFα seen in neurones within the first data chapter, the data presented above suggest a more plausible hypothesis of an indirect effect of TNFα on sensory neurones, via a non-neuronal cell type which could potentially drive chronic pain states.

It is noted that the primary read out of gene expression in this chapter, may not be taken as a direct indicator of protein expression. Future work could investigate the levels of protein expression in addition to the regulation of gene expression which is reported within this chapter.

4.6 Summary of Chapter

In summary, the data presented in this chapter suggest that TNFα is capable of modulating macrophage responses, while NGF does not show a direct effect in this particular cell type. In BMDM, we have demonstrated that TNFα can produce a strong and reproducible effect in a number of pain-relevant read-outs, including phospho-p38 activation, enhanced cytokine secretion and an increase in the expression of a number of pain-relevant genes. In contrast, NGF failed to produce any notable effects on the same readouts. The latter findings are in line with the receptor expression work we have reported. Once more, the lack of any additive or synergistic effects of the two inflammatory mediators on macrophages, suggest that this cell type is unlikely to be the sole site of action of the NGF/TNFα dual blockers which we have seen can deliver superior analgesic efficacy.

5. Investigating the Individual and Combined Effect of NGF and TNFα in a Co-Culture System of Sensory Neurones and Macrophages *In Vitro*

5.1 Introduction

Our previous data demonstrates that BMDM express high levels of *Tnfrsf1a*, whereas their expression of NGF receptors (*Ntrk1* and *Ngfr*) is low or absent. However, the situation in sensory neurones is much the converse, with only low levels of *Tnfrsf1a* expression and high levels of *Ntrk1* and *Ngfr* expression (Figure 35A). Therefore, any potential interaction between NGF and TNFα is unlikely to be occurring at the level of an individual cell type.

This chapter will focus on the optimisation of a co-culture system between sensory neurones and macrophages, two cell types which we have seen can respond to NGF and TNFα, respectively. We believe a co-culture of these two cell types, both of which are known to have critical roles in chronic pain signalling (Cheng and Ji, 2008, Ristoiu, 2013, Pinho-Ribeiro et al., 2017a), can provide a proxy of the DRG *in vivo* in such disease states. Furthermore, given the apparent selectivity of the sensory neurone to NGF, and the macrophage to TNFα, a co-culture can provide a useful system in which to assay any additive or synergistic pain-relevant effects of these two algogenic factors.

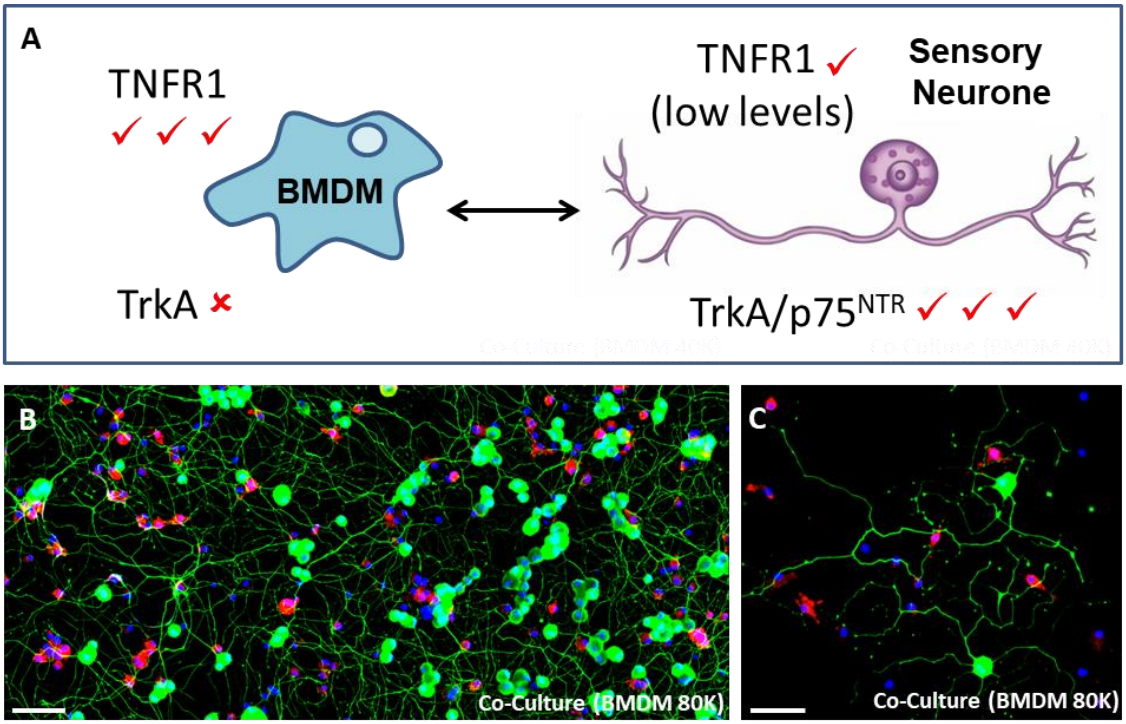

Figure 35. Rationale for and development of a co-culture of sensory neurones and macrophages. A) Schematic representing the rationale behind a co-culture set-up, focussing particularly on the levels of NGF and TNFα receptors in each cell type (adult DRG sensory neurone or BMDM). B-C) Representative fluorescent micrographs following immunostaining with the neuronal marker β-III tubulin (green), macrophage associated marker IBA1 (red) and the nuclear stain DAPI (blue) with BMDM plated at 80K cells/well. Scale bar represents 50 µM.

Abbreviations: NGF: nerve growth factor; TNFα: tumour necrosis factor alpha; DRG: dorsal root ganglia; BMDM: bone marrow-derived macrophages; IBA1: ionised calcium-binding adapter molecule 1; DAPI: 4',6-diamidino-2-phenylindole.

5.2 Aims and Experimental Strategy

The aims of this chapter are to test the hypothesis that:

- Additive or synergistic pain-relevant effects of NGF and TNFα can be detected in a system where sensory neurones and macrophages can communicate with one another

Specifically, we aim to:

- to develop a direct co-culture system between sensory DRG neurones and BMDM
- to utilise the above co-culture system to further elucidate the interaction between NGF and TNFα *in vitro* on pain-relevant readouts
- to determine the effect of BMDM-derived conditioned medium (CM) on DRG neurones *in vitro* on pain-relevant readouts

The results presented below originate from the use of the following key assays to assess the effect of NGF/TNFα in this system: levels of stimulus-evoked sensory neuronal CGRP release, levels of stimulus-evoked IL-1β release, quantification of mRNA transcripts (for a panel of inflammatory and pain-related genes) and determination of sensory neuronal calcium levels.

In addition to using direct co-culture methods (where cells exist in direct cell-cell contact), data is also presented from the effect of BMDM-derived CM on purified DRG neuronal cultures. This allows us to identify if any changes in pain-relevant readouts occur in sensory neurones as a result of secreted factor(s) from macrophages. Additionally, this method removes the complication of a secondary cell type being physically present in the neuronal culture and the corresponding biological variation associated with this physical contact.

5.3 Methods

All animals were obtained from Charles River and housed in a designated facility and maintained in accordance with the United Kingdom Home Office Animals (Scientific Procedures) Act (1986) and Home Office regulations. Animals were kept in a 12 h light dark cycle and fed *ad libitum*. All animals were sacrificed using schedule 1.

5.3.1 Mixed DRG Neuronal/Glia and BMDM Co-Cultures

All direct co-culture experiments were undertaken using mixed DRG neuronal/glia cultures to enable a high enough cell yield for subsequent assays described. Both cell type cultures (mixed DRG neuronal/glia cultures and BMDM cultures) were carried out as previously described (sections 3.3.1.1 and 4.3.1.1). Neurones were plated at 8K/well in 100 µL BS medium on pre-coated poly-D-lysine coated Greiner 96 well plates incubated with laminin diluted 1:50 in basal F12 for at least 2 h. Mixed DRG neuronal/glia cultures were left to settle overnight prior to the addition of BMDM the following day. BMDM were added to the culture at a density of either 20K cells/well, 40K cells/well or 80K cells/well in 50 µL BS medium. These cell densities were based on reports in the literature that had utilised macrophage co-cultures *in vitro* (Dobbertin et al., 1997, Kwon et al., 2015, Massier et al., 2015). Additionally, it has been shown that the number of macrophages infiltrating the DRG, following transection of the sciatic nerve *in vivo*, increases 3-fold in the initial days following injury and up to 10-fold compared with control DRGs at day 7 post-injury (Kwon et al., 2013). The two cell types were acclimatised to one another overnight prior to any experimental protocols taking place.

5.3.2 LDH Viability Assay

To determine that the mixed DRG neuronal/glia + BMDM co-cultures were healthy and remained viable, we quantified viability using the Pierce LDH Cytotoxicity Assay Kit (ThermoFisher Scientific, 88953 88954). This assay is a colorimetric method used to quantify the level of lactate dehydrogenase (LDH) in the supernatant of samples, an indicator of cellular toxicity (Weyermann et al., 2005). Briefly, direct co-cultures (7-8K neurones/well + 80K BMDM) were treated with TNFα 10 ng/mL, staurosporine (as positive control for cell death), or with the kit supplied lysis solution (an additional positive control) for 48 h. 50 µL of culture supernatant was transferred to a new flat-bottomed, clear 96-well plate and an equal volume of reaction mixture added (0.6 mL of Assay Buffer with 11.4 mL of Substrate Mix). The above reaction was incubated at RT for 30 min before 50 µL of stop solution was added, taking care to avoid bubbles. Absorbance was measured at both 490 nm and 680 nm on FLUOstar Omega plate reader (BMG Labtech). LDH activity was determined via the subtraction of the 680 nm absorbance value from the 490 nm absorbance to remove background signal from the instrument.

5.3.3 Enzyme Immuno Assay to Quantify CGRP Release

Levels of CGRP in culture supernatants from mixed DRG neuronal/glia cultures, the co-culture system and BMDM alone were examined using SPI Bio's Rat CGRP EIA kit (SPI Bio/Bertin Pharma, A05482) as previously described in section 3.3.5, with the following changes:

At the point of stimulation, performed in either duplicate or triplicate, 50 µL of culture supernatant was removed (leaving 100 µL of culture supernatant) and a 6X stock of the desired concentration of stimulators (NGF, TNFα, or a combination of the two) added in a volume of 20 µL BS medium. Cultures were stimulated for 48 h (see Table 8 for details). On

the day of the CGRP release assay, culture supernatants were removed and cultures were challenged with either 100 µL 25 mM K^+ solution (made as previously described in section 3.3.5), 100 nM capsaicin (Sigma Aldrich, 50 mg stock, M2028-50MG) or 31.25 µM veratridine (Sigma Aldrich, 10 mg stock, V5754-10MG) made up in 1X HBSS, followed by a 30 min incubation at 37 °C for both high K^+ and capsaicin and a 10 min incubation at 37 °C for veratridine.

Table 8. Table of concentrations of NGF and TNFα used throughout the CGRP release experiments.

NGF Concentration	TNFα Concentration	
	0 ng/mL	10 ng/mL
0 ng/mL	✓	✓
0.1 ng/mL	✓	✓
1 ng/mL	✓	✓
10 ng/mL	✓	✓

5.3.4 Gene Expression Analysis of Purified DRG Neurones after Treatment with BMDM-Derived Conditioned Medium

To further examine the possible relationship between DRG sensory neurones and BMDM, a series of CM experiments were performed. Throughout these experiments purified DRG neuronal cultures were utilised.

5.3.4.1 Purified DRG Neuronal Cultures

Following the culture and purification of adult mouse DRG neurones (as previously described in section 3.3.1.2), purified DRG neuronal cultures were plated on Poly-L-lysine coated 13 mm

coverslips placed in a 4 well plate incubated with growth-factor reduced matrigel as previously described. Initially, purified DRG neurones were plated at a density of approximately 5000 cells/well in a small volume (80 µL) of B27 medium. Following a time period of 1 h to allow for the attachment of the purified DRG neurones, 500 µL BMDM-derived CM was added and cells allowed to incubate at 37 °C for 24 h prior to RNA collection.

5.3.4.2 BMDM-Derived Conditioned Medium Collection and Transfer to Purified DRG Neuronal Cultures

CM was collected from BMDM which had been cultured as previously described (section 4.3.1.1). Following the 7-day differentiation period, BMDM were re-plated in a 24-well plate at a density of either 40K cells/well or 80K cells/well. BMDM then received media only (control) or TNFα (10 ng/mL) for 24 h. Following this time period, the CM was removed from the BMDM and centrifuged at 212 *g* for 5 min (Hettich Zentrifugen) to remove any cellular debris. Purified DRG neuronal cultures could then be treated with one of the following conditions for 24 h:

1. Untreated, no BMDM control (media only)
2. TNFα (10 ng/mL), no BMDM control (media with TNFα)
3. CM from untreated BMDM plated at 40K cells/well
4. CM from TNFα (10 ng/mL) treated BMDM plated at 40K cells/well
5. CM from untreated BMDM plated at 80K cells/well
6. CM from TNFα (10 ng/mL) treated BMDM plated at 80K cells/well

Following the addition of CM to the purified DRG neuronal cultures, one set of wells received no further treatment whereas the second set of wells received an additional stimulation with NGF (10 ng/mL). This enabled us to test whether the neuronal action of NGF could summate

with the TNFα effect on BMDM and therefore further contribute to pain signalling pathways. Wells which did not receive NGF, had the Trk-Inhibitor (Sigma Aldrich, PZ0254) added at a concentration of 200 μM to prevent any basal NGF signalling occurring.

5.3.4.3 RNA Collection, Amplification and Qubit Quantification

Following the 24 h neuronal treatment period, RNA was collected using the Qiagen RNAeasy Micro Kit and samples checked for quantity and quality on the Agilent 2100 Bioanalyzer instrument as previously described (section 3.3.4.1). Only samples with a RIN < than 7 were taken forward for further analysis.

Due to the relatively low number of purified DRG neurones plated, it was necessary to amplify the sample material to be able to run the samples on custom made TaqMan 384-well PCR array microfluidic cards (Applied Biosystems).

Amplification of cDNA samples was performed using the REPLI-g® WTA Single Cell Kit (Qiagen, 150065). Briefly, 3 μL of NA Denaturation Buffer was added to 8 μL of purified RNA in a microcentrifuge tube. The resulting product was mixed by vortexing and incubated at 95 °C for 3 min. Subsequently, 2 μL of gDNA Wipeout Buffer WTA was added and incubated for a further 10 min at 42 °C. During this latter incubation, the Quantiscript RT mix was prepared fresh as outlined in Table 9, before 7 μL were added to the lysed cell sample. After being vortexed, this solution was incubated at 42 °C for 60 min;

Table 9. Table displaying the components and associated volumes for the Quantiscript RT mix.

Component	Volume/reaction
RT/Polymerase Buffer	4 µL
Random Primer	1 µL
Oligo dT Primer	1 µL
Quantiscript RT Enzyme Mix	1 µL
Total volume	7 µL

To stop the reaction, samples were incubated at 95 °C for 3 min before being cooled on ice. At this stage, 10 µL ligation mix was added and the resulting mix was vortexed and incubated for 24 °C for 30 min. The ligation mix was prepared as shown in Table 10:

Table 10. Table displaying the components and associated volumes for the ligation mix.

Component	Volume/reaction
Ligase Buffer	8 µL
Ligase Mix	2 µL
Total volume	10 µL

To stop the reaction, samples were incubated at 95 °C for 5 min. Following this step, the REPLI-g SensiPhi amplification mix was prepared (as shown in Table 11), 30 µL added to the solution from above and the resulting mix vortexed and incubated at 30 °C for 2 h.

Table 11. Table displaying the components and associated volume for the REPLI-g SensiPhi amplification mix.

Component	Volume/reaction
REPLI-g sc Reaction Buffer	29 µL
REPLI-g SensiPhi DNA Polymerase	1 µL
Total volume	30 µL

The above reaction was stopped by incubating at 65 °C for 5 min. Amplified cDNA was stored at -20 °C until ready for cDNA quantification and downstream use.

cDNA was quantified using the Qubit dsDNA Broad Range Assay Kit (ThermoFisher Scientific, Q32853) and read on the Qubit Fluorometer (ThermoFisher, Scientific) as illustrated below (Figure 36).

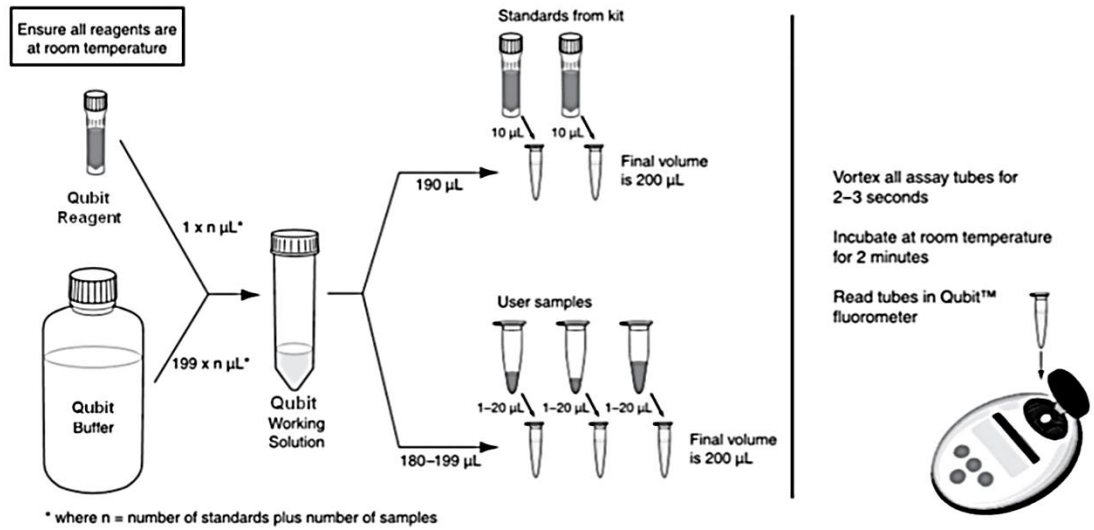

Figure 36. Schematic detailing the process of cDNA quantification using Qubit technology (ThermoFisher).

5.3.4.4 RT-qPCR

Custom made TaqMan 384-well PCR array microfluidic cards (Applied Biosystems) were used to analyse the effect of CM on purified DRG neurones. These were composed of 48 pain-related gene transcripts simultaneously, including three housekeeping genes; *18s*, *Ywhaz* and *Gapdh*. See Table 12 for full list of gene transcripts quantified. Sample cDNA was diluted to 6 ng/mL in 50 µL molecular grade water before a TaqMan universal PCR master mix (Applied Biosystems, 4304437) was added at a 1:1 ratio to give a final volume of 100 µL. Each custom card held eight cDNA samples and was allowed to acclimatise to RT prior to loading. Once thoroughly mixed, 95 µL of the sample mix was loaded into the corresponding channel and centrifuged at 158 *g* for 1 min (Sorvall ST 40 Centrifuge) twice. The card was sealed, and the entry wells removed prior to the card being run on the ABI 7900HT Real Time PCR instrument (Applied Biosystems, serial number: 201276). The following cycling conditions were used: 25 °C for 10 min, 42 °C for 60 min and 85 °C for 5 min.

5.3.4.5 Data Analysis

mRNA transcripts were normalised to the expression of the housekeeping genes (*18s*, *YWhaz* and *Gapdh*) using the ΔΔCt method and data expressed as ΔΔCt changes from the basal condition.

Table 12. List of gene transcripts included on the PCR TaqMan card (DRG pain-related). Housekeeping genes are highlighted in bold font.

Gene Transcripts						
Adcyap1	*Ccl20*	*Cxcl12*	*Il-1ß*	*Npy*	*Scn10a*	*Trpa1*
Areg	*Ccl3*	*Ereg*	*Il-6*	*Ntrk1*	*Scn11a*	*Trpv1*
Atf3	*Ccl4*	*Gal*	*Il-6ra*	*Ntrk2*	*Scn9a*	*Vgf*
Bdnf	*Ccl5*	*Gch1*	*Il-6st*	*Ntrk3*	*Stat3*	***18s***
Cacna2d1	*Csf1*	*Il-11*	*Ngf*	*Oprm1*	*Tac1*	***Ywhaz***
Calca	*Csf2ra*	*Il-17a*	*Ngfr*	*P2xr3*	*Tlr4*	***Gapdh***
Ccl2	*Csf3*	*Il-18*	*Nos1*	*P2xr4*	*Tnf*	

5.3.5 Gene Expression Analysis of Direct Co-Cultures of Mixed DRG Neuronal/Glia Cultures with BMDM

Direct co-cultures between mixed DRG neuronal cultures and BMDM were set-up as previously described (section 5.3.1). These experiments followed the exact timeline of those of the CGRP assay (section 5.3.3) to align experimental results. Following the 48 h stimulation period (with NGF, TNFα or a combination of the two) samples were collected, the RNA extracted and amplified and cDNA measured on the Qubit as previously described (section 5.3.4.3). Samples were run on the same pain-related custom made TaqMan 384-well PCR array microfluidic cards as for the CM experiments (section 5.3.4.4).

5.3.5.1 Data analysis

mRNA transcripts were normalised to the expression of the housekeeping genes (*18s*, *Ywhaz* and *Gapdh*) using the ΔΔCt method and data expressed as ΔΔCt changes from the basal condition.

5.3.6 IL-1β ELISA

Levels of IL-1β secretion in mixed DRG neuronal/glia cultures, BMDM cultures or mixed DRG neuronal/glia + BMDM co-cultures in response to NGF (10 ng/mL, 48 h), TNFα (10 ng/mL, 48 h) or NGF + TNFα (10 ng/mL, 48 h) were examined using a Mouse IL-1β ELISA kit (R&D Systems, DY401-05). A 96-well microplate was coated with 100 µL/well of the Mouse IL-1β Capture Antibody at a working concentration of 4 µg/mL, diluted in PBS without carrier protein. The plate was sealed and left to incubate overnight at RT. The plate was washed three times with 400 µL of wash buffer and then blocked via the addition of 300 µL/well of Reagent Diluent for 1 h at RT. The wash step described above was repeated. 100 µL of either standard (1000 pg/mL, 500 pg/mL, 250 pg/mL, 125 pg/mL, 62.5 pg/mL, 31.25 pg/mL, 15.6 pg/mL or 0 pg/mL) or sample diluted in Reagent Diluent were added to the plate and incubated for 2 h at RT. The wash step was repeated. Subsequently, 100 µL/well of the Mouse IL-1β Detection Antibody, diluted to a working concentration of 500 ng/mL in Reagent Diluent, was added to the plate and incubated for 2 h at RT. The wash step was repeated. 100 µL/well of Streptavidin-HRP, diluted 1:40 in Reagent Diluent, was added to the plate and incubated for 20 min at RT, protected from direct sunlight. Following a final wash step, 100 µL of Substrate Solution was added to the plate and incubated for 20 min at RT (protected against direct sunlight). To stop the reaction, 50 µL/well of Stop Solution was added to the plate and the absorbance measured.

5.3.6.1 Data Analysis for IL-1β ELISA Data

The absorbance was read at 450 nm and 540 nm on a FLUOstar Omega microplate reader (BMG Labtech). Readings at 540 nm were subtracted from the readings at 450 nm to correct for optical imperfections in the plate. The absorbance values of the standards were used to plot a standard curve, from which absorbance values of experimental samples were interpolated to determine their concentrations.

5.3.7 Calcium Imaging

Following the culture and purification of adult mouse DRG neurones, purified DRG neuronal cultures were plated on Poly-L-lysine coated 13 mm coverslips placed in a 4 well plate incubated with growth-factor reduced matrigel as previously described (section 3.3.1.2). Initially, neurones were plated at a density of ~1500 cells/well in a small (10 µL) volume of B27 medium. Following a time period of 30 min to allow for the attachment of the purified DRG neurones, 500 µL BMDM-derived CM was added and allowed to incubate at 37 °C for 24 h prior to calcium imaging. BMDM-derived CM was collected as previously described and the treatment groups remained the same (for CM experiments BMDM were used at a density of 80K cells/well).

Calcium imaging was performed as previously described (section 3.3.6). To determine if the CM was able to sensitise the purified DRG neurones, the response to capsaicin 50 nM was determined. Both capsaicin and KCl solutions were made up in the previously described physiological solution. The protocol followed is illustrated in the below schematic (Figure 37).

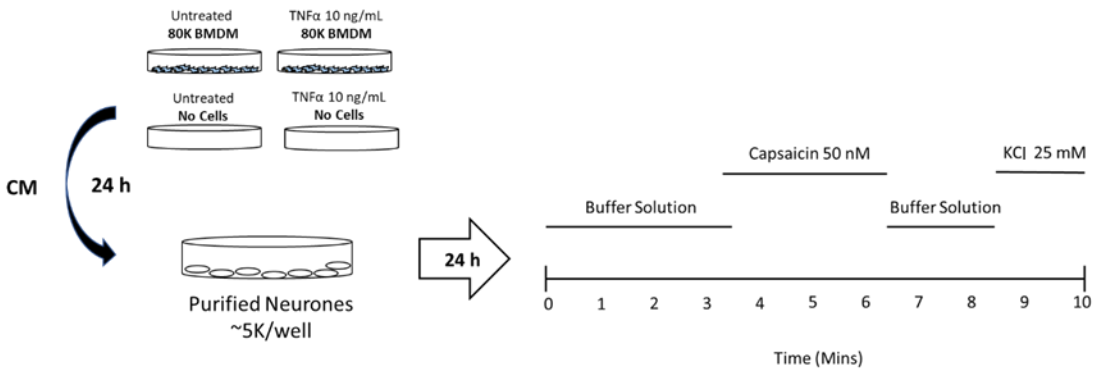

Figure 37. Schematic displaying the timeline of the CM experiments and the associated calcium imaging protocol.

5.3.7.1 Data Analysis for Calcium Imaging Experiments

Images were extracted from the Easy Ratio Pro software as Tiff files and further image processing was undertaken using ImageJ Version 1.8. In order to generate traces of calcium signals from time lapse images, cell bodies of neurons were circled using the oval selection tool in ImageJ. Cell bodies were circled with minimal overlap where possible. To generate normalised data (as neurones show differences in their baseline fluorescence), the baseline period (at least 3 min) of fluorescence for each cell and changes from this baseline fluorescence were calculated as ΔF/F.

$$\frac{\Delta F}{F} = \frac{Ft - F0}{F0}$$

Where F_t is the fluorescence at time t and F_0 is the fluorescence average over a baseline period.

5.3.8 Statistical Analysis

All statistical analysis was performed using GraphPad software (version 7.04). Prior to any statistical analysis taking place, the data were tested for normality using the Shapiro-Wilk normality test. Within this chapter, all data was analysed using the following statistical tests; Two-tailed t-tests, One-Way ANOVA, Two-Way ANOVA or LIMMA (for the TaqMan card data)

followed by *post-hoc* correction tests for multiple comparisons. In all instances, data are displayed as Mean ± SEM, n numbers and specific *post-hoc* correction tests used are reported within the figure legend. A P value <0.05 was considered to be significant.

5.4 Results

5.4.1 Direct Co-Culture Viability is Comparable to that of Mixed DRG Neuronal/Glia Cultures

Following the culture of mixed DRG neuronal/glia and BMDM together, a number of methods were employed to determine that no significant detrimental effects (of macrophage presence on neuronal health) were occurring. The % of cell death was examined in a mixed DRG neuronal/glia culture vs a mixed DRG neuronal/glia + BMDM co-culture and analysed using a Two-Way ANOVA. A significant treatment effect was observed ($F(2,12)=89.23$, $P<0.0001$), with the positive control of staurosporine producing a significant increase in cell death (Figure 38A, B and C). In a naïve state, *i.e.* unstimulated, the co-culture showed no significant increase in cell death compared to mixed DRG neuronal/glia cultures (8.14 ± 2.39 % cell death in mixed DRG neuronal/glia cultures (n=3 biological replicates) to 22.42 ± 4.36 % cell death in mixed DRG neuronal/glia + BMDM co-cultures (n=3 biological replicates). In cultures where there had been a stimulation period with TNFα, no significant differences were observed, with 10.08 ± 2.02 % cell death in the mixed DRG neuronal/glia cultures (n=3 biological replicates) and 11.87 ± 4.13 % cell death in the mixed DRG neuronal/glia + BMDM co-cultures (n=3 biological replicates).

Additionally, the expression levels of three housekeeping genes were examined; *18s*, *Ywhaz* and *Gapdh*, to ensure that no unexpected changes were occurring at the transcriptional level. Using a Two-Way ANOVA, no significant culture type effect was observed ($F(1, 18)=0.3075$, $P=0.5861$). No significant changes in the mRNA levels of *18s*, *Ywhaz* or *Gapdh* were detected between the mixed DRG neuronal/glia cultures and the mixed DRG neuronal/glia + BMDM co-culture groups (Figure 38D). In the mixed DRG neuronal/glia cultures, *18s, Ywhaz and*

Gapdh displayed ΔΔCt values of 9.59 ± 1.64, 23.71 ± 2.12 and 17.01 ± 0.88 respectively (n=4 biological replicates). In the mixed DRG neuronal/glia + BMDM co-cultures, *18s*, *Ywhaz* and *Gapdh* displayed ΔΔCt values of 8.36 ± 1.04, 23.53 ± 1.66 and 16.48 ± 0.65 respectively (n=4 biological replicates) (Figure 38D).

It was important to determine if the neurones within the mixed DRG neuronal/glia + BMDM co-cultures showed significant functional differences compared to neurones of the mixed DRG neuronal/glia cultures. In terms of average neurite outgrowth, the co-culture system responded to NGF-stimulation (10 ng/mL) as expected, with 12 times increase in neurite outgrowth from 17.72 ± 2.62 µm (n=3 biological replicates,) in the untreated condition to 220.2 ± 4.71 µm (n=3 biological replicates, One-Way ANOVA; $F(3,8)=11.19$, $P=0.0104$) following NGF (10 ng/mL) treatment (Figure 39B). This effect is comparable with the response of mixed DRG neuronal/glia cultures to NGF treatment (Figure 39A and B), which saw an increase in neurite outgrowth from 9.55 ± 5.39 µm to 184.7 ± 65.35 µm (n=3 biological replicates, One-Way ANOVA; $F(3,8)=11.19$, $P=0.0229$) following NGF 10 ng/mL treatment. Furthermore, the levels of CGRP release in response to NGF 100 ng/mL were examined using a Two-Way ANOVA (Figure 39C). A significant treatment effect was observed ($F(1, 26)=82.73$, $P<0.0001$). In co-cultures with BMDM added in at both 40K and 80K, a significant increase in stimulated CGRP release was observed following NGF treatment (Figure 39C) of between 4-5 times the release in untreated conditions, from 698.8 ± 75.59 pg/mL to 3507 ± 223.9 pg/mL and 732.6 ± 53.18 pg/mL to 3143 ± 375.8 pg/mL respectively (n=4-6 biological replicates). The above data indicates that the mixed DRG neuronal/glia + BMDM co-culture remains viable and healthy, maintaining responsiveness to stimuli such as NGF.

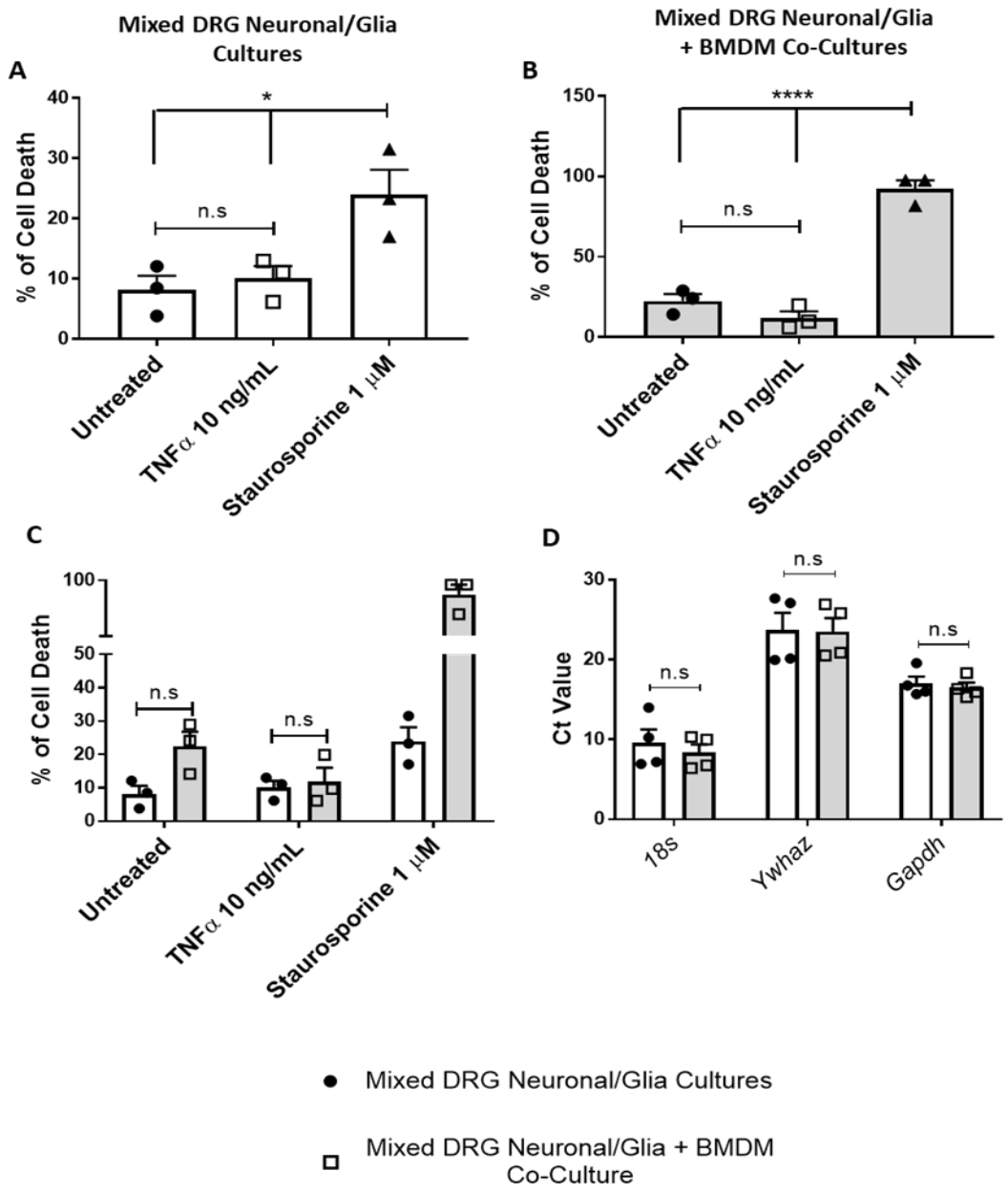

Figure 38. Comparison of culture viability and health in mixed DRG neuronal/glia cultures or mixed DRG neuronal/glia + BMDM co-cultures. A) % of cell death measured using the LDH assay in mixed DRG neuronal/glia cultures (white bars) or (B) mixed DRG neuronal/glia + BMDM co-cultures (shaded bars) in response to TNFα (10 ng/mL, 48 h, hollow squares) or staurosporine (1 μM, 48 h, black triangles) as a positive control. C) Direct comparison of different treatment groups between mixed DRG neuronal/glia cultures (white bars, black circles) and mixed DRG neuronal/glia + BMDM co-cultures (shaded bars, hollow squares). Data displayed as Mean ± SEM, n=3 biological replicates (displayed as individual data points). Data analysed using One-Way ANOVA followed by Tukey's multiple comparisons test for (A-B) and Two-Way ANOVA followed by Sidak's multiple comparisons test for (C). D) The basal expression level of *18s, Ywhaz* or *Gapdh* in either mixed DRG neuronal/glia cultures (white bars, black circles) or mixed DRG neuronal/glia + BMDM co-cultures (shaded bars, hollow squares). Data displayed as Mean ± SEM, n=4 biological replicates. Data analysed using Two-Way ANOVA followed by Sidak's multiple comparison test.

Abbreviations: DRG: dorsal root ganglia; BMDM: bone marrow-derived macrophages; LDH: lactate dehydrogenase; TNFα: tumour necrosis factor alpha; *18s*: 18s ribosomal RNA; *Ywhaz*: tyrosine 3-monooxygenase/tryptophan 5 monooxygenase activation protein; *Gapdh*: glyceraldehyde 3-phosphate dehydrogenase; n.s: not significant.

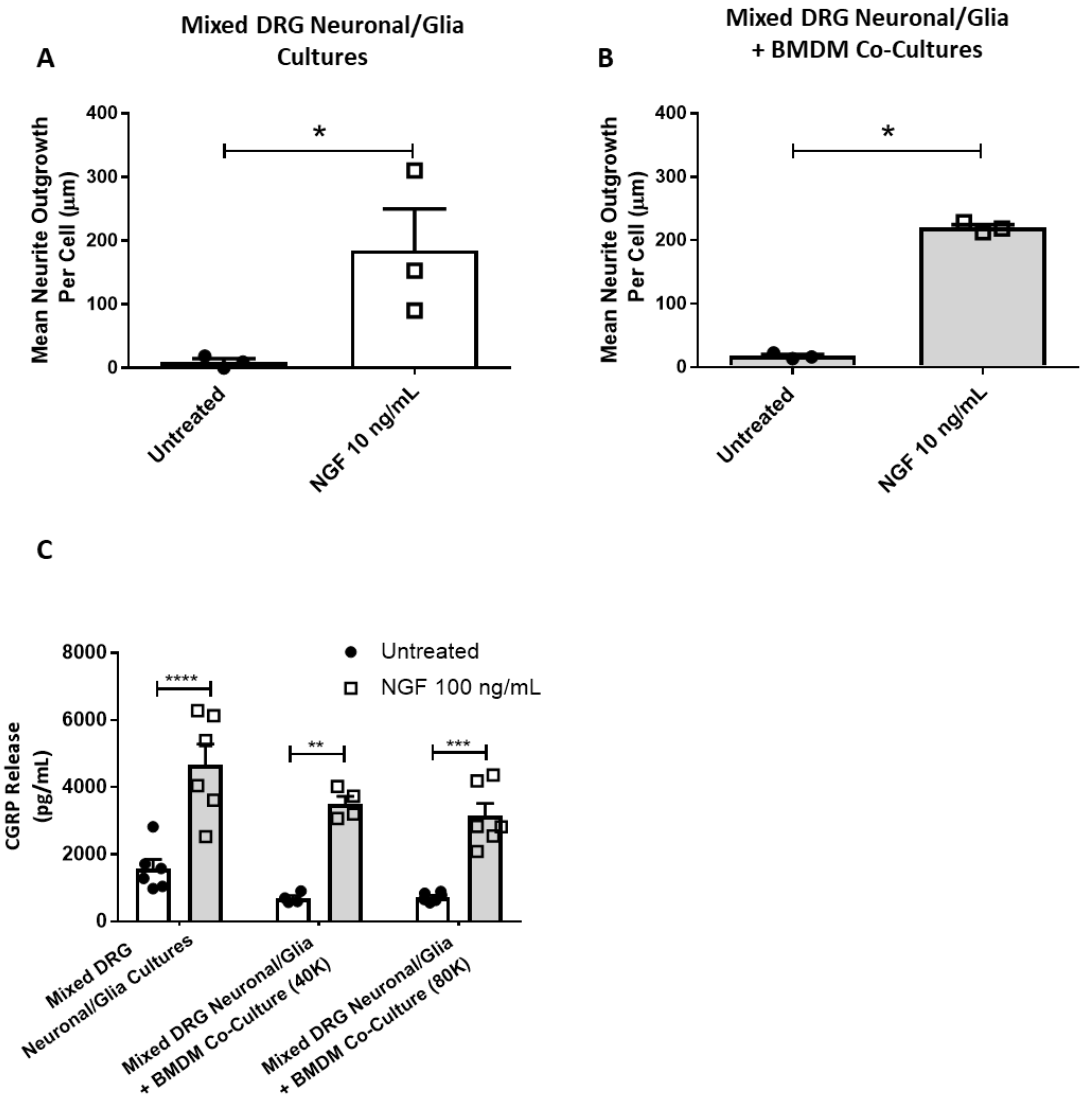

Figure 39. Co-culture response to NGF stimulation. A-B) Average neurite outgrowth in response to NGF (10 ng/mL, 24 h, hollow squares) in either mixed DRG neuronal/glia cultures (white bars) or mixed DRG neuronal/glia + BMDM co-cultures (shaded bars). C) High K^+-evoked CGRP release in response to high concentration NGF stimulation (100 ng/mL, 48 h, hollow squares) in either a mixed DRG neuronal/glia cultures or mixed DRG neuronal/glia + BMDM, with BMDM added in at 40K/well or 80K/well. Data displayed as Mean ± SEM, n=3 biological replicates (displayed as individual data points) for neurite outgrowth experiments and n=4-6 biological replicates (displayed as individual data points) for CGRP release experiments. Data were analysed using One-Way ANOVA followed by Tukey's multiple comparisons test or Two-Way ANOVA followed by Sidak's multiple comparisons test. * P<0.05, ** P<0.01, *** P<0.001, **** P<0.0001.

Abbreviations: NGF: nerve growth factor; DRG: dorsal root ganglia; BMDM: bone marrow-derived macrophages; CGRP: calcitonin gene-related peptide.

5.4.2 Stimulation of Co-cultures with TNFα, in the Presence of NGF, Results in a Potentiation of CGRP Release

CGRP release has been shown to represent a pain-relevant read-out at the level of the sensory neurone (Schou et al., 2017). Therefore, CGRP levels in the co-culture system were examined to determine whether NGF and TNFα could synergistically contribute to pain states via CGRP release. The timeline used in the following experiments are outlined in Figure 40.

The effect of different densities of BMDM, 20K, 40K or 80K on CGRP release in the presence/absence of TNFα (10 ng/mL), were examined. At a density of 20K BMDM (in co-culture with 8K neurones), there was no significant effect on K^+-evoked CGRP release between cultures which were stimulated with or without TNFα (10 ng/mL) (Figure 41A). However, BMDM at higher densities of 40K and 80K (in co-culture with 8K neurones), significantly increased K^+-evoked CGRP release (Figure 41A). This was apparent in co-cultures which had been stimulated with TNFα for 48 h, with an average increase in CGRP release of 229.4 pg/mL (40K BMDM) and 245.5 pg/mL (80K BMDM) respectively (Figure 41A). Worth noting however, is the large variation of baselines seen in this co-culture system; most likely due to combining two primary cells together. Based on the above data set it was decided to use the highest density of BMDM of 80K for all future co-culture experiments.

It has been shown that growing BMDM in GMCSF, as opposed to MCSF, can create BMDM with a different phenotypic profile (Na et al., 2016), an effect which may alter their response to subsequent stimulation (*e.g.* TNFα). Therefore, CGRP release following TNFα stimulation was further examined in co-cultures where BMDM had been differentiated either in the presence of MCSF or GMCSF using a Two-Way ANOVA. No significant difference in the BMDM growth condition effect was seen ($F(1,32)=0.2559$, $P=0.6164$), however a significant

treatment effect was observed (F(1,32)=16.36, P=0.0003). There was no significant difference between cultures grown in MCSF and GMCSF in their response to TNFα stimulation (Figure 41B). In MCSF grown cultures, an increase in CGRP release from 872.9 ± 43.73 pg/mL to 1061 ± 28.09 pg/mL (n=minimum 4 biological replicates) was observed following TNFα stimulation, compared to an increase in CGRP release from 829.3 ± 51.06 pg/mL to 1053 ± 71.1 pg/mL (n=minimum 4 biological replicates) in GMCSF grown cultures (Figure 41B). All subsequent BMDM cultures used in the co-culture system were therefore differentiated in MCSF to provide consistency with the previous chapter in this thesis.

Following a 48 h stimulation period, CGRP release was triggered from mixed DRG neuronal/glia cultures or from mixed DRG neuronal/glia + BMDM co-cultures using three different challenges; K^+ (25 mM), capsaicin (100 nM) or veratridine (31.25 µM). The above challenges were used to establish the mechanism by which an effect was produced. For example, if a strong effect was seen using veratridine but not capsaicin, it could be assumed that the mechanism responsible for producing said effect may involve voltage-gated sodium channel modulation.

Throughout the forthcoming experiments, the effect of NGF was examined at a range of concentrations (0.1 ng/mL, 1 ng/mL, 10 ng/mL, 100 ng/mL), whereas TNFα was kept at a constant concentration of 10 ng/mL.

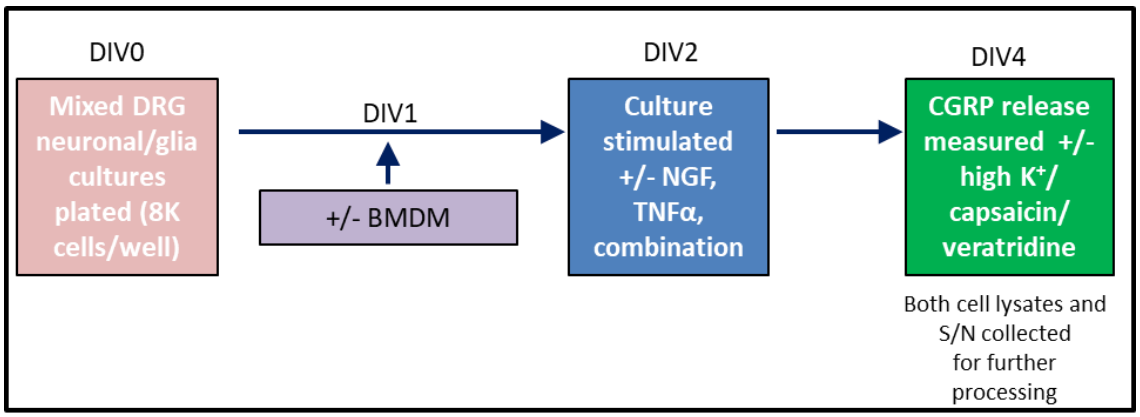

Figure 40. Schematic demonstrating the timeline of all CGRP experiments conducted in the co-culture system. Mixed DRG neuronal/glia cultures were plated at desired density and left to settle overnight prior to the addition of BMDM at varying densities. The co-cultures were left for a further 24 h to allow the sensory neurones and BMDM to acclimatise to each other prior to stimulation with either NGF, TNFα or a combination of the two for 48 h. Following this stimulation period, CGRP release was triggered via either high K^+, capsaicin or a veratridine challenge.

Abbreviations: CGRP: calcitonin gene-related peptide; DRG: dorsal root ganglia; BMDM: bone marrow-derived macrophages; NGF: nerve growth factor; TNFα: tumour necrosis factor alpha; DIV: days *in vitro*; S/N: supernatant.

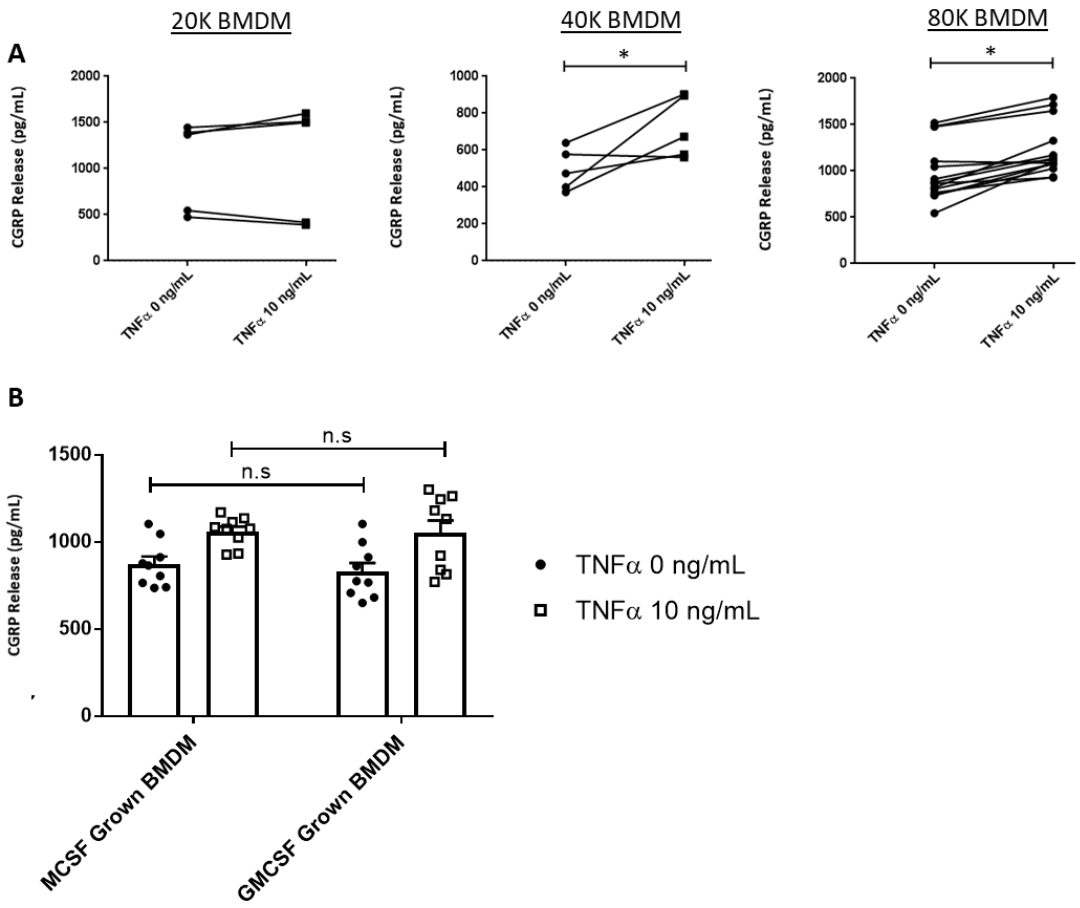

Figure 41. Determining optimal conditions for the co-culture system (mixed DRG neuronal/glia + BMDM). A) CGRP release in the co-culture system with increasing densities of BMDM (grown in MCSF); 20K cells/well, 40K cells/well or 80K cells/well +/- TNFα (10 ng/mL, 48 h) stimulation. Each line represents data from the same culture. B) Effect on CGRP release when BMDM were grown in either MCSF or GMCSF +/- TNFα (10 ng/mL) stimulation. Data displayed as Mean ± SEM, n=minimum 4 biological replicates (displayed as individual data points). Data were analysed using unpaired two-tailed t-tests for (A) and Two-Way ANOVA followed by Tukey's multiple comparisons test (B). * P<0.05.

Abbreviations: DRG: dorsal root ganglia; BMDM: bone marrow-derived macrophages; TNFα: tumour necrosis factor alpha; CGRP: calcitonin gene-related peptide; MCSF: macrophage colony-stimulating factor; GMCSF: granulocyte-macrophage colony-stimulating factor; n.s: not significant.

5.4.2.1 Potassium Evoked CGRP Release

Application of high extracellular K^+ solution results in the general depolarisation of mouse DRG neurones, triggering peptide secretion (Bost et al., 2017). The effect of NGF, TNFα or a combination of the two was examined using a Two-Way ANOVA. In both the mixed DRG neuronal/glia + BMDM co-cultures (Figure 42A) and the mixed DRG neuronal/glia cultures (Figure 42B), the concentration of NGF effect was significant ($F(3,63)=10.02$, $P<0.0001$ and $F(3,61)=29.94$, $P<0.0001$ respectively). NGF at a concentration of 10 ng/mL resulted in enhanced CGRP release (reaching significance at 10 ng/mL). The addition of TNFα (10 ng/mL) alone (*i.e.* with 0 ng/mL NGF) produced no significant changes in CGRP release in mixed DRG neuronal/glia + BMDM co-cultures (Figure 42A). Pre-treatment of co-cultures with TNFα (10 ng/mL), in addition to NGF stimulation, showed no significant enhancement of NGF (10 ng/mL)-induced potentiation of K^+ evoked CGRP release (Figure 42A) (an increase from 1435 ± 371.6 pg/mL in the NGF alone group to 2233 ± 303.1 pg/mL in the combination group of NGF/TNFα, n=minimum 4 biological replicates).

5.4.2.2 Capsaicin Evoked CGRP Release

Capsaicin, an agonist of TRPV1, stimulates the release of neurotransmitters, including CGRP from sensory neurones expressing TRPV1 (Yang et al., 2018). This was of particular interest to us due to the previously discussed literature surrounding the TNFα regulation of TRPV1 (Kochukov et al., 2009, Wang et al., 2018, Hensellek et al., 2007a). The effect of NGF, TNFα or a combination of the two was examined using a Two-Way ANOVA. In both the mixed DRG neuronal/glia + BMDM co-cultures (Figure 42C) and the mixed DRG neuronal/glia cultures (Figure 42D) the concentration of NGF effect was significant ($F(3,40)=37.48$, $P<0.0001$ and $F(3,31)=85.35$, $P<0.0001$ respectively). NGF at a concentration of 10 ng/mL resulted in

enhanced CGRP release in response to capsaicin challenge (reaching significance at 10 ng/mL). The addition of TNFα (10 ng/mL) alone (*i.e.* with 0 ng/mL NGF) showed no significant increase in CGRP release in mixed DRG neuronal/glia co-cultures (Figure 42C), or in the mixed DRG neuronal/glia cultures (Figure 42D). In co-cultures it was found that the presence of TNFα effect was significant ($F(1,40)=14.2$, $P=0.0005$). Pre-treatment of co-cultures with TNFα (10 ng/mL), in addition to NGF stimulation, produced a significant enhancement of NGF (10 ng/mL)-induced potentiation of capsaicin evoked CGRP release (Figure 42C) (an increase from 1957 ± 160.4 pg/mL in the NGF alone group to 2513 ± 307.9 pg/mL in the combination group, n=minimum 4 biological replicates). In the presence of BMDM, this effect was only apparent at the higher NGF concentration of 10 ng/mL (Figure 42C and D). For all other treatment groups within the co-culture system, no significant differences were observed (Figure 42C). In contrast to high K^+ as a challenge, a significant difference in the mixed DRG neuronal/glia cultures was observed between NGF (1 ng/mL) alone and the combination group (NGF 1 ng/mL + TNFα 10 ng/mL) (Figure 42D). No other significant differences were detected in the mixed DRG neuronal/glia cultures.

5.4.2.3 Veratridine as a Challenge

The last challenge used was veratridine 31.25 µM. Veratridine is a neurotoxin that acts by binding to a receptor site on voltage gated sodium channels (VGSC), thus inhibiting their activation and shifting the channel activation threshold toward a more negative membrane potential (Fekete et al., 2009). Veratridine has previously been shown to evoke CGRP release in capsaicin-sensitive nerves of the rat urinary bladder (Tramontana et al., 1992). TNFα has been reported to modulate VGSCs and affect primary sensory neurone excitability in rats, contributing to neuropathic and inflammatory pain states (Leo et al., 2015).

The effect of NGF, TNFα or a combination of the two was examined using a Two-Way ANOVA. It was found that, similar to both high K^+ and capsaicin, in both the mixed DRG neuronal/glia + BMDM co-cultures (Figure 42E) and the mixed DRG neuronal/glia cultures (Figure 42F) the concentration of NGF effect was significant ($F(3,42)=55.64$, $P<0.0001$ and $F(3,24)=28.01$, $P<0.0001$ respectively). NGF at a concentration of 10 ng/mL resulted in enhanced CGRP release in response to veratridine challenge (reaching significance at 10 ng/mL). The addition of TNFα (10 ng/mL) alone (*i.e.* with 0 ng/mL NGF) showed no significant increase in CGRP release in both types of culture (Figure 42E and F). In co-cultures it was found that the presence of TNFα effect was significant ($F(1,42)=10.03$, $P=0.0029$). Pre-treatment of co-cultures with TNFα (10 ng/mL), in addition to NGF stimulation, produced a significant enhancement of NGF (10 ng/mL)-induced potentiation of veratridine evoked CGRP release (Figure 42E) (an increase from 902.9 ± 90.8 pg/mL to 1391 ± 207.7 pg/mL, n=minimum 4 biological replicates). In agreement with previous data, this effect was only apparent in the presence of BMDM, and not in the mixed DRG neuronal/glia cultures and only at the higher NGF concentration of 10 ng/mL (Figure 42E and F).

Overall, a consistent increase in the combination group (where both mediators were at 10 ng/mL) compared to the NGF or TNFα alone groups (10 ng/mL) was observed across all three different challenges in the co-culture set-up (Figure 43). Therefore, when considering all data together, a potentiation of CGRP release can be observed in the co-culture when pre-treatment with TNFα (10 ng/mL) is combined with NGF treatment (10 ng/mL) (Figure 44A) (1432 ± 184.5 pg/mL in the NGF (10 ng/mL) alone group to 2072 ± 188.5 pg/mL in the combination group, n=minimum of 12 biological replicates). This effect is however not observed in the mixed DRG neuronal glia cultures (Figure 44B), suggesting that the presence

of BMDM is crucial for this observed synergistic effect between NGF and TNFα. An important aspect to note is that BMDM themselves do not release CGRP, either basally or in response to NGF, TNFα or a combination of the two (Appendix Figure 2), therefore any increases in CGRP release observed here is likely to originate from the sensory neurone cultures.

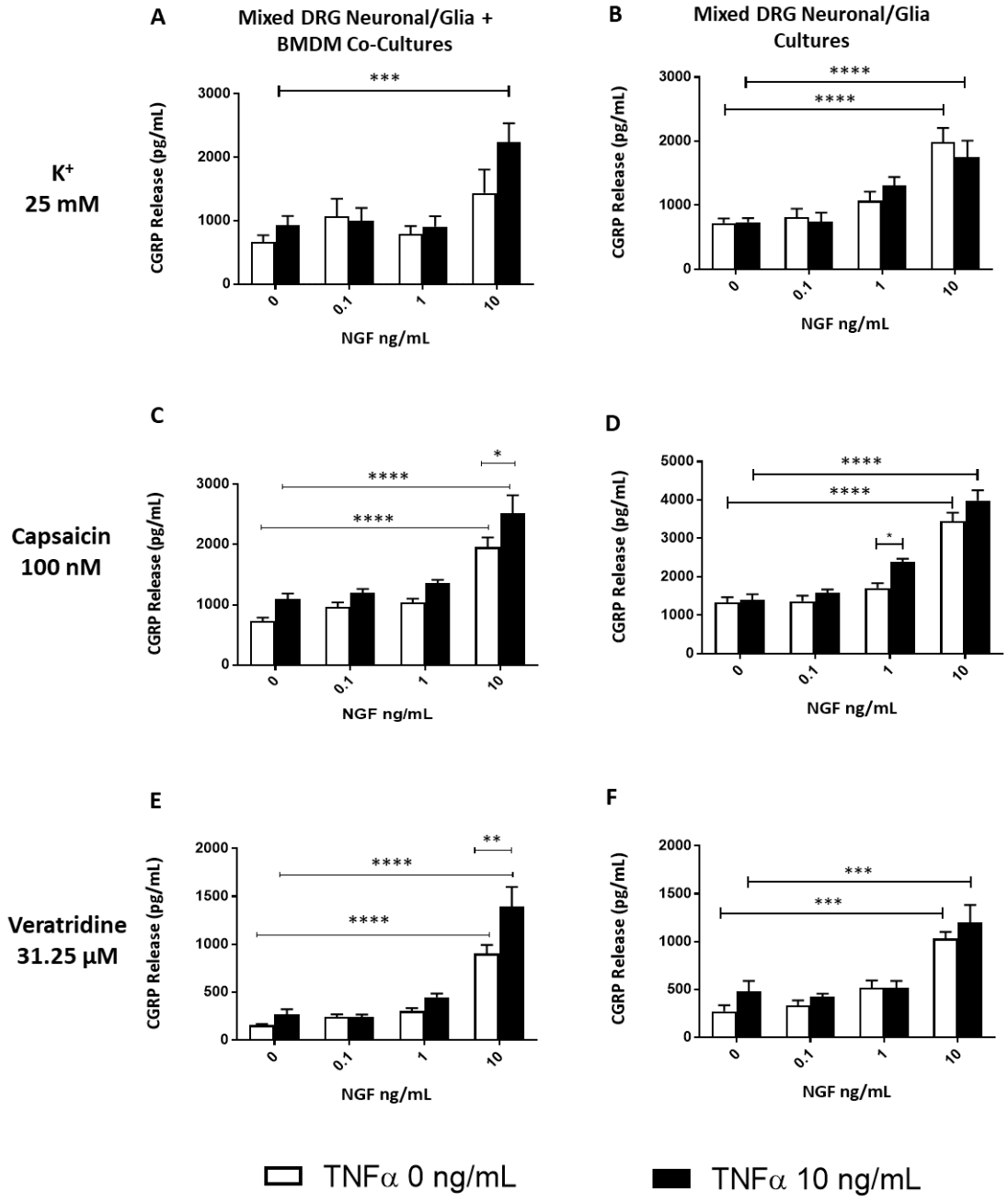

Figure 42. Effect of stimulus-evoked CGRP release in mixed DRG neuronal/glia + BMDM co-cultures vs mixed DRG neuronal/glia cultures. A) High K^+ (25 mM)-evoked CGRP release in mixed DRG neuronal/glia + BMDM co-cultures (80K BMDM/well) in response to a range of NGF concentrations (0.1 ng/mL to 10 ng/mL), TNFα (10 ng/mL), combination of the two B) as above but in mixed DRG neuronal/glia cultures (no BMDM present). C) Capsaicin (100 nM)-evoked CGRP release in mixed DRG neuronal/glia + BMDM co-cultures (80K BMDM/well) in response to a range of NGF concentrations (0.1 ng/mL to 10 ng/mL), TNFα (10 ng/mL), combination of the two D) as above but in mixed DRG neuronal/glia cultures (no BMDM present). E) Veratridine (31.25 µM)-evoked CGRP release in mixed DRG neuronal/glia + BMDM co-cultures (80K BMDM/well) in response to a range of NGF concentrations (0.1 ng/mL to 10 ng/mL), TNFα (10 ng/mL), combination of the two E) as above but in mixed DRG neuronal/glia cultures (no BMDM present). In all graphs displayed, white bars represent cultures with no TNFα whereas black bars represent cultures that have received TNFα (10 ng/mL). Data displayed as Mean ± SEM, n=minimum 4 biological replicates. Data were analysed using Two-Way ANOVA followed by Sidak's multiple comparisons test. * P<0.05, ** P<0.01, *** P<0.001, **** P<0.0001.

Abbreviations: CGRP: calcitonin gene-related peptide; DRG: dorsal root ganglia; BMDM: bone marrow-derived macrophages; K^+: potassium; NGF: nerve growth factor; TNFα: tumour necrosis factor alpha.

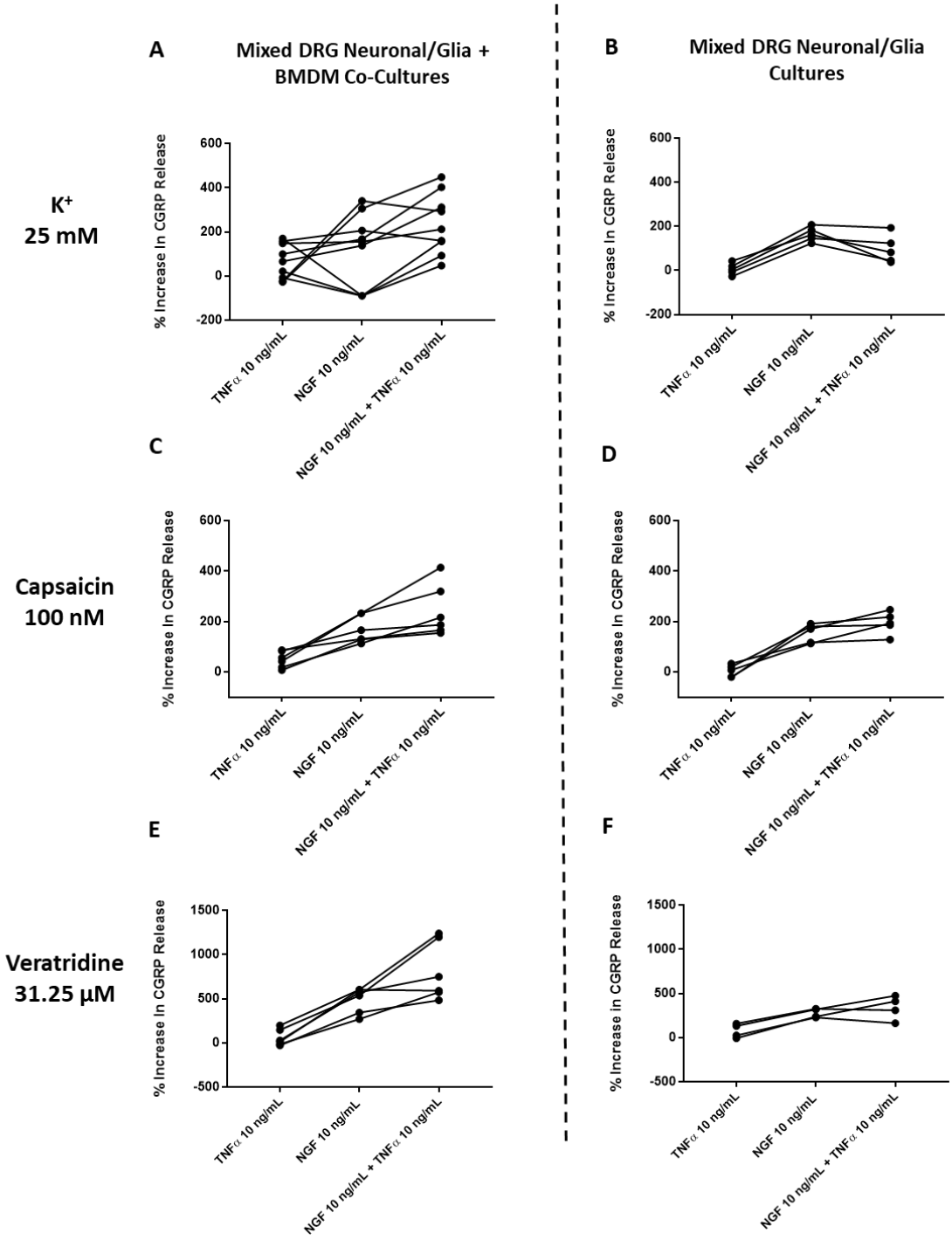

Figure 43. % of CGRP release in response to NGF alone (10 ng/mL), TNFα alone (10ng/mL) or a combination of the two in either mixed DRG neuronal/glia cultures or mixed DRG neuronal/glia + BMDM co-cultures. A-B) % of CGRP release following K^+ (25 mM) C-D) capsaicin (100 nM) or E-F) veratridine (31.25 µM). Data displayed as individual data points, with each line representing a different culture.

Abbreviations: CGRP: calcitonin gene-related peptide; DRG: dorsal root ganglia; BMDM: bone marrow-derived macrophages; K^+: potassium; NGF: nerve growth factor; TNFα: tumour necrosis factor alpha.

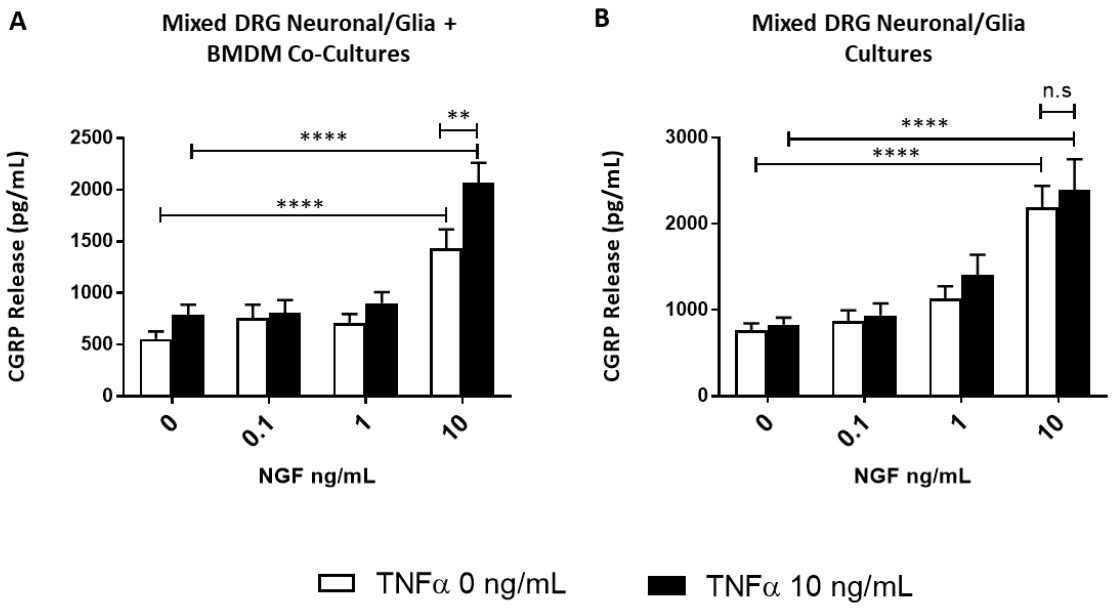

Figure 44. Combined effect of all stimuli (K^+, capsaicin and veratridine) used to evoke CGRP release. CGRP release in A) mixed DRG neuronal/glia + BMDM co-cultures or B) mixed DRG neuronal/glia cultures. Data displayed as Mean ± SEM, n=minimum of 12 biological replicates. Data were analysed using Two-Way ANOVA followed by Sidak's multiple comparisons test. ** P<0.01, **** P<0.0001.

Abbreviations: CGRP: calcitonin gene-related peptide; DRG: dorsal root ganglia; BMDM: bone marrow-derived macrophages; K^+: potassium; NGF: nerve growth factor; TNFα: tumour necrosis factor alpha; n.s: not significant.

5.4.3 TNFα-Stimulated BMDM-Derived Conditioned Medium Increases the Expression of Pain-Relevant Genes in Purified DRG Neuronal Cultures

To help dissect the mechanism by which TNFα could modulate DRG sensory neurones, a set of CM experiments were performed to determine if any neuronal transcriptional changes were evoked by factor(s) secreted by TNFα-stimulated BMDM. CM was added both in the absence and presence of NGF 10 ng/mL to address the following questions:

1) What is the effect of BMDM secreted factor(s) (+/- TNFα stimulation) on the transcription of pain-relevant genes in purified DRG neuronal cultures?
2) Can adding NGF, in addition to CM, result in synergistic effects, regarding transcriptional modulation, driven by secreted factors from TNFα-activated macrophages?

The effect of CM from TNFα-stimulated BMDM was examined using a Two-Way ANOVA, a significant treatment effect was found ($F(3,132)=9.701$, $P<0.0001$). Interestingly, CM from TNFα-stimulated BMDM significantly increased the average gene expression change of a panel of 45 pain-relevant genes (0.77 ± 0.21 ΔΔCt, n=3 biological replicates) when compared to cultures exposed to media only controls, +/- TNFα (Figure 45A and B) (-0.17 ± 0.18 ΔΔCt, n=3 biological replicates). No significant differences in the average gene expression change (of the 45-gene panel) evoked by CM of naïve BMDM, or media only controls (*i.e.* non BMDM CM, +/- TNFα) were observed (Figure 45B). Although the average difference in gene expression (of the 45-gene panel) evoked by CM from naïve BMDM was not significantly different from TNFα-stimulated BMDM, a trend for an increase was observed (0.33 ± 0.18 ΔΔCt to 0.78 ± 0.21 ΔΔCt, n=3 biological replicates) (Figure 45B).

Figure 47 displays neuronal gene expression changes in purified DRG neuronal cultures treated with media only controls (+/- TNFα), naïve BMDM CM or TNFα-stimulated BMDM CM. Expression levels of *Ccl2*, *Nos1* and *Ccl3* all displayed significant differences following treatment with TNFα-stimulated BMDM CM compared to media only controls (Figure 47A, B and C). Of particular interest was the neuronal expression levels of *Ccl2*. A significant difference between the media only control group and the TNFα-stimulated BMDM CM (increase of 2.40 ± 0.49 ΔΔCt, n=3 biological replicates) was observed, but also between the naïve BMDM CM and the TNFα-stimulated BMDM groups (0.31 ± 0.18 ΔΔCt to 2.40 ± 0.49 ΔΔCt, n=3 biological replicates) (Figure 47A). These findings suggest that the increase in neuronal *Ccl2* expression is dependent on both the presence of BMDM and TNFα-stimulation. Expression levels of *Atf3*, *Il-1β* and *Trpa1* all displayed a trend for an increase in neuronal expression following treatment with TNFα-stimulated BMDM CM (Figure 47D,E and F).

The above data suggest that BMDM secreted factor(s), driven by TNFα-stimulation, are capable of affecting sensory neurone expression of pain-relevant genes. To investigate whether any additive or synergistic actions occur (between the TNFα-stimulated BMDM secreted factor(s) and NGF itself) the same experiment, examining gene expression, was performed but in the presence of NGF (*i.e.* NGF added to the purified DRG neurones at time of treatment with BMDM-derived CM). Using a Two-Way ANOVA, no significant treatment effect was observed ($F(4,176)=1.275$, $P=0.2815$), with concomitant NGF neuronal treatment displaying no significant differences in neuronal gene expression (of the 45-gene panel) were evoked by naïve BMDM CM or TNFα-stimulated BMDM CM (Figure 46A and B).

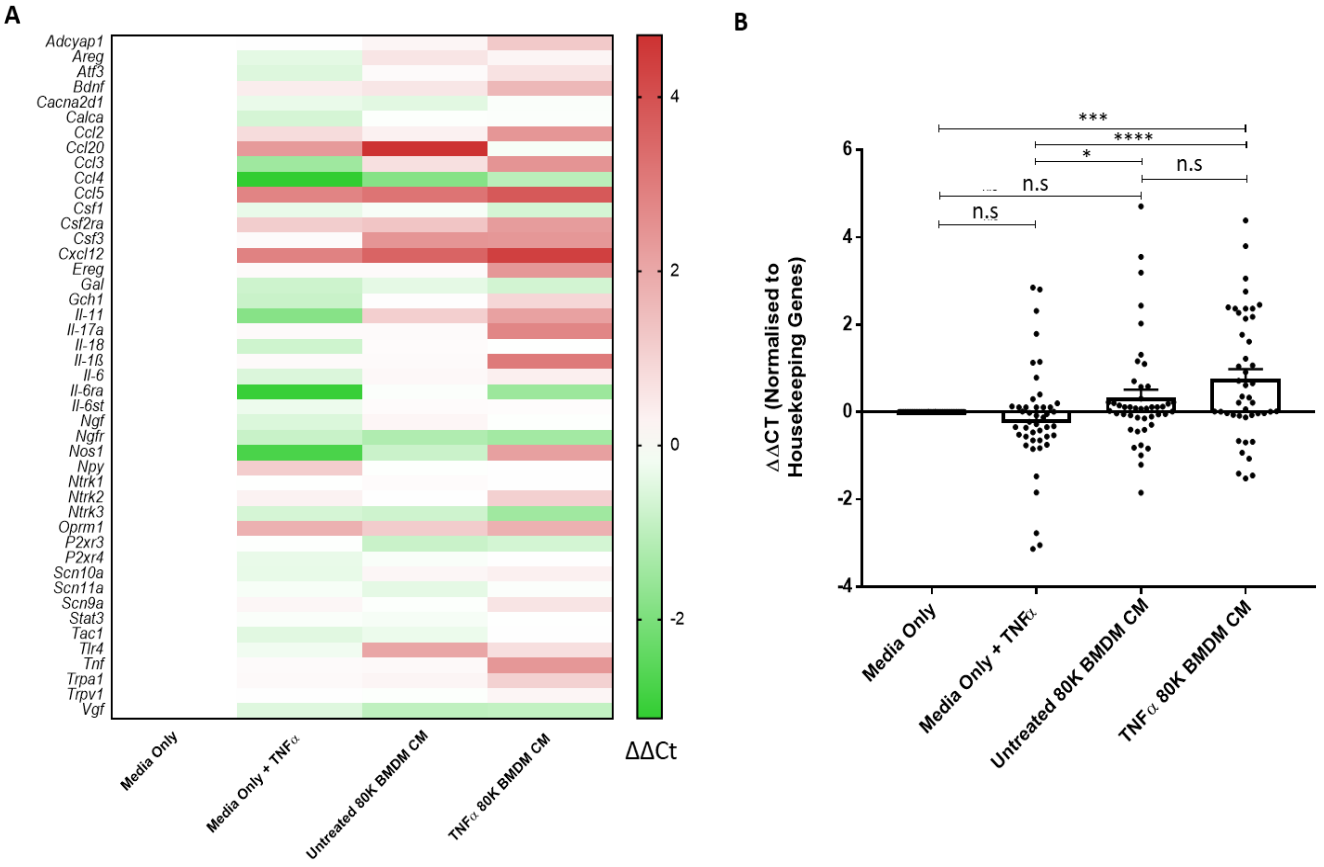

Figure 45. Gene expression changes in purified DRG neuronal cultures in response to treatment with CM from untreated or TNFα-stimulated BMDM (in absence of NGF). A) Heat map displaying the regulation of 45 pain-related genes (normalised to three housekeeping genes *(18s, Ywhaz* and *Gapdh*) and relative to the media only control group) in response to CM from naïve or TNFα 10 ng/mL treated BMDM (80K cells/well). Naïve and TNFα treated media (no BMDM) conditions were included as appropriate controls. Data represents the average ΔΔCt value over 3 biological replicates. Genes which are upregulated are signified in red whereas genes which are downregulated are signified in green. B) Comparing the effect of BMDM-derived CM (stimulated +/- TNFα 10 ng/mL) on expression changes in purified DRG neuronal cultures. Media only treatment groups (+/- TNFα) served as controls. Each data point represents the average ΔΔCt value of an individual gene. Data displayed as Mean ± SEM, n= 3 biological replicates. Data were analysed using Two-Way ANOVA followed by Tukey's multiple comparisons test. *P<0.05, ***P<0.001, ****P<0.0001. CM: conditioned medium.

Abbreviations: DRG: dorsal root ganglia; CM: conditioned medium; TNFα: tumour necrosis factor alpha; BMDM: bone marrow-derived macrophages; NGF: nerve growth factor; *18s*: 18s ribosomal RNA; *Ywhaz*: tyrosine 3-monooxygenase/tryptophan 5 monooxygenase activation protein; *Gapdh*: glyceraldehyde 3-phosphate dehydrogenase; n.s: not significant; further details of all genes examined can be found in the abbreviation list.

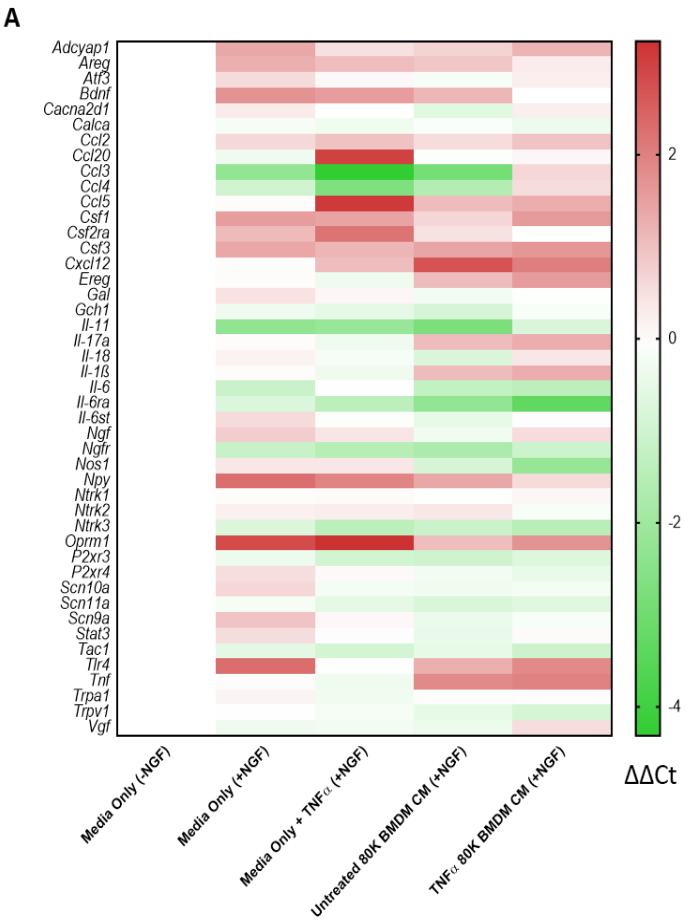

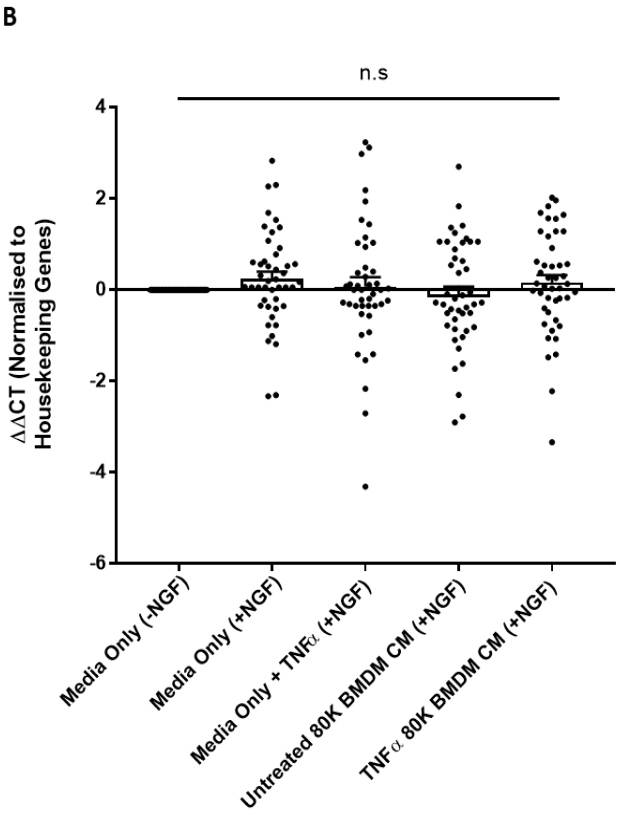

Figure 46. Gene expression changes in purified DRG neuronal cultures in response to treatment with CM from untreated or TNFα-stimulated BMDM (in presence of NGF 10 ng/mL). A) Heat map displaying the regulation of 45 pain-related genes (normalised to three housekeeping genes (*18s, Ywhaz* and *Gapdh* and relative to the media only control group) in response to CM from naïve or TNFα 10 ng/mL treated BMDM (80K cells/well) with added NGF 10 ng/mL in the purified DRG neuronal culture. Data represents the average ΔΔCt value over 3 biological replicates. Genes which are upregulated are signified in red whereas genes which are downregulated are signified in green. B) Comparing the effect of BMDM-derived CM (stimulated +/- TNFα 10 ng/mL), on expression changes in purified DRG neuronal cultures (also stimulated with NGF 10 ng/mL). Media only treatment groups (+/- TNFα, +NGF) served as controls. Each data point represents the average ΔΔCt value of an individual gene. Data displayed as Mean ± SEM, n= 3 biological replicates.

Abbreviations: DRG: dorsal root ganglia; CM: conditioned medium; TNFα: tumour necrosis factor alpha; BMDM: bone marrow-derived macrophages; NGF: nerve growth factor; *18s*: 18s ribosomal RNA; *Ywhaz*: tyrosine 3-monooxygenase/tryptophan 5 monooxygenase activation protein; *Gapdh*: glyceraldehyde 3-phosphate dehydrogenase; n.s: not significant; further details of all genes examined can be found in the abbreviation list.

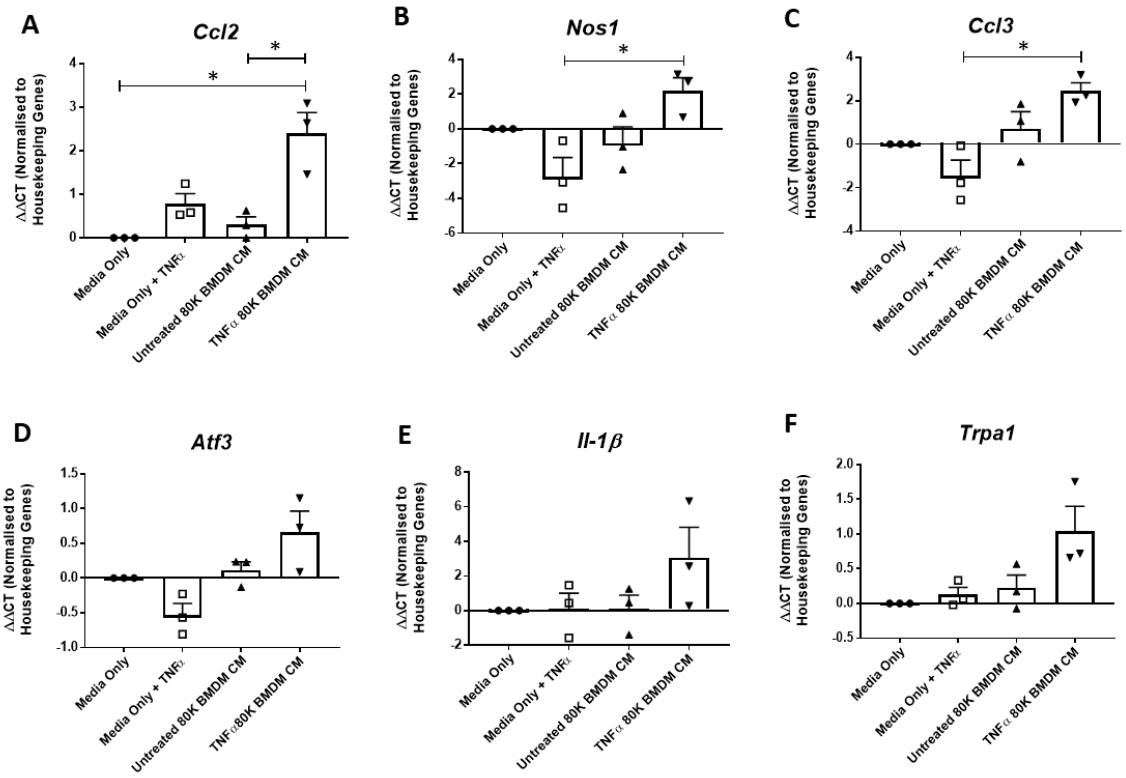

Figure 47. Transcriptional effect on individual genes following treatment of purified DRG neuronal cultures with BMDM derived CM (in absence of NGF). Genes displayed; A) *Ccl2*, B) *Nos1*, C) *Ccl3*, D) *Atf3*, E) *Il-1β* and F) *Trpa1*. Data displayed as Mean ± SEM, n=3 biological replicates (displayed as individual data points). Data were analysed using LIMMA analysis and adjusted for multiple comparisons. * P<0.05.

Abbreviations: DRG: dorsal root ganglia; BMDM: bone marrow-derived macrophages; CM: conditioned medium; NGF: nerve growth factor; TNFα: tumour necrosis factor; *Ccl2*: chemokine (C-C motif) ligand 2; *Nos1*: nitric oxide synthase; *Ccl3*: chemokine (C-C motif) ligand 3; *Atf3*: activating transcription factor 3; *Il-1β*: interleukin-1β; *Trpa1*: transient receptor ankyrin 1.

5.4.4 BMDM Co-Cultured with Mixed DRG Neuronal/Glia Cultures Display Enhanced Responsiveness to Stimuli

For a complete picture, the transcriptional changes (of the same 45-gene panel) from direct co-cultures were also examined. In this instance, direct co-cultures (mixed DRG neuronal/glia cultures + BMDM) were compared with mixed DRG neuronal/glia cultures alone and BMDM cultures alone. All cultures were stimulated with NGF, TNFα or a combination of the two. A heat-map displaying the overall changes in genes from these cultures are shown in Figure 48. For clarity, the heat-map is divided into genes which are known to be expressed in BMDM and genes which are more associated with neuronal function. Genes shown to be upregulated are signified by the colour red, and genes shown to be downregulated are signified by the colour green. The heat-map shows that the co-culture system may drive higher expression of a number of genes (known to be expressed in BMDM) compared to either the mixed DRG neuronal/glia cultures or BMDM alone, for example, *Ccl5, Il-1β* and *Tnf* (Figure 48 and 49A, B and C). The latter suggesting that within the co-culture system, the presence of the neurones may be impacting BMDM response to pain-related stimuli. However, the fact that both cell types are adherent and therefore impossible to separate from each other in the RNA extraction process, makes it hard to definitively say which cell type is responsible for the observed changes in expression.

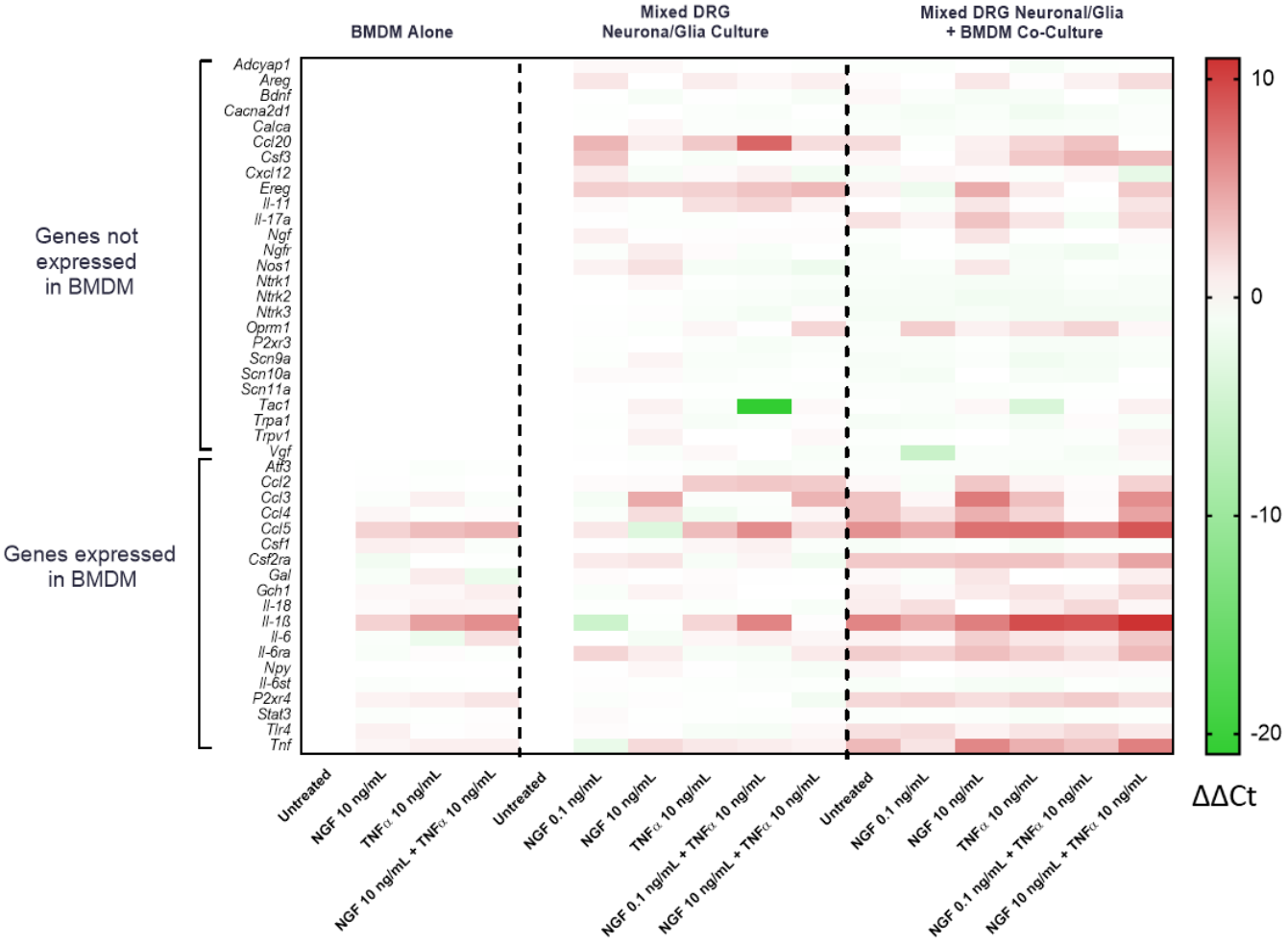

Figure 48. Heat map displaying the regulation of 45 pain-related genes in direct co-cultures. Transcriptional changes in response to NGF (0.1 ng/mL, 10 ng/mL, 48 h), TNFα (10 ng/mL, 48 h), NGF (0.1 ng/mL, 48 h) + TNFα (10 ng/mL, 48 h) or NGF + TNFα (both at 10 ng/mL, 48 h) in mixed DRG neuronal/glia cultures, direct co-cultures (mixed DRG neuronal/glia + BMDM) or BMDM alone cultures. Data represents the average ΔΔCt value over a number of biological replicates. n= minimum of 3 biological replicates across all groups except NGF 0.1 ng/mL and NGF 0.1 ng/mL + TNFα 10 ng/mL in the DRG mixed neuronal culture where n=2 biological replicates.

Abbreviations: DRG: dorsal root ganglia; NGF: nerve growth factor; TNFα: tumour necrosis factor alpha; BMDM: bone marrow-derived macrophages; further details of all genes examined can be found in the abbreviation list.

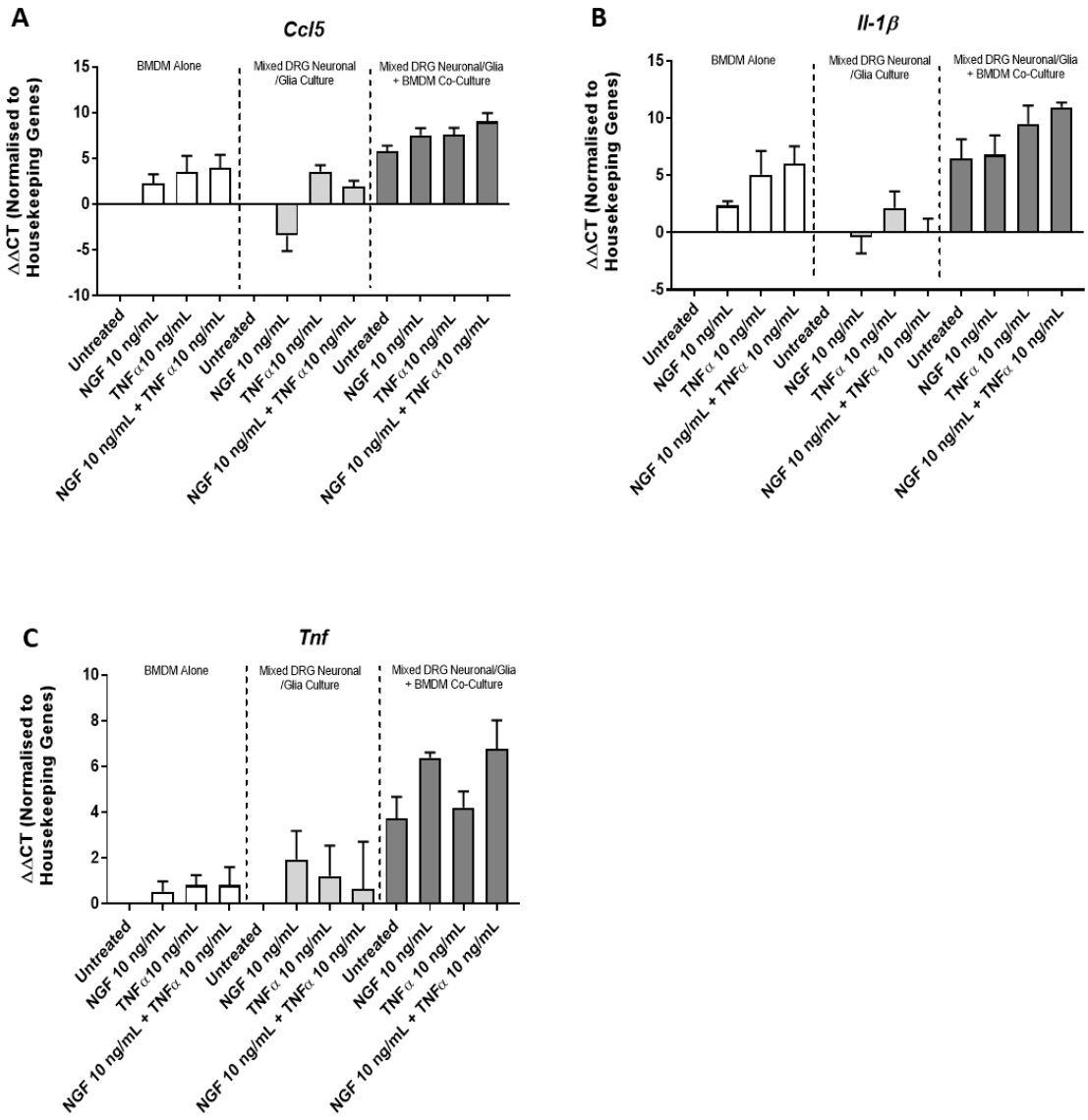

Figure 49. Transcriptional effect on individual genes in response to NGF and TNFα in BMDM alone cultures, mixed DRG neuronal/glia cultures or mixed DRG neuronal/glia + BMDM co-cultures. Genes displayed; A) *Ccl5*, B) *Il-1β* and C) *Tnf*. Data displayed as Mean ± SEM, n= minimum of 3 biological replicates.

Abbreviations: NGF: nerve growth factor; TNFα: tumour necrosis factor alpha; BMDM: bone marrow-derived macrophages; *Ccl5*: Chemokine (C-C motif) ligand 5*; Il-1β*: interleukin-1β; *Tnf*: tumour necrosis factor.

5.4.5 Direct Co-cultures Display Enhanced IL-1β Secretion in Response to TNFα Stimulation

The transcriptional data from section 5.4.4 highlighted BMDM-derived IL-1β as a potential inflammatory mediator which was being modulated by the presence of DRG sensory neurones. Therefore, the release of IL-1β at the cellular level was examined in these culture systems. Both mixed DRG neuronal/glia cultures and BMDM alone cultures showed no detectable release of IL-1β in response to NGF 10 ng/mL, TNFα 10 ng/mL or a combination of the two (Figure 50). However, in the co-culture set-up, not only was IL-1β detectable in all groups, there was a significant increase in IL-1β (of almost 95 %) after TNFα 10 ng/mL treatment (60.7 ± 8.16 pg/mL, n=3 biological replicates, One-Way ANOVA; $F(12,26)=37.48$, $P<0.0001$), when compared to the untreated group (31.28 ± 3.32 pg/mL, n=3 biological replicates). However, there was no detectable additive or synergistic actions occurring in the combination group of NGF and TNFα-stimulation (49.96 ± 3.31 pg/mL, n=3 biological replicates). The response from the combination group was almost identical to the IL-1β release triggered via NGF stimulation (49.72 ± 1.34 pg/mL, n=3 biological replicates) (Figure 50).

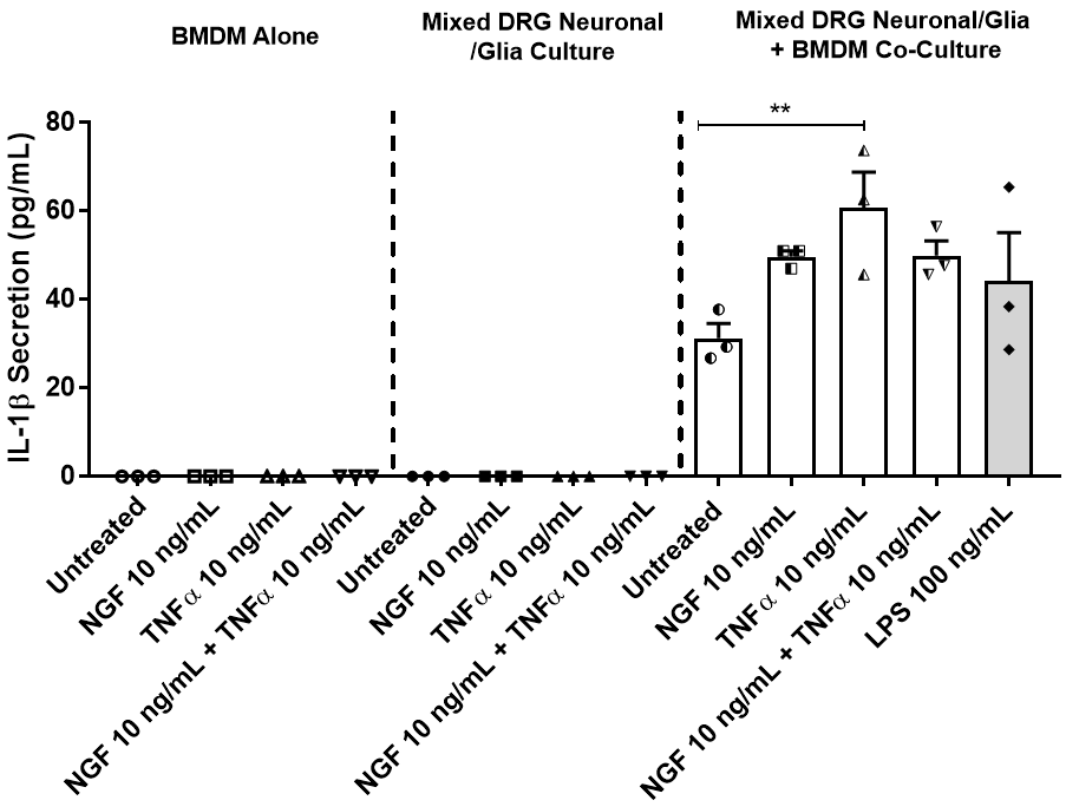

Figure 50. IL-1β secretion in different culture set-ups. IL-1β secretion in BMDM alone cultures, mixed DRG neuronal/glia cultures or mixed DRG neuronal/glia + BMDM co-cultures in response to NGF (10 ng/mL, 48 h), TNFα (10 ng/mL, 48 h) or a combination of the two (10 ng/mL, 48 h). LPS (100 ng/mL) was used as a positive control. Data displayed as Mean ± SEM, n=3 biological replicates (displayed as individual data points). Data analysed using One-Way ANOVA followed by Tukey's multiple comparisons test. ** P<0.01.

Abbreviations: IL-1β: interleukin-1β; BMDM: bone marrow-derived macrophages; DRG: dorsal root ganglia; NGF: nerve growth factor; TNFα: tumour necrosis factor alpha; LPS: lipopolysaccharide.

5.4.6 Conditioned Medium from TNFα-Stimulated BMDM does not Acutely Regulate Sensory Neuronal Calcium Transients

Given the observed effect of CM (from TNFα-stimulated BMDM) on DRG sensory neuronal gene expression, it was decided to investigate whether the same CM may acutely modulate calcium dynamics in sensory neurones. Calcium imaging was utilised to actively visualise and quantify neuronal activation in response to CM derived from BMDM (+/- TNFα-stimulation).

On application of CM (from either naïve BMDM or TNFα-stimulated BMDM) to purified DRG neuronal cultures, we saw no evidence of increased cytosolic calcium over an acute period (Figure 51). The latter was true regardless of the presence of NGF in the purified DRG neuronal cultures (Figure 51A and B). Regarding the % of neurones responding to capsaicin, it was found that 14.19 ± 2.58 % of cells (n=399 neurones across 4-5 mice) responded in the media only condition (no BMDM media only control) (-NGF) condition compared to 13.36 ± 2.41 % of cells (n=499 neurones across 4-5 mice) in purified DRG neuronal cultures exposed to TNFα-stimulated BMDM CM (-NGF) group (Figure 51C). Likewise, no difference was detected in the magnitude of the capsaicin response (0.53 ± 0.09 ΔF/F and 0.52 ± 0.04 ΔF/F respectively) or the magnitude of the KCl response (0.53 ± 0.07 ΔF/F and 0.51 ± 0.05 ΔF/F respectively) in cultures exposed to CM from TNFα-stimulated BMDM (Figure 51E and F). On average > 90 % of neurones responded to KCl stimulation in all cultures tested (Figure 51D), confirming the viability of neurones in this experimental set-up.

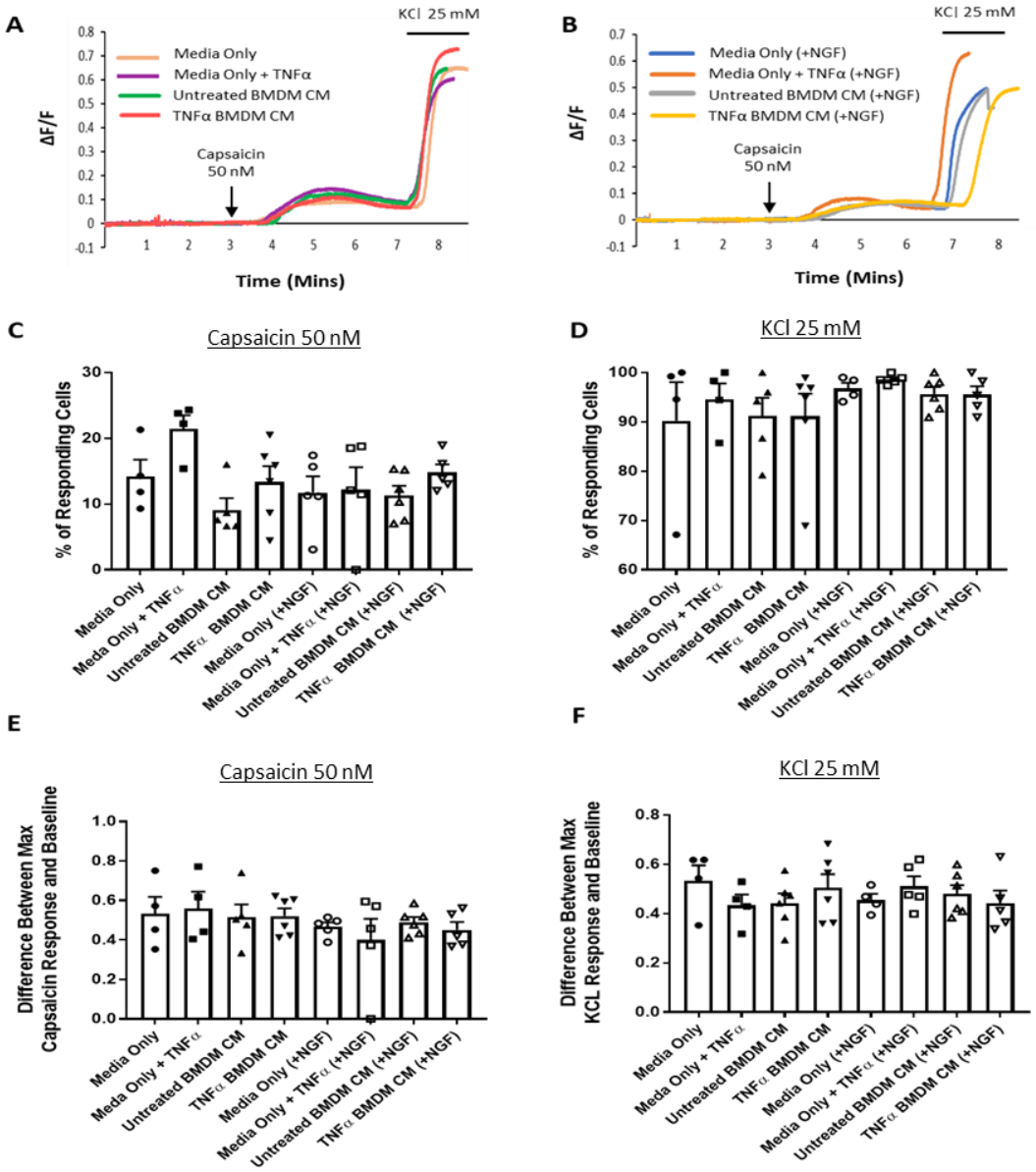

Figure 51. Calcium signals in purified DRG neuronal cultures +/- NGF (10 ng/mL) following 24 h in culture with CM derived from BMDM treated with or without TNFα (10 ng/mL). A-B) Representative traces from coverslips displaying ΔF/F versus time, A) –NGF and B) +NGF. Each line represents the average values of all neurones on one coverslip. Capsaicin (50 nM) was applied for 3 min followed by a wash-out period and a final KCl (25 mM) stimulus to ensure cell viability. C-D) Quantification of % of responding cells to both C) capsaicin 50 nM or D) KCl 25 mM. E-F) The maximum response seen from E) capsaicin (50 nM) or F) KCl (25 mM) (calculated by taking the difference between the maximum capsaicin/KCl response recorded and the average of baseline ten frames pre-capsaicin/KCl stimulus.) Data displayed as Mean ± SEM, n=6858 neurones across 4-5 mice per group. Untreated No BMDM –NGF (399 neurones), TNFα No BMDM –NGF (348 neurones), Untreated 80K BMDM –NGF (456 neurones), TNFα 80K BMDM –NGF (499 neurones), Untreated No BMDM +NGF (1281 neurones), TNFα No BMDM +NGF (1136 neurones), Untreated 80K BMDM +NGF (1347 neurones), TNFα 80K BMDM +NGF (1392 neurones). Data points on graphs represent individual cover slips.

Abbreviations: DRG: dorsal root ganglia; NGF: nerve growth factor; CM: conditioned medium; BMDM: bone marrow-derived macrophages; TNFα: tumour necrosis factor; KCl: potassium chloride.

5.5 Discussion

This chapter aimed to address two primary questions; does TNFα affect sensory neurone function indirectly via BMDM activation and could synergistic actions of NGF and TNFα be detected using a co-culture system between sensory neurones and BMDM.

In the first instance, the focus was ensuring appropriate levels of viability within the co-cultures. The data presented in this chapter suggests that the sensory DRG neurones function as expected in the presence of BMDM in terms of neurite outgrowth and CGRP release. We have shown that in the presence of TNFα, in both mixed DRG neuronal/glia cultures and mixed DRG neuronal/glia + BMDM co-cultures, the viability of the sensory DRG neurones are unaffected. The latter is in line with evidence in the literature which shows that rat neurone-macrophage co-culture viability is only reduced following LPS/IFNγ stimulation, and not TNFα stimulation (Massier et al., 2015). However, one study showed the addition of macrophages for 24 h to neurones caused rapid cell death, an effect only seen in the direct co-cultures and not in a conditioned medium set-up (Arantes et al., 2000). The difference between the above study and our results could be explained by the latter study using peritoneal macrophages, which may have a more activated phenotype, and looking at sympathetic neurones isolated from neo-natal mice.

We found that levels of evoked-CGRP release from primary sensory neurones could be significantly potentiated when combining the two inflammatory mediators together (only observed at 10 ng/mL) in a direct co-culture set-up (mixed DRG neuronal/glia + BMDM). This effect was reproducible across all three challenges used to evoke CGRP release and only seen with the additional presence of BMDM in the co-culture system.

Previous work within the literature supports the ability of macrophages to stimulate CGRP release from sensory neurones (Massier et al., 2015), an effect which was seen as early as 1 h in neurone-macrophage co-cultures obtained from rats with antigen-induced arthritis. Despite some evidence to suggest that invading macrophages may upregulate their own production of CGRP in response to pro-inflammatory stimuli, thus contributing to pain states (Ma and Quirion, 2006), we showed that BMDM were unable to produce CGRP themselves (including stimulation with TNFα).

Future experiments could examine the effect of our co-culture system on release of other neuropeptides known to be involved in pain processing, for example substance P (Lisowska et al., 2016, Mashaghi et al., 2016, Teodoro et al., 2013, Sahbaie et al., 2009). A co-culture system comprised of pig DRG sensory neurones and skin keratinocytes demonstrated an increase in substance P release triggered by capsaicin stimulation (Pereira et al., 2010). Similar to our own experiments, the authors highlight that substance P was secreted exclusively by the neurones, an effect enhanced via the presence of keratinocytes. This provides further evidence for sensory neurone modulation via non-neuronal cell types.

A number of genes in purified DRG neuronal cultures displayed an increase in expression following treatment with CM from TNFα treated BMDM. This effect was observed despite no effects of TNFα on sensory DRG neurones being detectable previously (section 3.4). This suggests that TNFα-stimulated BMDM can release factor(s) that can act directly on the sensory neurone itself. In this instance, intriguing changes were detected in the following neuronal genes; *Ccl2, Nos1, Ccl3, Atf3, Il-1β* and *Trpa1*.

It has previously been shown that CCL2 can act as a key mediator in the communication between neurones and macrophages, enhancing regenerative capacity following a

peripheral nerve injury (Kwon et al., 2015). However, it has also been shown that CCL2 and its receptor, CCR2, are upregulated in the DRG following chemotherapy-induced peripheral neuropathy, an effect which is correlated with mechanical hypersensitivity (Illias et al., 2018). Furthermore, the use of an anti-CCL2 antibody could successfully prevent the development of the described hypersensitivity (Illias et al., 2018). CCL2 is known to trigger CGRP release from cultured DRG neurones obtained from neonatal rats, an effect dependent on both phospholipase C and protein kinase C signalling (Qin et al., 2005b).

NOS1 is one of three isoforms of nitric oxide (NO) synthase which produces NO, a messenger molecule with widespread affects throughout the body (Thomas et al., 2008). NOS1 is expressed in central and peripheral neurones, in addition to other cell types, such as endothelial cells (Forstermann et al., 1994). NOS1 has been implicated in a myriad of physiological functions, including learning and memory, regulation of synaptic transmission and regulation of vascular tone in the periphery (Förstermann and Sessa, 2012). However, NO is also an important mediator in both chronic and acute inflammation (Laroux et al., 2000). For example, it has been shown that mice pre-treated with a selective NOS1 inhibitor failed to develop thermal hyperalgesia induced by intraplantar injection of CFA (Chen et al., 2010). The authors demonstrate that CFA-induced increases in pro-inflammatory cytokines (*e.g. Tnf* and *Il-1β*) were prevented following the use of the NOS1 inhibitor, along with an increase in the expression of the anti-inflammatory cytokine, *Il-10* (Chen et al., 2010). Additionally, NOS1 was upregulated in the spinal cords of mice exposed to a model of neuropathic pain (sciatic nerve ligation), while NOS1-KO mice showed a significant reduction in mechanical and thermal hyperalgesia compared to wildtype mice (Hervera et al., 2010). Interestingly,

recently NOS1 has also been linked with regulating macrophage phenotype, with NOS1 deficiency in mice resulting in a switch from pro- to anti-inflammatory properties in macrophages (Blajszczak et al., 2017) and reduced pro-inflammatory NF-κB transcriptional activity (Baig et al., 2015).

CCL3 (also known as macrophage inflammatory protein-1α) is a chemokine secreted by macrophages with various biological functions, primarily in the recruitment of inflammatory cells and maintenance of the effector immune response (Bhavsar et al., 2014). However, its role in nociceptive processing is being increasingly recognised, with involvement in both acute and chronic inflammatory states (Llorián-Salvador et al., 2016). Following remifentanil-induced hyperalgesia in rats, the expression of both CCL3 and its receptor, CCR5, were significantly increased (at both the mRNA level and the protein level) in the DRG, when compared to the control saline group (Li et al., 2016b). Additionally, CCL3 has been shown to be upregulated following peripheral nerve injury in mice, an effect thought to be due to the epigenetic histone modification in infiltrating macrophages (Kiguchi et al., 2013). One proposed mechanism for CCL3-induced hyperalgesia has been the sensitisation of sensory neurone TRPV1 (Zhang et al., 2005a). The authors show, using immunohistochemistry, that CCR1 (an additional CCL3 receptor) is co-expressed with TRPV1 in >85 % of small-diameter neurones within the DRG. They also show that pre-treatment with CCL3 enhanced calcium transients of DRG neurones in response to capsaicin and that an intraplantar injection of CCL3 in mice decreased their hot-plate response latency (Zhang et al., 2005a).

TRPA1 is instrumental in the detection of noxious cold stimuli and involved in a number of chronic painful states, including inflammation, neuropathic pain and fibromyalgia (as reviewed by (Garrison and Stucky, 2011)). However, its regulation via mediators such as

TNFα is not well understood. TNFα treatment of odontoblast-like cells has been shown to result in an increase in *Trpa1* expression, an effect which is dependent on p38 activation (El Karim et al., 2015). Additionally, TNFα treatment of rat trigeminal sensory neurons resulted in an elevated surface TRPA1 content (Meng et al., 2016). However, one study demonstrated that despite TNFα enhancing *Trpv1* expression in synoviocytes, TNFα was unable to modulate the expression of *Trpa1* (Kochukov et al., 2009). Interestingly, despite the literature surrounding the TNFα effect on *Trpv1* expression (as previously described), we were not able to replicate this finding.

The data collected from the conditioned medium experiments, looking at transcriptional changes, support the hypothesis that TNFα is more likely to act indirectly via the BMDM than on the neurones themselves. This is particularly compelling due to the use of purified DRG neuronal cultures in these experiments. Figure 52 illustrates how this may occur. The hypothesis is that NGF added into the system could act on the neurones themselves, while TNFα could increase the release of other inflammatory molecules from macrophages. Thereby, the two inflammatory mediators would act together to produce a heightened pain state.

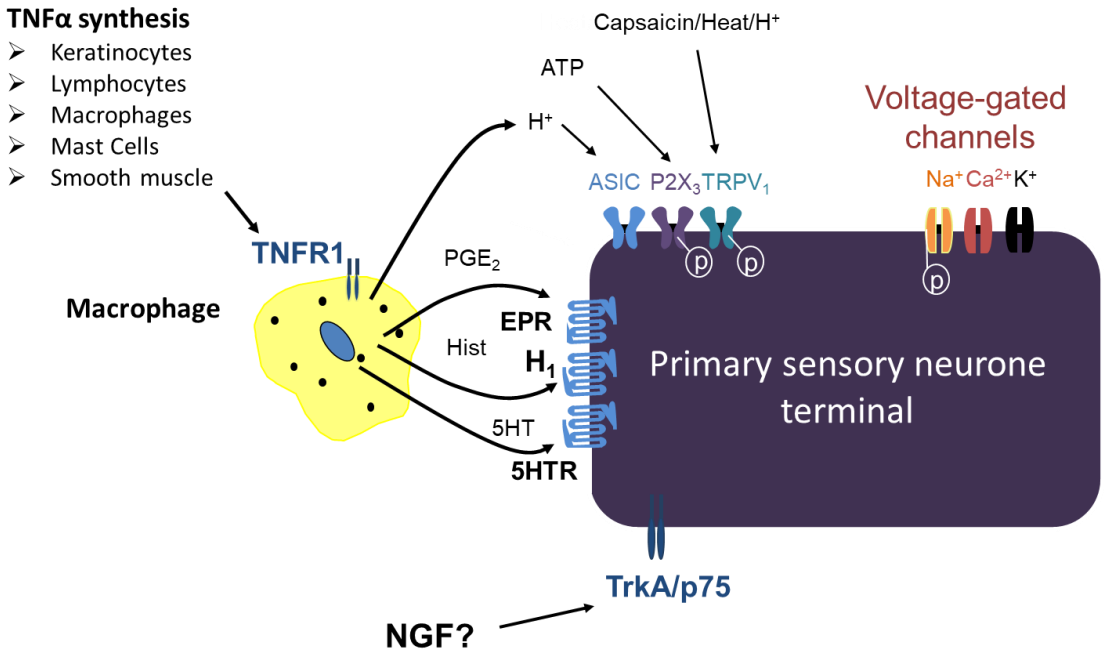

Figure 52. Schematic demonstrating the possible indirect action of TNFα on sensory neurones. (Schematic courtesy of Prof. Stephen McMahon). TNFα, from a variety of sources, may act directly via TNFR1 on a non-neuronal cell type, for example, a macrophage, resulting in the release of numerous inflammatory mediators which can then directly act upon the sensory neurone itself. These inflammatory mediators include H+, PGE2, Histamine, 5-HT, ATP, NGF and heat which act on their respective receptors residing on the sensory neurone terminal.

Abbreviations: TNFα: tumour necrosis factor; TNFR1: tumour necrosis factor receptor 1; PGE_2: Prostaglandin E2; 5-HT: serotonin; ATP: adenosine triphosphate; NGF: nerve growth factor; EPR: prostaglandin E2 receptor; 5-HTR: serotonin receptor; ASIC: acid sensing ion channel.

In line with this, our data shows enhanced CGRP release when NGF and TNFα are used in combination and only in the presence of BMDM. However, when examining changes at the transcriptional level (experiments involving CM from TNFα-stimulated BMDM (+NGF)) we saw no further changes. One explanation for this finding could be that adding NGF at 10 ng/mL was saturating the system and therefore any further modulation with CM was undetectable.

Although we saw a possible TNFα-driven effect on neurones (mediated via the CM released from TNFα stimulated BMDM) at the transcriptional level, this effect failed to translate into functional changes detected via calcium imaging. There are a number of reasons that this may have been the case. In our case we used 24 h as a time-point (24 h of neuronal exposure to the CM), in order to stay as consistent as possible with

previous experiments. However, it may be that changes would be detectable at either a much more acute time point (*e.g.* minutes-hours) or a more chronic one (*e.g.* days). Alternatively, it is possible that calcium imaging is not sensitive enough to pick up subtle changes in neuronal function.

One read-out that was not assessed following the addition of CM from BMDM on purified DRG neuronal cultures was that of neurite outgrowth. It has been shown that painful conditions, such as chronic low back pain caused by intervertebral disc degeneration, is associated with increased neurite outgrowth and increased CGRP expression via the release of nociceptive factors (Krock et al., 2014), A recent study has shown that conditioned medium collected from neurone-peritoneal macrophage cultures treated with dibutyryl cyclic AMP for 24 h, stimulated robust neurite outgrowth activity when applied to adult DRG neurone cultures alone (Au - Yun et al., 2018). These findings highlight the crucial role that macrophages play in modulating sensory neurone behaviour and suggest a possible future assay to explore in the context of this project.

Within this chapter, the emphasis has been on how the BMDM may be influencing neurones to produce changes which may be crucial to the generation and maintenance of pain states. However, it is important to note that the reverse may also be true, *i.e.* that neurones may influence the behaviour of the macrophages. Our co-culture data corroborates this idea, with macrophage-associated mediators appearing to be enhanced compared to macrophage or neuronal alone cultures (*e.g.* macrophage expressed gene transcripts and IL-1β release). In line with this, it has been shown that cerebral cortical neurones secrete TGF-β2, a factor that can significantly enhance the proliferation of macrophages (Dobbertin et al., 1997) and enteric neurones can secrete CSF1, a factor required for macrophage development (Muller et al., 2014). Furthermore,

it has recently been shown that CGRP reduced the mRNA levels of pro-IL-1β and subsequent secretion of IL-1β following LPS treatment by murine macrophages, as well as enhancing the expression of anti-inflammatory cytokines (*e.g.* IL-10) (Duan et al., 2017). The above suggests that following macrophage infiltration at the site of injury, there is most likely extensive bidirectional crosstalk between neurones and macrophages, with each cell type capable of modulating the behaviour of the other.

5.6 Summary of Chapter

In summary, the data presented throughout this chapter displays the successful optimisation and use of a co-culture system between adult DRG sensory neurones and BMDM to assess pain-relevant changes. It was found that the presence of BMDM, greatly enhanced the capacity of TNFα to potentiate neuronal evoked-CGRP release. Furthermore, we show that the effects of TNFα (likely via BMDM) can further enhance NGF-sensitised CFRP release in co-cultures of sensory neurones and BMDM. In addition to the above, expression analysis data provides supporting evidence for the existence of an indirect action of TNFα, via BMDM, to modulate sensory neurone behaviour.

6. Investigating the Combined Individual Antagonism of NGF and TNFα in an *In Vivo* Setting

6.1 Introduction

The previous chapters have presented and discussed results using *in vitro* methods. In this chapter, data will be presented using individual antagonists against NGF/TNFα *in vivo.* Appendix 1 displays the behavioural data obtained previously from chronic pain studies conducted at MedImmune wherein a bispecific molecule against NGF and TNFα was used. The following *in vivo* behavioural data mirrors this study with the exception that individual antagonists against NGF and TNFα were used. The data in Appendix 1 has been included for clarity and comparative reasons between the two studies.

Our data so far has investigated the relationship between DRG neurones and macrophages, and how this is modulated by NGF/TNFα, via a range of *in vitro* assays (Chapter 5). *In vitro* methods are fundamental to our understanding of basic biological processes; however, these are isolated systems that lack the presence of multiple other cell types and the corresponding complex environment that exists *in vivo*. Up to now, we have attempted to understand potential additive or synergistic effects following application of exogenous recombinant NGF or TNFα. In a disease state (such as chronic pain) these factors will be endogenously expressed (McMahon et al., 1995, Kidd and Urban, 2001), a scenario in which dual antagonism (of low concentrations of NGF or TNFα) provides synergistic pain relief. Thus, an alternative approach to understand the potential downstream mediators regulating the functional analgesic synergy (seen with antagonism of NGF and TNFα, Appendix Figure 1) would be to perform expression analysis of pain-relevant tissues in rodent models of chronic pain. The latter may lead to the discovery of genes which are specifically regulated by the dual antagonism of the NGF and TNFα signalling pathway.

Here, we investigate the effects of antagonising NGF or TNFα (both alone and in combination) on the expression of pain-relevant genes, in pain relevant tissues taken from two commonly used mouse models of chronic pain:

1. Intra-articular CFA model of inflammatory joint pain, and
2. Seltzer model (partial nerve ligation) of neuropathic pain

Importantly, the dose of NGF/TNFα antagonists used throughout this chapter have been carefully chosen based on their capacity to drive functional synergy (in terms of analgesia, Appendix Figure 1). Therefore, by comparing gene expression changes between mice dosed with these combined concentrations of antagonists and mice who do not receive the dual antagonism, we may gain insight into molecular drivers behind the synergistic analgesia observed.

6.1.1 Inflammatory Model of Pain- Intra-Articular Injection of Complete Freund's Adjuvant

CFA is composed of inactivated and dried *Mycobacterium* and is a common model used to mimic chronic inflammatory pain conditions, such as OA (Gregory et al., 2013). It is known to produce a persistent inflammatory state compared to other compounds, such as carrageenan, and is commonly used as a screening model to assess anti-inflammatory and analgesic drugs (Matson et al., 2007). Following CFA injection into the rat hind paw, the cardinal signs of inflammation occur (including redness, heat and swelling), followed by both allodynia and hyperalgesia, which can occur as early as 30 min after injection and persist for up to two weeks (Ren and Dubner, 1999). This time frame mimics the chronic pain experienced in humans closer than other models. CFA can be injected into

a number of anatomical sites including the paw and the tail; in our case CFA was injected into the knee joint to simulate the development of arthritis.

In this model, levels of pain-related gene transcripts in L3, L4, L5 DRG and fat pad tissue (taken from the injected knee site) were analysed. L3, L4 and L5 DRG were chosen as it known that these DRGs innervate the knee (Aso et al., 2014). Additionally, it has been shown that neuronal changes, following an inflammatory insult, were primarily located in the L3 and L4 ganglia, with a smaller contribution from L5. This differs substantially from rats, where the L3 ganglia do not contribute at all (Rigaud et al., 2008).

The fat pad tissue in the injected knee was collected due to the growing literature suggesting a crucial role for this tissue type in pain development, as described below. This tissue is an intracapsular, extrasynovial structure that fills the anterior knee compartment and is richly vascularised and innervated (Dragoo et al., 2012). The presence and distribution of substance P positive fibres within the fat pad of patients suffering from anterior knee pain syndrome suggest a role in nociceptive function (Bohnsack et al., 2005). It has been shown that the fat pad tissue from the knees of patients suffering with OA contained increased levels of pro-inflammatory cytokines (Ushiyama et al., 2003) and fatty acids such as palmitic acid, which are also known to have pro-inflammatory actions (Ioan-Facsinay and Kloppenburg, 2013). The fat pad of OA patients are infiltrated with high levels of immune cells, such as T cells and macrophages, the latter of which have been shown to be a mix of both pro- and anti-inflammatory phenotypes (Klein-Wieringa et al., 2011). Additionally, the level of CGRP expression in the fat pad of OA patients are increased depending on the grade of OA and positively correlated with COX-2 expression (Aikawa et al., 2017). A recent study showed that injection of NGF, into the fat pad tissue of healthy volunteers, resulted in

significantly reduced pressure pain thresholds (Munkholm and Arendt-Nielsen, 2017) and patients with anterior knee pain syndrome displayed a significantly higher expression of TNFα in the fat pad when compared to control subjects (Witonski et al., 2010). The above studies point to a tissue in which pain-related signalling may be modulated via the antagonism of inflammatory mediators, such as NGF and TNFα.

The levels of circulating cytokines in the plasma were also analysed due to reports of pro-inflammatory cytokines in the blood being associated with increased pain sensitivity and severity (Owens et al., 2018, Zu et al., 2016, Si et al., 2017). For example, a cross-sectional study demonstrated that levels of TNFα and IL-6 were higher in blood samples from patients suffering with chronic lower back pain compared to healthy controls (Kraychete et al., 2010). Additionally, higher serum levels of the soluble receptors of TNFα were associated with increased symptoms of pain and stiffness, increased OA symptoms and worse knee radiographic scores (Penninx et al., 2004). This is in line with data that shows that enhanced serum levels of IL-6 and TNFα are associated with knee cartilage loss in older people suffering from OA (Stannus et al., 2010), as well as in synovial fluid from patients who had meniscectomies (leading to OA) (Larsson et al., 2015).

6.1.2 Neuropathic Model of Pain- Seltzer Model

The Seltzer model involves a partial nerve injury whereby part of the sciatic nerve is unilaterally ligated. This model results in allodynia, thermal hyperalgesia and mechanical hyperalgesia, the effects of which can last for several months after the initial surgery (Seltzer et al., 1990). Similarly to the CFA model, L3, L4 and L5 DRG were collected for transcriptional analysis. We chose to examine the effect of NGF and TNFα antagonism in a model of neuropathic pain (in addition to studying an inflammatory model), due to

the difficulty in finding effective pharmacological treatments to control symptoms with this pain type (Teixeira, 2009). Therefore, discovering novel signalling pathways and interactions in this system may offer opportunities to unearth novel pain targets with improved efficacy compared to current treatments.

In both models, collection of tissue samples occurred 1-day or 7-day post-vehicle/test compound administration. These time points were based on previous mouse model data which displayed a significant reversal in mechanical hypersensitivity in the dual NGF/TNFα antagonist group when compared to either antagonist alone (Appendix Figure 1). Gene panels for each time point and tissue type (DRG or fat pad tissue) were based on genes known to be relevant in pain signalling *e.g. Trpv1 (*Zhang and Wang, 2017), as well as knowledge gained in our laboratory. Dawes and colleagues have previously shown time-dependent modulation of a range of genes in the knee fat pad tissue of rats injected with monosodium iodoacetate, including *Nos2, CCL3*, *CXCL5* (Dawes et al., 2013). Gene transcripts for both NGF and TNFα (along with their respective receptors) were also examined. Additionally, *Itgam* and *Cd14* were chosen to assess the effect of blockade on non-neuronal cell type infiltration into DRG/fat pad tissue.

6.2 Aims and Experimental Strategy

The aims of this chapter are to test the hypotheses that:

- Dual antagonism of NGF and TNFα results in a superior analgesia (compared to antagonising either factor alone) in both an inflammatory and neuropathic mouse model of chronic pain (to confirm previous findings, Appendix Figure 1)

- Dual antagonism of NGF and TNFα (at low doses which provide synergistic analgesia) normalise the expression of pain-related genes/levels of circulating cytokines in both an inflammatory and neuropathic mouse model of chronic pain

The data presented below arises from the intra-articular CFA model of inflammatory joint pain and the Seltzer model of pain (PNL) in mice. Behavioural changes in response to the different antagonists ('MEDI578' (a human anti-NGF IgG), TNFRII-fc (recombinant Fc-tagged TNFRII, acting as a TNFα antagonist)) alone or in combination, are presented along with the subsequent analysis of any changes occurring at the transcriptional level (in DRG or fat pad tissue) or circulating plasma cytokine levels.

6.3 Methods

I would like to extend my greatest gratitude to Jon Hatcher (Senior Research Scientist, MedImmune) who conducted the necessary surgeries and performed all behavioural testing presented throughout this chapter.

All experiments were performed in accordance with the United Kingdom Home Office Animals (Scientific Procedures) Act (1986). Experiments were performed under Home Office Licence PPL 70/7994 (Development of Novel Analgesics) and in accordance with ARRIVE (Animal Research: Reporting of *In Vivo* Experiments) guidelines. Mice were group housed and had food and water available *ad libitum.*

6.3.1 Complete Freund's Adjuvant Pain Model

CFA injection and behavioural testing was carried out by Jon Hatcher from MedImmune, *In Vivo* Senior Research Scientist. A schematic representing the time course of this study can be seen in Figure 53.

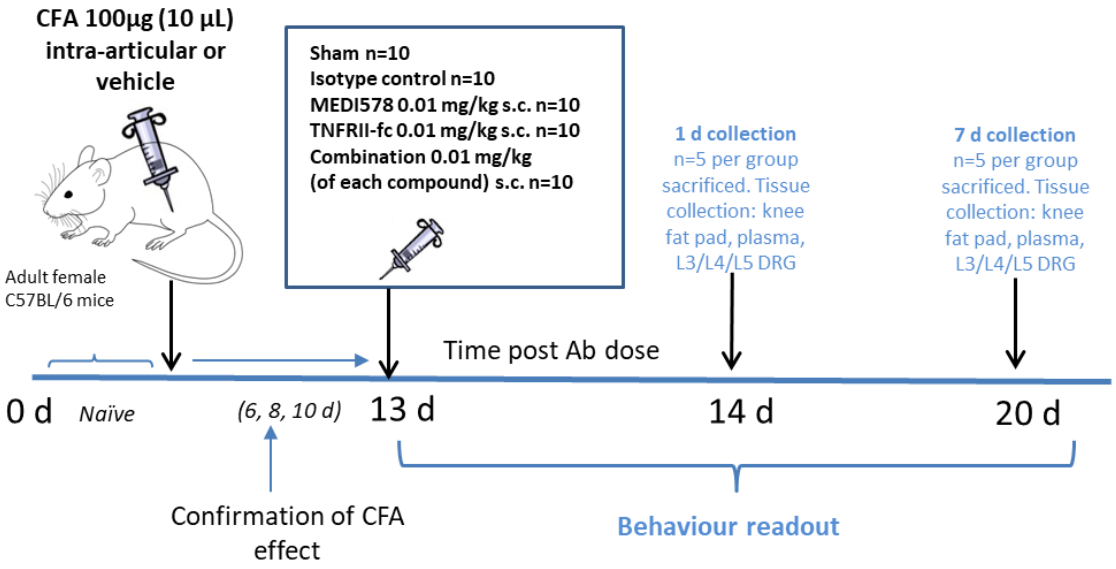

Figure 53. Schematic displaying the experimental timeline of the effect of NGF/TNFα antagonism in the intra-articular CFA model of inflammatory joint pain.

Abbreviations: NGF: nerve growth factor; TNFα: tumour necrosis factor; CFA; complete Freund's adjuvant; DRG: dorsal root ganglia; Ab: antibody.

50 adult female C57BL/6 mice were used for this study. Female mice were utilised in these experiments to allow for the mice to be group housed for a prolonged period of time (4-5 weeks in total). It is known that female mice are less aggressive than male mice (Miczek et al., 2001) and therefore do not show the same level of aggressive behaviour towards each other, thus avoiding the need to isolate any of the mice.

All mice underwent insertion of transponders (IPTT-300 Electronic ID, Plexx) for identification purposes 5 days prior to the start of the study. Transponders were implanted sub-cutaneously under general anaesthetic (isoflurane 3.5 %). Mechanical hypersensitivity was determined using a mouse incapacitance tester (Linton Instrumentation). Mice were placed in the incapacitance tester with their hind paws on separate sensors, and the body weight distribution calculated over a period of 4 secs. Data was expressed as ipsilateral and contralateral weight bearing measurements in

grams. Following the establishment of baseline readings mice were divided into 2 groups (of 40 in the CFA group and 10 in the vehicle group) with approximately equal ipsilateral/contralateral ratios. For CFA injection, animals were anesthetised using 3 % isoflurane in oxygen. The left knee was shaved, cleaned and the joint of each mouse injected with either CFA or mineral oil vehicle using a 25 g needle mounted on a 100 µl Hamilton syringe. Injections were made directly into the synovial space of the knee joint.

Mice were re-tested for changes in mechanical hypersensitivity on day 6, 8 and 10 post-injection, as described above, in order to confirm the development of mechanical hypersensitivity. Baseline readings were taken on day 10, from which the groups were further sub-divided into the final treatment groups (see below). Any mice showing an ipsilateral/contralateral ratio of greater than 80 % were classed as non-responders and removed from the study.

The final treatment groups were as follows (described in section 6.3.1.1):

- Group 1: Vehicle + CAT-251 0.01 mg/kg s.c. + PBS vehicle 10 ml/kg s.c. (n=10)
- Group 2: CFA + CAT-251 0.01 mg/kg s.c. + PBS vehicle 10 ml/kg s.c. (n=9)
- Group 3: CFA + CAT-251 0.01 mg/kg s.c. + TNFRII-fc 0.01 mg/kg s.c. (n=9)
- Group 4: CFA + MEDI578 0.01 mg/kg s.c. + PBS vehicle 1 0ml/kg s.c. (n=9)
- Group 5: CFA + MEDI578 0.01 mg/kg s.c. + TNFRII-fc 0.01 mg/kg s.c. (n=9)

Mice were administered vehicle control or test compound on day 13 post CFA injection and were subsequently re-tested for changes in mechanical hypersensitivity at 4 h, 1 day, 4 days and 7 days post dose. Following testing on day 1 post dose approximately half of the mice were culled and DRGs (L3, L4 and L5) as well as the fat pad of the ipsilateral knee were removed for subsequent analysis. Plasma was also obtained from

these mice. The remaining mice were culled following testing on day 7 and also underwent tissue removal as the first group.

6.3.1.1 Details of Drugs Used Throughout Study

CFA- 100 mg of dried mycobacterium tuberculosis (BD Biosciences; Batch number 9138946) was suspended in 10 ml of light mineral oil (Sigma Aldrich, 330779-1L) to give a stock solution of 10 mg/ml and stored at 4 ^{o}C until required for use. The solution was removed from the fridge and allowed to acclimatise to RT prior to use. The solution was shaken frequently to ensure thorough mixing. Used at a final concentration of 10 µg/µL.

CAT251- (isotype control human IgG4 antibody, MedImmune) 0.5 ml of 0.1 mg/ml solution diluted 0.5:5.0 to give 0.01 mg/ml = 0.1 mg/kg. This was then further diluted 0.5:5.0 to give a solution of 0.001 mg/ml = 0.01 mg/kg.

MEDI578- (anti-NGF human IgG4 antibody, MedImmune) Supplied as 50 mg/ml. Used at a final concentration of 0.01 mg/kg, made up in PBS.

TNFRII-fc- (recombinant Fc-tagged TNFRII, MedImmune) Supplied at 50 mg/ml. Used at a final concentration of 0.01 mg/kg, made up in PBS.

6.3.1.2 Behavioural Data Analysis

For the behavioural data, ipsilateral and contralateral readings were taken for each animal at each test time and ipsilateral/contralateral ratios calculated. PRISM was used for graphical and statistical analysis. Results were analysed using Two-Way ANOVA. Pairwise comparisons where appropriate were made using Tukey's test.

6.3.2 Gene Expression Analysis in Response to Intra-Articular CFA

6.3.2.1 RNA Isolation and cDNA Conversion

Following collection, samples from both day 1 collection and day 7 collection were snap frozen on dry ice and stored at -80 °C until subsequent analysis took place. On the day of experiment, samples were prevented from defrosting and kept on dry ice until RLT plus buffer + β-mercaptoethanol had been added, at which point they were transferred to wet ice.

6.3.2.2 L3, L4, L5 DRG Samples

DRG RNA was isolated using the RNeasy plus micro kit according to the manufacturer's instructions. Samples were homogenised in 700 µL RLT plus buffer + β-mercaptoethanol, first using a 19 g needle, followed by a 25 g needle until the DRG tissue was visually dispersed completely. Following complete homogenisation, the lysate was centrifuged at full speed for 3 min (Eppendorf centrifuge 5424) before the resulting supernatant was collected and an equal volume of 70 % ethanol added. The subsequent steps, including quantification on the Agilent 2100 Bioanalyzer, followed the same process as outlined in section 3.3.4.

Only samples with a RIN < than 7 were taken forward for further analysis. Based on this quantification 15 ng of RNA was reverse transcribed. cDNA samples were diluted 2-fold in RNase-free water and kept at 4 °C until ready for use.

6.3.2.3 Fat Pad Samples

Fat pad RNA was isolated using the RNeasy Plus Mini Kit (Qiagen, 74134) according to the manufacturer's instructions. Samples were homogenised in 350 µL RLT plus buffer + β-mercaptoethanol, first using a 19 g needle, followed by a 25 g needle until the fat pad

tissue was visually dispersed completely. Following complete homogenisation, the lysate was centrifuged at full speed for 3 min (Eppendorf centrifuge 5424) before the resulting supernatant was collected. The homogenised lysate was transferred to a gDNA Eliminator spin column and centrifuged for 30 s at 8000 *g* (Eppendorf centrifuge 5424). The column was discarded and the flow through saved. An equal volume of 70 % ethanol was added, and the sample transferred to an RNeasy Mini spin column prior to being centrifuged for 15 s at 8000 *g* (Eppendorf centrifuge 5424). The sample was transferred to an RNeasy spin column, centrifuged for 15 s at 8000 *g* (Eppendorf centrifuge 5424) and the flow-through discarded. At each of the following steps the flow through was discarded. The column was washed with 700 µL RW1 buffer, centrifuged for 15 s at 8000 *g* (Eppendorf centrifuge 5424), followed by 500 µL RPE buffer and centrifuged once more (same settings). Subsequently, 500 µL RPE buffer was added to the column and centrifuged for 2 min at 8000 *g* (Eppendorf centrifuge 5424) to further wash the membrane. At this point the column was transferred to a new collection tube and centrifuged at full speed for 1 min in order to fully air dry the membrane. Finally, the column was placed in a new 1.5 mL collection tube and 40 µL RNase-free water added directly to the centre of the membrane. To elute the RNA, the column was spun for a final time at 8000 *g* for 1 min (Eppendorf centrifuge 5424).

Quantification and sample quality assessment of RNA was conducted as described above (section 6.3.2.2), with the exception that 25 ng of RNA was reverse transcribed.

6.3.2.4 RT-qPCR

Quantification of gene transcripts, for both DRG and fat pad cDNA samples, used the same TaqMan technology and protocol as previously described in section 3.3.4.2. Mouse gene transcripts analysed are listed below (Table 13, 14 and 15) and *18s* used as the

housekeeping control gene. A blank sample of water was used as a negative control in all experiments. Where possible the assays selected were those recommended by Applied Biosystems and ones whose probes spanned an exon junction, and therefore would not detect any genomic DNA (denoted by _m1 within the catalogue numbers of Table 13, 14 and 15). For the fat pad samples, either leptin or adiponectin was quantified as a positive control to ensure that the correct tissue type was collected.

6.3.2.5 Data Analysis

mRNA transcripts were normalised to the expression of the housekeeping gene *18s* using the ΔΔCt method and data expressed as ΔΔCt changes from the basal condition. Gene transcripts analysed are listed below.

Table 13. List of mouse gene transcripts and the associated catalogue reference number used for L3, L4 and L5 DRG tissue (following intra-articular CFA administration) day 1 and day 7.

Gene Transcript	Applied Biosystems Catalogue Number
Vgf VGF Nerve Growth Factor Inducible	Mm01204485_s1
Bdnf Brain-Derived Neurotrophic Facto	Mm04230576_m1
Il-6 Interleukin 6	Mm00446190_m1
Areg Amphiregulin	Mm01354339_m1
P2x4 P2X Purinoceptor 4	Mm00501787_m1
Trpv1 Transient Receptor Potential Vanilloid 1	Mm01246300_m1
Itgam Integrin Alpha M	Mm00434455_m1
F2rl1 Protease Activated Receptor 2	Mm00433160_m1
Ntrk1	Mm01219406_m1

Neurotrophic Receptor Tyrosine 1	
Ngfr Nerve Growth Factor Receptor	Mm01219406_m1
Ngf Nerve Growth Factor	Mm00443039_m1
Tnf Tumour Necrosis Factor	Mm00443258_m1
Calca Calcitonin Related Polypeptide Alpha	Mm00801462_m1
Scn10a Sodium Voltage-Gated Channel Alpha Subunit 10	Mm00501467_m1
Tnfrsf1a Tumour Necrosis Factor Receptor 1	Mm00441875_m1
Tac1 Tachykinin Precursor 1	Mm01166996_m1
Cd14 Cluster of Differentiation 14	Mm00438094_g1

Table 14. List of mouse gene transcripts and the associated catalogue reference number used for knee fat pad samples (following intra-articular CFA administration) at day 1.

Gene Transcript	Applied Biosystems Catalogue Number
Ereg Epiregulin	Mm00514794_m1
Nos2 Nitric Oxide Synthase 2	Mm00440502_m1
Areg Amphiregulin	Mm01354339_m1
Cxcl5 C-X-C Motif Chemokine 5	Mm00436451_g1
Ccl3 Chemokine (C-C Motif) Ligand 3	Mm00441259_g1
Ccl12 Chemokine (C-C Motif) Ligand 12	Mm01617100_m1
Itgam Integrin Alpha M	Mm00434455_m1
Ngf Nerve Growth Factor	Mm00443039_m1
Tnf Tumour Necrosis Factor	Mm00443258_m1
Ptgs2	Mm00478374_m1

Prostaglandin-Endoperoxide Synthase 2	
Csf3 Colony Stimulating Factor 3	Mm00438334_m1
Cd14 Cluster of Differentiation 14	Mm00438094_g1
Calca Calcitonin Related Polypeptide Alpha	Mm00801462_m1
Tac1 Tachykinin Precursor 1	Mm01166996_m1
Lep Leptin	Mm00434759_m1

Table 15. List of mouse gene transcripts and the associated catalogue reference number used for knee fat pad samples (following intra-articular CFA administration) at day 7.

Gene Transcript	Applied Biosystems Catalogue Number
Ccl1 Chemokine (C-C Motif) Ligand 1	Mm00441236_m1
Nos2 Nitric Oxide Synthase 2	Mm00440502_m1
Ccl21 Chemokine (C-C Motif) Ligand 21	Mm03646971_gH
Ngf Nerve Growth Factor	Mm00443039_m1
Tnf Tumour Necrosis Factor	Mm00443258_m1
Csf3 Colony Stimulating Factor 3	Mm00438334_m1
Itgam Integrin Alpha M	Mm00434455_m1
Ccl5 Chemokine (C-C Motif) Ligand 5	Mm01302427_m1
Cxcl5 C-X-C Motif Chemokine 5	Mm00436451_g1
Ccl3 Chemokine (C-C Motif) Ligand 3	Mm00441259_g1

Cd14 Cluster of Differentiation 14	Mm00438094_g1
Bdnf Brain-Derived Neurotrophic Factor	Mm04230576_m1
Il-3 Interleukin 3	Mm00439631_m1
Calca Calcitonin Related Polypeptide Alpha	Mm00801462_m1
Tac1 Tachykinin Precursor 1	Mm01166996_m1
AdipoQ Adiponectin	Mm00456425_m1

6.3.3 MSD® U-PLEX Platform for CFA Experimental Plasma Sample Analysis

To measure the circulating levels of pain-relevant cytokines in each condition, MSD® U-PLEX technology was utilised. The following cytokine protein levels, at day 1 and day 7, were collected and analysed from plasma samples; IL-6, TNFα, IL-1β, KC/GRO, MCP1, MIP-3α and GM-CSF (Finn et al., 2014). Briefly, plasma samples were collected in the following way; whole blood was collected in anticoagulant-treated tubes and mixed by inverting several times prior to being left for 30 mins at room temperature. The samples were then centrifuged for 10 mins at 1000 *g* at 4 °C in order to deplete the number of platelets in the plasma sample. The resulting plasma was transferred into clean 0.5 eppendorfs and placed immediately on dry ice. Plasma samples were stored at -80 °C until further processing occurred, and numerous freeze/thaw cycles actively avoided. The MSD assay was performed according to manufacturer's instructions as previously described in section 4.3.4.

6.3.4 Seltzer Pain Model

Partial nerve ligation (PNL) surgeries and subsequent behavioural testing was carried out by Jon Hatcher from MedImmune, *In Vivo* Senior Research Scientist. A schematic representing the time course of this study can be seen in Figure 54.

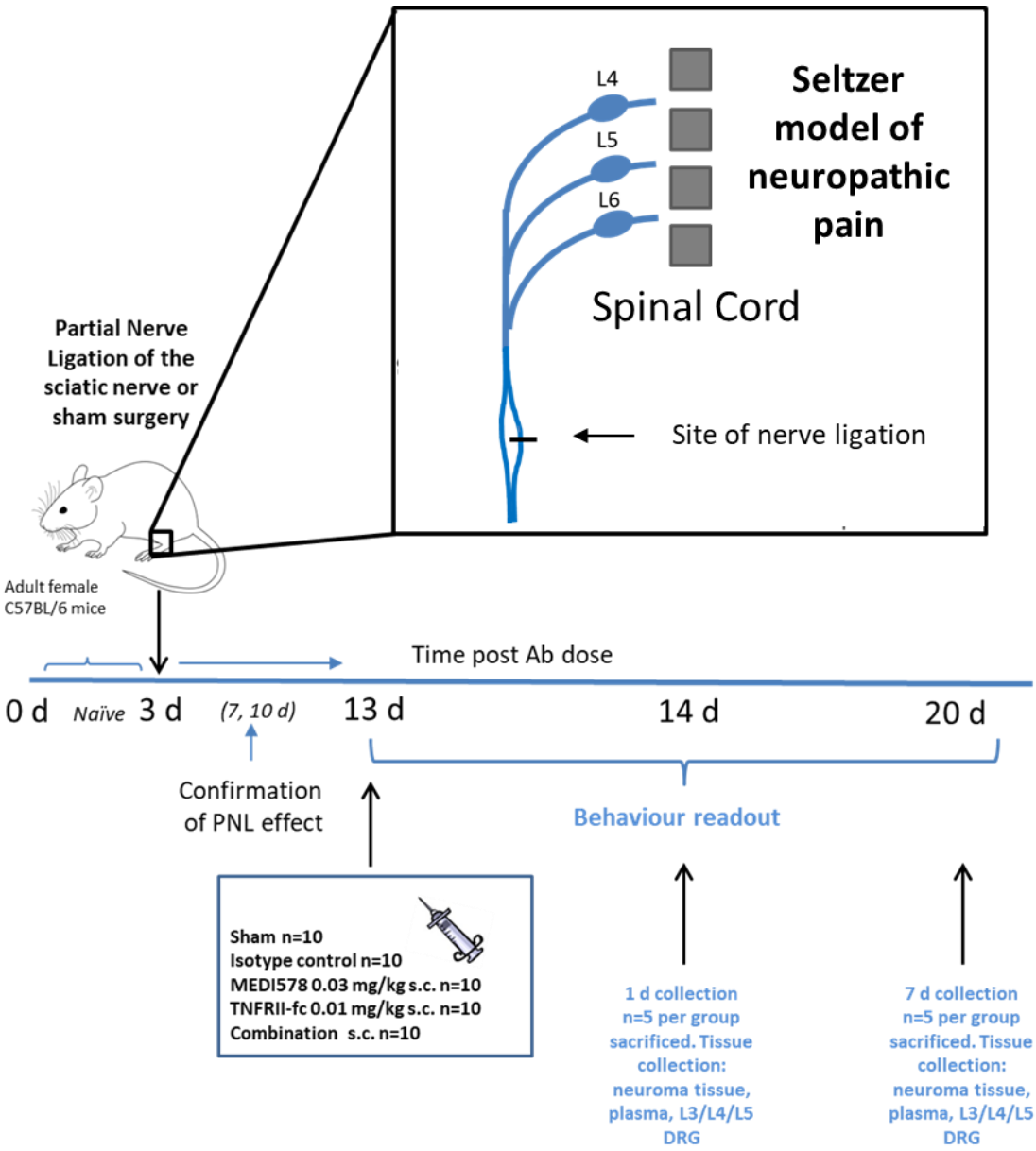

Figure 54. Schematic displaying the experimental timeline of the effect of NGF/TNFα antagonism in a PNL model of neuropathic pain. PNL schematic modified from (Zhao et al., 2014).

Abbreviations: PNL: partial nerve ligation; DRG: dorsal root ganglia.

50 female C57BL/6 mice were used for the studies. All mice underwent insertion of transponders (IPTT-300 Electronic ID, Plexx) for identification purposes at least 5 days before the start of the study. Transponders were implanted sub-cutabeously under general anaesthetic (isoflurane, 3.5 %). Mechanical hyperalgesia was determined using an analgesiometer (Randall & Selitto 1957) (Ugo Basile). An increasing force was applied

to the dorsal surface of each hind paw in turn until a withdrawal response was observed. The application of force was halted at this point and the weight in grams recorded. Data was expressed as withdrawal threshold in grams for ipsilateral and contralateral paws. Following the establishment of baseline readings mice were divided into 2 groups with approximately equal ipsilateral/contralateral ratios which underwent surgery to partially ligate the sciatic nerve or served as sham operated controls. Operated mice were anaesthetised with 3 % isoflurane. Following this approximately 1 cm of the left sciatic nerve was exposed by blunt dissection through an incision at the level of the mid-thigh. A suture (8/0 Virgin Silk: Ethicon) was then passed through the dorsal third of the nerve and tied tightly. The incision was then closed using glue and the mice were allowed to recover for at least six days prior to commencement of testing. Sham operated mice underwent the same protocol but following exposure of the nerve the mice were sutured and allowed to recover.

Mice were tested for onset of hyperalgesia on days 7 and 10 post surgery. Any mice showing an ipsilateral/contralateral ratio of greater than 80 % were classed as non-responders and removed from the study. Following testing on day 10, mice were further sub-divided into groups.

The final treatment groups were as follows;

- Group 1: Sham operated + CAT-251 0.03 mg/kg s.c. + PBS vehicle 10 ml/kg s.c. (n=10)
- Group 2: Nerve ligated + CAT-251 0.03 mg/kg s.c. + PBS vehicle 10 ml/kg s.c. (n=9)
- Group 3: Nerve ligated + CAT-251 0.03 mg/kg s.c. + TNFRII-fc 0.01 mg/kg s.c. (n=9)

- Group 4: Nerve ligated + MEDI578 0.03 mg/kg s.c. + PBS vehicle 10 ml/kg s.c. (n=9)
- Group 5: Nerve ligated + MEDI578 0.03 mg/kg s.c. + TNFRII-fc 0.01 mg/kg s.c. (n=9)

Mice were administered PBS control or test molecules on day 13 and were re-tested for changes in mechanical hyperalgesia at 1 and 4 h post dose and also at 1, 4 and 7 days post dose. Following testing on day 1 post dose approximately half of the mice were culled. DRGs (L3, L4 and L5) were removed for subsequent analysis. The remaining mice were culled following testing on day 7 and also underwent tissue removal as the first group.

Details of drugs were as described in section 6.3.1.1, with the exceptions of CAT251 and MEDI578 being used at the higher dose of 0.03 mg/kg. Data analysis was performed as described in section 6.3.1.2.

6.3.5 Gene Expression Analysis in Response to PNL

Following the collection of L3, L4, L5 DRG from the above animals, samples were handled as for the intra-articular CFA model samples. RNA isolation, cDNA conversion and RT-qPCR were performed as previously described in section 6.3.2. Gene transcripts examined are listed in Table 16 and *18s* used as the housekeeping control gene.

Table 16. List of mouse gene transcripts and the associated catalogue reference number used for L3, L4, L5 DRG samples at day 1 and day 7 following PNL.

Gene Transcript	Applied Biosystems Catalogue Number
Il-6 Interleukin 6	Mm00446190_m1
Areg Amphiregulin	Mm01354339_m1
P2x4 P2X Purinoceptor 4	Mm00501787_m1
Trpv1 Transient Receptor Potential Vanilloid 1	Mm01246300_m1
Itgam Integrin Alpha M	Mm00434455_m1
F2rl1 Protease Activated Receptor 2	Mm00433160_m1
Ntrk1 Neurotrophic Receptor Tyrosine Kinase	Mm01219406_m1
Ngfr Nerve Growth Factor Receptor	Mm01219406_m1
Ngf Nerve Growth Factor	Mm00443039_m1

Tnf Tumour Necrosis Factor	Mm00443258_m1
Calca Calcitonin Related Polypeptide Alpha	Mm00801462_m1
Scn10a Sodium Voltage-Gated Channel Alpha Subunit 10	Mm00501467_m1
Tnfsf1a Tumour Necrosis Factor Receptor 1	Mm00441875_m1
Tac1 Tachykinin Precursor 1	Mm01166996_m1
Atf3 Activating Transcription Factor 3	Mm00476033_m1

6.3.6 Statistical Analysis

All statistical analysis was performed using GraphPad software (version 7.04). Prior to any statistical analysis taking place, the data were tested for normality using the Shapiro-Wilk normality test. Within this chapter, all data was analysed using the following statistical tests; One-Way ANOVA or Two-Way ANOVA followed by *post-hoc* correction tests for multiple comparisons. In all instances, data are displayed as Mean ± SEM, n numbers and specific *post-hoc* correction tests used are reported within the figure legend. A P value <0.05 was considered to be significant.

6.4 Results

6.4.1 Behavioural Results from the CFA Model Support the Finding of a Superior Analgesic Effect when Antagonising NGF and TNFα Together in an Inflammatory Model of Joint Pain

Results demonstrated a clear effect of administration of CFA 100 µg on the ipsilateral side, an effect which was evident throughout the 7-day period (Figure 55B and C). The effect of CFA was evident as early as 4 post-injection, with the weight bearing reduced from 7.53 ± 0.53 g to 4.89 ± 0.41 g (n=8-10 mice/group) (Figure 55B). This effect was not present in the sham group or on the contralateral side (Figure 55A). The effect of treatment on reversal of mechanical hypersensitivity was examined using a Two-Way ANOVA. A significant treatment effect was present ($F(4,284)=102.4$, $P<0.0001$). When examining the ipsilateral/contralateral ratio, the administration of the isotype control, MEDI578 or TNFRII-fc failed to significantly reverse the mechanical hypersensitivity associated with CFA injection (Figure 55C). In the case of the combination treatment (ipsi/contra ratio: 82.04 ± 4.48, n=4-5 mice/group), a significant reversal from both the MEDI578 (ipsi/contra ratio: 43.3 ± 7.11, n=4-5 mice/group) and TNFRII-fc (ipsi/contra ratio: 40.17 ± 8.7, n=4-5 mice/group) alone treatment groups was observed. This effect was only observed at day 4 post-dosing with antagonists (Figure 55C). The reversal observed in the combination group at day 7 was no longer significant compared to the other treatment groups (MEDI578 ipsi/contra ratio: 54.76 ± 3.73, TNFRII-fc ipsi/contra ratio: 45.58 ± 4.84), displaying a ipsi/contra ratio of 67.36 ± 4.72 (n=4-5 mice/group) (Figure 55C).

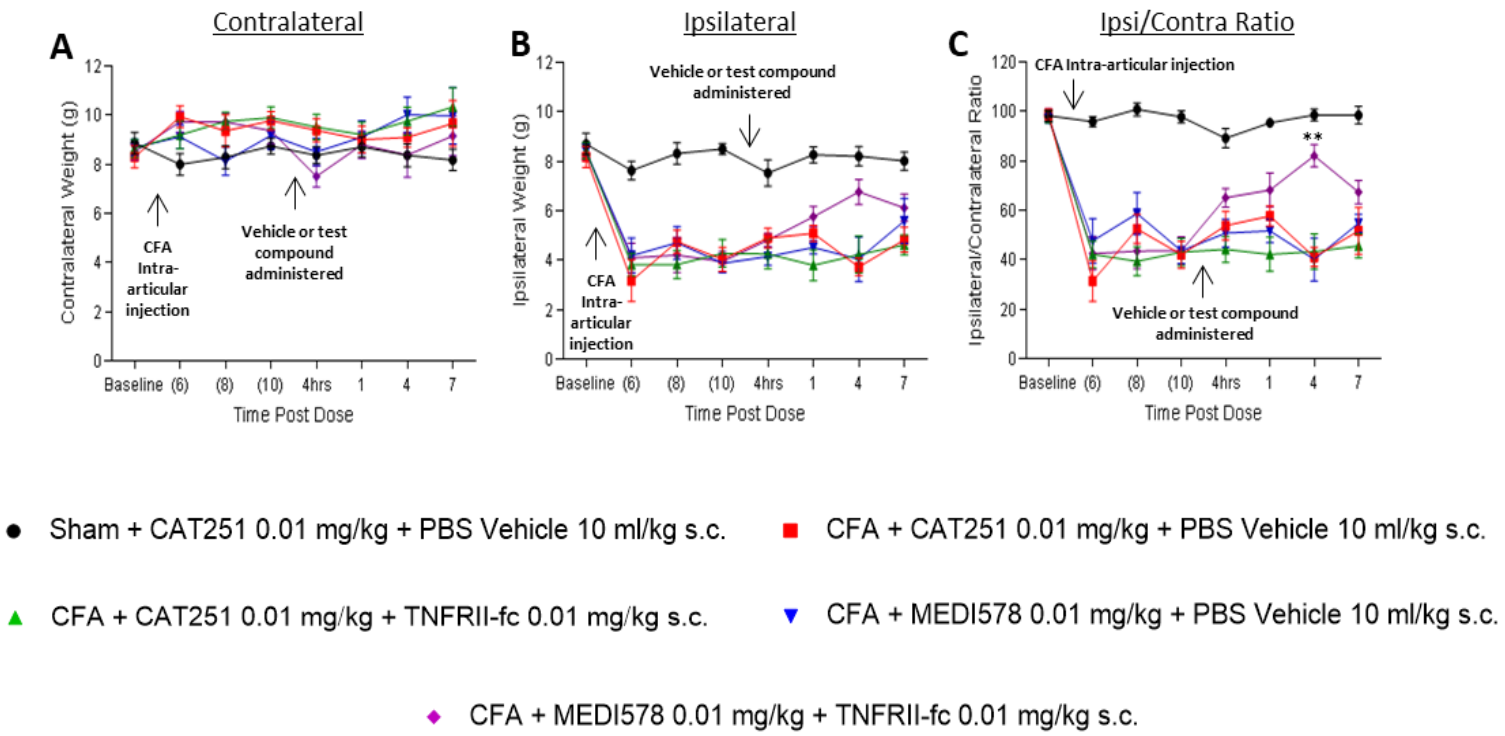

Figure 55. Effect of TNFRII-fc and MEDI578 on the reversal of intra-articular CFA induced mechanical hypersensitivity. A) Effect of sham, CFA alone, CFA + TNFRII-fc, CFA + MEDI578 or CFA + TNFRII-fc + MEDI578 on contralateral weight bearing B) ipsilateral weight bearing or C) the ipsi/contra ratio at 4 h, 1 d, 4 d, and 7 d post-vehicle/test compound administration. Data presented as Mean ± SEM, n= 8-10 mice/group up to 1 d, n= 4-5 mice/group for 4 d and 7 d. Data were analysed using Two-Way ANOVA followed by Tukey's multiple comparisons test. ** P< 0.01 compared to CFA alone, CFA + TNFRII-fc and CFA + MEDI578.

Abbreviations: CFA: complete Freund's adjuvant; Ipsi: ipsilateral; Contra: contralateral.

6.4.2 Minimal Modulation at the Transcriptional Level Occurs Following CFA Administration in the L3, L4, L5 DRG

CFA administration evoked limited DRG gene expression changes compared to sham-operated mice at both day 1 and day 7 (Figure 56). The effect of CFA was examined using a Two-Way ANOVA; no overall significant CFA effect was observed ($F(1,78)=3.245$, $P=0.0755$). However, at day 1, a significant increase in *Itgam* was observed between the sham group and CFA only group, with an increase from -0.0025 ± 0.47 ΔΔCt (n=4 mice/group) to 2.02 ± 0.36 ΔΔCt (n=4 mice/group) (Figure 56A). Amongst all other genes examined (at day 1) there was only a trend for an increase in the expression of *Tnf*, with an increase from 0.0 ± 0.21 ΔΔCt to 1.46 ± 0.22 ΔΔCt (n=4 mice/group) (Figure 56A). At the later time point of day 7, the above changes were no longer as evident, suggesting a possible resolution of earlier changes by this time point (Figure 56B).

Administration of test compounds (MEDI578, TNFRII-fc or a combination of the two) following CFA administration, had no effect on the gene expression profile evoked by CFA administration alone (1-day post-test compound addition). This was true for both *Ngf*, *Tnf*, their respective receptors (*Ntrk1*, *Ngfr*, *Tnfrsf1a*) and *Itgam* (Figure 57A-F), the latter of which had displayed a significant increase from the sham group at day 1. Similar to day 1, at day 7, administration of test compounds following CFA administration, evoked no differential expression (compared to CFA alone) (Figure 58A-F). Data for all other genes examined can be viewed in Appendix Tables 1 and 2.

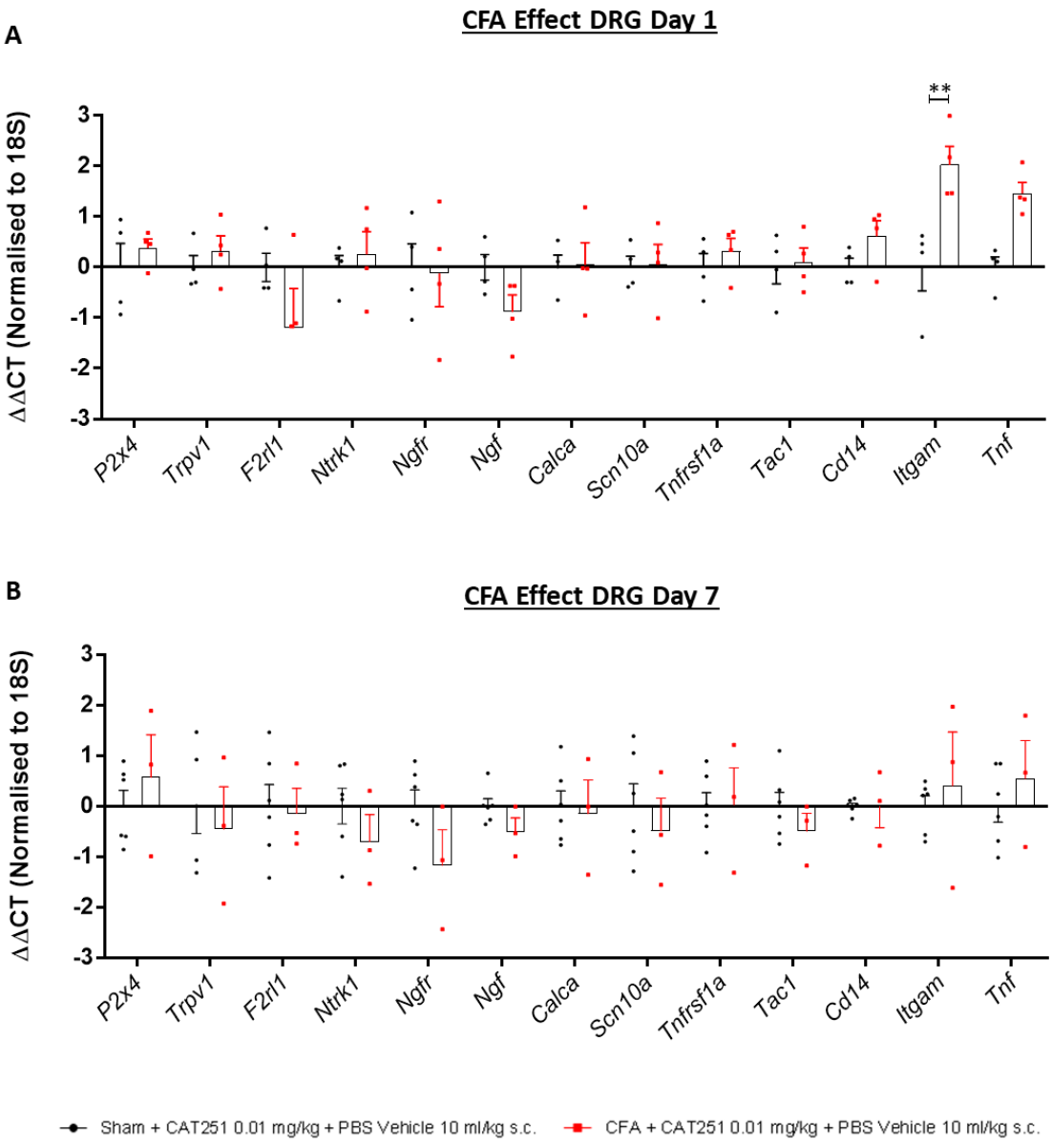

Figure 56. Transcriptional changes of DRG pain-relevant transcripts in response to intra-articular CFA administration. A) ΔΔCT values for both the sham (n=4 mice/group) and CFA group (n=4 mice/group) at day 1 and B) ΔΔCT values for both the sham (n=6 mice/group) and CFA group (n=3 mice/group) at day 7. Data displayed as Mean ± SEM. Individual data points represent individual mice. Data were analysed using Two-Way ANOVA followed by Sidak's multiple comparisons test. ** P< 0.01.

Abbreviations: DRG: dorsal root ganglia; CFA: complete Freund's adjuvant; *P2x4*: P2x purinoceptor 4; *Trpv1*: transient receptor potential vanilloid 1; *F2rl1*: coagulation factor II receptor-like 1; *Ntrk1*: neurotrophin tyrosine kinase 1; *Ngfr*; nerve growth factor receptor; *Calca:* calcitonin related polypeptide alpha; *Scn10a*: sodium voltage-gated channel alpha subunit 10; *Tnfrsf1a*: tumour necrosis factor receptor superfamily member 1a; *Tac1*: tachykinin precursor 1; *Cd14*: cluster of differentiation 14; *Itgam*: integrin subunit alpha M; *Tnf*: tumour necrosis factor.

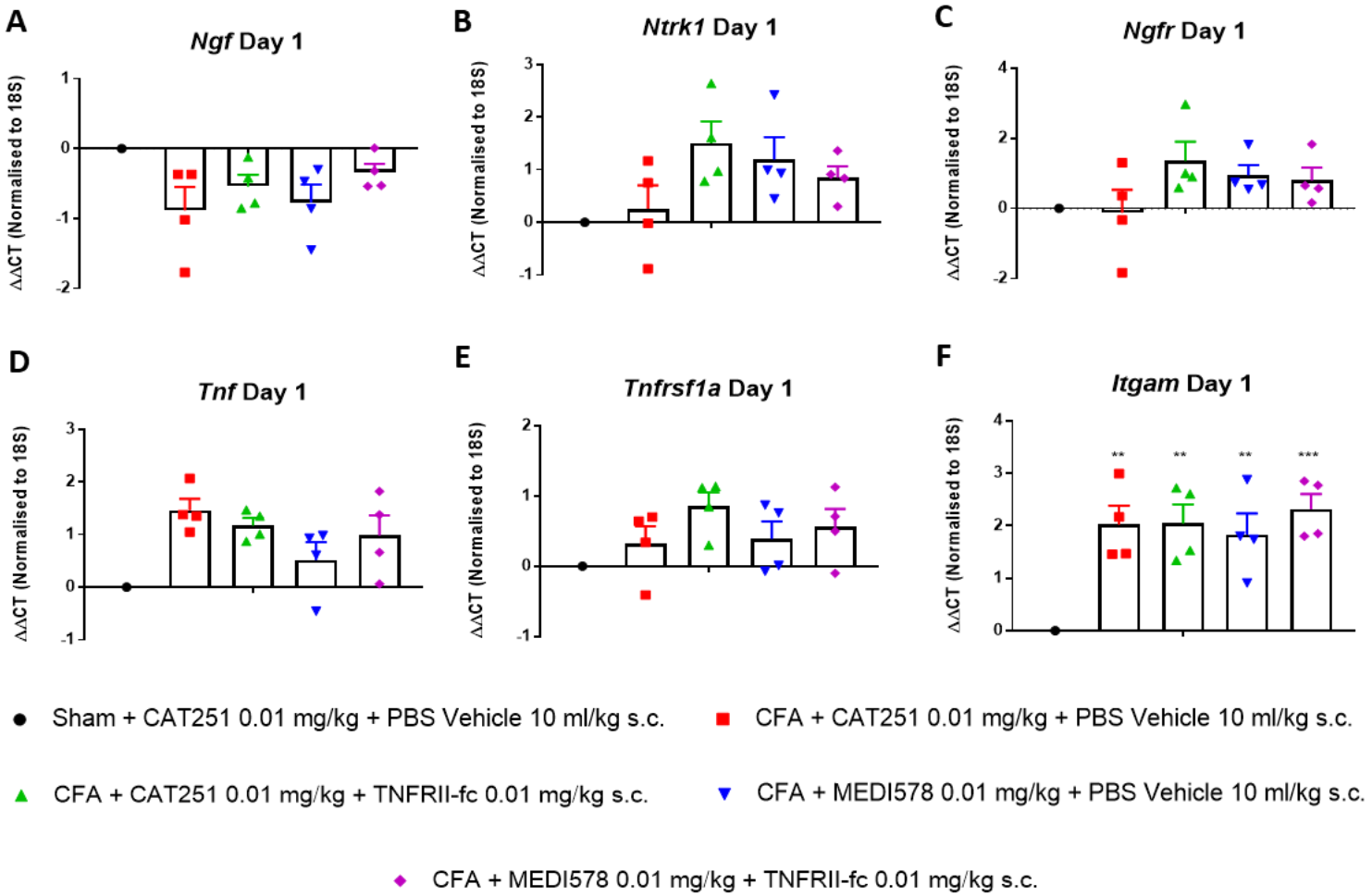

Figure 57. DRG transcriptional changes 1-day post-vehicle or test compound administration in the mouse intra-articular CFA model. ΔΔCt values for A) *Ngf* B) *Ntrk1* C) *Ngfr* D) *Tnf* E) *Tnfrsf1a* or F) *Itgam* expression. Data displayed as Mean ± SEM, n=4 mice/group (displayed as individual data points). Data were analysed using One-Way ANOVA followed by Tukey's multiple comparisons test. ** P<0.01, *** P<0.001 compared to sham group.

Abbreviations: DRG: dorsal root ganglia; CFA: complete Freund's adjuvant; *Ngf*: nerve growth factor; *Ntrk1*: neurotrophic receptor tyrosine kinase 1; *Ngfr*: nerve growth factor receptor; *Tnf*: tumour necrosis factor; *Tnfrsf1a*: tumour necrosis factor receptor superfamily member 1a; *Itgam*: integrin subunit alpha M.

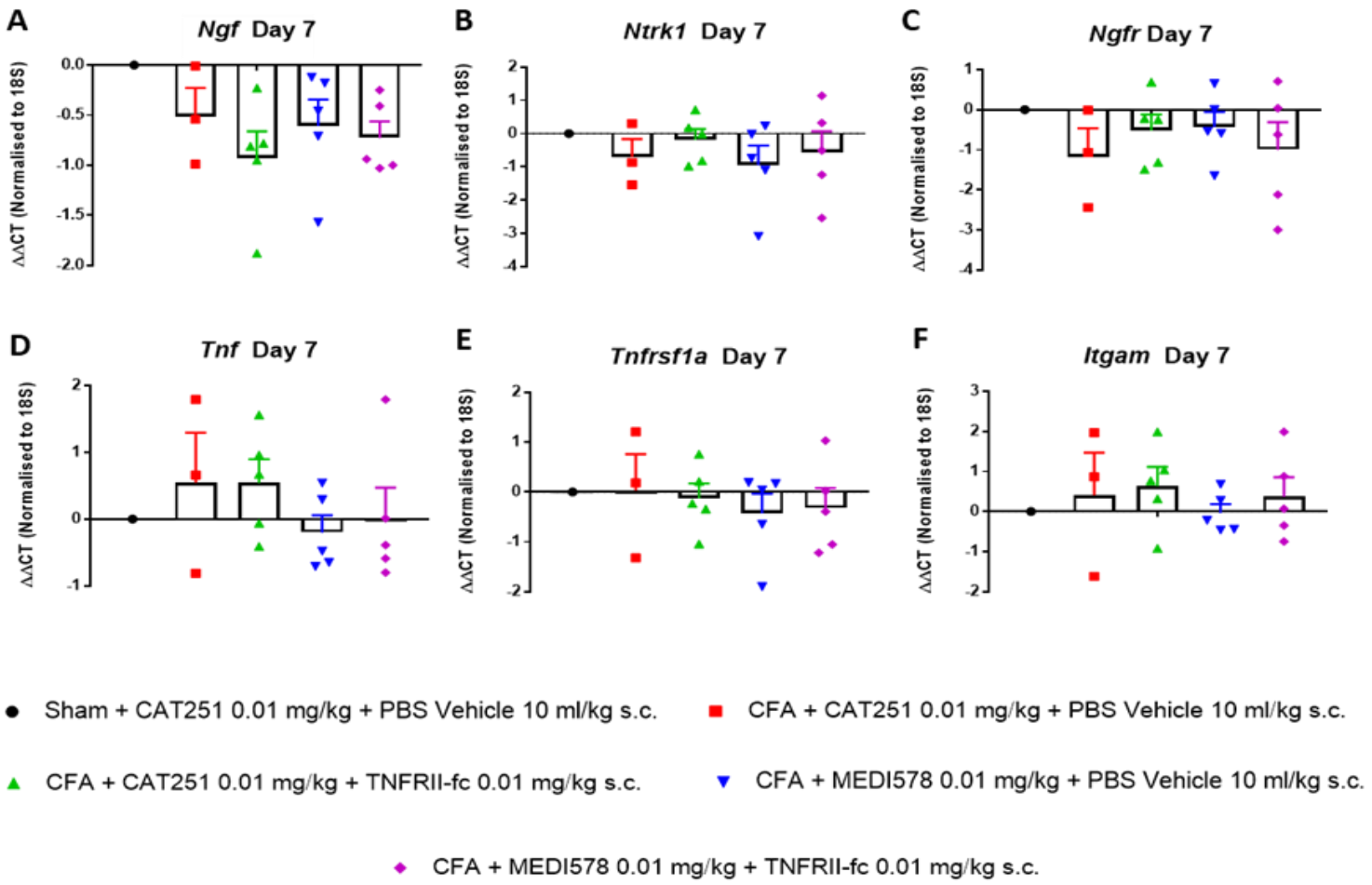

Figure 58. DRG transcriptional changes 7-days post-vehicle or test compound administration in the mouse intra-articular CFA model. ΔΔCt values for A) *Ngf* B) *Ntrk1* C) *Ngfr* D) *Tnf* E) *Tnfrsf1a* or F) *Itgam* expression. Data displayed as Mean ± SEM, n=3-5 mice/group (displayed as individual data points). Data were analysed using One-Way ANOVA followed by Tukey's multiple comparisons test.

Abbreviations: DRG: dorsal root ganglia; CFA: complete Freund's adjuvant; *Ngf*: nerve growth factor; *Ntrk1*: neurotrophic receptor tyrosine kinase 1; *Ngfr*: nerve growth factor receptor; *Tnf*: tumour necrosis factor; *Tnfrsf1a*: tumour necrosis factor receptor superfamily member 1a; *Itgam:* integrin subunit alpha M.

6.4.3 Intra-articular CFA Administration Drives a Profound Inflammatory Response at Day 1 in the Knee Fat Pad

In contrast to the DRG, CFA evoked marked changes in gene expression in the knee fat pad tissue when compared to sham-operated mice. The effect of CFA was examined using a Two-Way ANOVA; an overall CFA effect was observed ($F(1,70)=62.95$, $P<0.0001$). Significant increases in gene expression from the sham group were seen in *Nos2* (0.0 ± 0.25 ΔΔCt to 6.03 ± 0.85 ΔΔCt, n=4 mice/group), *Cxcl5* (0.003 ± 0.29 ΔΔCt to 4.58 ± 0.80 ΔΔCt, n=4 mice/group) and *Ptgs2* (0.0 ± 0.42 ΔΔCt to 3.97 ± 0.84 ΔΔCt, n=4 mice/group) (Figure 59A). Similar to the DRG tissue, these changes appeared to be returning to their baseline levels at the day 7 timepoint (Figure 59B), with the above CFA-induced gene expression changes no longer reaching significance. One exception is the expression of *Cd14*. Our data indicates that there are higher levels of *Cd14* following CFA administration at day 7 than at day 1 (1.87 ± 0.72 ΔΔCt (n=4 mice/group) to 6.59 ± 0.82 ΔΔCt (n=2 mice/group). However, due to technical issues in the CFA alone group at the day 7 timepoint, the n number (2 mice) is too low to draw any further conclusions.

Figure 60 displays all gene transcripts examined at day 1 in the knee fat pad. In terms of the test compound groups, both the TNFRII-fc and combination group behaved in a very similar manner to the CFA alone group. However, one effect of interest was seen in the MEDI578 (anti-NGF) group. Across an array of genes, we saw a consistent and reproducible increase in levels of expression in this group (Figure 60A-K, Table 17). These genes included *Tnf*, *Ereg*, *Nos2*, *Areg*, *Ccl3*, *Itgam*, *Ptgs2* and *Csf3*. Individual ΔΔCt values for all groups are displayed in Table 17, and results for the MEDI578 group highlighted in red. In each case, combined dosing of MEDI578 with TNFRII-fc, appeared to prevent these MEDI578-induced gene expression increases from occurring (Figure 60A-K, Table

17). Additionally, this effect of MEDI578 was no longer present at day 7, possibly suggesting an initial acute mechanism of action, however further experiments will be needed to confirm this finding. There were no significant changes across the genes examined at day 7, data for individual genes can be found in Appendix Table 3.

Table 17. ΔΔCt values of pain-relevant transcripts in the knee fat pad 1-day post vehicle or test compound administration in the intra-articular CFA model of joint pain. ΔΔCt values for each treatment group (CFA Only (n=4 mice), CFA + TNFRII-fc (n=4 mice), CFA + MEDI578 (n=3 mice) and CFA + TNFRII-fc + MEDI578 (n=3 mice)) relative to the sham-operated mice. Data for the MEDI578 alone group are highlighted in red.

Gene	Change from Sham Group (ΔΔCt) Mean ± SEM			
	CFA Only	CFA + TNFRII-fc	CFA + MEDI578	CFA + TNFRII-fc + MEDI578
Tnf	2.07 ± 0.62	2.28 ± 0.57	4.75 ± 0.16	1.62 ± 0.29
Ereg	1.23 ± 1.11	0.99 ± 0.41	2.81 ± 0.37	0.41 ± 0.31
Inos	6.03 ± 0.85	6.48 ± 0.34	10.21 ± 0.38	6.56 ± 0.56
Areg	0.28 ± 0.57	0.32 ± 0.35	2.74 ± 0.78	0.18 ± 0.24
Ccl3	2.33 ± 0.83	2.72 ± 0.87	6.72 ± 0.19	2.31 ± 0.59
Itgam	0.87 ± 0.46	0.89 ± 0.34	2.95 ± 0.03	0.78 ± 0.46
Ptgs2	3.97 ± 0.84	3.98 ± 0.62	7.42 ± 0.20	1.13 ± 0.61
Csf3	2.26 ± 0.86	1.97 ± 0.39	4.65 ± 0.39	2.35 ± 0.41

The levels of cytokines in the plasma of these test mice were examined using Two-Way ANOVA. Although a significant treatment effect was observed for both TNFα and IL-6 ($F(4,33)=12.1$, $P<0.0001$ and $F(4,33)=4.4$, $P=0.0058$ respectively), no changes were

observed when comparing the treatment groups with the CFA only group (Figure 61A and B). All other cytokines examined showed no significant differences across any of the groups at either time point, with levels of IL-1β being below the limits of detection (Appendix Figure 3). TNFα showed a significant increase from the sham group following CFA administration at day 1 (8.08 ± 1.12 pg/mL (n=4 mice/group) to 29.45 ± 5.13 pg/mL (n=4 mice/group), an effect which was unchanged by dosing with all test compounds (Figure 61A). A similar effect was seen at day 7 (6.39 ± 0.40 pg/mL (n=3 mice/group) to 18.4 ± 2.37 pg/mL (n=3 mice/group)) (Figure 61A). Regarding IL-6 release, we did not detect a CFA-induced effect (when compared to sham). Treatment with test compounds did not affect CFA-induced levels of plasma IL-6 relative to the CFA only treated animals (Figure 61B).

To summarise, in the DRG and knee fat pad tissue, we saw no evidence that antagonism of NGF or TNFα, or combined antagonism of NGF and TNFα (in animals dosed with MEDI578 and TNFRII-fc respectively) could differentially affect gene expression changes evoked by intra-articular CFA injection in mice (Figures 57, 58 and 60). Similarly, CFA-evoked increases in plasma TNFα or IL-6 were unaffected by antagonism of NGF and TNFα, or a combination of the two (Figure 61).

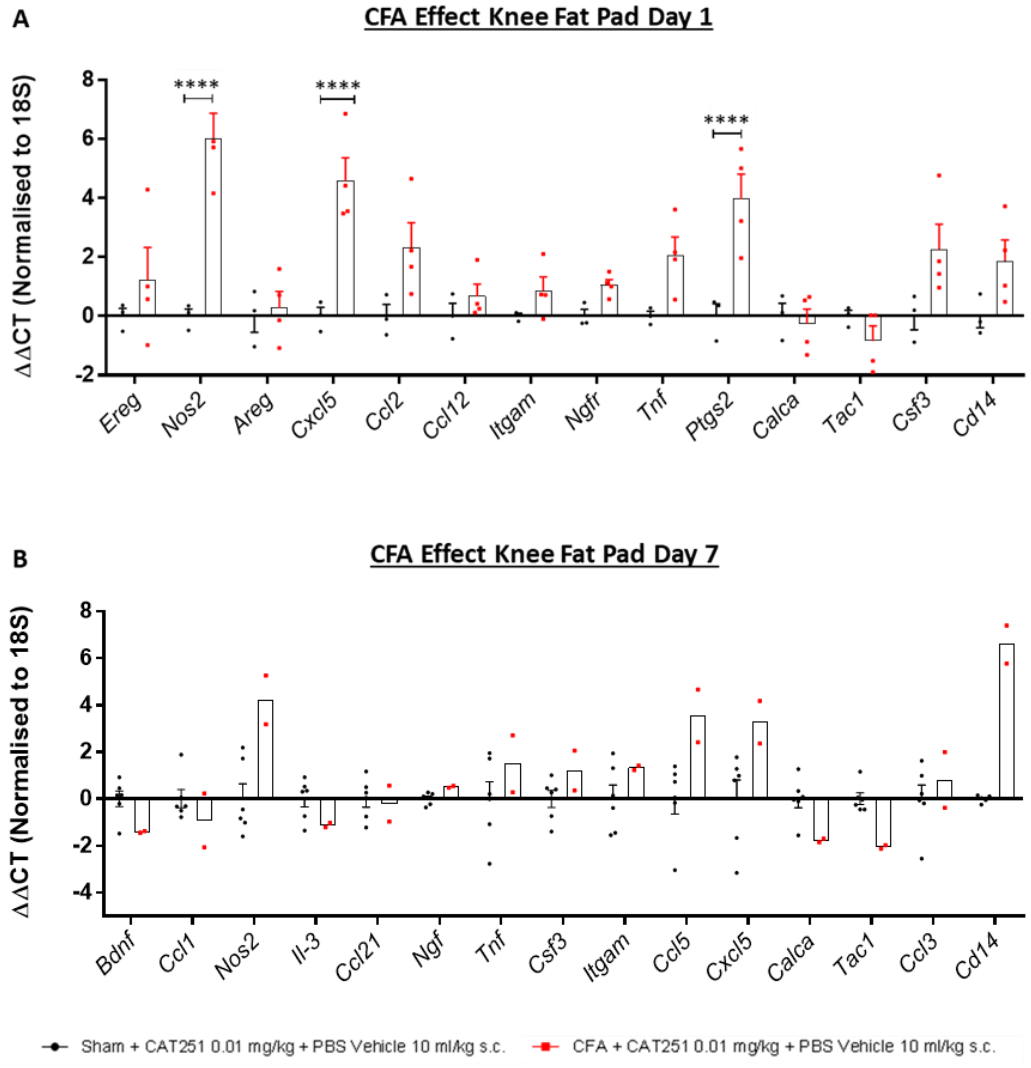

Figure 59. Transcriptional changes of knee fat pad transcripts following intra-articular CFA administration. A) ΔΔCT values for both the sham (n=4 mice/group) and CFA group (n=4 mice/group) at day 1 and B) ΔΔCT values for both the sham (n=6 mice/group) and CFA group (n=2 mice/group) at day 7. Data displayed as Mean ± SEM. Individual data points represent individual mice. Data were analysed using Two-Way ANOVA followed by Sidak's multiple comparisons test. **** P< 0.0001.

Abbreviations: CFA: complete Freund's adjuvant; *Bdnf*: brain-derived neurotrophic factor; *Ccl1*: chemokine (C-C motif) ligand 1; *Nos2*: nitrogen oxide synthase 2; *Il-3*: interleukin-3; *Ccl21*: chemokine (C-C motif) ligand 21; *Ngf*: nerve growth factor; *Tnf*: tumour necrosis factor; *Csf3*: colony-stimulating factor; *Itgam*: integrin subunit alpha M; *Ccl5*: chemokine (C-C) ligand 5; *Cxcl5*: chemokine (C-X-C motif) ligand 5; *Calca*: calcitonin related polypeptide alpha; *Tac1*: tachykinin precursor 1; *Ccl3*: chemokine (C-C motif) ligand 3; *Cd14*: cluster of differentiation 14.

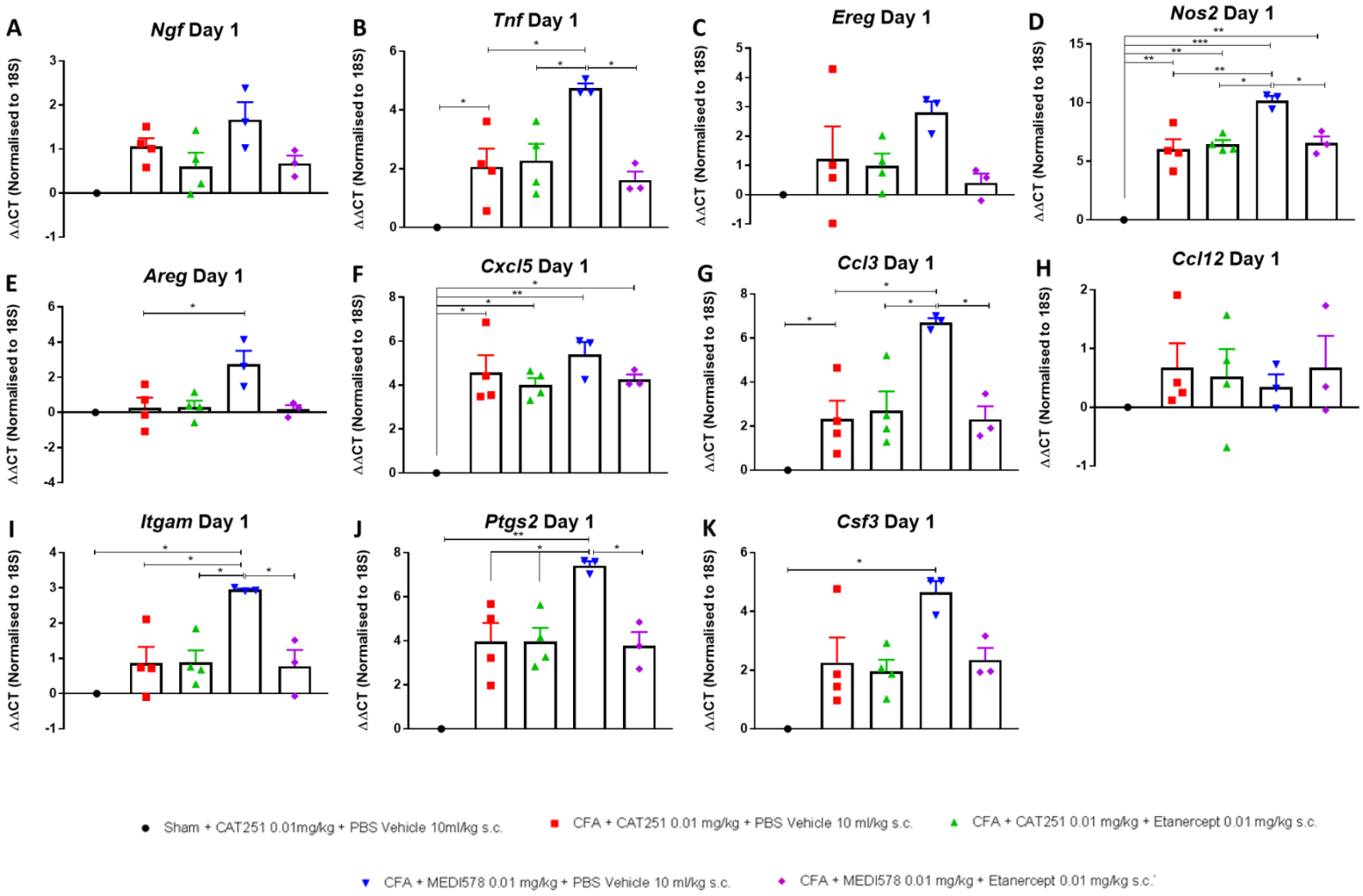

Figure 60. Knee fat pad transcriptional changes 1-day post-vehicle or test compound administration in the mouse intra-articular CFA model. Genes displayed A) *Ngf*, B) *Tnf,* C) *Ereg,* D) *Nos2,* E) *Areg,* F) *Cxcl5,* G) *Ccl3,* H) *Ccl12,* I) I*tgam,* J) *Ptgs2 and* K) *Csf3.* Data displayed as Mean ± SEM, n=3-4 mice/group (displayed as individual data points). Data were analysed using One-Way ANOVA followed by Tukey's multiple comparisons test. * P< 0.05, ** P<0.01, *** P<0.001.

Abbreviations: CFA: complete Freund's adjuvant; *Ngf*: nerve growth factor; *Tnf:* tumour necrosis factor; *Ereg*: epiregulin; *Nos2*: nitrogen oxide synthase 2; *Areg*: amphiregulin; *Cxcl5*: Chemokine (C-X-C motif) ligand 5; *Ccl3*: chemokine (C-C) ligand 3; *Ccl12*: chemokine (C-C) ligand 12; *Itgam*: integrin subunit alpha M; *Ptgs2*: prostaglandin-endoperoxide synthase 2; *Csf3*: colony-stimulating factor 3.

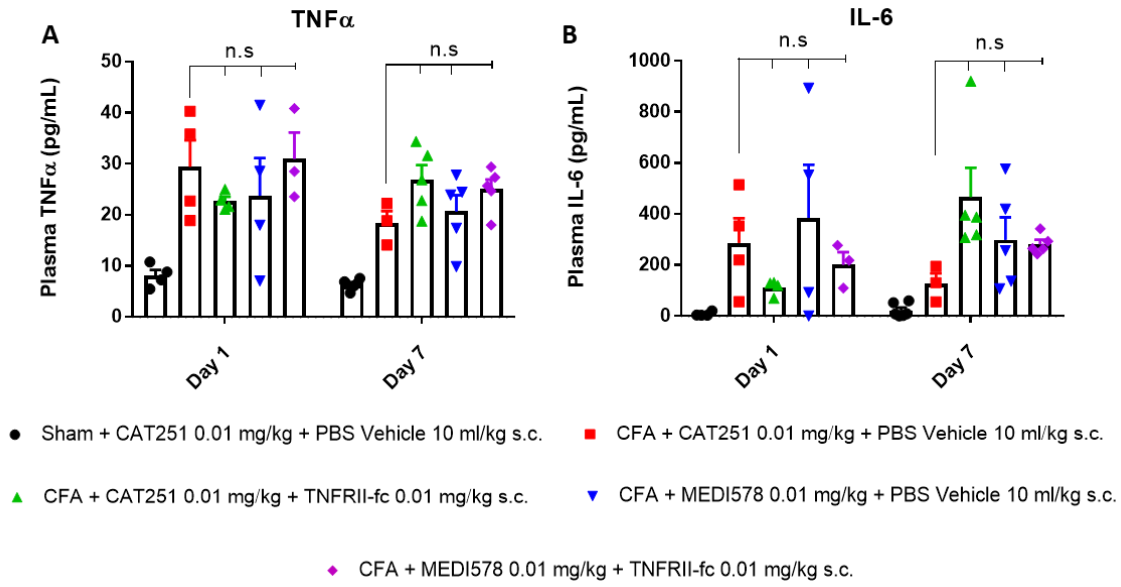

Figure 61. Levels of TNFα and IL-6 in plasma following intra-articular CFA administration. A) Levels of TNFα release (pg/mL) or B) IL-6 release (pg/mL) in the sham group or following vehicle or test compound administration at both day 1 and day 7. Data displayed as Mean ± SEM, n=3-6 mice/group (displayed as individual data points). Data analysed using Two-Way ANOVA with Tukey's multiple comparisons test. Lower limits of quantification (LLOQ) for these assays were 1.3 pg/mL (TNFα) and 4.8 pg/mL (IL-6).

Abbreviations: TNFα: tumour necrosis factor alpha; IL-6: interleukin-6; CFA: complete Freund's adjuvant; n.s: not significant.

6.4.4 Behavioural Results from the Seltzer Model Support the Finding of a Superior Analgesic Effect when Antagonising NGF and TNFα Together

Partial ligation of the sciatic nerve resulted in a profound mechanical hypersensitivity on the ipsilateral side (Figure 62B). The effect of treatment on reversal of mechanical hypersensitivity was examined using a Two-Way ANOVA. A significant treatment effect was present ($F(4,284)=161.2$, $P<0.0001$). This was clearly demonstrated when looking at the ipsilateral/contralateral ratio at day 7 (ipsi/contra ratio: from 107.5 ± 3.82 to 73.89 ± 4.31, n=9-10 mice/group) and day 10 post surgery (ipsi/contra ratio: 111 ± 2.21 to 70 ± 2.36, n=9-10 mice/group) (Figure 62C). This effect was not observed on the contralateral side (Figure 62A). The administration of a vehicle compound (CAT-251 isotype control) had no effect on the reversal of mechanical hyperalgesia, as was the case for MEDI578 and TNFRII-fc by themselves (Figure 62B and C). However, combined dosing of MEDI578 and TNFRII-fc (at doses 0.03 mg/kg and 0.01 mg/kg respectively) reversed PNL-evoked mechanical hypersensitivity at 4 h (ipsi/contra ratio: 83 ± 2.55, n=9-10 mice/group), day 1 (89 ± 4, n=9-10 mice/group) and day 7 (82.91 ± 2.92, n=4-5 mice/group) (Figure 62C) following administration of test compounds. However, as with the intra-articular CFA model of inflammatory joint pain, day 4 and day 7 represent the behavioural data from half the number of mice used at earlier time points due to tissue collection (for day 1 tissue harvest timepoint).

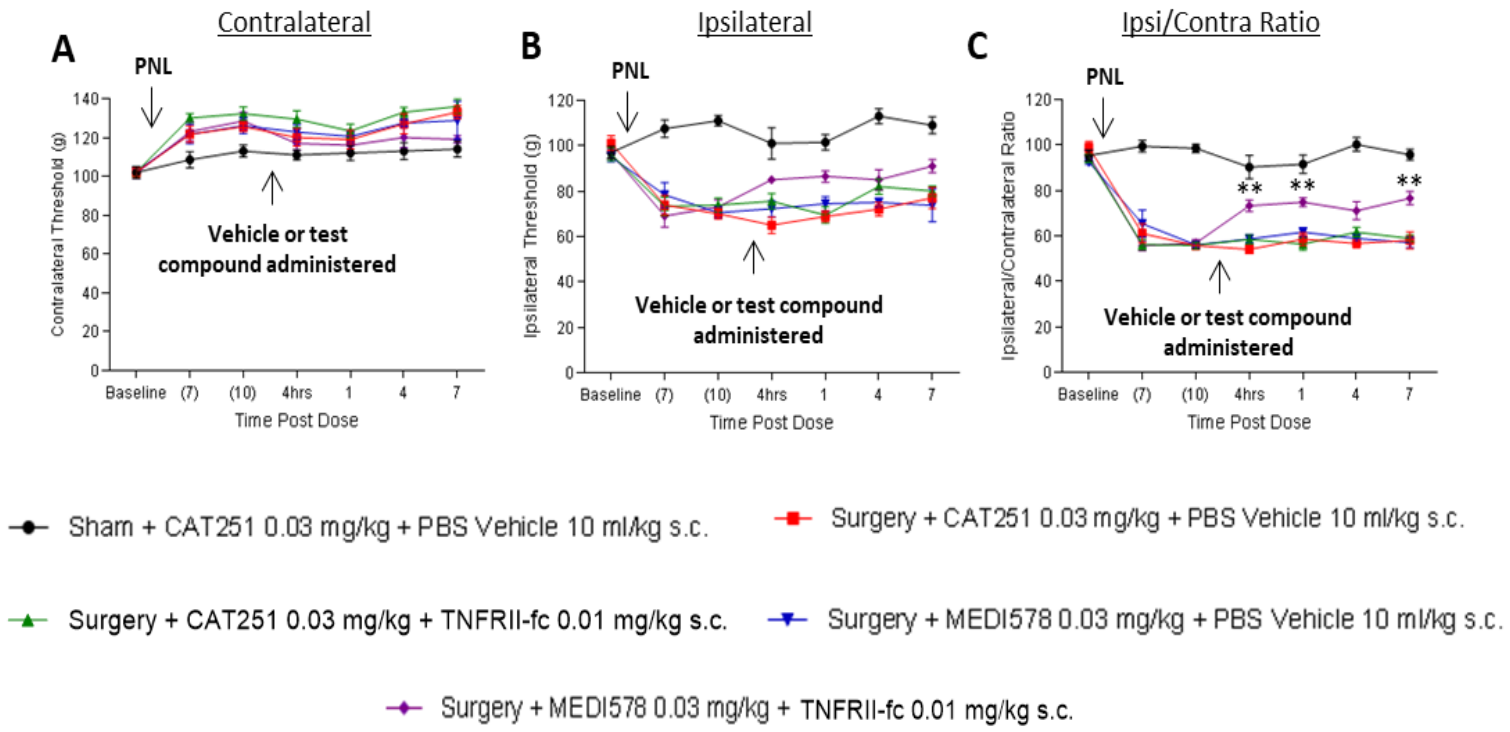

Figure 62. Effect of TNFRII-fc and MEDI578 on the reversal of PNL induced mechanical hypersensitivity. A) Effect of sham, PNL alone, PNL+ TNFRII-fc, PNL + MEDI578 or PNL + TNFRII-fc + MEDI578 on contralateral weight bearing, B) ipsilateral weight bearing or C) the ipsi/contra ratio at 4 h, 1 d, 4 d, and 7 d post-vehicle/test compound administration at day 13 post surgery. Data presented as Mean ± SEM, n= 9-10 mice/group up to 1 d, n= 4-5 mice/group for 4 d and 7 d. Data were analysed using Two-Way ANOVA followed by Tukey's multiple comparisons test. ** P<0.01 compared to PNL surgery alone, PNL surgery + TNFRII-fc and PNL surgery alone + MEDI578.

Abbreviations: PNL: partial nerve ligation; Ipsi: ipsilateral; Contra: contralateral.

6.4.5 Partial Nerve Ligation Causes a Modest Upregulation of Several Genes in L3, L4 and L5 DRG

Following PNL, a significant effect of treatment was observed at day 1 ($F(1,104)=14.29$, $P=0.0003$). Several genes showed a trend for an increase in expression when compared to the sham surgery group at day 1 (Figure 63A). These included *Il-6* (increase of 2.10 ± 0.40 ΔΔCt, n=4 mice/group), *Areg* (increase of 1.13 ± 0.33 ΔΔCt, n=4 mice/group), *F2rl1* (increase of 1.63 ± 0.16 ΔΔCt, n=4 mice/group) and a significant increase in the expression of *Atf3* (increase of 4.60 ± 1.82 ΔΔCt, n=4 mice/group) (Figure 63A). At day 7, these changes were less prominent, and no genes displayed a significant change from the sham surgery group (Figure 63B).

When looking at the effect of the test compounds on the above regulated genes at day 1, there were no significant differences detected between the vehicle, MEDI578 alone, TNFRII-fc alone and the combination groups (Figure 64A, C, E). No significant differences between the test compounds were seen at day 7 (Figure 64B, D, F and H). The effects of the test compounds on the remaining genes can be seen in Appendix Tables 4 and 5).

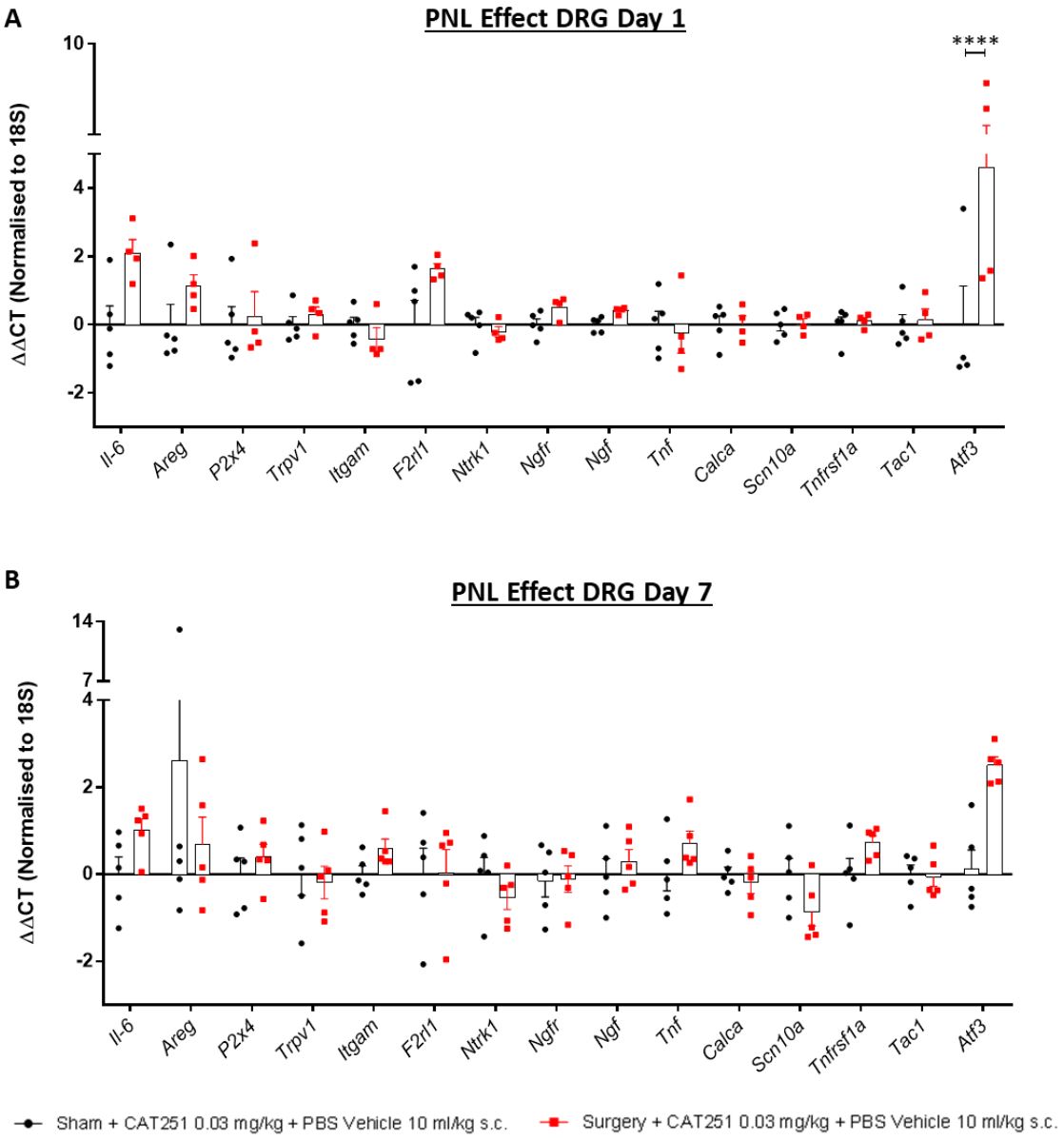

Figure 63. Transcriptional changes of DRG pain-relevant transcripts in response to PNL. A) ΔΔCT values for both the sham (n=5 mice/group) and the PNL group (n=4 mice/group) at day 1 and B) ΔΔCT values for both the sham (n=5 mice/group) and PNL group (n=5 mice/group) at day 7. Data displayed as Mean ± SEM. Individual data points represent individual mice. Data were analysed using Two-Way ANOVA followed by Sidak's multiple comparisons test. **** P< 0.0001.

Abbreviations: DRG: dorsal root ganglia; PNL: partial nerve ligation; *Il-6*: interleukin-6; *Areg*: amphiregulin; *P2x4*: P2x purinoceptor 4; *Trpv1*: transient receptor potential vanilloid 1; *Itgam*: integrin subunit alpha M; *F2rl1*: coagulation factor II receptor-like 1; *Ntrk1*: neurotrophic receptor tyrosine kinase 1; *Ngfr*: nerve growth factor receptor; *Ngf*: nerve growth factor; *Tnf*: tumour necrosis factor alpha; *Calca*: calcitonin related polypeptide alpha; *Scn10a*: sodium voltage-gated channel alpha subunit 10; *Tnfrsf1a*: tumour necrosis factor receptor superfamily member 1a; *Tac1*: tachykinin precursor 1; *Atf3*: activating transcription factor 3.

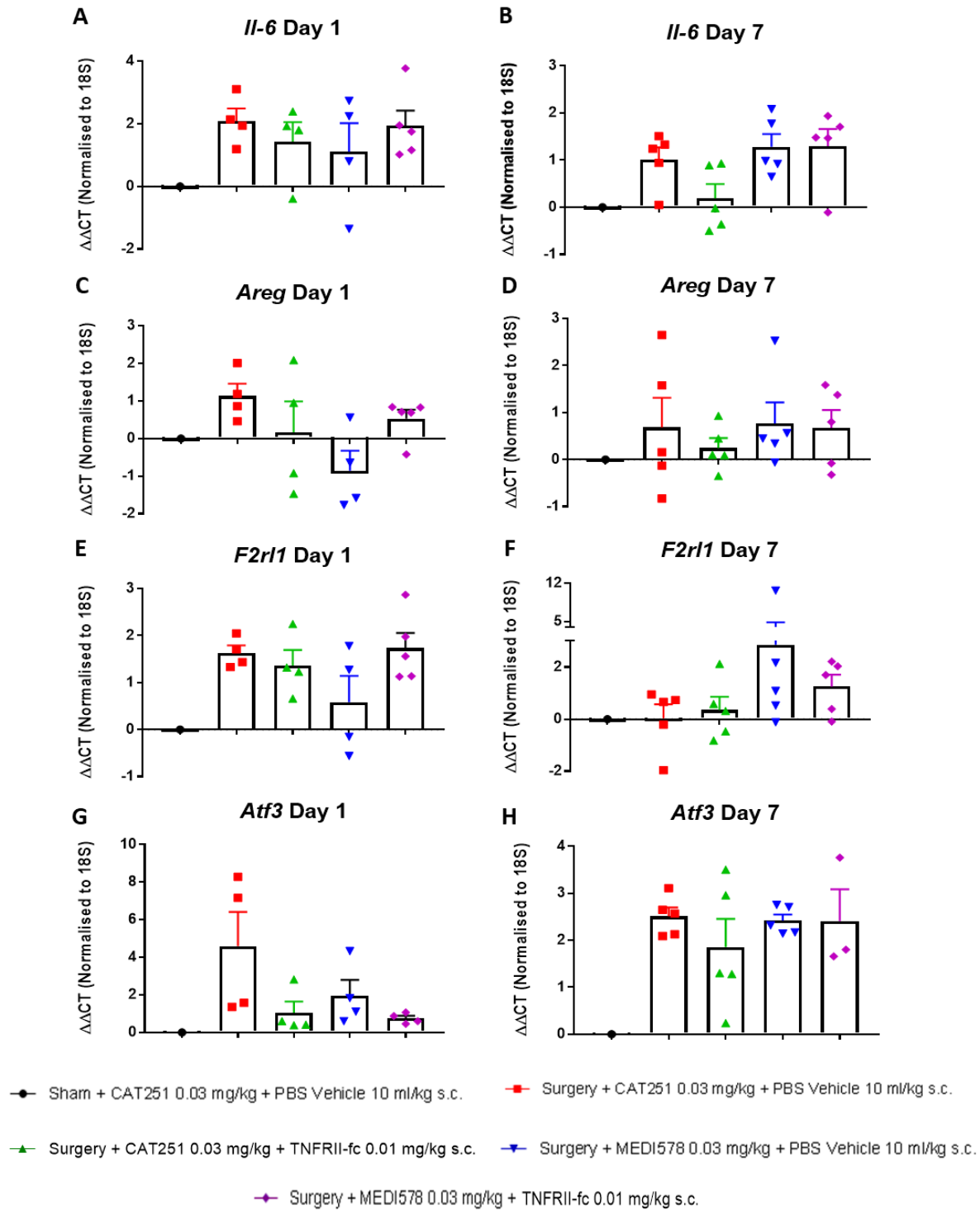

Figure 64. DRG transcriptional changes 1-day or 7-day post-vehicle or test compound administration following PNL. Expression levels of *Il-6* at A) day 1 and B) day 7, *Areg* at C) day 1 and D) day 7, *F2rl1* at E) day 1 and F) day 7 and *Atf3* at G) day 1 and H) day 7. Data displayed as Mean ± SEM, n=3-5 mice/group (displayed as individual data points). Data were analysed using One-Way ANOVA followed by Tukey's multiple comparisons test.

Abbreviations: DRG: dorsal root ganglia; PNL: partial nerve ligation; *Il-6*: interleukin-6; *Areg*: amphiregulin; *F2rl1*: coagulation factor II receptor-like 1; *Atf3*: activating transcription factor 3.

6.5 Discussion

The principal aim of this chapter was to determine if NGF/TNFα antagonism *in vivo* could synergistically reduce behavioural read-outs of pain and/or the expression of pain-relevant mediators/circulating cytokines. Two models of pain were used; the intra-articular CFA model of inflammatory joint pain and the Seltzer model of neuropathic pain (PNL).

Behavioural read-outs from both models (inflammatory and neuropathic) demonstrated a reversal in mechanical hypersensitivity following the combined blockade of NGF and TNFα compared to the blockade of each factor alone. This supports previous data collected using these models. The ability of the combination group to produce a superior analgesia compared to the individual components at the same dose could be a distinct advantage if this effect is translatable into humans. There are known adverse effects associated with both anti-NGF and anti-TNFα therapy in humans, including reports of osteonecrosis and rapidly progressive OA of the hip knee and shoulder (Lane and Corr, 2017) and development of infections, malignancies and cardiovascular effects (Atzeni et al., 2015) respectively. Therefore, a combination therapy which is efficacious at lower doses could substantially reduce these undesirable side effects.

Intra-articular CFA administration evoked limited changes in the expression of pain transcripts in DRG at the earlier time pints of tissue collection (day 1). At the later time point (day 7) of tissue collection, the effect of intra-articular CFA on DRG gene expression was nearly non-existent. One DRG gene which was significantly induced by intra-articular CFA (at the earlier timepoint of tissue collection) was *Itgam*. This molecule is commonly used as a marker for a range of cell types including monocytes, granulocytes,

neutrophils and macrophages (Yu et al., 2016). Its increase in expression following CFA administration may be indicative of non-neuronal cell type infiltration into the DRG compared to the sham group. In keeping with this, it has been shown that CFA injection into the hind paw of rats results in an increase of monocyte chemoattractant protein-1 immunoreactivity in inflammatory cells within the DRG, suggesting an infiltration of non-neuronal cell types (Jeon et al., 2008). Furthermore, CFA administration, in the hind paw of rats, has been shown to induce a 10-fold increase in the amount of perineuronal macrophages in the DRG, a finding which correlated with the level of mechanical hyperalgesia seen (Inglis et al., 2005a). Furthermore, the above infiltration was shown to be completely abolished with pre-treatment with etanercept (an anti-TNFα antibody), although etanercept application was shown to be ineffective if administered after inflammation onset. This is in line with our data which showed that despite the increase in *Itgam* expression following CFA administration, this increase was unaffected by any of the test compounds, including TNFRII-fc. The latter suggests that the mechanism by which the combination group produces superior analgesic responses is not via a mechanism which is preventing the infiltration of non-neuronal cells into the DRG.

Although not significant, there was a trend for an increase in *Tnf* expression in the DRG tissue collected at day 1 following intra-articular CFA administration, suggesting that an inflammatory response is occurring. The above finding is corroborated by a study which analysed the level of gene expression across a number of pain-relevant genes in L3-L5 rat DRG (Im et al., 2010). The authors found that across a number of rat OA knee pain models (MIA-induced, anterior cruciate ligament transection and surgical destabilisation of the medial meniscus) both *Tnf* and *Il-1β* were significantly upregulated. For example, following intra-articular injection of MIA in rats, *Il-1β* expression were increased more

than 20-fold and *Tnf* increased approximately 4-fold at the lumbar DRG level of 4/5 (Im et al., 2010). Interestingly, the same paper reported a significant down regulation of CGRP and substance P, an effect that we did not observe. This difference may be due to the use of small cohorts of mice in our case, or the use of the intra-articular CFA model as opposed to the pain models aforementioned.

The lack of gene expression changes was somewhat unexpected due to their known involvement in pain states. Changes in DRG gene expression have previously been examined in the CFA model. One study examined the effect of intraplantar CFA administration in rats on DRG gene expression at day 4 post-injection (Chang et al., 2010). Using microarrays, they were able to assay a large range of genes and showed that in general, genes associated with the immune and inflammatory response were down-regulated, whilst those associated with neuron growth and survival were enhanced (Chang et al., 2010). One of the main reasons we could not replicate the above findings could be that the CFA in our study was administered to the knee and not the plantar surface of the paw- as was the case in the study by Chang et al. It has previously been shown that a high dose of CFA into the hind paw results in multiple joints undergoing arthritic changes and causing systemic symptoms (Almarestani et al., 2011), therefore possibly producing a more widespread and perhaps a more profound response. Furthermore, a much broader range of genes were examined (by Chang et al.), while we focussed on a more limited panel of pain-related genes.

Another reason why we may not be detecting any changes in gene expression at the level of the DRG may be due to an effect of dilution. An intra-articular injection into the knee of an inflammatory substance affects far fewer DRG neurones that those innervating skin (Cook et al., 2018a). One study used an intra-articular injection of DiI (a

fluorescent dye) to demonstrate that on average only 15.9 % of L4 DRG neurones were positively labelled (and thereby innervating the joint) (Miller et al., 2018), whereas an injection of True Blue dye into plantar surface of the paw in mice showed approximately 60 % of DRG neurones were positively labelled (Rigaud et al., 2008). Additionally, when considering the ganglia as whole, only 10 % represent neurones, with the remainder being satellite glia cells and other non-neuronal cell types (Thakur et al., 2014). Therefore, important changes may be occurring to a small proportion of the cells in the DRG but remain undetected due to the large number of unaffected neurones and other cell types present within the whole DRG. As there was no effect on gene expression following intra-articular CFA administration, it is unsurprising that no further modulation was seen with any of the test compounds. One way to circumvent the above issue would be to incorporate a cell dye within the injection and then FACS sort the cells that were dye positive. This technique of using differential neuronal labelling has been previously shown to be successful in distinguishing damaged neurones from intact neurones (Reinhold et al., 2015).

Compared to the data from the DRG, several significant changes were apparent in the fat pad tissue, confirming the presence of an inflammatory reaction post-CFA administration. The most highly regulated genes in the fat pad (post-CFA administration) were identified at the earlier collection time point (day 1), with increases seen in *Nos2*, *Cxcl5* and *Ptgs2* expression. Both *Nos2* and *Cxcl5* have been shown to be highly up-regulated in the rat knee fat pad three days following monosodium iodoacetate (Dawes et al., 2013). The same dataset showed that the most highly up-regulated gene in this model (day 3) was *Ereg*. *Ereg* encodes for the protein epiregulin; a protein that belongs to the Epidermal Growth Factor family of peptide hormones. EREG is known to

contribute to a variety of physiological processes, including inflammation, wound healing and tissue repair via binding to the EGF receptor (EGFR) (Riese and Cullum, 2014). A recent study showed that blockade of EGFR signalling resulted in strongly reduced nociceptive behaviour in mouse models of both inflammatory and chronic pain. Additionally, the authors demonstrate that EREG application to sensory neurones resulted in potentiation of capsaicin-induced calcium influx (Martin et al., 2017). In line with the above evidence, single nucleotide polymorphisms (SNPs) in the gene loci encoding for EGFR and EREG have been shown to be associated with risk of chronic pain conditions, for example, temporomandibular disorder (Diatchenko, 2014). Although not significant, our dataset also showed a trend for an increase in the expression of *Ereg* in the knee fat pad (day 1). Dawes et al. may have observed a stronger increase in the levels of *Ereg*, either due to the different pain model used (MIA opposed to CFA) or due to the limited number of mice used in our study. Furthermore, the increase in *Ptgs2* expression is in line with research showing that that macrophage-dependent inflammation is significantly reduced in adipose tissue of *Ptgs2*-deficient mice (Ghoshal et al., 2011).

Most of the gene expression changes detected in the knee fat pad (post-CFA) at day 1 in our dataset were reduced at day 7, suggesting an acute response. Interestingly, at day 7, *Cd14* was more highly expressed than at day 1. *Cd14* encodes the protein CD14; a cell surface marker primarily expressed by macrophages, and to a lesser extent neutrophils and dendritic cells (Ziegler-Heitbrock and Ulevitch, 1993). One study, which would support the temporal changes in *Cd14* expression that we observed, showed an initial neutrophil accumulation into the articular space of the knee subsequent to intra-articular CFA administration in rats, followed by an infiltration of macrophages observed

at the later time point of 5 days (Chung et al., 2016). Using flow cytometry methods, macrophages, T cells and mast cells have all been shown to be present within arthritic knee joints in their activated state (Klein-Wieringa et al., 2016) further adding to the pro-inflammatory environment.

At day 1 in the fat pad tissue, MEDI578 alone further enhanced CFA-induced increases in the expression of a number of pain-relevant genes; *Tnf*, *Nos2*, *Areg*, *Ccl3*, *Itgam*, *Ptgs2* and *Csf3*. This effect was only observed 1-day post-MEDI578 administration and was lost by 7-days post-administration. Furthermore, the apparent potentiating effect of MEDI578 on these CFA-induced genes appeared to be negated by co-administration of TNFRII-fc. One potential explanation for this effect may be that the expression levels of several pro-inflammatory genes are upregulated to compensate for the blockade of NGF signalling. By day 7, the system may have 're-adjusted' and therefore this compensation is no longer required. This issue of compensation by alternative inflammatory mediators has been highlighted in the use of chemokine and chemokine receptor blockade in treating chronic synovial inflammation (Haringman and Tak, 2004). The above data would need to be repeated in a larger cohort of mice to determine if this is a reproducible effect.

Relative to sham, intra-articular CFA administration drove an increase in plasma levels of TNFα. It is known that CFA administration can induce a range of pro-inflammatory cytokines in synovial fluid and blood (Finn et al., 2014). Similarly to TNFα, IL-6 is a pleiotropic inflammatory cytokine with increasing evidence to suggest a crucial role in pain states. Following tissue injury, IL-6 is known to be upregulated, an effect which is positively correlated with pain intensity (Wang et al., 2009). Intra-articular injection of IL-6 in rats causes a gradual increase in the responses of C-fibres supplying the knee joint

in response to innocuous and noxious rotation (Brenn et al., 2007) and mice that lack its signal transducing receptor (gp130), specifically in nociceptors, showed significantly reduced levels of inflammatory and tumour-induced pain (Andratsch et al., 2009). The use of anti-IL-6 antibodies have been shown to be effective analgesics. For example, in a model of experimental autoimmune encephalomyelitis (EAE), the use of the anti-IL-6 receptor antibody MR16-1 could prevent the increase in sensitivity to pain in EAE mice, as measured via the von Frey test (Serizawa et al., 2018). Additionally, the use of the anti-IL-6 receptor antibody, tocilizumab, in patients with neuromyelitis optica (characterised in part by nerve pain) displayed a significant improvement in neuropathic pain scores following a year of treatment (Araki et al., 2014). The increase in plasma TNFα and IL-6 plasma levels that we observe most likely reflects the leakage of cytokines from the inflamed joint, therefore suggesting an ongoing state of inflammation at the site of pain.

Despite the detectable increase in TNFα (post-CFA administration), there was no significant effect of NGF or TNFα blockade (or combination of the two) on the enhanced TNFα plasma levels. This indicates that this cytokine is therefore unlikely to be contributing to the observed analgesia in Figure 55. Doses of NGF and TNFα antagonists (MEDI578 and TNFRII-fc respectively) used in this study were deliberately kept low (0.01 mg/kg and 0.03 mg/kg), to enable the detection of their efficacy *only* when used in combination. Therefore, it is not surprising that the raised TNFα plasma level is not reduced following treatment with TNFRII-fc. The data does however suggest that the mechanism of analgesia observed (driven by the combination of the two antagonists) is unlikely to be dependent on TNFα protein levels.

One explanation for a lack of effect seen from any of the treatment groups (MEDI578, TNFRII-fc or a combination of the two) post-CFA administration could be the collection of tissue at the wrong timepoint. Retrospectively, the behavioural effects of intra-articular CFA were significant at day-4 post-CFA injection, with only a trend for reversal in mechanical hypersensitivity observed at day 1 and day 7 (post-CFA injection) (Figure 51). Therefore, future studies could collect tissue at day-4 post-CFA administration and re-examine if there are any changes (either at the transcriptional level or in circulating cytokines) which correlate with the analgesia observed when MEDI578 and TNFRII-fc are dosed together.

Similarly to the intra-articular CFA model of inflammatory joint pain, L3, L4 and L5 DRG from mice that had received a PNL of the sciatic nerve showed limited changes across several genes at both time points investigated. However, a recent study reported that within the L4 DRG (7 day post injury), 75 genes were upregulated and 131 were downregulated in a neuropathic pain model (Chen et al., 2017a), changes which have been shown to produce effects for up to 30 days (Uttam et al., 2018). Additionally, one study used laser-capture microdissection to separate out injured neurons from the whole DRG ganglia and thereby demonstrated the regulation of several novel transcripts (Berta et al., 2017). The primary differences between the above studies and our own, which may account for the differences observed, was the use of a spinal nerve ligation model and our relatively narrow selection of analysed genes.

One gene that did show an increase in expression was *Atf3*. ATF3 is considered a reliable marker of neuronal damage and therefore confirmed that an injury had occurred. In a model of joint pain, *Atf3* was highly induced, primarily showing co-localisation with CGRP and IB4, displaying its specificity for peptidergic neurones (Nascimento et al.,

2011). *Atf3* is also upregulated in models of neuropathic pain, with a significant level of *Atf3* induction following spinal nerve ligation in rats (Thacker et al., 2009). It has been shown that transcription factors, such as ATF3, orchestrate the extensive transcriptional changes in neurones following an injury and induce important changes such as the altered regulation of ion channels (Costigan et al., 2009).

A further consideration when examining the *in vivo* data is the use of TNFRII-fc as an antagonist for TNFα signalling. It is known that this decoy receptor is capable of not only binding to TNFα but also lymphotoxin (also known as TNFβ) (Mpofu et al., 2005). Similar to TNFα, lymphotoxin can exist in a soluble homotrimer and is known to bind to TNFR1 and TNFR2, in addition to the herpesvirus entry mediator receptor (Calmon-Hamaty et al., 2011). High levels of lymphotoxin gene expression in the synovium of RA patients, measured using RT-PCR, have been reported to correlate with the degree of inflammation and patient pain scores compared to healthy controls (O'Rourke et al., 2008). Furthermore, one study reported a patient suffering with RA who was resistant to repeated high doses of infliximab, obtaining no clinical benefit. However, when the patient was treated with etanercept (blocking both lymphotoxin and TNFα) the patient went into clinical remission of the disease (Buch et al., 2004). Although the above study describes the situation for just one individual patient, it highlights the potential role of lymphotoxin in a disease where pain is a hallmark symptom. Therefore, future work could examine the potential role of lymphotoxin in the superior analgesia observed with the bispecific blocker.

6.6 Summary of Chapter

The behavioural data shown in this chapter demonstrates the previously observed superior analgesia (Appendix Figure 1) when antagonising NGF and TNFα at the same time in two models of pain; the intra-articular CFA model of inflammatory pain and the Seltzer model of neuropathic pain (PNL). Our data shows an increase in the expression levels of *Itgam* and *Cd14*, suggesting an infiltration of non-neuronal cell types in pain-relevant tissue types and further supporting our *in vitro* co-culture work. However, we have been unable to show changes in the expression level of se

veral pain-related genes in DRG/knee fat pad or cytokine plasma levels that reflect the behavioural changes triggered by the blockade of NGF together with TNFα. These data would suggest that the mechanism by which superior analgesia occurring may not be via regulation of transcriptional changes (in the genes examined) or circulating TNFα or IL-6 levels at these time points.

7. Conclusions, Limitations and Future Work

This PhD project has attempted to dissect the mechanisms by which a dual blocker directed against both NGF and TNFα demonstrates superior analgesic properties (in a number of pain models) compared to the blockade of either factor alone. To address this question, the effects of NGF and TNFα, either alone or in combination, were assessed using a variety of *in vitro* techniques in adult mouse sensory DRG neurones cultures, murine BMDM cultures or a co-culture system of the two. Additionally, *in vivo* experiments were used to assess the combined individual antagonism of NGF and TNFα.

We have shown that in our hands, NGF and TNFα display distinct effects on different cell types; NGF acts directly upon sensory DRG neurones whereas TNFα has a profound effect on BMDMs. We have shown that pre-treatment of neurones with NGF can enhance stimuli-evoked CGRP release, whereas TNFα requires the presence of BMDM (in a co-culture set-up). In the co-culture we have shown that the presence of BMDM, in conjunction with TNFα treatment, can significantly potentiate the CGRP release observed with NGF (over and above the NGF effect alone). Furthermore, conditioned medium derived from TNFα-stimulated BMDM showed modulation of purified neurones at the transcriptional level. These experiments suggest a likely *indirect* action of TNFα on sensory DRG neurones. This finding is contrary to some reports within the literature (previously described in section 3.1.2). However, our data is in line with other literature reporting an indirect action of TNFα. For example, mirror-image pain has been shown to be mediated by NGF produced from TNFα-activated satellite glia following PNI in rats (Cheng et al., 2014). Finally, in mouse models of chronic pain, combined blockade of NGF and TNFα failed to prevent increases in mRNA levels of genes indicative of non-neuronal cell infiltration in the knee fat pad tissue and possibly the DRG.

This thesis demonstrates that TNFα does not appear to have a direct action upon sensory DRG neurones when studied in highly purified cultures. Our work has showed that purified neuronal cultures do express low levels of the TNFα receptor, *Tnfrsf1a*, however, it may be possible that in order for TNFα to exert a direct effect on sensory neurones, an initial insult is required resulting in an upregulation of functional TNFα receptors. Therefore, future experiments could include culturing purified DRG neuronal cultures that have been extracted from mice which have undergone a partial nerve ligation or CFA injection and then assessing their response to TNFα stimulation.

Additionally, this project has focussed on the TNFα signalling mediated via the TNFR1 receptor, however, TNFα also exerts its actions via the TNFR2 receptor. Although evidence in the literature suggests that TNFα exerts the majority of its effect via the TNFR1 receptor, future work could examine if TNFR2 contributes in any way to pain-relevant signalling *e.g.* determine levels of TNFR2 in purified DRG neuronal cultures and if this is altered following treatment with NGF/TNFα. This thesis has presented some intriguing data, however, as with all scientific work, there are a number of caveats to consider. One such caveat is the use of BMDM in the co-culture set-up. BMDM were used as the most quiescent form of macrophage and therefore deemed the most suitable for assaying a response to a range of treatments. However, *in vivo*, in response to a painful stimulus, the macrophages which are infiltrating the DRG are likely to have a distinct phenotype compared to the BMDM used in our model, possibly altering the response (Komori et al., 2011). Therefore, future work could use the CGRP paradigm to assess the co-culture response when using either peritoneal macrophages or activated peritoneal macrophages (in place of BMDM) to further investigate the above. A further caveat to consider is the architecture of the co-culture set-up. Our model may closely

resemble changes occurring at the level of the DRG following a painful stimulus (*i.e.* infiltration of non-neuronal cell types), however, it may not resemble the environment at the peripheral site of injury (Dubin and Patapoutian, 2010). Additionally, *in vivo,* there are numerous other cell types involved in pain-relevant signalling pathways than merely the neurones and macrophages. Therefore, when drawing conclusions from the data presented in this thesis it is important to recognise that this multi-cellular environment was not recapitulated *in vitro*, for example, no satellite glial cells were present. In line with this, it may be that the TNFα-driven BMDM effects observed (*e.g.* increases in mRNA levels of pro-inflammatory cytokines, chemokines) require an additional cell type in order to impact the neurone, an effect that we would be missing in our current co-culture system.

In a broader context, a further consideration of our work is the use of rodents. The ability to be able to translate basic scientific research into therapies which could be effective at the clinical level is a key issue in the drug discovery process (Rezaee and Abdollahi, 2017). This is an area where many previous drugs have failed. For example, NK1 (substance P) receptor antagonists failed to exhibit efficacy in clinical trials as an analgesic, despite promising results in preclinical animal studies (Hill, 2000). It has also been shown that there is a low correlation between gene expression changes in human patients who have experienced burns or trauma and the corresponding mouse model (Burkhardt and Zlotnik, 2013). Additionally, differences between mouse and human nociceptors have been identified, with the co-expression of *Trpv1* with *TrkA* found to be present in a much larger population of neurones in humans compared to mice (Rostock et al., 2017). The above highlights the need to be cautious when interpreting the data

collected and the need to progress the work within this thesis into higher order of species to confirm our findings.

Our work highlights the importance of cross-talk between sensory neurones and non-neuronal cell types in driving changes at the level of the nociceptor that could impact the development and maintenance of pain states. We have focussed on the role of BMDM in the above process. However, future work could utilise the co-culture set-up we have used in this PhD project to investigate the effect of other non-neuronal cell types on sensory neurone function, or to assess the interaction between nociceptors and multiple non-neuronal cell types to better simulate an *in vivo* environment. In line with this, the use of *in vivo* calcium imaging could be harnessed to study the effect of NGF/TNFα application on nociceptor activation within the DRG. Additionally, the effect of NGF/TNFα blockade on nociceptor activation following an injury or insult (*i.e.* PNL, CFA injection) could be assessed. This technique would limit the potential caveats associated with cellular extractions (for *in vitro* studies), take into account the complication of intact cellular networks and has previously been used to characterise the response of large populations of sensory neurones to a variety of innocuous and noxious stimuli (Chisholm et al., 2018).

In conclusion, this thesis proposes that the mechanism(s) by which the combined individual blockade (of NGF and TNFα) regulates analgesia is not simply by an inhibition of non-neuronal cell type infiltration into pain-relevant tissue types, but more likely to be dependent on a combined dampening of neuronal sensitisation evoked by the TNFα-induced macrophage secretome and the direct activity of NGF at nociceptors. Thus, the interaction between NGF and TNFα signalling may significantly contribute to the development of chronic pain states.

8. References

Biotium [Online]. Available: https://biotium.com/technology/flow-cytometry-reagents/live-dye-fixable-viability-stains-flow-cytometry/ [Accessed 10/09/2018 2018].

1979. Pain terms: a list with definitions and notes on usage. Recommended by the IASP Subcommittee on Taxonomy. *Pain,* 6**,** 249.

AIKAWA, J., UCHIDA, K., TAKANO, S., INOUE, G., MINATANI, A., MIYAGI, M., IWASE, D., SEKIGUCHI, H., MUKAI, M. & TAKASO, M. 2017. Expression of calcitonin gene-related peptide in the infrapatellar fat pad in knee osteoarthritis patients. *Journal of Orthopaedic Surgery and Research,* 12**,** 65.

AKSENTIJEVICH, I., GALON, J., SOARES, M., MANSFIELD, E., HULL, K., OH, H.H., GOLDBACH-MANSKY, R., DEAN, J., ATHREYA, B., REGINATO, A., HENRICKSON, M., PONS-ESTERL, B.,O'SHEA, J.J. and KASTNER, D.L. 2001. The Tumor-Necrosis-Factor Receptor–Associated Periodic Syndrome: New Mutations inTNFRSF1A, Ancestral Origins, Genotype-Phenotype Studies, and Evidence for Further Genetic Heterogeneity of Periodic Fevers. *The American Journal of Human Genetics*, 69(5), pp.1160-1160.

AKSENTIJEVICH, I. & ZHOU, Q. 2017. NF-κB Pathway in Autoinflammatory Diseases: Dysregulation of Protein Modifications by Ubiquitin Defines a New Category of Autoinflammatory Diseases. *Frontiers in Immunology,* 8**,** 399.

ALETAHA, D. & BLÜML, S. 2016. Therapeutic implications of autoantibodies in rheumatoid arthritis. *RMD Open,* 2.

ALMARESTANI, L., FITZCHARLES, M.-A., BENNETT, G. J. & RIBEIRO-DA-SILVA, A. 2011. Imaging studies in Freund's complete adjuvant model of regional polyarthritis, a model suitable for the study of pain mechanisms, in the rat. *Arthritis & Rheumatism,* 63**,** 1573-1581.

ALOE, L., ROCCO, M. L., BIANCHI, P. & MANNI, L. 2012. Nerve growth factor: from the early discoveries to the potential clinical use. *Journal of Translational Medicine,* 10**,** 239-239.

AMANN, R., SCHULIGOI, R., HOLZER, P. & DONNERER, J. 1995. The non-peptide NK1 receptor antagonist SR140333 produces long-lasting inhibition of neurogenic inflammation, but does not influence acute chemo- or thermonociception in rats. *Naunyn Schmiedebergs Arch Pharmacol,* 352**,** 201-5.

ANDERSON, D. J. 2000. Genes, lineages and the neural crest: a speculative review. *Philosophical Transactions of the Royal Society B: Biological Sciences,* 355**,** 953-964.

ANDRADE, P., HOOGLAND, G., TEERNSTRA, O. P., VAN AALST, J., VAN MAREN, E., DAEMEN, M. A. & VISSER-VANDEWALLE, V. 2016. Elevated levels of tumor necrosis factor-α and TNFR1 in recurrent herniated lumbar discs correlate with chronicity of postoperative sciatic pain. *The Spine Journal,* 16**,** 243-251.

ANDRADE, P., VISSER-VANDEWALLE, V., PHILIPPENS, M., DAEMEN, M. A., STEINBUSCH, H. W., BUURMAN, W. A. & HOOGLAND, G. 2011. Tumor necrosis factor-alpha levels correlate with postoperative pain severity in lumbar disc hernia patients:

opposite clinical effects between tumor necrosis factor receptor 1 and 2. *Pain,* 152**,** 2645-52.

ANDRATSCH, M., MAIR, N., CONSTANTIN, C. E., SCHERBAKOV, N., BENETTI, C., QUARTA, S., VOGL, C., SAILER, C. A., ÜCEYLER, N., BROCKHAUS, J., MARTINI, R., SOMMER, C., ULRICH ZEILHOFER, H., MÜLLER, W., KUNER, R., DAVIS, J. B., ROSE-JOHN, S. & KRESS, M. 2009. A Key Role for gp130 Expressed on Peripheral Sensory Nerves in Pathological Pain. *The Journal of Neuroscience,* 29**,** 13473-13483.

ANG, D. C., MOORE, M. N., HILLIGOSS, J. & TABBEY, R. 2011. MCP-1 and IL-8 as pain biomarkers in fibromyalgia: a pilot study. *Pain Med,* 12**,** 1154-61.

APKARIAN, A. V., SOSA, Y., SONTY, S., LEVY, R. M., HARDEN, R. N., PARRISH, T. B. & GITELMAN, D. R. 2004. Chronic back pain is associated with decreased prefrontal and thalamic gray matter density. *J Neurosci,* 24**,** 10410-5.

ARADILLAS, E., SCHWARTZMAN, R. J., GROTHUSEN, J. R., GOEBEL, A. & ALEXANDER, G. M. 2015. Plasma Exchange Therapy in Patients with Complex Regional Pain Syndrome. *Pain Physician,* 18**,** 383-94.

ARAKI, M., MATSUOKA, T., MIYAMOTO, K., KUSUNOKI, S., OKAMOTO, T., MURATA, M., MIYAKE, S., ARANAMI, T. & YAMAMURA, T. 2014. Efficacy of the anti–IL-6 receptor antibody tocilizumab in neuromyelitis optica: A pilot study. *Neurology,* 82**,** 1302-1306.

ARANGO DUQUE, G. & DESCOTEAUX, A. 2014. Macrophage Cytokines: Involvement in Immunity and Infectious Diseases. *Frontiers in Immunology,* 5**,** 491.

ARANTES, R., LOURENSSEN, S., R. S. MACHADO, C. & BLENNERHASSETT, M. 2000. *Early damage of sympathetic neurons after co-culture with macrophages: A model of neuronal injury in vitro*.

AREND, W. P. 2002. The mode of action of cytokine inhibitors. *The Journal of Rheumatology,* 65**,** 16-21.

ASO, K., IKEUCHI, M., IZUMI, M., SUGIMURA, N., KATO, T., USHIDA, T. & TANI, T. 2014. Nociceptive phenotype of dorsal root ganglia neurons innervating the subchondral bone in rat knee joints. *European Journal of Pain,* 18**,** 174-181.

ATES, O., KURT, S., ALTINISIK, J., KARAER, H. & SEZER, S. 2011. Genetic Variations in Tumor Necrosis Factor Alpha, Interleukin-10 Genes, and Migraine Susceptibility. *Pain Medicine,* 12**,** 1464-1469.

ATZENI, F., GIANTURCO, L., TALOTTA, R., VARISCO, V., DITTO, M. C., TURIEL, M. & SARZI-PUTTINI, P. 2015. Investigating the potential side effects of anti-TNF therapy for rheumatoid arthritis: cause for concern? *Immunotherapy,* 7**,** 353-361.

AU - YUN, H. J., AU - KIM, E.-H. & AU - KIM, B. G. 2018. Neuron-Macrophage Co-cultures to Activate Macrophages Secreting Molecular Factors with Neurite Outgrowth Activity. *JoVE***,** e56920.

AXELROD, F. B. & GOLD-VON SIMSON, G. 2007. Hereditary sensory and autonomic neuropathies: types II, III, and IV. *Orphanet J Rare Dis,* 2**,** 39.

BAI, Q., LIU, S., SHU, H., TANG, Y., GEORGE, S., DONG, T., SCHMIDT, B. L. & TAO, F. 2018. TNFα in the Trigeminal Nociceptive System Is Critical for Temporomandibular Joint Pain. *Molecular Neurobiology*.

BAIG, M. S., ZAICHICK, S. V., MAO, M., DE ABREU, A. L., BAKHSHI, F. R., HART, P. C., SAQIB, U., DENG, J., CHATTERJEE, S., BLOCK, M. L., VOGEL, S. M., MALIK, A. B., CONSOLARO, M. E. L., CHRISTMAN, J. W., MINSHALL, R. D., GANTNER, B. N. & BONINI, M. G. 2015. NOS1-derived nitric oxide promotes NF-κB transcriptional activity through inhibition of suppressor of cytokine signaling-1. *The Journal of Experimental Medicine,* 212**,** 1725-1738.

BALESTRA, E., PERNO, C. F., AQUARO, S., PANTI, S., BERTOLI, A., PIACENTINI, M., FORBICI, F., D'ARRIGO, R., CALIO, R. & GARACI, E. 2001. Macrophages: a crucial reservoir for human immunodeficiency virus in the body. *J Biol Regul Homeost Agents,* 15**,** 272-6.

BALKWILL, F. 2006. TNF-α in promotion and progression of cancer. *Cancer and Metastasis Reviews,* 25**,** 409.

BARKER, P. A. & SHOOTER, E. M. 1994. Disruption of NGF binding to the low affinity neurotrophin receptor p75LNTR reduces NGF binding to TrkA on PC12 cells. *Neuron,* 13**,** 203-215.

BAROUCH, R., KAZIMIRSKY, G., APPEL, E. & BRODIE, C. 2001. Nerve growth factor regulates TNF-alpha production in mouse macrophages via MAP kinase activation. *J Leukoc Biol,* 69**,** 1019-26.

BARRETO-CHANG, O. L. & DOLMETSCH, R. E. 2009. Calcium Imaging of Cortical Neurons using Fura-2 AM. *Journal of Visualized Experiments : JoVE***,** 1067.

BAUGH, J. A. & BUCALA, R. 2001. Mechanisms for modulating TNF alpha in immune and inflammatory disease. *Curr Opin Drug Discov Devel,* 4**,** 635-50.

BAYLISS, W. M. 1901. On the origin from the spinal cord of the vaso-dilator fibres of the hind-limb, and on the nature of these fibres. *The Journal of Physiology,* 26**,** 173-209.

BEAN, A. G., ROACH, D. R., BRISCOE, H., FRANCE, M. P., KORNER, H., SEDGWICK, J. D. & BRITTON, W. J. 1999. Structural deficiencies in granuloma formation in TNF gene-targeted mice underlie the heightened susceptibility to aerosol Mycobacterium tuberculosis infection, which is not compensated for by lymphotoxin. *J Immunol,* 162**,** 3504-11.

BECKERS, K., VANDER, L. M., PENDERS, J., HEYLEN, R., VAN ZUNDERT, J. & VANELDEREN, P. 2013. Neuropathic pain in humans is associated with elevated TNF-α concentrations in blood and cerebrospinal fluid: 14AP8-1. *European Journal of Anaesthesiology (EJA),* 30**,** 223-224.

BEGGS, S. 2015. Long-Term Consequences of Neonatal Injury. *The Canadian Journal of Psychiatry,* 60**,** 176-180.

BEGGS, S. & SALTER, M. W. 2010. Microglia–neuronal signalling in neuropathic pain hypersensitivity 2.0. *Current Opinion in Neurobiology,* 20**,** 474-480.

BENYAMIN, R., TRESCOT, A. M., DATTA, S., BUENAVENTURA, R., ADLAKA, R., SEHGAL, N., GLASER, S. E. & VALLEJO, R. 2008. Opioid complications and side effects. *Pain physician,* 11**,** S105-S120.

BERGER, M., KREBS, P., CROZAT, K., LI, X., CROKER, B. A., SIGGS, O. M., POPKIN, D., DU, X., LAWSON, B. R., THEOFILOPOULOS, A. N., XIA, Y., KHOVANANTH, K., MORESCO, E. M. Y., SATOH, T., TAKEUCHI, O., AKIRA, S. & BEUTLER, B. 2010. A Slfn2 mutation causes lymphoid and myeloid immunodeficiency due to loss of immune cell quiescence. *Nature immunology,* 11**,** 335-343.

BERGMANN, I., REITER, R., TOYKA, K. V. & KOLTZENBURG, M. 1998. Nerve growth factor evokes hyperalgesia in mice lacking the low-affinity neurotrophin receptor p75. *Neuroscience Letters,* 255**,** 87-90.

BERTA, T., PERRIN, F. E., PERTIN, M., TONELLO, R., LIU, Y.-C., CHAMESSIAN, A., KATO, A. C., JI, R.-R. & DECOSTERD, I. 2017. Gene Expression Profiling of Cutaneous Injured and Non-Injured Nociceptors in SNI Animal Model of Neuropathic Pain. *Scientific Reports,* 7**,** 9367.

BHAVSAR, I., MILLER, C. S. & AL-SABBAGH, M. 2014. Macrophage Inflammatory Protein-1 Alpha (MIP-1 Alpha)/CCL3: As a Biomarker MIP-1α/CCL3. *In:* PREEDY, V. R. & PATEL, V. B. (eds.) *General Methods in Biomarker Research and their Applications.* Dordrecht: Springer Netherlands.

BIAL, E. & COPE, D. K. 2011. Introduction to Pain Management, Historical Perspectives, and Careers in Pain Management. *In:* VADIVELU, N., URMAN, R. D. & HINES, R. L. (eds.) *Essentials of Pain Management.* New York, NY: Springer New York.

BIBER, K., NEUMANN, H., INOUE, K. and BODDEKE, H. 2007. Neuronal 'On' and 'Off' signals control microglia. *Trends in Neurosciences*, 30(11), pp.596-602.

BLAJSZCZAK, C., HE, C., GANTNER, B. N. & BONINI, M. 2017. NOS1 and SOC1 work as a switch of macrophage functional phenotypes. *The FASEB Journal,* 31**,** lb502-lb502.

BLISS, T. V. & COLLINGRIDGE, G. L. 1993. A synaptic model of memory: long-term potentiation in the hippocampus. *Nature,* 361**,** 31-9.

BOHNSACK, M., MEIER, F., WALTER, G. F., HURSCHLER, C., SCHMOLKE, S., WIRTH, C. J. & RÜHMANN, O. 2005. Distribution of substance-P nerves inside the infrapatellar fat pad and the adjacent synovial tissue: a neurohistological approach to anterior knee pain syndrome. *Archives of Orthopaedic and Trauma Surgery,* 125**,** 592-597.

BOLAY, H. and MOSKOWITZ, M. 2002. Mechanisms of pain modulation in chronic syndromes. *Neurology*, 59(Issue 5, Supplement 2), pp.S2-S7.

BONDESON, J., WAINWRIGHT, S. D., LAUDER, S., AMOS, N. & HUGHES, C. E. 2006. The role of synovial macrophages and macrophage-produced cytokines in driving aggrecanases, matrix metalloproteinases, and other destructive and inflammatory responses in osteoarthritis. *Arthritis Research & Therapy,* 8**,** R187-R187.

BONGARTZ, T., SUTTON, A. J., SWEETING, M. J., BUCHAN, I., MATTESON, E. L. & MONTORI, V. 2006. Anti-tnf antibody therapy in rheumatoid arthritis and the risk

of serious infections and malignancies: Systematic review and meta-analysis of rare harmful effects in randomized controlled trials. *JAMA,* 295**,** 2275-2285.

BONNINGTON, J. K. & MCNAUGHTON, P. A. 2003. Signalling pathways involved in the sensitisation of mouse nociceptive neurones by nerve growth factor. *J Physiol,* 551**,** 433-46.

BOST, A., SHAIB, A. H., SCHWARZ, Y., NIEMEYER, B. A. & BECHERER, U. 2017. Large dense-core vesicle exocytosis from mouse dorsal root ganglion neurons is regulated by neuropeptide Y. *Neuroscience,* 346**,** 1-13.

BOUCHARD, C., PAGÉ, J., BÉDARD, A., TREMBLAY, P. & VALLIÈRES, L. 2007. G protein-coupled receptor 84, a microglia-associated protein expressed in neuroinflammatory conditions. *Glia,* 55**,** 790-800.

BOWEN, E. J., SCHMIDT, T. W., FIRM, C. S., RUSSO, A. F. & DURHAM, P. L. 2006a. Tumor necrosis factor-alpha stimulation of calcitonin gene-related peptide expression and secretion from rat trigeminal ganglion neurons. *J Neurochem,* 96**,** 65-77.

BOWEN, E. J., SCHMIDT, T. W., FIRM, C. S., RUSSO, A. F. & DURHAM, P. L. 2006b. Tumor necrosis factor-α stimulation of calcitonin gene-related peptide expression and secretion from rat trigeminal ganglion neurons. *Journal of neurochemistry,* 96**,** 65-77.

BRADLEY, J. 2008. TNF-mediated inflammatory disease. *The Journal of Pathology,* 214**,** 149-160.

BRADLEY, L. M., HAYNES, L. & SWAIN, S. L. 2005. IL-7: maintaining T-cell memory and achieving homeostasis. *Trends in Immunology,* 26**,** 172-176.

BREIVIK, H., COLLETT, B., VENTAFRIDDA, V., COHEN, R. & GALLACHER, D. 2006. Survey of chronic pain in Europe: prevalence, impact on daily life, and treatment. *Eur J Pain,* 10**,** 287-333.

BRENN, D., RICHTER, F. & SCHAIBLE, H.-G. 2007. Sensitization of unmyelinated sensory fibers of the joint nerve to mechanical stimuli by interleukin-6 in the rat: An inflammatory mechanism of joint pain. *Arthritis & Rheumatism,* 56**,** 351-359.

BRESNIHAN, B., ALVARO-GRACIA, J. M., COBBY, M., DOHERTY, M., DOMLJAN, Z., EMERY, P., NUKI, G., PAVELKA, K., RAU, R., ROZMAN, B., WATT, I., WILLIAMS, B., AITCHISON, R., MCCABE, D. & MUSIKIC, P. 1998. Treatment of rheumatoid arthritis with recombinant human interleukin-1 receptor antagonist. *Arthritis & Rheumatism,* 41**,** 2196-2204.

BRIDGES, D., THOMPSON, S. W. N. & RICE, A. S. C. 2001. Mechanisms of neuropathic pain. *BJA: British Journal of Anaesthesia,* 87**,** 12-26.

BUCH, M., CONAGHAN, P., QUINN, M., BINGHAM, S., VEALE, D. & EMERY, P. 2004. True infliximab resistance in rheumatoid arthritis: a role for lymphotoxin α? *Annals of the Rheumatic Diseases,* 63**,** 1344-1346.

BURKHARDT, A. M. & ZLOTNIK, A. 2013. Translating translational research: mouse models of human disease. *Cellular And Molecular Immunology,* 10**,** 373.

CALMON-HAMATY, F., COMBE, B., HAHNE, M. & MOREL, J. 2011. Lymphotoxin α revisited: general features and implications in rheumatoid arthritis. *Arthritis Research & Therapy,* 13**,** 232-232.

CAO, D. L., ZHANG, Z. J., XIE, R. G., JIANG, B. C., JI, R. R. & GAO, Y. J. 2014. Chemokine CXCL1 enhances inflammatory pain and increases NMDA receptor activity and COX-2 expression in spinal cord neurons via activation of CXCR2. *Exp Neurol,* 261**,** 328-36.

CAO, X. C., PAPPALARDO, L. W., WAXMAN, S. G. & TAN, A. M. 2017. Dendritic spine dysgenesis in superficial dorsal horn sensory neurons after spinal cord injury. *Molecular Pain,* 13**,** 1744806916688016.

CAROLEO, M. C., COSTA, N., BRACCI-LAUDIERO, L. & ALOE, L. 2001. Human monocyte/macrophages activate by exposure to LPS overexpress NGF and NGF receptors. *Journal of Neuroimmunology,* 113**,** 193-201.

CARSWELL, E. A., OLD, L. J., KASSEL, R. L., GREEN, S., FIORE, N. & WILLIAMSON, B. 1975. An endotoxin-induced serum factor that causes necrosis of tumors. *Proceedings of the National Academy of Sciences,* 72**,** 3666-3670.

CAVANAUGH, D. J., CHESLER, A. T., BRÁZ, J. M., SHAH, N. M., JULIUS, D. & BASBAUM, A. I. 2011. Restriction of Transient Receptor Potential Vanilloid-1 to the Peptidergic Subset of Primary Afferent Neurons Follows Its Developmental Downregulation in Nonpeptidergic Neurons. *The Journal of Neuroscience,* 31**,** 10119-10127.

CHANG, D. S., HSU, E., HOTTINGER, D. G. & COHEN, S. P. 2016. Anti-nerve growth factor in pain management: current evidence. *Journal of Pain Research,* 9**,** 373-383.

CHANG, M., SMITH, S., THORPE, A., BARRATT, M. J. & KARIM, F. 2010. Evaluation of phenoxybenzamine in the CFA model of pain following gene expression studies and connectivity mapping. *Molecular Pain,* 6**,** 56-56.

CHAVAN, S. S., PAVLOV, V. A. & TRACEY, K. J. 2017. Mechanisms and Therapeutic Relevance of Neuro-immune Communication. *Immunity,* 46**,** 927-942.

CHEN, C.-C., ZIMMER, A., SUN, W.-H., HALL, J., BROWNSTEIN, M. J. & ZIMMER, A. 2002. A role for ASIC3 in the modulation of high-intensity pain stimuli. *Proceedings of the National Academy of Sciences,* 99**,** 8992-8997.

CHEN, C.-J., LIU, D.-Z., YAO, W.-F., GU, Y., HUANG, F., HEI, Z.-Q. & LI, X. 2017a. Identification of key genes and pathways associated with neuropathic pain in uninjured dorsal root ganglion by using bioinformatic analysis. *Journal of Pain Research,* 10**,** 2665-2674.

CHEN, L., YANG, G. & GROSSER, T. 2017b. Macrophage COX-2/mPGES-1/PGE2 mediates inflammatory pain in peripheral tissues. *The FASEB Journal,* 31**,** 812.9-812.9.

CHEN, Y., BOETTGER, M. K., REIF, A., SCHMITT, A., ÜÇEYLER, N. & SOMMER, C. 2010. Nitric oxide synthase modulates CFA-induced thermal hyperalgesia through cytokine regulation in mice. *Molecular Pain,* 6**,** 13-13.

CHENG, C. F., CHENG, J. K., CHEN, C. Y., LIEN, C. C., CHU, D., WANG, S. Y. & TSAUR, M. L. 2014. Mirror-image pain is mediated by nerve growth factor produced from tumor necrosis factor alpha-activated satellite glia after peripheral nerve injury. *Pain,* 155**,** 906-20.

CHENG, J.-K. & JI, R.-R. 2008. Intracellular signaling in primary sensory neurons and persistent pain. *Neurochemical research,* 33**,** 1970-1978.

CHISHOLM, K. I., KHOVANOV, N., LOPES, D. M., LA RUSSA, F. & MCMAHON, S. B. 2018. Large Scale in Vivo Recording of Sensory Neuron Activity with GCaMP6. *eneuro*.

CHIU, I. M., HEESTERS, B. A., GHASEMLOU, N., VON HEHN, C. A., ZHAO, F., TRAN, J., WAINGER, B., STROMINGER, A., MURALIDHARAN, S., HORSWILL, A. R., WARDENBURG, J. B., HWANG, S. W., CARROLL, M. C. & WOOLF, C. J. 2013. Bacteria activate sensory neurons that modulate pain and inflammation. *Nature,* 501**,** 52-57.

CHIU, I. M., VON HEHN, C. A. & WOOLF, C. J. 2012. Neurogenic Inflammation – The Peripheral Nervous System's Role in Host Defense and Immunopathology. *Nature neuroscience,* 15**,** 1063-1067.

CHU, W.-M. 2013. Tumor necrosis factor. *Cancer letters,* 328**,** 222-225.

CHUANG, H.-H., PRESCOTT, E. D., KONG, H., SHIELDS, S., JORDT, S.-E., BASBAUM, A. I., CHAO, M. V. & JULIUS, D. 2001. Bradykinin and nerve growth factor release the capsaicin receptor from PtdIns(4,5)P2-mediated inhibition. *Nature,* 411**,** 957-962.

CHUNG, J.-I., MIN, B.-H. & BAIK, E. J. 2016. Effect of Continuous-Wave Low-Intensity Ultrasound in Inflammatory Resolution of Arthritis-Associated Synovitis. *Physical Therapy,* 96**,** 808-817.

COGHILL, R. C. 2010. Individual Differences in the Subjective Experience of Pain: New Insights into Mechanisms and Models. *Headache,* 50**,** 1531-1535.

COHEN, A., BEN-ABU, Y. & ZILBERBERG, N. 2009. Gating the pore of potassium leak channels. *European Biophysics Journal,* 39**,** 61.

COHEN, S., CHANG, D., HSU, E. and HOTTINGER, D. 2016. Anti-nerve growth factor in pain management: current evidence. *Journal of Pain Research*, p.373.

COOK, A. D., CHRISTENSEN, A. D., TEWARI, D., MCMAHON, S. B. & HAMILTON, J. A. 2018a. Immune Cytokines and Their Receptors in Inflammatory Pain. *Trends in Immunology,* 39**,** 240-255.

COOK, A. D., CHRISTENSEN, A. D., TEWARI, D., MCMAHON, S. B. & HAMILTON, J. A. 2018b. Immune Cytokines and Their Receptors in Inflammatory Pain. *Trends in Immunology*.

COSTIGAN, M., SCHOLZ, J. & WOOLF, C. J. 2009. Neuropathic Pain: A Maladaptive Response of the Nervous System to Damage. *Annual review of neuroscience,* 32**,** 1-32.

COSTIGAN, M. & WOOLF, C. J. 2000. Pain: Molecular mechanisms. *The Journal of Pain,* 1**,** 35-44.

CROWLEY, C., SPENCER, S. D., NISHIMURA, M. C., CHEN, K. S., PITTS-MEEK, S., ARMANINI, M. P., LING, L. H., MCMAHON, S. B., SHELTON, D. L., LEVINSON, A. D. & ET AL. 1994. Mice lacking nerve growth factor display perinatal loss of sensory

and sympathetic neurons yet develop basal forebrain cholinergic neurons. *Cell,* 76**,** 1001-11.

CUNNANE, G., MADIGAN, A., MURPHY, E., FITZGERALD, O. & BRESNIHAN, B. 2001. The effects of treatment with interleukin-1 receptor antagonist on the inflamed synovial membrane in rheumatoid arthritis. *Rheumatology (Oxford),* 40**,** 62-9.

DAGHESTANI, H. N., PIEPER, C. F. & KRAUS, V. B. 2015. Soluble macrophage biomarkers indicate inflammatory phenotypes in patients with knee osteoarthritis. *Arthritis Rheumatol,* 67**,** 956-65.

DAVIES, A. M., LEE, K. F. & JAENISCH, R. 1993. p75-deficient trigeminal sensory neurons have an altered response to NGF but not to other neurotrophins. *Neuron,* 11**,** 565-74.

DAVIS, J. B., GRAY, J., GUNTHORPE, M. J., HATCHER, J. P., DAVEY, P. T., OVEREND, P., HARRIES, M. H., LATCHAM, J., CLAPHAM, C., ATKINSON, K., HUGHES, S. A., RANCE, K., GRAU, E., HARPER, A. J., PUGH, P. L., ROGERS, D. C., BINGHAM, S., RANDALL, A. & SHEARDOWN, S. A. 2000. Vanilloid receptor-1 is essential for inflammatory thermal hyperalgesia. *Nature,* 405**,** 183-187.

DAWES, J. M., KIESEWETTER, H., PERKINS, J. R., BENNETT, D. L. H. & MCMAHON, S. B. 2013. Chemokine expression in peripheral tissues from the Monosodium Iodoacetate model of chronic joint pain. *Molecular Pain,* 9**,** 57-57.

DAWES, J. M. & VINCENT, A. 2016. Autoantibodies and pain. *Curr Opin Support Palliat Care,* 10**,** 137-42.

DAWES, J. M., WEIR, G. A., MIDDLETON, S. J., PATEL, R., CHISHOLM, K. I., PETTINGILL, P., PECK, L. J., SHERIDAN, J., SHAKIR, A., JACOBSON, L., GUTIERREZ-MECINAS, M., GALINO, J., WALCHER, J., KÜHNEMUND, J., KUEHN, H., SANNA, M. D., LANG, B., CLARK, A. J., THEMISTOCLEOUS, A. C., IWAGAKI, N., WEST, S. J., WERYNSKA, K., CARROLL, L., TRENDAFILOVA, T., MENASSA, D. A., GIANNOCCARO, M. P., COUTINHO, E., CERVELLINI, I., TEWARI, D., BUCKLEY, C., LEITE, M. I., WILDNER, H., ZEILHOFER, H. U., PELES, E., TODD, A. J., MCMAHON, S. B., DICKENSON, A. H., LEWIN, G. R., VINCENT, A. & BENNETT, D. L. 2018. Immune or Genetic-Mediated Disruption of CASPR2 Causes Pain Hypersensitivity Due to Enhanced Primary Afferent Excitability. *Neuron,* 97**,** 806-822.e10.

DE FILIPPO, K., DUDECK, A., HASENBERG, M., NYE, E., VAN ROOIJEN, N., HARTMANN, K., GUNZER, M., ROERS, A. & HOGG, N. 2013. Mast cell and macrophage chemokines CXCL1/CXCL2 control the early stage of neutrophil recruitment during tissue inflammation. *Blood,* 121**,** 4930-7.

DELCROIX, J.-D., VALLETTA, J. S., WU, C., HUNT, S. J., KOWAL, A. S. & MOBLEY, W. C. 2003. NGF Signaling in Sensory Neurons: Evidence that Early Endosomes Carry NGF Retrograde Signals. *Neuron,* 39**,** 69-84.

DEMA, B. & CHARLES, N. 2016. Autoantibodies in SLE: Specificities, Isotypes and Receptors. *Antibodies,* 5**,** 2.

DENK, F., BENNETT, D. L. & MCMAHON, S. B. 2017. Nerve Growth Factor and Pain Mechanisms. *Annu Rev Neurosci,* 40**,** 307-325.

DENK, F., CROW, M., DIDANGELOS, A., LOPES, DOUGLAS M. & MCMAHON, STEPHEN B. 2016. Persistent Alterations in Microglial Enhancers in a Model of Chronic Pain. *Cell Reports,* 15**,** 1771-1781.

DHIMOLEA, E. 2010. Canakinumab. *mAbs,* 2**,** 3-13.

DI FILIPPO, M., SARCHIELLI, P., PICCONI, B. & CALABRESI, P. 2008. Neuroinflammation and synaptic plasticity: theoretical basis for a novel, immune-centred, therapeutic approach to neurological disorders. *Trends in Pharmacological Sciences,* 29**,** 402-412.

DI MARCO, E., MARCHISIO, P. C., BONDANZA, S., FRANZI, A. T., CANCEDDA, R. & DE LUCA, M. 1991. Growth-regulated synthesis and secretion of biologically active nerve growth factor by human keratinocytes. *Journal of Biological Chemistry,* 266**,** 21718-21722.

DIATCHENKO, L. 2014. Translational research in the genomic era: OPPERA study. *Molecular Pain,* 10**,** O1-O1.

DINARELLO, C. A. 2011. Interleukin-1 in the pathogenesis and treatment of inflammatory diseases. *Blood,* 117**,** 3720-32.

DINARELLO, C. A., SIMON, A. & VAN DER MEER, J. W. M. 2012. Treating inflammation by blocking interleukin-1 in a broad spectrum of diseases. *Nature reviews. Drug discovery,* 11**,** 633-652.

DING, S., ZHU, L., TIAN, Y., ZHU, T., HUANG, X. & ZHANG, X. 2017. P2X3 receptor involvement in endometriosis pain via ERK signaling pathway. *PLoS ONE,* 12**,** e0184647.

DJOUHRI, L., DAWBARN, D., ROBERTSON, A., NEWTON, R. & LAWSON, S. N. 2001. Time Course and Nerve Growth Factor Dependence of Inflammation-Induced Alterations in Electrophysiological Membrane Properties in Nociceptive Primary Afferent Neurons. *The Journal of Neuroscience,* 21**,** 8722-8733.

DJOUHRI, L. and LAWSON, S. 2004. Aβ-fiber nociceptive primary afferent neurons: a review of incidence and properties in relation to other afferent A-fiber neurons in mammals. *Brain Research Reviews,* 46(2), pp.131-145.

DOBBERTIN, A., SCHMID, P., GELMAN, M., GLOWINSKI, J. & MALLAT, M. 1997. Neurons Promote Macrophage Proliferation by Producing Transforming Growth Factor-β2. *The Journal of Neuroscience,* 17**,** 5305-5315.

DONG, F., DU, Y. R., XIE, W., STRONG, J. A., HE, X. J. & ZHANG, J. M. 2012. Increased function of the TRPV1 channel in small sensory neurons after local inflammation or in vitro exposure to the pro-inflammatory cytokine GRO/KC. *Neurosci Bull,* 28**,** 155-64.

DONG, Y., FISCHER, R., NAUDE, P. J., MAIER, O., NYAKAS, C., DUFFEY, M., VAN DER ZEE, E. A., DEKENS, D., DOUWENGA, W., HERRMANN, A., GUENZI, E., KONTERMANN, R. E., PFIZENMAIER, K. & EISEL, U. L. 2016. Essential protective role of tumor necrosis factor receptor 2 in neurodegeneration. *Proc Natl Acad Sci U S A,* 113**,** 12304-12309.

DRAGOO, J. L., JOHNSON, C. & MCCONNELL, J. 2012. Evaluation and Treatment of Disorders of the Infrapatellar Fat Pad. *Sports Medicine,* 42**,** 51-67.

DRAY, A., URBAN, L. & DICKENSON, A. 1999. Pharmacology of Chronic Pain. *In:* NAHAS, G., SUTIN, K., HARVEY, D., AGURELL, S., PACE, N. & CANCRO, R. (eds.) *Marihuana and Medicine.* Humana Press.

DRENTH, J. P. & WAXMAN, S. G. 2007. Mutations in sodium-channel gene SCN9A cause a spectrum of human genetic pain disorders. *J Clin Invest,* 117**,** 3603-9.

DREYFUS, C. F. 1989. Effects of nerve growth factor on cholinergic brain neurons. *Trends in Pharmacological Sciences,* 10**,** 145-149.

DRUBIN, D. G., FEINSTEIN, S. C., SHOOTER, E. M. & KIRSCHNER, M. W. 1985. Nerve growth factor-induced neurite outgrowth in PC12 cells involves the coordinate induction of microtubule assembly and assembly-promoting factors. *The Journal of Cell Biology,* 101**,** 1799-1807.

DUAN, J.-X., ZHOU, Y., ZHOU, A.-Y., GUAN, X.-X., LIU, T., YANG, H.-H., XIE, H. & CHEN, P. 2017. Calcitonin gene-related peptide exerts anti-inflammatory property through regulating murine macrophages polarization in vitro. *Molecular Immunology,* 91**,** 105-113.

DUBIN, A. E. & PATAPOUTIAN, A. 2010. Nociceptors: the sensors of the pain pathway. *The Journal of Clinical Investigation,* 120**,** 3760-3772.

DUBOVÝ, P., JANČÁLEK, R., KLUSÁKOVÁ, I., SVÍŽENSKÁ, I. & PEJCHALOVÁ, K. 2006. Intra- and Extraneuronal Changes of Immunofluorescence Staining for TNF- and TNFR1 in the Dorsal Root Ganglia of Rat Peripheral Neuropathic Pain Models. *Cellular and Molecular Neurobiology,* 26**,** 1203-1215.

DUMAS, E. O. & POLLACK, G. M. 2008. Opioid Tolerance Development: A Pharmacokinetic/Pharmacodynamic Perspective. *The AAPS Journal,* 10**,** 537.

DURHAM, P. L. 2006. Calcitonin Gene-Related Peptide (CGRP) and Migraine. *Headache,* 46**,** S3-S8.

EDELMAYER, R. M., BREDERSON, J.-D., JARVIS, M. F. & BITNER, R. S. 2014. Biochemical and pharmacological assessment of MAP-kinase signaling along pain pathways in experimental rodent models: a potential tool for the discovery of novel antinociceptive therapeutics. *Biochemical Pharmacology,* 87**,** 390-398.

EDWARDS, M. A., LOXLEY, R. A., WILLIAMS, A. J., CONNOR, M. & PHILLIPS, J. K. 2007. Lack of functional expression of NMDA receptors in PC12 cells. *Neurotoxicology,* 28**,** 876-85.

EHLERS, S. 2003. Role of tumour necrosis factor (TNF) in host defence against tuberculosis: implications for immunotherapies targeting TNF. *Annals of the Rheumatic Diseases,* 62**,** ii37-ii42.

EISSNER, G., KIRCHNER, S., LINDNER, H., KOLCH, W., JANOSCH, P., GRELL, M., SCHEURICH, P., ANDREESEN, R. & HOLLER, E. 2000. Reverse signaling through transmembrane TNF confers resistance to lipopolysaccharide in human monocytes and macrophages. *J Immunol,* 164**,** 6193-8.

EL-ZORKANY, B. K., GAMAL, S. M. & EL-MOFTY, S. A. 2013. Frequency and causes of discontinuation of methotrexate in a cohort of Egyptian patients. *The Egyptian Rheumatologist,* 35**,** 53-57.

EL KARIM, I., MCCRUDDEN, M. T. C., LINDEN, G. J., ABDULLAH, H., CURTIS, T. M., MCGAHON, M., ABOUT, I., IRWIN, C. & LUNDY, F. T. 2015. TNF-α–Induced p38MAPK Activation Regulates TRPA1 and TRPV4 Activity in Odontoblast-Like Cells. *The American Journal of Pathology,* 185**,** 2994-3002.

ELKON, K. & CASALI, P. 2008. Nature and functions of autoantibodies. *Nature clinical practice. Rheumatology,* 4**,** 491-498.

EMPL, M., RENAUD, S., ERNE, B., FUHR, P., STRAUBE, A., SCHAEREN–WIEMERS, N. & STECK, A. J. 2001. TNF-alpha expression in painful and nonpainful neuropathies. *Neurology,* 56**,** 1371-1377.

ENOMOTO, M., MANTYH, P., MURRELL, J., INNES, J. and LASCELLES, B. 2018. Anti-nerve growth factor monoclonal antibodies for the control of pain in dogs and cats. *Veterinary Record*, pp.vetrec-2017-104590.

EVANS, R. J., MOLDWIN, R. M., COSSONS, N., DAREKAR, A., MILLS, I. W. & SCHOLFIELD, D. 2011. Proof of concept trial of tanezumab for the treatment of symptoms associated with interstitial cystitis. *J Urol,* 185**,** 1716-21.

FAGAN, A. M., ZHANG, H., LANDIS, S., SMEYNE, R. J., SILOS-SANTIAGO, I. & BARBACID, M. 1996. TrkA, But Not TrkC, Receptors Are Essential for Survival of Sympathetic Neurons In Vivo . *The Journal of Neuroscience,* 16**,** 6208-6218.

FAHNESTOCK, M., MICHALSKI, B., XU, B. & COUGHLIN, M. D. 2001. The precursor pro-nerve growth factor is the predominant form of nerve growth factor in brain and is increased in Alzheimer's disease. *Mol Cell Neurosci,* 18**,** 210-20.

FAHNESTOCK, M., YU, G., MICHALSKI, B., MATHEW, S., COLQUHOUN, A., ROSS, G. M. & COUGHLIN, M. D. 2004. The nerve growth factor precursor proNGF exhibits neurotrophic activity but is less active than mature nerve growth factor. *Journal of Neurochemistry,* 89**,** 581-592.

FAYAZ, A., CROFT, P., LANGFORD, R. M., DONALDSON, L. J. & JONES, G. T. 2016. Prevalence of chronic pain in the UK: a systematic review and meta-analysis of population studies. *BMJ Open,* 6.

FEHRENBACHER, J. C., BURKEY, T. H., NICOL, G. D. & VASKO, M. R. 2005. Tumor necrosis factor α and interleukin-1β stimulate the expression of cyclooxygenase II but do not alter prostaglandin E2 receptor mRNA levels in cultured dorsal root ganglia cells. *PAIN,* 113**,** 113-122.

FEKETE, Á., FRANKLIN, L., IKEMOTO, T., RÓZSA, B., LENDVAI, B., SYLVESTER VIZI, E. & ZELLES, T. 2009. Mechanism of the persistent sodium current activator veratridine-evoked Ca2+ elevation: implication for epilepsy. *Journal of Neurochemistry,* 111**,** 745-756.

FINN, A., ANGEBY MOLLER, K., GUSTAFSSON, C., ABDELMOATY, S., NORDAHL, G., FERM, M. & SVENSSON, C. 2014. Influence of model and matrix on cytokine profile in rat and human. *Rheumatology (Oxford),* 53**,** 2297-305.

FIORENTINO, D. F., ZLOTNIK, A., MOSMANN, T. R., HOWARD, M. & O'GARRA, A. 1991. IL-10 inhibits cytokine production by activated macrophages. *J Immunol,* 147**,** 3815-22.

FIROUZI, M. 2012. Multiple Functions of the P75 Neurotrophin Receptor in the Nervous System. *Zahedan Journal of Research in Medical Sciences,* 14**,** 1-5.

FISCHER, R., KONTERMANN, R. & MAIER, O. 2015. Targeting sTNF/TNFR1 Signaling as a New Therapeutic Strategy. *Antibodies,* 4**,** 48.

FISCHIETTI, M., ARSLAN, A. D., SASSANO, A., SALEIRO, D., MAJCHRZAK-KITA, B., EBINE, K., MUNSHI, H. G., FISH, E. N. & PLATANIAS, L. C. 2018. Slfn2 Regulates Type I Interferon Responses by Modulating the NF-κB Pathway. *Molecular and Cellular Biology,* 38.

FORSTERMANN, U., CLOSS, E. I., POLLOCK, J. S., NAKANE, M., SCHWARZ, P., GATH, I. & KLEINERT, H. 1994. Nitric oxide synthase isozymes. Characterization, purification, molecular cloning, and functions. *Hypertension,* 23**,** 1121-31.

FÖRSTERMANN, U. & SESSA, W. C. 2012. Nitric oxide synthases: regulation and function. *European Heart Journal,* 33**,** 829-837.

FOUCQUIER, J. and GUEDJ, M. 2015. Analysis of drug combinations: current methodological landscape. *Pharmacology Research & Perspectives*, 3(3), p.e00149.

FRIESS, H., ZHU, Z.-W., DI MOLA, F. F., KULLI, C., GRABER, H. U., ANDREN-SANDBERG, Å., ZIMMERMANN, A., KORC, M., REINSHAGEN, M. & BÜCHLER, M. W. 1999. Nerve Growth Factor and Its High-Affinity Receptor in Chronic Pancreatitis. *Annals of Surgery,* 230**,** 615-615.

FROBERT, Y., NEVERS, M., AMADESI, S., VOLLAND, H., BRUNE, P., GEPPETTI, P., GRASSI, J. and CRÉMINON, C. 1999. A sensitive sandwich enzyme immunoassay for calcitonin gene-related peptide (CGRP): Characterization and application. *Peptides*, 20(2), pp.275-284.

FUKUOKA, H., KAWATANI, M., HISAMITSU, T. & TAKESHIGE, C. 1994. Cutaneous hyperalgesia induced by peripheral injection of interleukin-1 beta in the rat. *Brain Res,* 657**,** 133-40.

FUNG, T. C., OLSON, C. A. & HSIAO, E. Y. 2017. Interactions between the microbiota, immune and nervous systems in health and disease. *Nature Neuroscience,* 20**,** 145.

GALAN, A., LAIRD, J. M. & CERVERO, F. 2004. In vivo recruitment by painful stimuli of AMPA receptor subunits to the plasma membrane of spinal cord neurons. *Pain,* 112**,** 315-23.

GALLI, S., BORREGAARD, N. and WYNN, T. 2011. Phenotypic and functional plasticity of cells of innate immunity: macrophages, mast cells and neutrophils. *Nature Immunology*, 12(11), pp.1035-1044.

GANGADHARAN, V. and KUNER, R. 2013. Pain hypersensitivity mechanisms at a glance. *Disease Models & Mechanisms*, 6(4), pp.889-895.

GARACI, E., CAROLEO, M. C., ALOE, L., AQUARO, S., PIACENTINI, M., COSTA, N., AMENDOLA, A., MICERA, A., CALIÒ, R., PERNO, C.-F. & LEVI-MONTALCINI, R. 1999. Nerve growth factor is an autocrine factor essential for the survival of macrophages infected with HIV. *Proceedings of the National Academy of Sciences,* 96**,** 14013-14018.

GARBER, K. 2011. Fate of novel painkiller mAbs hangs in balance. *Nat Biotech,* 29**,** 173-174.

GARRISON, S. R. & STUCKY, C. L. 2011. The Dynamic TRPA1 Channel: A Suitable Pharmacological Pain Target? *Current pharmaceutical biotechnology,* 12**,** 1689-1697.

GAURIAU, C. and BERNARD, J. 2003. A comparative reappraisal of projections from the superficial laminae of the dorsal horn in the rat: The forebrain. *The Journal of Comparative Neurology*, 468(1), pp.24-56.

GENOVESE, M. C., BATHON, J. M., MARTIN, R. W., FLEISCHMANN, R. M., TESSER, J. R., SCHIFF, M. H., KEYSTONE, E. C., WASKO, M. C., MORELAND, L. W., WEAVER, A. L., MARKENSON, J., CANNON, G. W., SPENCER-GREEN, G. & FINCK, B. K. 2002. Etanercept versus methotrexate in patients with early rheumatoid arthritis: Two-year radiographic and clinical outcomes. *Arthritis & Rheumatism,* 46**,** 1443-1450.

GHILARDI, J. R., FREEMAN, K. T., JIMENEZ-ANDRADE, J. M., MANTYH, W. G., BLOOM, A. P., BOUHANA, K. S., TROLLINGER, D., WINKLER, J., LEE, P., ANDREWS, S. W., KUSKOWSKI, M. A. & MANTYH, P. W. 2011. SUSTAINED BLOCKADE OF NEUROTROPHIN RECEPTORS TrkA, TrkB AND TrkC REDUCES NON-MALIGNANT SKELETAL PAIN BUT NOT THE MAINTENANCE OF SENSORY AND SYMPATHETIC NERVE FIBERS. *Bone,* 48**,** 389-398.

GHILARDI, J. R., FREEMAN, K. T., JIMENEZ-ANDRADE, J. M., MANTYH, W. G., BLOOM, A. P., KUSKOWSKI, M. A. & MANTYH, P. W. 2010. Administration of a tropomyosin receptor kinase inhibitor attenuates sarcoma-induced nerve sprouting, neuroma formation and bone cancer pain. *Molecular Pain,* 6**,** 87-87.

GHOSHAL, S., TRIVEDI, D. B., GRAF, G. A. & LOFTIN, C. D. 2011. Cyclooxygenase-2 Deficiency Attenuates Adipose Tissue Differentiation and Inflammation in Mice. *The Journal of Biological Chemistry,* 286**,** 889-898.

GOEBEL, A. 2016. Autoantibody pain. *Autoimmunity Reviews,* 15**,** 552-557.

GOLD, M. S. & GEBHART, G. F. 2010. Nociceptor sensitization in pain pathogenesis. *Nature Medicine,* 16**,** 1248.

GOLDEN, J., HOSHI, M., NASSAR, M., ENOMOTO, H., WOOD, J., MILBRANDT, J., GEREAU, R., JOHNSON, E. and JAIN, S. 2010. RET Signaling Is Required for Survival and Normal Function of Nonpeptidergic Nociceptors. *Journal of Neuroscience*, 30(11), pp.3983-3994.

GOMES, R. N., CASTRO-FARIA-NETO, H. C., BOZZA, P. T., SOARES, M. B., SHOEMAKER, C. B., DAVID, J. R. & BOZZA, M. T. 2005. Calcitonin gene-related peptide inhibits local acute inflammation and protects mice against lethal endotoxemia. *Shock,* 24**,** 590-4.

GONG, W.-Y., ABDELHAMID, R. E., CARVALHO, C. S. & SLUKA, K. A. 2016. Resident macrophages in muscle contribute to development of hyperalgesia in a mouse model of non-inflammatory muscle pain. *The journal of pain : official journal of the American Pain Society,* 17**,** 1081-1094.

GOODWIN, R. G., ANDERSON, D., JERZY, R., DAVIS, T., BRANNAN, C. I., COPELAND, N. G., JENKINS, N. A. & SMITH, C. A. 1991. Molecular cloning and expression of the type

1 and type 2 murine receptors for tumor necrosis factor. *Molecular and Cellular Biology,* 11**,** 3020-3026.

GORDON, S. 2016. Phagocytosis: An Immunobiologic Process. *Immunity,* 44**,** 463-475.

GORDON, S. & PLÜDDEMANN, A. 2017. Tissue macrophages: heterogeneity and functions. *BMC Biology,* 15**,** 53.

GOSSELIN, R.-D., SUTER, M. R., JI, R.-R. & DECOSTERD, I. 2010. Glial Cells and Chronic Pain. *The Neuroscientist : a review journal bringing neurobiology, neurology and psychiatry,* 16**,** 519-531.

GOTTLIEB, A. B., CHAMIAN, F., MASUD, S., CARDINALE, I., ABELLO, M. V., LOWES, M. A., CHEN, F., MAGLIOCCO, M. & KRUEGER, J. G. 2005. TNF Inhibition Rapidly Down-Regulates Multiple Proinflammatory Pathways in Psoriasis Plaques. *The Journal of Immunology,* 175**,** 2721-2729.

GOULD III, H. J., GOULD, T. N., ENGLAND, J. D., PAUL, D., LIU, Z. P. & LEVINSON, S. R. 2000. A possible role for nerve growth factor in the augmentation of sodium channels in models of chronic pain. *Brain Research,* 854**,** 19-29.

GRACE, P. M., HUTCHINSON, M. R., MAIER, S. F. & WATKINS, L. R. 2014. Pathological pain and the neuroimmune interface. *Nat Rev Immunol,* 14**,** 217-231.

GRASSI J., PRADELLES P. 1991. The use of Acetylcholinesterase as a Universal marker in Enzyme-Immunoassays. Proceedings of the Third International Meeting on Cholinesterases, American Chemical Society.

GREENE, L. A. 1978a. Nerve growth factor prevents the death and stimulates the neuronal differentiation of clonal PC12 pheochromocytoma cells in serum-free medium. *The Journal of Cell Biology,* 78**,** 747-755.

GREENE, L. A. 1978b. NGF-responsive clonal PC12 pheochromocytoma cells as tools for neuropharmacological investigation. *Advances in Pharmacology and Therapeutics*.

GREGORY, N., HARRIS, A. L., ROBINSON, C. R., DOUGHERTY, P. M., FUCHS, P. N. & SLUKA, K. A. 2013. An overview of animal models of pain: disease models and outcome measures. *The journal of pain : official journal of the American Pain Society,* 14**,** 10.1016/j.jpain.2013.06.008.

GRELL, M., DOUNI, E., WAJANT, H., LOHDEN, M., CLAUSS, M., MAXEINER, B., GEORGOPOULOS, S., LESSLAUER, W., KOLLIAS, G., PFIZENMAIER, K. & SCHEURICH, P. 1995. The transmembrane form of tumor necrosis factor is the prime activating ligand of the 80 kDa tumor necrosis factor receptor. *Cell,* 83**,** 793-802.

GRIENBERGER, C. & KONNERTH, A. 2012. Imaging calcium in neurons. *Neuron,* 73**,** 862-85.

GRIMES, M. L., ZHOU, J., BEATTIE, E. C., YUEN, E. C., HALL, D. E., VALLETTA, J. S., TOPP, K. S., LAVAIL, J. H., BUNNETT, N. W. & MOBLEY, W. C. 1996. Endocytosis of activated TrkA: evidence that nerve growth factor induces formation of signaling endosomes. *J Neurosci,* 16**,** 7950-64.

HAKIM, A. W., DONG, X. & CAIRNS, B. E. 2011. TNFα Mechanically Sensitizes Masseter Muscle Nociceptors by Increasing Prostaglandin E2 Levels. *Journal of Neurophysiology,* 105**,** 154-161.

HAMANOUE, M., MIDDLETON, G., WYATT, S., JAFFRAY, E., HAY, R. T. & DAVIES, A. M. 1999. p75-mediated NF-kappaB activation enhances the survival response of developing sensory neurons to nerve growth factor. *Mol Cell Neurosci,* 14**,** 28-40.

HANANI, M. 2005. Satellite glial cells in sensory ganglia: from form to function. *Brain Res Brain Res Rev,* 48**,** 457-76.

HANSEBOUT, C. R., SU, C., REDDY, K., ZHANG, D., JIANG, C., RATHBONE, M. P. & JIANG, S. 2012. Enteric glia mediate neuronal outgrowth through release of neurotrophic factors. *Neural Regeneration Research,* 7**,** 2165-2175.

HARINGMAN, J. J. & TAK, P. P. 2004. Chemokine blockade: a new era in the treatment of rheumatoid arthritis? *Arthritis Research & Therapy,* 6**,** 93-97.

HARTMANN, B., AHMADI, S., HEPPENSTALL, P. A., LEWIN, G. R., SCHOTT, C., BORCHARDT, T., SEEBURG, P. H., ZEILHOFER, H. U., SPRENGEL, R. & KUNER, R. 2004. The AMPA Receptor Subunits GluR-A and GluR-B Reciprocally Modulate Spinal Synaptic Plasticity and Inflammatory Pain. *Neuron,* 44**,** 637-650.

HAWKER, G., WRIGHT, J., COYTE, P., PAUL, J., DITTUS, R., CROXFORD, R., KATZ, B., BOMBARDIER, C., HECK, D. & FREUND, D. 1998. Health-related quality of life after knee replacement. *J Bone Joint Surg Am,* 80**,** 163-73.

HENSELLEK, S., BRELL, P., SCHAIBLE, H.-G., BRÄUER, R. & SEGOND VON BANCHET, G. 2007a. The cytokine TNFα increases the proportion of DRG neurones expressing the TRPV1 receptor via the TNFR1 receptor and ERK activation. *Molecular and Cellular Neuroscience,* 36**,** 381-391.

HENSELLEK, S., BRELL, P., SCHAIBLE, H. G., BRAUER, R. & SEGOND VON BANCHET, G. 2007b. The cytokine TNFalpha increases the proportion of DRG neurones expressing the TRPV1 receptor via the TNFR1 receptor and ERK activation. *Mol Cell Neurosci,* 36**,** 381-91.

HERVERA, A., NEGRETE, R., LEÁNEZ, S., MARTÍN-CAMPOS, J. M. & POL, O. 2010. The Spinal Cord Expression of Neuronal and Inducible Nitric Oxide Synthases and Their Contribution in the Maintenance of Neuropathic Pain in Mice. *PLoS ONE,* 5**,** e14321.

HESS, A., AXMANN, R., RECH, J., FINZEL, S., HEINDL, C., KREITZ, S., SERGEEVA, M., SAAKE, M., GARCIA, M., KOLLIAS, G., STRAUB, R. H., SPORNS, O., DOERFLER, A., BRUNE, K. & SCHETT, G. 2011. Blockade of TNF-α rapidly inhibits pain responses in the central nervous system. *Proceedings of the National Academy of Sciences,* 108**,** 3731-3736.

HILL, R. 2000. NK1 (substance P) receptor antagonists – why are they not analgesic in humans? *Trends in Pharmacological Sciences,* 21**,** 244-246.

HOESEL, B. & SCHMID, J. A. 2013. The complexity of NF-κB signaling in inflammation and cancer. *Molecular Cancer,* 12**,** 86.

HOFFMAN, H. M., YASOTHAN, U. & KIRKPATRICK, P. 2008. Rilonacept. *Nature Reviews Drug Discovery,* 7**,** 385.

HOLMES, D. 2012. Anti-NGF painkillers back on track? *Nat Rev Drug Discov,* 11**,** 337-8.

HOLTZMAN, D., KILBRIDGE, J., LI, Y., CUNNINGHAM, E., LENN, N., CLARY, D., REICHARDT, L. & MOBLEY, W. 1995. TrkA expression in the CNS: evidence for the existence of several novel NGF-responsive CNS neurons. *The Journal of Neuroscience,* 15**,** 1567-1576.

HORIUCHI, T., MITOMA, H., HARASHIMA, S.-I., TSUKAMOTO, H. & SHIMODA, T. 2010. Transmembrane TNF-α: structure, function and interaction with anti-TNF agents. *Rheumatology (Oxford, England),* 49**,** 1215-1228.

HORTON, A., LARAMEE, G., WYATT, S., SHIH, A., WINSLOW, J. & DAVIES, A. M. 1997. NGF binding to p75 enhances the sensitivity of sensory and sympathetic neurons to NGF at different stages of development. *Mol Cell Neurosci,* 10**,** 162-72.

HOSOI, J., MURPHY, G. F., EGAN, C. L., LERNER, E. A., GRABBE, S., ASAHINA, A. & GRANSTEIN, R. D. 1993. Regulation of Langerhans cell function by nerves containing calcitonin gene-related peptide. *Nature,* 363**,** 159.

HUGHES, P. A., ZOLA, H., PENTTILA, I. A., BLACKSHAW, L. A., ANDREWS, J. M. & KRUMBIEGEL, D. 2013. Immune Activation in Irritable Bowel Syndrome: Can Neuroimmune Interactions Explain Symptoms? *The American Journal Of Gastroenterology,* 108**,** 1066.

HULL, K., DREWE, E., AKSENTIJEVICH, I., SINGH, H., WONG, K., MCDERMOTT, E., DEAN, J., POWELL, R. and KASTNER, D. 2002. The TNF Receptor-Associated Periodic Syndrome (TRAPS). *Medicine*, 81(5), pp.349-368.

HUTTON, L. A., DEVELLIS, J. & PEREZ-POLO, J. R. 1992. Expression of p75NGFR trkA, and trkB mRNA in rat C6 glioma and type I astrocyte cultures. *Journal of Neuroscience Research,* 32**,** 375-383.

IDRISS, H. T. & NAISMITH, J. H. 2000. TNF alpha and the TNF receptor superfamily: structure-function relationship(s). *Microsc Res Tech,* 50**,** 184-95.

IKEDA, H., STARK, J., FISCHER, H., WAGNER, M., DRDLA, R., JAGER, T. & SANDKUHLER, J. 2006. Synaptic amplifier of inflammatory pain in the spinal dorsal horn. *Science,* 312**,** 1659-62.

ILLIAS, A. M., GIST, A. C., ZHANG, H., KOSTURAKIS, A. K. & DOUGHERTY, P. M. 2018. Chemokine CCL2 and its receptor CCR2 in the dorsal root ganglion contribute to oxaliplatin-induced mechanical hypersensitivity. *PAIN,* 159**,** 1308-1316.

IM, H.-J., KIM, J., LI, X., KOTWAL, N., SUMNER, D. R., VAN WIJNEN, A. J., DAVIS, F. J., YAN, D., LEVINE, B., HENRY, J. L., DESEVRÉ, J. & KROIN, J. S. 2010. Alteration of Sensory Neurons and Spinal Response To An Experimental Osteoarthritis Pain Model. *Arthritis and rheumatism,* 62**,** 2995-3005.

INDO, Y., TSURUTA, M., HAYASHIDA, Y., KARIM, M. A., OHTA, K., KAWANO, T., MITSUBUCHI, H., TONOKI, H., AWAYA, Y. & MATSUDA, I. 1996. Mutations in the TRKA/NGF receptor gene in patients with congenital insensitivity to pain with anhidrosis. *Nat Genet,* 13**,** 485-488.

INGLIS, J. J., NISSIM, A., LEES, D. M., HUNT, S. P., CHERNAJOVSKY, Y. & KIDD, B. L. 2005a. The differential contribution of tumour necrosis factor to thermal and mechanical hyperalgesia during chronic inflammation. *Arthritis Research & Therapy,* 7**,** R807-R816.

INGLIS, J. J., NISSIM, A., LEES, D. M., HUNT, S. P., CHERNAJOVSKY, Y. & KIDD, B. L. 2005b. The differential contribution of tumour necrosis factor to thermal and mechanical hyperalgesia during chronic inflammation. *Arthritis Res Ther,* 7**,** R807-16.

INOUE, K. & TSUDA, M. 2009. Microglia and neuropathic pain. *Glia,* 57**,** 1469-1479.

INOUE, K. & TSUDA, M. 2018. Microglia in neuropathic pain: cellular and molecular mechanisms and therapeutic potential. *Nature Reviews Neuroscience,* 19**,** 138.

IOAN-FACSINAY, A. & KLOPPENBURG, M. 2013. An emerging player in knee osteoarthritis: the infrapatellar fat pad. *Arthritis Research & Therapy,* 15**,** 225-225.

ITALIANI, P. & BORASCHI, D. 2014. From Monocytes to M1/M2 Macrophages: Phenotypical vs. Functional Differentiation. *Frontiers in Immunology,* 5**,** 514.

IYENGAR, S., OSSIPOV, M. H. & JOHNSON, K. W. 2017. The role of calcitonin gene–related peptide in peripheral and central pain mechanisms including migraine. *Pain,* 158**,** 543-559.

JADAD, A. 1995. The WHO Analgesic Ladder for Cancer Pain Management. *JAMA*, 274(23), p.1870.

JAUNEAU, A.-C., ISCHENKO, A., CHATAGNER, A., BENARD, M., CHAN, P., SCHOUFT, M.-T., PATTE, C., VAUDRY, H. & FONTAINE, M. 2006. Interleukin-1β and anaphylatoxins exert a synergistic effect on NGF expression by astrocytes. *Journal of Neuroinflammation,* 3**,** 8.

JEON, S.-M., LEE, K.-M., PARK, E.-S., JEON, Y.-H. & CHO, H.-J. 2008. Monocyte chemoattractant protein-1 immunoreactivity in sensory ganglia and hindpaw after adjuvant injection. *NeuroReport,* 19**,** 183-186.

JESUS, A. A. & GOLDBACH-MANSKY, R. 2014. IL-1 Blockade in Autoinflammatory Syndromes. *Annual review of medicine,* 65**,** 223-244.

JI, R.-R., BERTA, T. & NEDERGAARD, M. 2013. Glia and pain: Is chronic pain a gliopathy? *Pain,* 154**,** S10-S28.

JI, R.-R., CHAMESSIAN, A. & ZHANG, Y.-Q. 2016a. Pain regulation by non-neuronal cells and inflammation. *Science,* 354**,** 572-577.

JI, R.-R., CHAMESSIAN, A. & ZHANG, Y.-Q. 2016b. Pain Regulation by Non-neuronal Cells and Inflammation. *Science (New York, N.Y.),* 354**,** 572-577.

JI, R.-R., SAMAD, T. A., JIN, S.-X., SCHMOLL, R. & WOOLF, C. J. 2002. p38 MAPK Activation by NGF in Primary Sensory Neurons after Inflammation Increases TRPV1 Levels and Maintains Heat Hyperalgesia. *Neuron,* 36**,** 57-68.

JI, R.-R. & WEN, Y.-R. 2006. Neural-glial interaction in the spinal cord for the development and maintenance of nerve injury-induced neuropathic pain. *Drug Development Research,* 67**,** 331-338.

JI, R.-R., XU, Z.-Z. & GAO, Y.-J. 2014. Emerging targets in neuroinflammation-driven chronic pain. *Nat Rev Drug Discov,* 13**,** 533-548.

JIA, Y., QUINN, C.M., GAGNON, A.I. & TALANIAN, R. 2006. Homogenous time-resolved fluorescence and its applications for kinase assays in drug discovery. *Analytical Biochemistry,* 356(2): 273-281.

JIANG, Y., WORONICZ, J. D., LIU, W. & GOEDDEL, D. V. 1999. Prevention of constitutive TNF receptor 1 signaling by silencer of death domains. *Science,* 283**,** 543-6.

JIN, X. & GEREAU, R. W. T. 2006. Acute p38-mediated modulation of tetrodotoxin-resistant sodium channels in mouse sensory neurons by tumor necrosis factor-alpha. *J Neurosci,* 26**,** 246-55.

JINSMAA, Y., TAKAHASHI, M., TAKAHASHI, M. & YOSHIKAWA, M. 2000. Anti-analgesic and anti-amnesic effect of complement C3a. *Life Sci,* 67**,** 2137-43.

JOACHIM, R. A., SAGACH, V., QUARCOO, D., DINH, T., ARCK, P. C. & KLAPP, B. F. 2006. Upregulation of Tumor Necrosis Factor-Alpha by Stress and Substance P in a Murine Model of Allergic Airway Inflammation. *Neuroimmunomodulation,* 13**,** 43-50.

KALLIOMÄKI, M.-L., SANDBLOM, G., HALLBERG, M., GRÖNBLADH, A., GUNNARSSON, U., GORDH, T., GINYA, H. & NYBERG, F. 2016. Genetic susceptibility to postherniotomy pain. The influence of polymorphisms in the Mu opioid receptor, TNF-α, GRIK3, GCH1, BDNF and CACNA2D2 genes. *Scandinavian Journal of Pain,* 12**,** 1-6.

KANDA, H., KOBAYASHI, K., YAMANAKA, H., OKUBO, M. & NOGUCHI, K. 2017. Microglial TNFα Induces COX2 and PGI2 Synthase Expression in Spinal Endothelial Cells during Neuropathic Pain. *eNeuro,* 4**,** ENEURO.0064-17.2017.

KASHEM, SAKEEN W., RIEDL, MAUREEN S., YAO, C., HONDA, CHRISTOPHER N., VULCHANOVA, L. & KAPLAN, DANIEL H. 2015. Nociceptive Sensory Fibers Drive Interleukin-23 Production from CD301b+ Dermal Dendritic Cells and Drive Protective Cutaneous Immunity. *Immunity,* 43**,** 515-526.

KATO, K., LIU, H., KIKUCHI, S.-I., MYERS, R. R. & SHUBAYEV, V. I. 2010. Immediate Anti-tumor Necrosis Factor-α (Etanercept) Therapy Enhances Axonal Regeneration After Sciatic Nerve Crush. *Journal of neuroscience research,* 88**,** 360-368.

KATZ, N., BORENSTEIN, D. G., BIRBARA, C., BRAMSON, C., NEMETH, M. A., SMITH, M. D. & BROWN, M. T. 2011. Efficacy and safety of tanezumab in the treatment of chronic low back pain. *PAIN®,* 152**,** 2248-2258.

KE, J., LONG, X., LIU, Y., ZHANG, Y. F., LI, J., FANG, W. & MENG, Q. G. 2007. Role of NF-κB in TNF-α-induced COX-2 Expression in Synovial Fibroblasts from Human TMJ. *Journal of Dental Research,* 86**,** 363-367.

KERR, B. J., SOUSLOVA, V., MCMAHON, S. B. & WOOD, J. N. 2001. A role for the TTX-resistant sodium channel Nav 1.8 in NGF-induced hyperalgesia, but not neuropathic pain. *Neuroreport,* 12**,** 3077-80.

KIDD, B. L. & URBAN, L. A. 2001. Mechanisms of inflammatory pain. *BJA: British Journal of Anaesthesia,* 87**,** 3-11.

KIGUCHI, N., KOBAYASHI, Y., SAIKA, F. & KISHIOKA, S. 2013. Epigenetic upregulation of CCL2 and CCL3 via histone modifications in infiltrating macrophages after peripheral nerve injury. *Cytokine,* 64**,** 666-672.

KIM, H. S., KIM, D. C., KIM, H.-M., KWON, H.-J., KWON, S. J., KANG, S.-J., KIM, S. C. & CHOI, G.-E. 2015. STAT1 deficiency redirects IFN signalling toward suppression of TLR response through a feedback activation of STAT3. *Scientific Reports,* 5**,** 13414.

KLARESKOG, L., VAN DER HEIJDE, D., DE JAGER, J. P., GOUGH, A., KALDEN, J., MALAISE, M., MARTIN MOLA, E., PAVELKA, K., SANY, J., SETTAS, L., WAJDULA, J., PEDERSEN, R., FATENEJAD, S. & SANDA, M. 2004. Therapeutic effect of the combination of etanercept and methotrexate compared with each treatment alone in patients with rheumatoid arthritis: double-blind randomised controlled trial. *Lancet,* 363**,** 675-81.

KLEIN-WIERINGA, I. R., DE LANGE-BROKAAR, B. J. E., YUSUF, E., ANDERSEN, S. N., KWEKKEBOOM, J. C., KROON, H. M., VAN OSCH, G. J. V. M., ZUURMOND, A.-M., STOJANOVIC-SUSULIC, V., NELISSEN, R. G. H. H., TOES, R. E. M., KLOPPENBURG, M. & IOAN-FACSINAY, A. 2016. Inflammatory Cells in Patients with Endstage Knee Osteoarthritis: A Comparison between the Synovium and the Infrapatellar Fat Pad. *The Journal of Rheumatology,* 43**,** 771-778.

KLEIN-WIERINGA, I. R., KLOPPENBURG, M., BASTIAANSEN-JENNISKENS, Y. M., YUSUF, E., KWEKKEBOOM, J. C., EL-BANNOUDI, H., NELISSEN, R. G. H. H., ZUURMOND, A., STOJANOVIC-SUSULIC, V., VAN OSCH, G. J. V. M., TOES, R. E. M. & IOAN-FACSINAY, A. 2011. The infrapatellar fat pad of patients with osteoarthritis has an inflammatory phenotype. *Annals of the Rheumatic Diseases,* 70**,** 851-857.

KLEIN, R. 1994. Role of neurotrophins in mouse neuronal development. *The FASEB Journal,* 8**,** 738-44.

KLESSE, L. J. & PARADA, L. F. 1999. Trks: Signal transduction and intracellular pathways. *Microscopy Research and Technique,* 45**,** 210-216.

KOBAYASHI, H. & MIZISIN, A. P. 2001. Nerve growth factor and neurotrophin-3 promote chemotaxis of mouse macrophages in vitro. *Neurosci Lett,* 305**,** 157-60.

KOBAYASHI, Y., KIGUCHI, N., FUKAZAWA, Y., SAIKA, F., MAEDA, T. & KISHIOKA, S. 2015. Macrophage-T cell interactions mediate neuropathic pain through the glucocorticoid-induced tumor necrosis factor ligand system. *J Biol Chem,* 290**,** 12603-13.

KOCHUKOV, M. Y., MCNEARNEY, T. A., YIN, H., ZHANG, L., MA, F., PONOMAREVA, L., ABSHIRE, S. & WESTLUND, K. N. 2009. Tumor necrosis factor-alpha (TNF-α) enhances functional thermal and chemical responses of TRP cation channels in human synoviocytes. *Molecular Pain,* 5**,** 49-49.

KOH, T. J. & DIPIETRO, L. A. 2011. Inflammation and wound healing: The role of the macrophage. *Expert reviews in molecular medicine,* 13**,** e23-e23.

KOLE, M. H. P., ILSCHNER, S. U., KAMPA, B. M., WILLIAMS, S. R., RUBEN, P. C. & STUART, G. J. 2008. Action potential generation requires a high sodium channel density in the axon initial segment. *Nature Neuroscience,* 11**,** 178.

KOMORI, T., MORIKAWA, Y., INADA, T., HISAOKA, T. & SENBA, E. 2011. Site-specific subtypes of macrophages recruited after peripheral nerve injury. *Neuroreport,* 22**,** 911-7.

KRAUS, V. B., MCDANIEL, G., HUEBNER, J. L., STABLER, T. V., PIEPER, C. F., SHIPES, S. W., PETRY, N. A., LOW, P. S., SHEN, J., MCNEARNEY, T. A. & MITCHELL, P. 2016. Direct in vivo evidence of activated macrophages in human osteoarthritis. *Osteoarthritis Cartilage,* 24**,** 1613-21.

KRAYCHETE, D. C., SAKATA, R. K., ISSY, A. M., BACELLAR, O., SANTOS-JESUS, R. & CARVALHO, E. M. 2010. Serum cytokine levels in patients with chronic low back pain due to herniated disc: analytical cross-sectional study. *Sao Paulo Med J,* 128**,** 259-62.

KRESS, G. J. & MENNERICK, S. 2009. Action potential initiation and propagation: upstream influences on neurotransmission. *Neuroscience,* 158**,** 211-222.

KRESS, M. 2010. *Nociceptor Sensitization by Proinflammatory Cytokines And Chemokines*.

KROCK, E., ROSENZWEIG, D. H., CHABOT-DORÉ, A.-J., JARZEM, P., WEBER, M. H., OUELLET, J. A., STONE, L. S. & HAGLUND, L. 2014. Painful, degenerating intervertebral discs up-regulate neurite sprouting and CGRP through nociceptive factors. *Journal of Cellular and Molecular Medicine,* 18**,** 1213-1225.

KUCHINAD, A., SCHWEINHARDT, P., SEMINOWICZ, D. A., WOOD, P. B., CHIZH, B. A. & BUSHNELL, M. C. 2007. Accelerated brain gray matter loss in fibromyalgia patients: premature aging of the brain? *J Neurosci,* 27**,** 4004-7.

KUNER, R. 2010. Central mechanisms of pathological pain. *Nat Med,* 16**,** 1258-66.

KWON, M. J., KIM, J., SHIN, H., JEONG, S. R., KANG, Y. M., CHOI, J. Y., HWANG, D. H. & KIM, B. G. 2013. Contribution of macrophages to enhanced regenerative capacity of dorsal root ganglia sensory neurons by conditioning injury. *J Neurosci,* 33**,** 15095-108.

KWON, M. J., SHIN, H. Y., CUI, Y., KIM, H., THI, A. H. L., CHOI, J. Y., KIM, E. Y., HWANG, D. H. & KIM, B. G. 2015. CCL2 Mediates Neuron–Macrophage Interactions to Drive Proregenerative Macrophage Activation Following Preconditioning Injury. *The Journal of Neuroscience,* 35**,** 15934-15947.

LAMBRECHT, B. N., GERMONPRE, P. R., EVERAERT, E. G., CARRO-MUINO, I., DE VEERMAN, M., DE FELIPE, C., HUNT, S. P., THIELEMANS, K., JOOS, G. F. & PAUWELS, R. A. 1999. Endogenously produced substance P contributes to lymphocyte proliferation induced by dendritic cells and direct TCR ligation. *Eur J Immunol,* 29**,** 3815-25.

LANE, N. E. & CORR, M. 2017. Anti-NGF treatments for pain — two steps forward, one step back? *Nature Reviews Rheumatology,* 13**,** 76.

LAROUX, F. S., LEFER, D. J., KAWACHI, S., SCALIA, R., COCKRELL, A. S., GRAY, L., HEYDE, H. V. D., HOFFMAN, J. M. & GRISHAM, M. B. 2000. Role of Nitric Oxide in the Regulation of Acute and Chronic Inflammation. *Antioxidants & Redox Signaling,* 2**,** 391-396.

LARSSON, S., ENGLUND, M., STRUGLICS, A. & LOHMANDER, L. S. 2015. Interleukin-6 and tumor necrosis factor alpha in synovial fluid are associated with progression of radiographic knee osteoarthritis in subjects with previous meniscectomy. *Osteoarthritis and Cartilage,* 23**,** 1906-1914.

LASKIN, D. L. & PENDINO, K. J. 1995. Macrophages and inflammatory mediators in tissue injury. *Annu Rev Pharmacol Toxicol,* 35**,** 655-77.

LATREMOLIERE, A. & WOOLF, C. J. 2009. Central Sensitization: A Generator of Pain Hypersensitivity by Central Neural Plasticity. *The journal of pain : official journal of the American Pain Society,* 10**,** 895-926.

LEE, C. H. & RUBEN, P. C. 2008. Interaction between voltage-gated sodium channels and the neurotoxin, tetrodotoxin. *Channels (Austin),* 2**,** 407-12.

LEE, J.-I. & BURCKART, G. J. 1998. Nuclear Factor Kappa B: Important Transcription Factor and Therapeutic Target. *The Journal of Clinical Pharmacology,* 38**,** 981-993.

LEE, K.-M., KANG, B.-S., LEE, H.-L., SON, S.-J., HWANG, S.-H., KIM, D.-S., PARK, J.-S. & CHO, H.-J. 2004. Spinal NF-kB activation induces COX-2 upregulation and contributes to inflammatory pain hypersensitivity. *European Journal of Neuroscience,* 19**,** 3375-3381.

LEO, M., ARGALSKI, S., SCHÄFERS, M. & HAGENACKER, T. 2015. Modulation of Voltage-Gated Sodium Channels by Activation of Tumor Necrosis Factor Receptor-1 and Receptor-2 in Small DRG Neurons of Rats. *Mediators of Inflammation,* 2015**,** 124942.

LEVI-MONTALCINI, R. & ANGELETTI, P. U. 1968. Nerve growth factor. *Physiol Rev,* 48**,** 534-69.

LEVI-MONTALCINI, R. & HAMBURGER, V. 1951. Selective growth stimulating effects of mouse sarcoma on the sensory and sympathetic nervous system of the chick embryo. *J Exp Zool,* 116**,** 321-61.

LEVINE, J., FIELDS, H. & BASBAUM, A. 1993. Peptides and the primary afferent nociceptor. *The Journal of Neuroscience,* 13**,** 2273-2286.

LEVINE, J. D. & ALESSANDRI-HABER, N. 2007. TRP channels: Targets for the relief of pain. *Biochimica et Biophysica Acta (BBA) - Molecular Basis of Disease,* 1772**,** 989-1003.

LEVINSON, S. R., LUO, S. & HENRY, M. A. 2012. THE ROLE OF SODIUM CHANNELS IN CHRONIC PAIN. *Muscle & nerve,* 46**,** 155-165.

LEWIN, G., RITTER, A. & MENDELL, L. 1993. Nerve growth factor-induced hyperalgesia in the neonatal and adult rat. *The Journal of Neuroscience,* 13**,** 2136-2148.

LI, C. L., LI, K. C., WU, D., CHEN, Y., LUO, H., ZHAO, J. R., WANG, S. S., SUN, M. M., LU, Y. J., ZHONG, Y. Q., HU, X. Y., HOU, R., ZHOU, B. B., BAO, L., XIAO, H. S. & ZHANG, X. 2016a. Somatosensory neuron types identified by high-coverage single-cell RNA-sequencing and functional heterogeneity. *Cell Res,* 26**,** 83-102.

LI, H., XIE, W., STRONG, J. A. & ZHANG, J. M. 2007. Systemic antiinflammatory corticosteroid reduces mechanical pain behavior, sympathetic sprouting, and

elevation of proinflammatory cytokines in a rat model of neuropathic pain. *Anesthesiology,* 107**,** 469-77.

LI, K., TAN, Y.-H., LIGHT, A. R. & FU, K.-Y. 2013. Different Peripheral Tissue Injury Induces Differential Phenotypic Changes of Spinal Activated Microglia. *Clinical and Developmental Immunology,* 2013**,** 901420.

LI, N., ZHANG, L., SHU, R., DING, L., WANG, Z., WANG, H., YU, Y. & WANG, G. 2016b. Involvement of CCL3/CCR5 Signaling in Dorsal Root Ganglion in Remifentanil-induced Hyperalgesia in Rats. *The Clinical Journal of Pain,* 32**,** 702-710.

LI, P., ZHENG, Y. & CHEN, X. 2017. Drugs for Autoimmune Inflammatory Diseases: From Small Molecule Compounds to Anti-TNF Biologics. *Frontiers in Pharmacology,* 8.

LI, W.-W., GUO, T.-Z., LIANG, D.-Y., SUN, Y., KINGERY, W. S. & CLARK, J. D. 2012. Substance P Signaling Controls Mast Cell Activation, Degranulation, and Nociceptive Sensitization in a Rat Fracture Model of Complex Regional Pain Syndrome. *Anesthesiology,* 116**,** 882-895.

LI, Y., JI, A., WEIHE, E. & SCHAFER, M. K. 2004. Cell-specific expression and lipopolysaccharide-induced regulation of tumor necrosis factor alpha (TNFalpha) and TNF receptors in rat dorsal root ganglion. *J Neurosci,* 24**,** 9623-31.

LISOWSKA, B., SIEWRUK, K. & LISOWSKI, A. 2016. Substance P and Acute Pain in Patients Undergoing Orthopedic Surgery. *PLOS ONE,* 11**,** e0146400.

LIU, J., LAMB, D., CHOU, M. M., LIU, Y.-J. & LI, G. 2007. Nerve Growth Factor-mediated Neurite Outgrowth via Regulation of Rab5. *Molecular Biology of the Cell,* 18**,** 1375-1384.

LIU, F., SUN, Y., WANG, F., LI, Q., SU, L., ZHAO, Z., MENG, X., ZHAO, H., WU, X., SUN, Q., XING, G. and WAN, Y. 2012. Activation of satellite glial cells in lumbar dorsal root ganglia contributes to neuropathic pain after spinal nerve ligation. *Brain Research*, 1427, pp.65-77.

LLORIÁN-SALVADOR, M., GONZÁLEZ-RODRÍGUEZ, S., LASTRA, A., FERNÁNDEZ-GARCÍA, M. T., HIDALGO, A., MENÉNDEZ, L. & BAAMONDE, A. 2016. Involvement of CC Chemokine Receptor 1 and CCL3 in Acute and Chronic Inflammatory Pain in Mice. *Basic & Clinical Pharmacology & Toxicology,* 119**,** 32-40.

LONGO, F. M. & MASSA, S. M. 2013. Small-molecule modulation of neurotrophin receptors: a strategy for the treatment of neurological disease. *Nat Rev Drug Discov,* 12**,** 507-525.

LOUIS, S. M., JAMIESON, A., RUSSELL, N. J. W. & DOCKRAY, G. J. 1989. The role of substance P and calcitonin gene-related peptide in neurogenic plasma extravasation and vasodilatation in the rat. *Neuroscience,* 32**,** 581-586.

LOWE, E. M., ANAND, P., TERENGHI, G., WILLIAMS-CHESTNUT, R. E., SINICROPI, D. V. & OSBORNE, J. L. 1997. Increased nerve growth factor levels in the urinary bladder of women with idiopathic sensory urgency and interstitial cystitis. *Br J Urol,* 79**,** 572-7.

MA, C., SHU, Y., ZHENG, Z., CHEN, Y., YAO, H., GREENQUIST, K. W., WHITE, F. A. & LAMOTTE, R. H. 2003. Similar Electrophysiological Changes in Axotomized and

Neighboring Intact Dorsal Root Ganglion Neurons. *Journal of Neurophysiology,* 89**,** 1588-1602.

MA, F., ZHANG, L. & WESTLUND, K. N. 2009. Reactive oxygen species mediate TNFR1 increase after TRPV1 activation in mouse DRG neurons. *Molecular Pain,* 5**,** 31-31.

MA, W. & QUIRION, R. 2006. Increased calcitonin gene-related peptide in neuroma and invading macrophages is involved in the up-regulation of interleukin-6 and thermal hyperalgesia in a rat model of mononeuropathy. *Journal of Neurochemistry,* 98**,** 180-192.

MACEWAN, D. 2002. TNF ligands and receptors - a matter of life and death. *British Journal of Pharmacology*, 135(4), pp.855-875.

MAIZELS, M & MCCARBERG, B. 2005. Antidepressants and Antiepileptic Drugs for Chronic Non-Cancer Pain. *American Family Physician,* 71(3): 483-490.

MALON, J. & CAO, L. 2014. Involvement of CGRP in peripheral nerve injury-induced behavioral hypersensitivity and chemokine production (CCR5P.260). *The Journal of Immunology,* 192**,** 181.14-181.14.

MALON, J. T. & CAO, L. 2016. Potential anti-nociceptive role of chemokine CXCL1 in peripheral nerve injury-induced neuropathic pain. *The Journal of Immunology,* 196**,** 51.4-51.4.

MALONEY, J., KIVITZ, A., SCHNITZER, T. J., DAKIN, P., DI MARTINO, S., GAO, H., STEHMAN-BREEN, C. & GEBA, G. 2017. Fasinumab in the treatment of hip and knee osteoarthritic pain: efficacy and safety in a 36-week randomized, double-blind placebo-controlled clinical trial. *Osteoarthritis and Cartilage,* 25**,** S56-S57.

MAMET, J., LAZDUNSKI, M. & VOILLEY, N. 2003. How Nerve Growth Factor Drives Physiological and Inflammatory Expressions of Acid-sensing Ion Channel 3 in Sensory Neurons. *Journal of Biological Chemistry,* 278**,** 48907-48913.

MAMIDIPUDI, V. & WOOTEN, M. W. 2002. Dual role for p75NTR signaling in survival and cell death: Can intracellular mediators provide an explanation? *Journal of Neuroscience Research,* 68**,** 373-384.

MANTYH, P. W., KOLTZENBURG, M., MENDELL, L. M., TIVE, L. & SHELTON, D. L. 2011. Antagonism of nerve growth factor-TrkA signaling and the relief of pain. *Anesthesiology,* 115**,** 189-204.

MARLIN, M.C. and LI, G. 2015. Biogenesis and Function of the NGF/TrkA Signaling Endosome. *International Review of Cell and Molecular Biology*. 314: 239-257.

MAROTTE, H. & CIMAZ, R. 2014. Etanercept – TNF receptor and IgG1 Fc fusion protein: is it different from other TNF blockers? *Expert Opinion on Biological Therapy,* 14**,** 569-572.

MARRIOTT, I., MASON, M. J., ELHOFY, A. & BOST, K. L. 2000. Substance P activates NF-κB independent of elevations in intracellular calcium in murine macrophages and dendritic cells. *Journal of Neuroimmunology,* 102**,** 163-171.

MARTIN, L. J., SMITH, S. B., KHOUTORSKY, A., MAGNUSSEN, C. A., SAMOSHKIN, A., SORGE, R. E., CHO, C., YOSEFPOUR, N., SIVASELVACHANDRAN, S., TOHYAMA, S., COLE, T., KHUONG, T. M., MIR, E., GIBSON, D. G., WIESKOPF, J. S., SOTOCINAL, S.

G., AUSTIN, J. S., MELOTO, C. B., GITT, J. H., GKOGKAS, C., SONENBERG, N., GREENSPAN, J. D., FILLINGIM, R. B., OHRBACH, R., SLADE, G. D., KNOTT, C., DUBNER, R., NACKLEY, A. G., RIBEIRO-DA-SILVA, A., NEELY, G. G., MAIXNER, W., ZAYKIN, D. V., MOGIL, J. S. & DIATCHENKO, L. 2017. Epiregulin and EGFR interactions are involved in pain processing. *The Journal of Clinical Investigation,* 127**,** 3353-3366.

MARTINEZ, F. O. & GORDON, S. 2014. The M1 and M2 paradigm of macrophage activation: time for reassessment. *F1000Prime Reports,* 6**,** 13.

MASHAGHI, A., MARMALIDOU, A., TEHRANI, M., GRACE, P. M., POTHOULAKIS, C. & DANA, R. 2016. Neuropeptide Substance P and the Immune Response. *Cellular and molecular life sciences : CMLS,* 73**,** 4249-4264.

MASSIER, J., EITNER, A., SEGOND VON BANCHET, G. & SCHAIBLE, H.-G. 2015. Effects of Differently Activated Rodent Macrophages on Sensory Neurons: Implications for Arthritis Pain. *Arthritis & Rheumatology,* 67**,** 2263-2272.

MATSON, D. J., BROOM, D. C., CARSON, S. R., BALDASSARI, J., KEHNE, J. & CORTRIGHT, D. N. 2007. Inflammation-Induced Reduction of Spontaneous Activity by Adjuvant: A Novel Model to Study the Effect of Analgesics in Rats. *Journal of Pharmacology and Experimental Therapeutics,* 320**,** 194-201.

MATUSICA, D., SKELDAL, S., SYKES, A., PALSTRA, N., SHARMA, A. and COULSON, E. 2013. An Intracellular Domain Fragment of the p75 Neurotrophin Receptor (p75NTR) Enhances Tropomyosin Receptor Kinase A (TrkA) Receptor Function. *Journal of Biological Chemistry*, 288(16), pp.11144-11154.

MAVROMMATIS, E., FISH, E. N. & PLATANIAS, L. C. 2013. The schlafen family of proteins and their regulation by interferons. *J Interferon Cytokine Res,* 33**,** 206-10.

MAYORGA, A. J., WANG, S., KELLY, K. M. & THIPPHAWONG, J. 2016. Efficacy and safety of fulranumab as monotherapy in patients with moderate to severe, chronic knee pain of primary osteoarthritis: a randomised, placebo- and active-controlled trial. *International Journal of Clinical Practice,* 70**,** 493-505.

MAZAHERI, S., HAJILOOI, M. & RAFIEI, A. 2006. The G-308A promoter variant of the tumor necrosis factor-alpha gene is associated with migraine without aura. *J Neurol,* 253**,** 1589-93.

MCDONALD, N. Q., LAPATTO, R., MURRAY-RUST, J., GUNNING, J., WLODAWER, A. & BLUNDELL, T. L. 1991. New protein fold revealed by a 2.3-A resolution crystal structure of nerve growth factor. *Nature,* 354**,** 411-4.

MCMAHON, S. B. 1996. NGF as a Mediator of Inflammatory Pain. *Philosophical Transactions of the Royal Society of London. Series B: Biological Sciences* 351 431-440.

MCMAHON, S. B., BENNETT, D. L., PRIESTLEY, J. V. & SHELTON, D. L. 1995. The biological effects of endogenous nerve growth factor on adult sensory neurons revealed by a trkA-IgG fusion molecule. *Nat Med,* 1**,** 774-80.

MCMAHON, S. B., RUSSA, F. L. & BENNETT, D. L. H. 2015. Crosstalk between the nociceptive and immune systems in host defence and disease. *Nature Reviews Neuroscience,* 16**,** 389.

MEAROWA, K. M. & KRIL, Y. 1995. Anti-NGF treatment blocks the upregulation of NGF receptor mRNA expression associated with collateral sprouting of rat dorsal root ganglion neurons. *Neuroscience Letters,* 184**,** 55-58.

MELZACK, R. and WALL, P. 1996. Pain mechanisms: A new theory. *Pain Forum*, 5(1), pp.3-11.

MENG, J., WANG, J., STEINHOFF, M. & DOLLY, J. O. 2016. TNFα induces co-trafficking of TRPV1/TRPA1 in VAMP1-containing vesicles to the plasmalemma via Munc18–1/syntaxin1/SNAP-25 mediated fusion. *Scientific Reports,* 6**,** 21226.

MEENTS, J., NEEB, L. and REUTER, U. 2010. TRPV1 in migraine pathophysiology. *Trends in Molecular Medicine*, 16(4), pp.153-159.

MICO, J. A., ARDID, D., BERROCOSO, E. & ESCHALIER, A. 2006. Antidepressants and pain. *Trends Pharmacol Sci,* 27**,** 348-54.

MICZEK, K., MAXSON, S., FISH, E. and FACCIDOMO, S. 2001. Aggressive behavioral phenotypes in mice. *Behavioural Brain Research*, 125(1-2), pp.167-181.

MIKOVA, O., YAKIMOVA, R., BOSMANS, E., KENIS, G. & MAES, M. 2001. Increased serum tumor necrosis factor alpha concentrations in major depression and multiple sclerosis. *Eur Neuropsychopharmacol,* 11**,** 203-8.

MILLER, R. E., KIM, Y. S., TRAN, P. B., ISHIHARA, S., DONG, X., MILLER, R. J. & MALFAIT, A.-M. 2018. Visualization of Peripheral Neuron Sensitization in a Surgical Mouse Model of Osteoarthritis by In Vivo Calcium Imaging. *Arthritis & Rheumatology,* 70**,** 88-97.

MILLS, C. D. 2015. Anatomy of a Discovery: M1 and M2 Macrophages. *Frontiers in Immunology,* 6**,** 212.

MINNONE, G., DE BENEDETTI, F. & BRACCI-LAUDIERO, L. 2017. NGF and Its Receptors in the Regulation of Inflammatory Response. *International Journal of Molecular Sciences,* 18**,** 1028.

MITCHELL, E. 2006. Serum calcitonin gene-related petide concentrations in the horse and their relationship to the systemic inflammatory response. [Blacksburg, Va.]: [University Libraries, Virginia Polytechnic Institute and State University].

MIYAGI, M., UCHIDA, K., TAKANO, S., FUJIMAKI, H., AIKAWA, J., SEKIGUCHI, H., NAGURA, N., OHTORI, S., INOUE, G. & TAKASO, M. 2018. Macrophage-derived inflammatory cytokines regulate growth factors and pain-related molecules in mice with intervertebral disc injury. *Journal of Orthopaedic Research,* 36**,** 2274-2279.

MOALEM, G., GRAFE, P. & TRACEY, D. J. 2005. Chemical mediators enhance the excitability of unmyelinated sensory axons in normal and injured peripheral nerve of the rat. *Neuroscience,* 134**,** 1399-1411.

MOBASHERI, A. 2013. The Future of Osteoarthritis Therapeutics: Emerging Biological Therapy. *Current Rheumatology Reports,* 15**,** 385.

MÓCSAI, A., KOVÁCS, L. & GERGELY, P. 2014. What is the future of targeted therapy in rheumatology: biologics or small molecules? *BMC Medicine,* 12**,** 43.

MOLYVA, D. 2010. Neuropeptides and pain. *Annals of General Psychiatry,* 9**,** S3-S3.

MOROOKA, T. & NISHIDA, E. 1998. Requirement of p38 Mitogen-activated Protein Kinase for Neuronal Differentiation in PC12 Cells. *Journal of Biological Chemistry,* 273**,** 24285-24288.

MORRISON, T. E., FRASER, R. J., SMITH, P. N., MAHALINGAM, S. & HEISE, M. T. 2007. Complement Contributes to Inflammatory Tissue Destruction in a Mouse Model of Ross River Virus-Induced Disease. *Journal of Virology,* 81**,** 5132-5143.

MPOFU, S., FATIMA, F. & MOOTS, R. J. 2005. Anti-TNF-alpha therapies: they are all the same (aren't they?). *Rheumatology (Oxford),* 44**,** 271-3.

MULLARD, A. 2015. Drug developers reboot anti-NGF pain programmes. *Nat Rev Drug Discov,* 14**,** 297-298.

MULLER, P. A., KOSCSÓ, B., RAJANI, G. M., STEVANOVIC, K., BERRES, M.-L., HASHIMOTO, D., MORTHA, A., LEBOEUF, M., LI, X.-M., MUCIDA, D., STANLEY, E. R., DAHAN, S., MARGOLIS, K. G., GERSHON, M. D., MERAD, M. & BOGUNOVIC, M. 2014. Crosstalk between Muscularis Macrophages and Enteric Neurons Regulates Gastrointestinal Motility. *Cell,* 158**,** 300-313.

MUNKHOLM, T. K. & ARENDT-NIELSEN, L. 2017. The interaction between NGF-induced hyperalgesia and acid-provoked pain in the infrapatellar fat pad and tibialis anterior muscle of healthy volunteers. *European Journal of Pain,* 21**,** 474-485.

MURRAY, P. J. & WYNN, T. A. 2011. Protective and pathogenic functions of macrophage subsets. *Nature reviews. Immunology,* 11**,** 723-737.

NA, Y. R., JUNG, D., GU, G. J. & SEOK, S. H. 2016. GM-CSF Grown Bone Marrow Derived Cells Are Composed of Phenotypically Different Dendritic Cells and Macrophages. *Molecules and Cells,* 39**,** 734-741.

NADEAU, S., FILALI, M., ZHANG, J., KERR, B. J., RIVEST, S., SOULET, D., IWAKURA, Y., DE RIVERO VACCARI, J. P., KEANE, R. W. & LACROIX, S. 2011. Functional recovery after peripheral nerve injury is dependent on the pro-inflammatory cytokines IL-1beta and TNF: implications for neuropathic pain. *J Neurosci,* 31**,** 12533-42.

NAGASAKO, E., OAKLANDER, A. and DWORKIN, R. 2003. Congenital insensitivity to pain: an update. *Pain*, 101(3), pp.213-219.

NAHRENDORF, M. & SWIRSKI, F. K. 2016. Abandoning M1/M2 for a Network Model of Macrophage Function. *Circulation research,* 119**,** 414-417.

NASCIMENTO, D., POZZA, D. H., CASTRO-LOPES, J. M. & NETO, F. L. 2011. Neuronal Injury Marker ATF-3 Is Induced in Primary Afferent Neurons of Monoarthritic Rats. *Neurosignals,* 19**,** 210-221.

NASSAR, M. A., STIRLING, L. C., FORLANI, G., BAKER, M. D., MATTHEWS, E. A., DICKENSON, A. H. & WOOD, J. N. 2004. Nociceptor-specific gene deletion reveals a major role for Nav1.7 (PN1) in acute and inflammatory pain. *Proceedings of the National Academy of Sciences of the United States of America,* 101**,** 12706-12711.

NATHAN, C. & DING, A. 2010. Nonresolving Inflammation. *Cell,* 140**,** 871-882.

NEUMANN, H., SCHWEIGREITER, R., YAMASHITA, T., ROSENKRANZ, K., WEKERLE, H. & BARDE, Y. A. 2002. Tumor necrosis factor inhibits neurite outgrowth and

branching of hippocampal neurons by a rho-dependent mechanism. *J Neurosci,* 22**,** 854-62.

NICHOLSON, B. & VERMA, S. 2004. Comorbidities in Chronic Neuropathic Pain. *Pain Medicine,* 5**,** S9-S27.

NICOL, G. D. & VASKO, M. R. 2007. Unraveling the story of NGF-mediated sensitization of nociceptive sensory neurons: ON or OFF the Trks? *Mol Interv,* 7**,** 26-41.

NICOL, L. S., DAWES, J. M., LA RUSSA, F., DIDANGELOS, A. & CLARK, A. K. 2015. The role of G-protein receptor 84 in experimental neuropathic pain. 35**,** 8959-69.

NIE, F., WANG, J., SU, D., SHI, Y., CHEN, J., WANG, H., QIN, W. & SHI, L. 2013. Abnormal activation of complement C3 in the spinal dorsal horn is closely associated with progression of neuropathic pain. *Int J Mol Med,* 31**,** 1333-42.

NIETO, F. R., CLARK, A. K., GRIST, J., HATHWAY, G. J., CHAPMAN, V. & MALCANGIO, M. 2016. Neuron-immune mechanisms contribute to pain in early stages of arthritis. *Journal of Neuroinflammation,* 13**,** 96.

NOCKHER, W. A. & RENZ, H. 2003. Neurotrophins in inflammatory lung diseases: modulators of cell differentiation and neuroimmune interactions. *Cytokine & Growth Factor Reviews,* 14**,** 559-578.

NOLANO, M., CRISCI, C., SANTORO, L., BARBIERI, F., CASALE, R., KENNEDY, W. R., WENDELSCHAFER-CRABB, G., PROVITERA, V., DI LORENZO, N. & CARUSO, G. 2000. Absent innervation of skin and sweat glands in congenital insensitivity to pain with anhidrosis. *Clin Neurophysiol,* 111**,** 1596-601.

O'ROURKE, K. P., O'DONOGHUE, G., ADAMS, C., MULCAHY, H., MOLLOY, C., SILKE, C., MOLLOY, M., SHANAHAN, F. & O'GARA, F. 2008. High levels of Lymphotoxin-Beta (LT-Beta) gene expression in rheumatoid arthritis synovium: clinical and cytokine correlations. *Rheumatology International,* 28**,** 979-986.

OBATA, K., KATSURA, H., SAKURAI, J., KOBAYASHI, K., YAMANAKA, H., DAI, Y., FUKUOKA, T. & NOGUCHI, K. 2006. Suppression of the p75 Neurotrophin Receptor in Uninjured Sensory Neurons Reduces Neuropathic Pain after Nerve Injury. *The Journal of Neuroscience,* 26**,** 11974-11986.

OGAWA, N., KAWAI, H., TERASHIMA, T., KOJIMA, H., OKA, K., CHAN, L. & MAEGAWA, H. 2014. Gene Therapy for Neuropathic Pain by Silencing of TNF-α Expression with Lentiviral Vectors Targeting the Dorsal Root Ganglion in Mice. *PLOS ONE,* 9**,** e92073.

OH, D. Y. & LAGAKOS, W. S. 2011. The role of G-protein-coupled receptors in mediating the effect of fatty acids on inflammation and insulin sensitivity. *Current Opinion in Clinical Nutrition & Metabolic Care,* 14**,** 322-327.

OHARA, P., VIT, J., BHARGAVA, A., ROMERO, M., SUNDBERG, C., CHARLES, A. and JASMIN, L. 2009. Gliopathic Pain: When Satellite Glial Cells Go Bad. *The Neuroscientist*, 15(5), pp.450-463.

OHTORI, S., TAKAHASHI, K., MORIYA, H. & MYERS, R. R. 2004. TNF-alpha and TNF-alpha receptor type 1 upregulation in glia and neurons after peripheral nerve injury: studies in murine DRG and spinal cord. *Spine (Phila Pa 1976),* 29**,** 1082-8.

OKAMOTO, K., MARTIN, D. P., SCHMELZER, J. D., MITSUI, Y. & LOW, P. A. 2001. Pro- and anti-inflammatory cytokine gene expression in rat sciatic nerve chronic constriction injury model of neuropathic pain. *Exp Neurol,* 169**,** 386-91.

OPREE, A. & KRESS, M. 2000. Involvement of the proinflammatory cytokines tumor necrosis factor-alpha, IL-1 beta, and IL-6 but not IL-8 in the development of heat hyperalgesia: effects on heat-evoked calcitonin gene-related peptide release from rat skin. *J Neurosci,* 20**,** 6289-93.

OPRÉE, A. & KRESS, M. 2000. Involvement of the Proinflammatory Cytokines Tumor Necrosis Factor-α, IL-1β, and IL-6 But Not IL-8 in the Development of Heat Hyperalgesia: Effects on Heat-Evoked Calcitonin Gene-Related Peptide Release from Rat Skin. *The Journal of Neuroscience,* 20**,** 6289-6293.

OSSIPOV, M.H. MRIMURA, K. and PORRECA, F. 2015. Descending pain modulation and chronification of pain. *Current Opinion in Supportive and Palliative Care*, 8(2): 143-151.

ORITA, S., KOSHI, T., MITSUKA, T., MIYAGI, M., INOUE, G., ARAI, G., ISHIKAWA, T., HANAOKA, E., YAMASHITA, K., YAMASHITA, M., EGUCHI, Y., TOYONE, T., TAKAHASHI, K. & OHTORI, S. 2011. Associations between proinflammatory cytokines in the synovial fluid and radiographic grading and pain-related scores in 47 consecutive patients with osteoarthritis of the knee. *BMC Musculoskeletal Disorders,* 12**,** 144.

ORTEGA-GÓMEZ, A., PERRETTI, M. & SOEHNLEIN, O. 2013. Resolution of inflammation: an integrated view. *EMBO Molecular Medicine,* 5**,** 661-674.

OSTROWSKI, S. M., BELKADI, A., LOYD, C. M., DIACONU, D. & WARD, N. L. 2011. Cutaneous denervation of psoriasiform mouse skin improves acanthosis and inflammation in a sensory neuropeptide dependent manner. *The Journal of investigative dermatology,* 131**,** 1530-1538.

OUYANG, W., RUTZ, S., CRELLIN, N. K., VALDEZ, P. A. & HYMOWITZ, S. G. 2011. Regulation and Functions of the IL-10 Family of Cytokines in Inflammation and Disease. *Annual Review of Immunology,* 29**,** 71-109.

OWENS, M., WHITE, D., STRATH, L., ATA, A., HEATH, S., TURAN, J., MERLIN, J. & GOODIN, B. 2018. Circulating levels of pro-inflammatory cytokines are associated with increased pain sensitivity and greater clinical pain severity in people living with HIV (PLWH) and chronic pain. *The Journal of Pain,* 19**,** S105-S106.

PARADA, C. A., YEH, J. J., JOSEPH, E. K. & LEVINE, J. D. 2003. Tumor necrosis factor receptor type-1 in sensory neurons contributes to induction of chronic enhancement of inflammatory hyperalgesia in rat. *European Journal of Neuroscience,* 17**,** 1847-1852.

PARAMESWARAN, N. & PATIAL, S. 2010. Tumor Necrosis Factor-α Signaling in Macrophages. *Critical reviews in eukaryotic gene expression,* 20**,** 87-103.

PARTSCH, G., STEINER, G., LEEB, B. F., DUNKY, A., BRÖLL, H. & SMOLEN, J. S. 1997. Highly increased levels of tumor necrosis factor-alpha and other proinflammatory cytokines in psoriatic arthritis synovial fluid. *The Journal of rheumatology,* 24**,** 518-523.

PATRO, N., NAGAYACH, A. & PATRO, I. K. 2010. Iba1 expressing microglia in the dorsal root ganglia become activated following peripheral nerve injury in rats. *Indian J Exp Biol,* 48**,** 110-6.

PEARSON, G., ROBINSON, F., BEERS GIBSON, T., XU, B. E., KARANDIKAR, M., BERMAN, K. & COBB, M. H. 2001. Mitogen-activated protein (MAP) kinase pathways: regulation and physiological functions. *Endocr Rev,* 22**,** 153-83.

PENNINX, B. W. J. H., ABBAS, H., AMBROSIUS, W., NICKLAS, B. J., DAVIS, C., MESSIER, S. P. & PAHOR, M. 2004. Inflammatory markers and physical function among older adults with knee osteoarthritis. *The Journal of Rheumatology,* 31**,** 2027-2031.

PEREIRA, U., BOULAIS, N., LEBONVALLET, N., LEFEUVRE, L., GOUGEROT, A. & MISERY, L. 2010. Development of an in vitro coculture of primary sensitive pig neurons and keratinocytes for the study of cutaneous neurogenic inflammation. *Experimental Dermatology,* 19**,** 931-935.

PERKINS, N. M. & TRACEY, D. J. 2000. Hyperalgesia due to nerve injury: role of neutrophils. *Neuroscience,* 101**,** 745-757.

PETERS, C. M., JIMENEZ-ANDRADE, J. M., JONAS, B. M., SEVCIK, M. A., KOEWLER, N. J., GHILARDI, J. R., WONG, G. Y. & MANTYH, P. W. 2007. Intravenous paclitaxel administration in the rat induces a peripheral sensory neuropathy characterized by macrophage infiltration and injury to sensory neurons and their supporting cells. *Experimental Neurology,* 203**,** 42-54.

PETERSON, S. L., NGUYEN, H. X., MENDEZ, O. A. & ANDERSON, A. J. 2017. Complement Protein C3 Suppresses Axon Growth and Promotes Neuron Loss. *Scientific Reports,* 7**,** 12904.

PEZET, S. & MCMAHON, S. B. 2006. NEUROTROPHINS: Mediators and Modulators of Pain. *Annual Review of Neuroscience,* 29**,** 507-538.

PEZET, S., ONTÉNIENTE, B., JULLIEN, J., JUNIER, M.-P., GRANNEC, G., RUDKIN, B. B. & CALVINO, B. 2001. Differential regulation of NGF receptors in primary sensory neurons by adjuvant-induced arthritis in the rat. *Pain,* 90**,** 113-125.

PFEFFER, K. 2003. Biological functions of tumor necrosis factor cytokines and their receptors. *Cytokine & Growth Factor Reviews,* 14**,** 185-191.

PINHO-RIBEIRO, F. A., VERRI, W. A. & CHIU, I. M. 2017a. Nociceptor Sensory Neuron-Immune Interactions in Pain and Inflammation. *Trends in immunology,* 38**,** 5-19.

PINHO-RIBEIRO, F. A., VERRI, W. A. & CHIU, I. M. 2017b. Nociceptor Sensory Neuron–Immune Interactions in Pain and Inflammation. *Trends in Immunology,* 38**,** 5-19.

POLAZZI, E. and CONTESTABILE, A. 2003. Neuron-Conditioned Media Differentially Affect the Survival of Activated or Unstimulated Microglia: Evidence for Neuronal Control on Apoptotic Elimination of Activated Microglia. *Journal of Neuropathology & Experimental Neurology*, 62(4), pp.351-362.

POLLOCK, J., MCFARLANE, S. M., CONNELL, M. C., ZEHAVI, U., VANDENABEELE, P., MACEWAN, D. J. & SCOTT, R. H. 2002. TNF-α receptors simultaneously activate Ca2+ mobilisation and stress kinases in cultured sensory neurones. *Neuropharmacology,* 42**,** 93-106.

POOLE, S., DE QUEIROZ CUNHA, F. & FERREIRA, S. H. 1999. Hyperalgesia from subcutaneous cytokines. *In:* WATKINS, L. R. & MAIER, S. F. (eds.) *Cytokines and Pain.* Basel: Birkhäuser Basel.

PRADHAN, L., NABZDYK, C., ANDERSEN, N. D., LOGERFO, F. W. & VEVES, A. 2009. Inflammation and Neuropeptides: The Connection in Diabetic Wound Healing. *Expert reviews in molecular medicine,* 11**,** e2-e2.

PRINZ, M. & PRILLER, J. 2017. The role of peripheral immune cells in the CNS in steady state and disease. *Nature Neuroscience,* 20**,** 136.

QIN, L., LI, G., QIAN, X., LIU, Y., WU, X., LIU, B., HONG, J.-S. & BLOCK, M. L. 2005a. Interactive role of the toll-like receptor 4 and reactive oxygen species in LPS-induced microglia activation. *Glia,* 52**,** 78-84.

QIN, X., WAN, Y. & WANG, X. 2005b. CCL2 and CXCL1 trigger calcitonin gene-related peptide release by exciting primary nociceptive neurons. *Journal of Neuroscience Research,* 82**,** 51-62.

QU, Y., ZHAO, G. & LI, H. 2017. Forward and Reverse Signaling Mediated by Transmembrane Tumor Necrosis Factor-Alpha and TNF Receptor 2: Potential Roles in an Immunosuppressive Tumor Microenvironment. *Frontiers in Immunology,* 8**,** 1675.

RADIO, N. M. & MUNDY, W. R. 2008. Developmental neurotoxicity testing in vitro: Models for assessing chemical effects on neurite outgrowth. *NeuroToxicology,* 29**,** 361-376.

RECIO, C., LUCY, D., PURVIS, G. S. D., IVESON, P., ZEBOUDJ, L., IQBAL, A. J., LIN, D., O'CALLAGHAN, C., DAVISON, L., GRIESBACH, E., RUSSELL, A. J., WYNNE, G. M., DIB, L., MONACO, C. & GREAVES, D. R. 2018. Activation of the Immune-Metabolic Receptor GPR84 Enhances Inflammation and Phagocytosis in Macrophages. *Frontiers in Immunology,* 9**,** 1419.

REICHARDT, L. F. 2006a. Neurotrophin-regulated signalling pathways. *Philosophical Transactions of the Royal Society B: Biological Sciences,* 361**,** 1545-1564.

REICHARDT, L. F. 2006b. *Neurotrophin-regulated signalling pathways*.

REINHOLD, A. K., BATTI, L., BILBAO, D., BUNESS, A., RITTNER, H. L. & HEPPENSTALL, P. A. 2015. Differential Transcriptional Profiling of Damaged and Intact Adjacent Dorsal Root Ganglia Neurons in Neuropathic Pain. *PLOS ONE,* 10**,** e0123342.

REN, K. & DUBNER, R. 1999. Inflammatory Models of Pain and Hyperalgesia. *ILAR Journal,* 40**,** 111-118.

REN, K. & TORRES, R. 2009. Role of interleukin-1β during pain and inflammation. *Brain research reviews,* 60**,** 57-64.

REYES-GIBBY, C. C., SPITZ, M. R., YENNURAJALINGAM, S., SWARTZ, M., GU, J., WU, X., BRUERA, E. & SHETE, S. 2009. The role of inflammation gene polymorphisms on pain severity in lung cancer patients. *Cancer epidemiology, biomarkers & prevention : a publication of the American Association for Cancer Research, cosponsored by the American Society of Preventive Oncology,* 18**,** 2636-2642.

REYES-GIBBY, C. C., SWARTZ, M. D., YU, X., WU, X., YENNURAJALINGAM, S., ANDERSON, K. O., SPITZ, M. R. & SHETE, S. 2013. Symptom clusters of pain, depressed mood, and fatigue in lung cancer: assessing the role of cytokine genes. *Supportive Care in Cancer,* 21**,** 3117-3125.

REZAEE, R. & ABDOLLAHI, M. 2017. The importance of translatability in drug discovery. *Expert Opinion on Drug Discovery,* 12**,** 237-239.

RIBEIRO, R. A., VALE, M. L., THOMAZZI, S. M., PASCHOALATO, A. B., POOLE, S., FERREIRA, S. H. & CUNHA, F. Q. 2000. Involvement of resident macrophages and mast cells in the writhing nociceptive response induced by zymosan and acetic acid in mice. *Eur J Pharmacol,* 387**,** 111-8.

RICCI, A., FELICI, L., MARIOTTA, S., MANNINO, F., SCHMID, G., TERZANO, C., CARDILLO, G., AMENTA, F. & BRONZETTI, E. 2004. Neurotrophin and Neurotrophin Receptor Protein Expression in the Human Lung. *American Journal of Respiratory Cell and Molecular Biology,* 30**,** 12-19.

RICHARDS, N. & MCMAHON, S. B. 2013. Targeting novel peripheral mediators for the treatment of chronic pain. *British Journal of Anaesthesia,* 111**,** 46-51.

RICHTER, F., NATURA, G., LOSER, S., SCHMIDT, K., VIISANEN, H. & SCHAIBLE, H. G. 2010. Tumor necrosis factor causes persistent sensitization of joint nociceptors to mechanical stimuli in rats. *Arthritis Rheum,* 62**,** 3806-14.

RICKLIN, D., HAJISHENGALLIS, G., YANG, K. & LAMBRIS, J. D. 2010. Complement: a key system for immune surveillance and homeostasis. *Nature Immunology,* 11**,** 785.

RIESE, D. J. & CULLUM, R. L. 2014. Epiregulin: Roles in Normal Physiology and Cancer. *Seminars in cell & developmental biology,* 0**,** 49-56.

RIGAUD, M., GEMES, G., BARABAS, M.-E., CHERNOFF, D. I., ABRAM, S. E., STUCKY, C. L. & HOGAN, Q. H. 2008. Species and strain differences in rodent sciatic nerve anatomy: Implications for studies of neuropathic pain. *Pain,* 136**,** 188-201.

RINA, B., GILA, K., ELENA, A. & CHAYA, B. 2001. Nerve growth factor regulates TNF-α production in mouse macrophages via MAP kinase activation. *Journal of Leukocyte Biology,* 69**,** 1019-1026.

RISTOIU, V. 2013. Contribution of macrophages to peripheral neuropathic pain pathogenesis. *Life Sciences,* 93**,** 870-881.

RODRIGUEZ-RAECKE, R., NIEMEIER, A., IHLE, K., RUETHER, W. & MAY, A. 2009. Brain Gray Matter Decrease in Chronic Pain Is the Consequence and Not the Cause of Pain. *The Journal of Neuroscience,* 29**,** 13746-13750.

ROGERS, M., TANG, L., MADGE, D. J. & STEVENS, E. B. 2006. The role of sodium channels in neuropathic pain. *Seminars in Cell & Developmental Biology,* 17**,** 571-581.

ROMERO-SANDOVAL, A., CHAI, N., NUTILE-MCMENEMY, N. & DELEO, J. A. 2008. A comparison of spinal Iba1 and GFAP expression in rodent models of acute and chronic pain. *Brain Research,* 1219**,** 116-126.

ROSEN, J. M., YAGGIE, R. E., WOIDA, P. J., MILLER, R. J., SCHAEFFER, A. J. & KLUMPP, D. J. 2018. TRPV1 and the MCP-1/CCR2 Axis Modulate Post-UTI Chronic Pain. *Scientific Reports,* 8**,** 7188.

ROSTOCK, C., SCHRENK-SIEMENS, K., POHLE, J. & SIEMENS, J. 2017. Human vs. Mouse Nociceptors – Similarities and Differences. *Neuroscience*.

ROUX, P. P., BHAKAR, A. L., KENNEDY, T. E. & BARKER, P. A. 2001. The p75 neurotrophin receptor activates Akt (protein kinase B) through a phosphatidylinositol 3-kinase-dependent pathway. *J Biol Chem,* 276**,** 23097-104.

ROZAS, P., LAZCANO, P., PIÑA, R., CHO, A., TERSE, A., PERTUSA, M., MADRID, R., GONZALEZ-BILLAULT, C., KULKARNI, A. B. & UTRERAS, E. 2016. Targeted overexpression of Tumor Necrosis Factor-α increases Cyclin-dependent kinase 5 activity and TRPV1-dependent Ca(2+) influx in trigeminal neurons. *Pain,* 157**,** 1346-1362.

RUSSELL, F. A., KING, R., SMILLIE, S. J., KODJI, X. & BRAIN, S. D. 2014. Calcitonin gene-related peptide: physiology and pathophysiology. *Physiol Rev,* 94**,** 1099-142.

RYDER, S. and STANNARD, C. 2005. Treatment of chronic pain: antidepressant, antiepileptic and antiarrhythmic drugs. *Continuing Education in Anaesthesia Critical Care & Pain,* 5(1), pp.18-21.

SABIO, G. & DAVIS, R. J. 2014. TNF and MAP kinase signalling pathways. *Semin Immunol,* 26**,** 237-45.

SAFIEH-GARABEDIAN, B., POOLE, S., ALLCHORNE, A., WINTER, J. & WOOLF, C. J. 1995. Contribution of interleukin-1 beta to the inflammation-induced increase in nerve growth factor levels and inflammatory hyperalgesia. *British Journal of Pharmacology,* 115**,** 1265-1275.

SAHA, R. N. & PAHAN, K. 2006. TNF-α in CNS: Physiologic and Pathologic Roles. *In:* LAJTHA, A. & LIM, R. (eds.) *Handbook of Neurochemistry and Molecular Neurobiology.* Springer US.

SAHBAIE, P., SHI, X., GUO, T.-Z., QIAO, Y., YEOMANS, D. C., KINGERY, W. S. & CLARK, J. D. 2009. Role of Substance P Signaling in Enhanced Nociceptive Sensitization and Local Cytokine Production after Incision. *Pain,* 145**,** 341-349.

SANDKÜHLER, J. and GRUBER-SCHOFFNEGGER, D. 2012. Hyperalgesia by synaptic long-term potentiation (LTP): an update. *Current Opinion in Pharmacology*, 12(1), pp.18-27.

SANTULLI, P., MARCELLIN, L., TOSTI, C., CHOUZENOUX, S., CERLES, O., BORGHESE, B., BATTEUX, F. & CHAPRON, C. 2015. MAP kinases and the inflammatory signaling cascade as targets for the treatment of endometriosis? *Expert Opinion on Therapeutic Targets,* 19**,** 1465-1483.

SARAFI, M. N., GARCIA-ZEPEDA, E. A., MACLEAN, J. A., CHARO, I. F. & LUSTER, A. D. 1997. Murine Monocyte Chemoattractant Protein (MCP)-5: A Novel CC Chemokine That Is a Structural and Functional Homologue of Human MCP-1. *The Journal of Experimental Medicine,* 185**,** 99-110.

SARCHIELLI, P., ALBERTI, A., FLORIDI, A. & GALLAI, V. 2001. Levels of nerve growth factor in cerebrospinal fluid of chronic daily headache patients. *Neurology,* 57**,** 132-4.

SARCHIELLI, P., MANCINI, M. L., FLORIDI, A., COPPOLA, F., ROSSI, C., NARDI, K., ACCIARRESI, M., PINI, L. A. & CALABRESI, P. 2007. Increased Levels of

Neurotrophins Are Not Specific for Chronic Migraine: Evidence From Primary Fibromyalgia Syndrome. *The Journal of Pain,* 8**,** 737-745.

SARDER, K., MA, R., KHANDOKER MR & ANMN, K. 2016. Anticonvulsants and Antidepressants in Chronic Pain Management. *J Recent Adv Pain,* 2**,** 90-93.

SATOH, T., NAKAMURA, S., TAGA, T., MATSUDA, T., HIRANO, T., KISHIMOTO, T. & KAZIRO, Y. 1988. Induction of neuronal differentiation in PC12 cells by B-cell stimulatory factor 2/interleukin 6. *Molecular and Cellular Biology,* 8**,** 3546-3549.

SCACCIANOCE, S., CIGLIANA, G., NICOLAI, R., MUSCOLO, L. A. A., PORCU, A., NAVARRA, D., PEREZ-POLO, J. R. & ANGELUCCI, L. 1993. Hypothalamic Involvement in the Activation of the Pituitary-Adrenocortical Axis by Nerve Growth Factor. *Neuroendocrinology,* 58**,** 202-209.

SCHAFERS, M., LEE, D. H., BRORS, D., YAKSH, T. L. & SORKIN, L. S. 2003a. Increased sensitivity of injured and adjacent uninjured rat primary sensory neurons to exogenous tumor necrosis factor-alpha after spinal nerve ligation. *J Neurosci,* 23**,** 3028-38.

SCHAFERS, M., SORKIN, L. S., GEIS, C. & SHUBAYEV, V. I. 2003b. Spinal nerve ligation induces transient upregulation of tumor necrosis factor receptors 1 and 2 in injured and adjacent uninjured dorsal root ganglia in the rat. *Neurosci Lett,* 347**,** 179-82.

SCHÄFERS, M., SVENSSON, C. I., SOMMER, C. & SORKIN, L. S. 2003. Tumor necrosis factor-alpha induces mechanical allodynia after spinal nerve ligation by activation of p38 MAPK in primary sensory neurons. *Journal of Neuroscience,* 23**,** 2517-2521.

SCHINDLER, C., LEVY, D. E. & DECKER, T. 2007. JAK-STAT Signaling: From Interferons to Cytokines. *Journal of Biological Chemistry,* 282**,** 20059-20063.

SCHMIDT-WILCKE, T., LEINISCH, E., STRAUBE, A., KÄMPFE, N., DRAGANSKI, B., DIENER, H. C., BOGDAHN, U. & MAY, A. 2005. Gray matter decrease in patients with chronic tension type headache. *Neurology,* 65**,** 1483-1486.

SCHMIDT, R., SCHMELZ, M., FORSTER, C., RINGKAMP, M., TOREBJORK, E. & HANDWERKER, H. 1995. Novel classes of responsive and unresponsive C nociceptors in human skin. *The Journal of Neuroscience,* 15**,** 333-341.

SCHMITT, K. R. L., BOATO, F., DIESTEL, A., HECHLER, D., KRUGLOV, A., BERGER, F. & HENDRIX, S. 2010. Hypothermia-Induced Neurite Outgrowth is Mediated by Tumor Necrosis Factor-Alpha. *Brain Pathology,* 20**,** 771-779.

SCHMITTGEN, T. D. & LIVAK, K. J. 2008. Analyzing real-time PCR data by the comparative CT method. *Nature Protocols,* 3**,** 1101.

SCHOLZ, J. & WOOLF, C. J. 2007. The neuropathic pain triad: neurons, immune cells and glia. *Nat Neurosci,* 10**,** 1361-1368.

SCHOTTE, H., SCHLUTER, B., WILLEKE, P., MICKHOLZ, E., SCHORAT, M. A., DOMSCHKE, W. & GAUBITZ, M. 2004. Long-term treatment with etanercept significantly reduces the number of proinflammatory cytokine-secreting peripheral blood mononuclear cells in patients with rheumatoid arthritis. *Rheumatology (Oxford),* 43**,** 960-4.

SCHOU, W. S., ASHINA, S., AMIN, F. M., GOADSBY, P. J. & ASHINA, M. 2017. Calcitonin gene-related peptide and pain: a systematic review. *The Journal of Headache and Pain,* 18**,** 34.

SEDGER, L. M. & MCDERMOTT, M. F. 2014. TNF and TNF-receptors: From mediators of cell death and inflammation to therapeutic giants – past, present and future. *Cytokine & Growth Factor Reviews,* 25**,** 453-472.

SEGOND VON BANCHET, G., BOETTGER, M. K., FISCHER, N., GAJDA, M., BRAUER, R. & SCHAIBLE, H. G. 2009. Experimental arthritis causes tumor necrosis factor-alpha-dependent infiltration of macrophages into rat dorsal root ganglia which correlates with pain-related behavior. *Pain,* 145**,** 151-9.

SEIDEL, M. F., WISE, B. L. & LANE, N. E. 2013. Nerve growth factor: an update on the science and therapy. *Osteoarthritis and cartilage / OARS, Osteoarthritis Research Society,* 21**,** 1223-1228.

SELTZER, Z. E., DUBNER, R. & SHIR, Y. 1990. A novel behavioral model of neuropathic pain disorders produced in rats by partial sciatic nerve injury. *PAIN,* 43**,** 205-218.

SERIZAWA, K., TOMIZAWA-SHINOHARA, H., MAGI, M., YOGO, K. & MATSUMOTO, Y. 2018. Anti-IL-6 receptor antibody improves pain symptoms in mice with experimental autoimmune encephalomyelitis. *Journal of Neuroimmunology,* 319**,** 71-79.

SEYMOUR, H. E., WORSLEY, A., SMITH, J. M. & THOMAS, S. H. L. 2001. Anti-TNF agents for rheumatoid arthritis. *British Journal of Clinical Pharmacology,* 51**,** 201-208.

SHEPHERD, A. J., COPITS, B. A., MICKLE, A. D., KARLSSON, P., KADUNGANATTIL, S., HAROUTOUNIAN, S., TADINADA, S. M., DE KLOET, A. D., VALTCHEVA, M. V., MCILVRIED, L. A., SHEAHAN, T. D., JAIN, S., RAY, P. R., USACHEV, Y. M., DUSSOR, G., KRAUSE, E. G., PRICE, T. J., GEREAU, R. W. & MOHAPATRA, D. P. 2018. Angiotensin II triggers peripheral macrophage-to-sensory neuron redox crosstalk to elicit pain. *The Journal of Neuroscience*.

SHUTOV, L. P. & WARWICK, C. A. 2016. The Complement System Component C5a Produces Thermal Hyperalgesia via Macrophage-to-Nociceptor Signaling That Requires NGF and TRPV1. 36**,** 5055-70.

SHUTOV, L. P., WARWICK, C. A., SHI, X., GNANASEKARAN, A., SHEPHERD, A. J., MOHAPATRA, D. P., WOODRUFF, T. M., CLARK, J. D. & USACHEV, Y. M. 2016. The Complement System Component C5a Produces Thermal Hyperalgesia via Macrophage-to-Nociceptor Signaling That Requires NGF and TRPV1. *The Journal of Neuroscience,* 36**,** 5055-5070.

SI, H.-B., YANG, T.-M., ZENG, Y., ZHOU, Z.-K., PEI, F.-X., LU, Y.-R., CHENG, J.-Q. & SHEN, B. 2017. Correlations between inflammatory cytokines, muscle damage markers and acute postoperative pain following primary total knee arthroplasty. *BMC Musculoskeletal Disorders,* 18**,** 265.

SICA, A. & MANTOVANI, A. 2012. Macrophage plasticity and polarization: in vivo veritas. *The Journal of Clinical Investigation,* 122**,** 787-795.

SILVA, R. L., LOPES, A. H., GUIMARÃES, R. M. & CUNHA, T. M. 2017. CXCL1/CXCR2 signaling in pathological pain: Role in peripheral and central sensitization. *Neurobiology of Disease,* 105**,** 109-116.

SNIDER, W. D. & MCMAHON, S. B. 1998. Tackling pain at the source: new ideas about nociceptors. *Neuron,* 20**,** 629-32.

SORKIN, L. S., XIAO, W. H., WAGNER, R. & MYERS, R. R. 1997. Tumour necrosis factor-alpha induces ectopic activity in nociceptive primary afferent fibres. *Neuroscience,* 81**,** 255-62.

SOUZA, G., TALBOT, J., LOTUFO, C., CUNHA, F., CUNHA, T. and FERREIRA, S. 2013. Fractalkine mediates inflammatory pain through activation of satellite glial cells. *Proceedings of the National Academy of Sciences*, 110(27), pp.11193-11198.

SPRENT, J. & SURH, C. D. 2011. Normal T cell homeostasis: the conversion of naive cells into memory-phenotype cells. *Nature Immunology,* 12**,** 478.

STANNUS, O., JONES, G., CICUTTINI, F., PARAMESWARAN, V., QUINN, S., BURGESS, J. & DING, C. 2010. Circulating levels of IL-6 and TNF-α are associated with knee radiographic osteoarthritis and knee cartilage loss in older adults. *Osteoarthritis and Cartilage,* 18**,** 1441-1447.

STAUD, R. 2015. Cytokine and immune system abnormalities in fibromyalgia and other central sensitivity syndromes. *Curr Rheumatol Rev,* 11**,** 109-15.

STEEDS, C. 2009. The anatomy and physiology of pain. *Surgery (Oxford)*, 27(12), pp.507-511.

STEINMAN, L. 2004. Elaborate interactions between the immune and nervous systems. *Nature Immunology,* 5**,** 575.

STEINSHAMN, S., BEMELMANS, M. H., VAN TITS, L. J., BERGH, K., BUURMAN, W. A. & WAAGE, A. 1996. TNF receptors in murine Candida albicans infection: evidence for an important role of TNF receptor p55 in antifungal defense. *J Immunol,* 157**,** 2155-9.

STRICKLAND, I. T., MARTINDALE, J. C., WOODHAMS, P. L., REEVE, A. J., CHESSELL, I. P. & MCQUEEN, D. S. 2008. Changes in the expression of NaV1.7, NaV1.8 and NaV1.9 in a distinct population of dorsal root ganglia innervating the rat knee joint in a model of chronic inflammatory joint pain. *European Journal of Pain,* 12**,** 564-572.

STUART, G., SPRUSTON, N., SAKMANN, B. & HÄUSSER, M. 1997. Action potential initiation and backpropagation in neurons of the mammalian CNS. *Trends in Neurosciences,* 20**,** 125-131.

SU, H. P., RICKERT, K., BURLEIN, C., NARAYAN, K., BUKHTIYAROVA, M., HURZY, D. M., STUMP, C. A., ZHANG, X., REID, J., KRASOWSKA-ZOLADEK, A., TUMMALA, S., SHIPMAN, J. M., KORNIENKO, M., LEMAIRE, P. A., KROSKY, D., HELLER, A., ACHAB, A., CHAMBERLIN, C., SARADJIAN, P., SAUVAGNAT, B., YANG, X., ZIEBELL, M. R., NICKBARG, E., SANDERS, J. M., BILODEAU, M. T., CARROLL, S. S., LUMB, K. J., SOISSON, S. M., HENZE, D. A. & COOKE, A. J. 2017. Structural characterization of nonactive site, TrkA-selective kinase inhibitors. *Proc Natl Acad Sci U S A,* 114**,** E297-e306.

SUSAKI, Y., SHIMIZU, S., KATAKURA, K., WATANABE, N., KAWAMOTO, K., MATSUMOTO, M., TSUDZUKI, M., FURUSAKA, T., KITAMURA, Y. & MATSUDA, H. 1996. Functional properties of murine macrophages promoted by nerve growth factor. *Blood,* 88**,** 4630-7.

SUURVÄLI, J., BOUDINOT, P., KANELLOPOULOS, J. & RÜÜTEL BOUDINOT, S. 2017. P2X4: A fast and sensitive purinergic receptor. *Biomedical Journal,* 40**,** 245-256.

SUZUKI, M., TAKAISHI, S., NAGASAKI, M., ONOZAWA, Y., IINO, I., MAEDA, H., KOMAI, T. & ODA, T. 2013. Medium-chain Fatty Acid-sensing Receptor, GPR84, Is a Proinflammatory Receptor. *The Journal of Biological Chemistry,* 288**,** 10684-10691.

SVENSSON, P., CAIRNS, B. E., WANG, K. & ARENDT-NIELSEN, L. 2003. Injection of nerve growth factor into human masseter muscle evokes long-lasting mechanical allodynia and hyperalgesia. *Pain,* 104**,** 241-7.

SYKIOTIS, G. P., KALLIOLIAS, G. D. & PAPAVASSILIOU, A. G. 2005. Pharmacogenetic Principles in the Hippocratic Writings. *The Journal of Clinical Pharmacology,* 45**,** 1218-1220.

SZALLASI, A., CORTRIGHT, D. N., BLUM, C. A. & EID, S. R. 2007. The vanilloid receptor TRPV1: 10 years from channel cloning to antagonist proof-of-concept. *Nature Reviews Drug Discovery,* 6**,** 357.

SZTURZ, P., ADAM, Z., SEDIVA, A., FOJTIK, Z., CORBOVA, D., NEUBAUER, J., PRASEK, J., HAJEK, R. & MAYER, J. 2011. [Schnitzler syndrome: diagnostics and treatment]. *Klin Onkol,* 24**,** 271-7.

TAGLIALATELA, G., ANGELUCCI, L., SCACCIANOCE, S., FOREMAN, P. J. & PEREZ-POLO, J. R. 1991. Nerve Growth Factor Modulates the Activation of the Hypothalamo-Pituitary-Adrenocortical Axis during the Stress Response. *Endocrinology,* 129**,** 2212-2218.

TAGLIAZUCCHI, E., BALENZUELA, P., FRAIMAN, D. & CHIALVO, D. R. 2010. Brain resting state is disrupted in chronic back pain patients. *Neurosci Lett,* 485**,** 26-31.

TAKANO, S. & UCHIDA, K. 2016. Nerve Growth Factor Regulation by TNF-alpha and IL-1beta in Synovial Macrophages and Fibroblasts in Osteoarthritic Mice. 2016**,** 5706359.

TAKANO, S. & UCHIDA, K. 2017. Nerve growth factor regulation and production by macrophages in osteoarthritic synovium. 190**,** 235-243.

TAKANO, S., UCHIDA, K., MIYAGI, M., INOUE, G., FUJIMAKI, H., AIKAWA, J., IWASE, D., MINATANI, A., IWABUCHI, K. & TAKASO, M. 2016. Nerve Growth Factor Regulation by TNF-α and IL-1β in Synovial Macrophages and Fibroblasts in Osteoarthritic Mice. *Journal of Immunology Research,* 2016**,** 5706359.

TAKEDA, F. 1990. WHO cancer pain relief programme. *Pain,* 41, p.S476.

TAKEUCHI, O. & AKIRA, S. 2010. Pattern Recognition Receptors and Inflammation. *Cell,* 140**,** 805-820.

TAN, A. M., STAMBOULIAN, S., CHANG, Y. W., ZHAO, P., HAINS, A. B., WAXMAN, S. G. & HAINS, B. C. 2008. Neuropathic pain memory is maintained by Rac1-regulated dendritic spine remodeling after spinal cord injury. *J Neurosci,* 28**,** 13173-83.

TAN, Z.-Y., PIEKARZ, A. D., PRIEST, B. T., KNOPP, K. L., KRAJEWSKI, J. L., MCDERMOTT, J. S., NISENBAUM, E. S. & CUMMINS, T. R. 2014. Tetrodotoxin-Resistant Sodium Channels in Sensory Neurons Generate Slow Resurgent Currents That Are Enhanced by Inflammatory Mediators. *The Journal of Neuroscience,* 34**,** 7190-7197.

TARTAGLIA, L. A., PENNICA, D. & GOEDDEL, D. V. 1993. Ligand passing: the 75-kDa tumor necrosis factor (TNF) receptor recruits TNF for signaling by the 55-kDa TNF receptor. *J Biol Chem,* 268**,** 18542-8.

TAVES, S., BERTA, T., LIU, D.-L., GAN, S., CHEN, G., KIM, Y. H., VAN DE VEN, T., LAUFER, S. & JI, R.-R. 2016. Spinal inhibition of p38 MAP kinase reduces inflammatory and neuropathic pain in male but not female mice: sex-dependent microglial signaling in the spinal cord. *Brain, behavior, and immunity,* 55**,** 70-81.

TAYLOR, A. M. W., MURPHY, N. P., EVANS, C. J. & CAHILL, C. M. 2014. Correlation between ventral striatal catecholamine content and nociceptive thresholds in neuropathic mice. *The journal of pain : official journal of the American Pain Society,* 15**,** 878-885.

TAYLOR, P. C., PETERS, A. M., PALEOLOG, E., CHAPMAN, P. T., ELLIOTT, M. J., MCCLOSKEY, R., FELDMANN, M. & MAINI, R. N. 2000. Reduction of chemokine levels and leukocyte traffic to joints by tumor necrosis factor α blockade in patients with rheumatoid arthritis. *Arthritis & Rheumatism,* 43**,** 38-47.

TEIXEIRA, M. J. 2009. [Challenges in the treatment of neuropathic pain]. *Drugs of today (Barcelona, Spain : 1998),* 45 Suppl C**,** 1-5.

TEODORO, F. C., TRONCO JÚNIOR, M. F., ZAMPRONIO, A. R., MARTINI, A. C., RAE, G. A. & CHICHORRO, J. G. 2013. Peripheral substance P and neurokinin-1 receptors have a role in inflammatory and neuropathic orofacial pain models. *Neuropeptides,* 47**,** 199-206.

THACKER, M. A., CLARK, A. K., BISHOP, T., GRIST, J., YIP, P. K., MOON, L. D. F., THOMPSON, S. W. N., MARCHAND, F. & MCMAHON, S. B. 2009. CCL2 is a key mediator of microglia activation in neuropathic pain states. *European Journal of Pain,* 13**,** 263-272.

THAKUR, M., CROW, M., RICHARDS, N., DAVEY, G. I. J., LEVINE, E., KELLEHER, J. H., AGLEY, C. C., DENK, F., HARRIDGE, S. D. R. & MCMAHON, S. B. 2014. Defining the nociceptor transcriptome. *Frontiers in Molecular Neuroscience,* 7**,** 87.

THOMAS, D. D., RIDNOUR, L. A., ISENBERG, J. S., FLORES-SANTANA, W., SWITZER, C. H., DONZELLIE, S., HUSSAIN, P., VECOLI, C., PAOLOCCI, N., AMBS, S., COLTON, C., HARRIS, C., ROBERTS, D. D. & WINK, D. A. 2008. The Chemical Biology of Nitric Oxide. Implications in Cellular Signaling. *Free radical biology & medicine,* 45**,** 18-31.

THOMAZZI, S. M., RIBEIRO, R. A., CAMPOS, D. I., CUNHA, F. Q. & FERREIRA, S. H. 1997. Tumor necrosis factor, interleukin-1 and interleukin-8 mediate the nociceptive

activity of the supernatant of LPS-stimulated macrophages. *Mediators of Inflammation,* 6**,** 195-200.

TILLU, D. V., HASSLER, S. N., BURGOS-VEGA, C. C., QUINN, T. L., SORGE, R. E., DUSSOR, G., BOITANO, S., VAGNER, J. & J PRICE, T. 2015. Protease activated receptor 2 (PAR(2)) activation is sufficient to induce the transition to a chronic pain state. *Pain,* 156**,** 859-867.

TISEO, P. J., REN, H. & MELLIS, S. 2014. Fasinumab (REGN475), an antinerve growth factor monoclonal antibody, for the treatment of acute sciatic pain: results of a proof-of-concept study. *Journal of Pain Research,* 7**,** 523-530.

TODD, A. 2010. Neuronal circuitry for pain processing in the dorsal horn. *Nature Reviews Neuroscience*, 11(12), pp.823-836.

TODD, A. 2017. Identifying functional populations among the interneurons in laminae I-III of the spinal dorsal horn. *Molecular Pain*, 13, p.174480691769300.

TONI, T., DUA, P. and VAN DER GRAAF, P. 2014. Systems Pharmacology of the NGF Signaling Through p75 and TrkA Receptors. *CPT Pharmacometrics Syst. Pharmacol.*, 3(12), p.e150.

TOROCSIK, B. & SZEBERENYI, J. 2000. Anisomycin uses multiple mechanisms to stimulate mitogen-activated protein kinases and gene expression and to inhibit neuronal differentiation in PC12 phaeochromocytoma cells. *Eur J Neurosci,* 12**,** 527-32.

TRAMONTANA, M., DEL BIANCO, E., CECCONI, R., MAGGI, C. A. & GEPPETTI, P. 1992. Veratridine evokes release of calcitonin gene-related peptide from capsaicin-sensitive nerves of rat urinary bladder. *European Journal of Pharmacology,* 212**,** 137-142.

TREEDE, R. 2007. 2.2. Spinothalamic nociceptive pathways. *Clinical Neurophysiology*, 118(12), p.2808.

TREEDE, R., RIEF, W., BARKE, A., AZIZ, Q., BENNETT, M., BENOLIEL, R., COHEN, M., EVERS, S., FINNERUP, N., FIRST, M., GIAMBERADINO, M., KAASA, S., KOSEK, E., LAVAND'HOMME, P., NICHOLAS, M., PERROT, S., SCHOLZ, J., SCHUG, S., SMITH, B., SVENSSON, P., VLAEYEN, J. and WANG, S. 2015. A classification of chronic pain for ICD-11. *PAIN,* p.1.

TROUPLIN, V., BOUCHERIT, N., GORVEL, L., CONTI, F., MOTTOLA, G. & GHIGO, E. 2013. Bone Marrow-Derived Macrophage Production. *Journal of Visualised Experiments,* (81):50966.

TSENG, W.-Y., HUANG, Y.-S., LIN, H.-H., LUO, S.-F., MCCANN, F., MCNAMEE, K., CLANCHY, F. & WILLIAMS, R. 2018. TNFR signalling and its clinical implications. *Cytokine,* 101**,** 19-25.

TSUDA, M., INOUE, K. & SALTER, M. W. 2005. Neuropathic pain and spinal microglia: a big problem from molecules in 'small' glia. *Trends in Neurosciences,* 28**,** 101-107.

TSUDA, M., MASUDA, T., KITANO, J., SHIMOYAMA, H., TOZAKI-SAITOH, H. & INOUE, K. 2009. IFN-γ receptor signaling mediates spinal microglia activation driving neuropathic pain. *Proceedings of the National Academy of Sciences of the United States of America,* 106**,** 8032-8037.

TSUDA, M., SHIGEMOTO-MOGAMI, Y., KOIZUMI, S., MIZOKOSHI, A., KOHSAKA, S., SALTER, M. W. & INOUE, K. 2003. P2X4 receptors induced in spinal microglia gate tactile allodynia after nerve injury. *Nature,* 424**,** 778.

TUCKER, B. A., RAHIMTULA, M. & MEAROW, K. M. 2008. Src and FAK are key early signalling intermediates required for neurite growth in NGF-responsive adult DRG neurons. *Cellular Signalling,* 20**,** 241-257.

UNGER, T. J., CALDERON, G. A., BRADLEY, L. C., SENA-ESTEVES, M. & RIOS, M. 2007. Selective Deletion of Bdnf in the Ventromedial and Dorsomedial Hypothalamus of Adult Mice Results in Hyperphagic Behavior and Obesity. *The Journal of Neuroscience,* 27**,** 14265-14274.

USHIYAMA, T., CHANO, T., INOUE, K. & MATSUSUE, Y. 2003. Cytokine production in the infrapatellar fat pad: another source of cytokines in knee synovial fluids. *Annals of the Rheumatic Diseases,* 62**,** 108-112.

UTTAM, S., WONG, C., AMORIM, I. S., JAFARNEJAD, S. M., TANSLEY, S. N., YANG, J., PRAGER-KHOUTORSKY, M., MOGIL, J. S., GKOGKAS, C. G. & KHOUTORSKY, A. 2018. Translational profiling of dorsal root ganglia and spinal cord in a mouse model of neuropathic pain. *Neurobiology of Pain*.

VALLEJO, R., TILLEY, D. M., VOGEL, L. & BENYAMIN, R. 2010. The Role of Glia and the Immune System in the Development and Maintenance of Neuropathic Pain. *Pain Practice,* 10**,** 167-184.

VAN DER BRUGGEN, T., NIJENHUIS, S., VAN RAAIJ, E., VERHOEF, J. & SWEDER VAN ASBECK, B. 1999. Lipopolysaccharide-Induced Tumor Necrosis Factor Alpha Production by Human Monocytes Involves the Raf-1/MEK1-MEK2/ERK1-ERK2 Pathway. *Infection and Immunity,* 67**,** 3824-3829.

VAN DER VELDEN, V. H. J., SZCZEPAŃSKI, T. & VAN DONGEN, J. J. M. 2001. Polymerase Chain Reaction, Real-Time Quantitative. *In:* BRENNER, S. & MILLER, J. H. (eds.) *Encyclopedia of Genetics.* New York: Academic Press.

VAN DEVENTER, S. J. 1997. Tumour necrosis factor and Crohn's disease. *Gut,* 40**,** 443-448.

VARGAS-SCHAFFER, G. 2010. Is the WHO analgesic ladder still valid?: Twenty-four years of experience. *Canadian Family Physician,* 56**,** 514-517.

VASSALLE, M. 1987. Contribution of the Na+/K+-pump to the membrane potential. *Experientia,* 43**,** 1135-40.

VEIGA-FERNANDES, H. & PACHNIS, V. 2017. Neuroimmune regulation during intestinal development and homeostasis. *Nature Immunology,* 18**,** 116.

VILLARREAL, C. F., FUNEZ, M. I., CUNHA, F. D. Q., PARADA, C. A. & FERREIRA, S. H. 2013. The long-lasting sensitization of primary afferent nociceptors induced by inflammation involves prostanoid and dopaminergic systems in mice. *Pharmacology Biochemistry and Behavior,* 103**,** 678-683.

WADACHI, R. & HARGREAVES, K. M. 2006. Trigeminal Nociceptors Express TLR-4 and CD14: a Mechanism for Pain due to Infection. *Journal of Dental Research,* 85**,** 49-53.

WALLIS, R. S. 2008. Tumour necrosis factor antagonists: structure, function, and tuberculosis risks. *The Lancet Infectious Diseases,* 8**,** 601-611.

WALLIS, R. S., BRODER, M. S., WONG, J. Y., HANSON, M. E. & BEENHOUWER, D. O. 2004. Granulomatous infectious diseases associated with tumor necrosis factor antagonists. *Clin Infect Dis,* 38**,** 1261-5.

WALSH, D. A., MAPP, P. I. & KELLY, S. 2015a. Calcitonin gene-related peptide in the joint: contributions to pain and inflammation. *British Journal of Clinical Pharmacology,* 80**,** 965-978.

WALSH, D. A., MAPP, P. I. & KELLY, S. 2015b. Calcitonin gene-related peptide in the joint: contributions to pain and inflammation. *Br J Clin Pharmacol,* 80**,** 965-78.

WALSH, D. A. & MCWILLIAMS, D. F. 2012. Pain in Rheumatoid Arthritis. *Current Pain and Headache Reports,* 16**,** 509-517.

WANG, H., WANG, R., THRIMAWITHANA, T., LITTLE, P. J., XU, J., FENG, Z.-P. & ZHENG, W. 2014. The Nerve Growth Factor Signaling and Its Potential as Therapeutic Target for Glaucoma. *BioMed Research International,* 2014**,** 759473.

WANG, H., ZHANG, X., HE, J.-Y., ZHENG, X.-F., LI, D., LI, Z., ZHU, J.-F., SHEN, C., CAI, G.-Q. & CHEN, X.-D. 2015. Increasing expression of substance P and calcitonin gene-related peptide in synovial tissue and fluid contribute to the progress of arthritis in developmental dysplasia of the hip. *Arthritis Research & Therapy,* 17**,** 4.

WANG, J.-G., STRONG, J. A., XIE, W., YANG, R.-H., COYLE, D. E., WICK, D. M., DORSEY, E. D. & ZHANG, J.-M. 2008. The chemokine CXCL1/growth related oncogene increases sodium currents and neuronal excitability in small diameter sensory neurons. *Molecular Pain,* 4**,** 38-38.

WANG, X.-M., HAMZA, M., WU, T.-X. & DIONNE, R. A. 2009. Upregulation of IL-6, IL-8 and CCL2 gene expression after acute inflammation: Correlation to clinical pain. *PAIN®,* 142**,** 275-283.

WANG, Y., FENG, C., HE, H., HE, J., WANG, J., LI, X., WANG, S., LI, W., HOU, J., LIU, T., FANG, D. & XIE, S.-Q. 2018. Sensitization of TRPV1 receptors by TNF-α orchestrates the development of vincristine-induced pain. *Oncology Letters,* 15**,** 5013-5019.

WARREN, G. L., HULDERMAN, T., JENSEN, N., MCKINSTRY, M., MISHRA, M., LUSTER, M. I. & SIMEONOVA, P. P. 2002. Physiological role of tumor necrosis factor alpha in traumatic muscle injury. *Faseb j,* 16**,** 1630-2.

WATANABE, T., ITO, T., INOUE, G., OHTORI, S., KITAJO, K., DOYA, H., TAKAHASHI, K. & YAMASHITA, T. 2008. The p75 receptor is associated with inflammatory thermal hypersensitivity. *J Neurosci Res,* 86**,** 3566-74.

WEI, S.-T., SUN, Y.-H., ZONG, S.-H. & XIANG, Y.-B. 2015. Serum Levels of IL-6 and TNF-α May Correlate with Activity and Severity of Rheumatoid Arthritis. *Medical Science Monitor : International Medical Journal of Experimental and Clinical Research,* 21**,** 4030-4038.

WEINBLATT, M. E., KREMER, J. M., BANKHURST, A. D., BULPITT, K. J., FLEISCHMANN, R. M., FOX, R. I., JACKSON, C. G., LANGE, M. & BURGE, D. J. 1999. A trial of etanercept, a recombinant tumor necrosis factor receptor:Fc fusion protein, in

patients with rheumatoid arthritis receiving methotrexate. *N Engl J Med,* 340**,** 253-9.

WEISCHENFELDT, J. & PORSE, B. 2008a. Bone Marrow-Derived Macrophages (BMM): Isolation and Applications. *Cold Spring Harbor Protocols,* 2008**,** pdb.prot5080.

WEISCHENFELDT, J. & PORSE, B. 2008b. Bone Marrow-Derived Macrophages (BMM): Isolation and Applications. *CSH Protoc,* 2008**,** pdb.prot5080.

WEYERMANN, J., LOCHMANN, D. & ZIMMER, A. 2005. A practical note on the use of cytotoxicity assays. *International Journal of Pharmaceutics,* 288**,** 369-376.

WHEELER, M. A., HEFFNER, D. L., KIM, S., ESPY, S. M., SPANO, A. J., CLELAND, C. L. & DEPPMANN, C. D. 2014. TNFα/TNFR1 signaling is required for the development and function of primary nociceptors. *Neuron,* 82**,** 587-602.

WILLIAMS, K. S., KILLEBREW, D. A., CLARY, G. P., SEAWELL, J. A. & MEEKER, R. B. 2015. Differential regulation of macrophage phenotype by mature and pro-nerve growth factor. *Journal of neuroimmunology,* 285**,** 76-93.

WILSON, K. P., FITZGIBBON, M. J., CARON, P. R., GRIFFITH, J. P., CHEN, W., MCCAFFREY, P. G., CHAMBERS, S. P. & SU, M. S.-S. 1996. Crystal Structure of p38 Mitogen-activated Protein Kinase. *Journal of Biological Chemistry,* 271**,** 27696-27700.

WINTER, J., ALISTAIR FORBES, C., STERNBERG, J. & LINDSAY, R. M. 1988. Nerve growth factor (NGF) regulates adult rat cultured dorsal root ganglion neuron responses to the excitotoxin capsaicin. *Neuron,* 1**,** 973-981.

WITONSKI, D., WAGROWSKA-DANILEWICZ, M., KESKA, R., RACZYNSKA-WITONSKA, G. & STASIKOWSKA-KANICKA, O. 2010. Increased interleukin 6 and tumour necrosis factor alpha expression in the infrapatellar fat pad of the knee joint with the anterior knee pain syndrome: a preliminary report. *Pol J Pathol,* 61**,** 213-8.

WONG, A. W., K. P. YEUNG, J., PAYNE, S. C., KEAST, J. R. & OSBORNE, P. B. 2015. Neurite outgrowth in normal and injured primary sensory neurons reveals different regulation by nerve growth factor (NGF) and artemin. *Molecular and Cellular Neuroscience,* 65**,** 125-134.

WOOLF, C. J., ALLCHORNE, A., SAFIEH-GARABEDIAN, B. & POOLE, S. 1997. Cytokines, nerve growth factor and inflammatory hyperalgesia: the contribution of tumour necrosis factor α. *British Journal of Pharmacology,* 121**,** 417-424.

WOOLF, C. J. & COSTIGAN, M. 1999. Transcriptional and posttranslational plasticity and the generation of inflammatory pain. *Proceedings of the National Academy of Sciences,* 96**,** 7723-7730.

WOOLF, C. J. & MA, Q. 2007. Nociceptors—Noxious Stimulus Detectors. *Neuron,* 55**,** 353-364.

WOOLF, C. J., SAFIEH-GARABEDIAN, B., MA, Q. P., CRILLY, P. & WINTER, J. 1994. Nerve growth factor contributes to the generation of inflammatory sensory hypersensitivity. *Neuroscience,* 62**,** 327-31.

WU, X.-B., CAO, D.-L., ZHANG, X., JIANG, B.-C., ZHAO, L.-X., QIAN, B. & GAO, Y.-J. 2016. CXCL13/CXCR5 enhances sodium channel Nav1.8 current density via p38 MAP

kinase in primary sensory neurons following inflammatory pain. *Scientific Reports,* 6**,** 34836.

WYNN, T. A., CHAWLA, A. & POLLARD, J. W. 2013. Origins and Hallmarks of Macrophages: Development, Homeostasis, and Disease. *Nature,* 496**,** 445-455.

XIE, W.-R., DENG, H., LI, H., TRAVIS, L. B., JUDITH, A. S. & ZHANG, J.-M. 2006. Robust Increase of Cutaneous Sensitivity, Cytokine Production and Sympathetic Sprouting in Rats with Localized Inflammatory Irritation of the Spinal Ganglia. *Neuroscience,* 142**,** 809-822.

XUE, J., SCHMIDT, SUSANNE V., SANDER, J., DRAFFEHN, A., KREBS, W., QUESTER, I., DE NARDO, D., GOHEL, TRUPTI D., EMDE, M., SCHMIDLEITHNER, L., GANESAN, H., NINO-CASTRO, A., MALLMANN, MICHAEL R., LABZIN, L., THEIS, H., KRAUT, M., BEYER, M., LATZ, E., FREEMAN, TOM C., ULAS, T. & SCHULTZE, JOACHIM L. 2014. Transcriptome-Based Network Analysis Reveals a Spectrum Model of Human Macrophage Activation. *Immunity,* 40**,** 274-288.

YANG, Y., CHEN, Q., JIA, S., HE, L., WANG, A., LI, D., LI, Y. & LI, X. 2018. Involvement of TRPV1 in the expression and release of calcitonin gene-related peptide induced by rutaecarpine. *Molecular Medicine Reports,* 17**,** 5168-5174.

YARILINA, A., PARK-MIN, K.-H., ANTONIV, T., HU, X. & IVASHKIV, L. B. 2008a. TNF activates an IRF1-dependent autocrine loop leading to sustained expression of chemokines and STAT1-dependent type I interferon-response genes. *Nat Immunol,* 9**,** 378-387.

YARILINA, A., PARK-MIN, K.-H., ANTONIV, T., HU, X. & IVASHKIV, L. B. 2008b. TNF activates an IRF1-dependent autocrine loop leading to sustained expression of chemokines and STAT1-dependent type I interferon–response genes. *Nature Immunology,* 9**,** 378.

YEH, J.-F., AKINCI, A., AL SHAKER, M., CHANG, M. H., DANILOV, A., GUILLEN, R., JOHNSON, K. W., KIM, Y.-C., EL-SHAFEI, A. A., SKLJAREVSKI, V., DUEÑAS, H. J. & TASSANAWIPAS, W. 2017. Monoclonal antibodies for chronic pain: A practical review of mechanisms and clinical applications. *Molecular Pain,* 13**,** 1744806917740233.

YILMAZ, I. A., OZGE, A., ERDAL, M. E., EDGUNLU, T. G., CAKMAK, S. E. & YALIN, O. O. 2010. Cytokine polymorphism in patients with migraine: some suggestive clues of migraine and inflammation. *Pain Med,* 11**,** 492-7.

YIN, Y., YI, M. and KIM, D. 2018. Impaired Autophagy of GABAergic Interneurons in Neuropathic Pain. *Pain Research and Management*, 2018, pp.1-8.

YIP, H. K. & JOHNSON, E. M. 1984. Developing dorsal root ganglion neurons require trophic support from their central processes: evidence for a role of retrogradely transported nerve growth factor from the central nervous system to the periphery. *Proceedings of the National Academy of Sciences of the United States of America,* 81**,** 6245-6249.

YOON, S. O., CASACCIA-BONNEFIL, P., CARTER, B. & CHAO, M. V. 1998. Competitive Signaling Between TrkA and p75 Nerve Growth Factor Receptors Determines Cell Survival. *The Journal of Neuroscience,* 18**,** 3273-3281.

YU, Y.-R. A., O'KOREN, E. G., HOTTEN, D. F., KAN, M. J., KOPIN, D., NELSON, E. R., QUE, L. & GUNN, M. D. 2016. A Protocol for the Comprehensive Flow Cytometric Analysis of Immune Cells in Normal and Inflamed Murine Non-Lymphoid Tissues. *PLOS ONE,* 11**,** e0150606.

ZELLER, J., POULSEN, K. T., SUTTON, J. E., ABDICHE, Y. N., COLLIER, S., CHOPRA, R., GARCIA, C. A., PONS, J., ROSENTHAL, A. & SHELTON, D. L. 2008. CGRP function-blocking antibodies inhibit neurogenic vasodilatation without affecting heart rate or arterial blood pressure in the rat. *British Journal of Pharmacology,* 155**,** 1093-1103.

ZENG, X.-Y., ZHANG, Q., WANG, J., YU, J., HAN, S.-P. & WANG, J.-Y. 2014. Distinct role of tumor necrosis factor receptor subtypes 1 and 2 in the red nucleus in the development of neuropathic pain. *Neuroscience Letters,* 569**,** 43-48.

ZHANG, H., YANG, H. & HE, S. 2010. TNF increases expression of IL-4 and PARs in mast cells. *Cell Physiol Biochem,* 26**,** 327-36.

ZHANG, J.-M. & AN, J. 2007. Cytokines, Inflammation and Pain. *International anesthesiology clinics,* 45**,** 27-37.

ZHANG, L., BERTA, T., XU, Z.-Z., LIU, T., PARK, J. Y. & JI, R.-R. 2011. TNF-alpha contributes to spinal cord synaptic plasticity and inflammatory pain: Distinct role of TNF receptor subtypes 1 and 2. *PAIN®,* 152**,** 419-427.

ZHANG, N., INAN, S., COWAN, A., SUN, R., WANG, J. M., ROGERS, T. J., CATERINA, M. & OPPENHEIM, J. J. 2005a. A proinflammatory chemokine, CCL3, sensitizes the heat- and capsaicin-gated ion channel TRPV1. *Proceedings of the National Academy of Sciences of the United States of America,* 102**,** 4536-4541.

ZHANG, X., GONCALVES, R. & MOSSER, D. M. 2008. The isolation and characterization of murine macrophages. *Curr Protoc Immunol,* Chapter 14**,** Unit 14.1.

ZHANG, X., HUANG, J. & MCNAUGHTON, P. A. 2005b. NGF rapidly increases membrane expression of TRPV1 heat-gated ion channels. *Embo j,* 24**,** 4211-23.

ZHANG, X., HUANG, J. & MCNAUGHTON, P. A. 2005c. NGF rapidly increases membrane expression of TRPV1 heat-gated ion channels. *The EMBO Journal,* 24**,** 4211-4223.

ZHANG, Y. & WANG, Y. 2017. [TRPV1: an important molecule involved in the peripheral sensitization during chronic pain and central pain modulation]. *Sheng Li Xue Bao,* 69**,** 677-684.

ZHANG, Z., CAO, D., ZHANG, X., JI, R. and GAO, Y. 2013. Chemokine contribution to neuropathic pain: Respective induction of CXCL1 and CXCR2 in spinal cord astrocytes and neurons. *Pain*, 154(10), pp.2185-2197.

ZHAO, F.Y., JEGGOO, R., WEI, H., WHYMENT, A., FANG, X and SPANSWICK, D. 2014. In vivo electrophysiological recording techniques for the study of neuropathic pain in rodent models. *Current Protocols in Pharmacology*, 66:11.

ZHAO, P., HILL, M., LIU, S., CHEN, L., BANGALORE, L., WAXMAN, S. G. & TAN, A. M. 2016. Dendritic spine remodeling following early and late Rac1 inhibition after spinal cord injury: evidence for a pain biomarker. *Journal of Neurophysiology,* 115**,** 2893-2910.

ZHU, W., GALOYAN, S. M., PETRUSKA, J. C., OXFORD, G. S. & MENDELL, L. M. 2004. *A Developmental Switch in Acute Sensitization of Small Dorsal Root Ganglion (DRG) Neurons to Capsaicin or Noxious Heating by NGF*.

ZHU, W. & OXFORD, G. S. 2007. Phosphoinositide-3-kinase and mitogen activated protein kinase signaling pathways mediate acute NGF sensitization of TRPV1. *Molecular and cellular neurosciences,* 34**,** 689-700.

ZIEGLER-HEITBROCK, H. W. L. & ULEVITCH, R. J. 1993. CD14: Cell surface receptor and differentiation marker. *Immunology Today,* 14**,** 121-125.

ZU, B., PAN, H., ZHANG, X.-J. & YIN, Z.-S. 2016. Serum Levels of the Inflammatory Cytokines in Patients with Lumbar Radicular Pain Due to Disc Herniation. *Asian Spine Journal,* 10**,** 843-849.

ZWEIFEL, L. S., KURUVILLA, R. & GINTY, D. D. 2005. Functions and mechanisms of retrograde neurotrophin signalling. *Nat Rev Neurosci,* 6**,** 615-625.

Biotium. 2018. LIVE-OR-DYE™ Fixable Viability for Flow Cytometry & Microscopy. [ONLINE]. Available at: https://biotium.com/technology/flow-cytometry-reagents/live-dye-fixable-viability-stains-flow-cytometry/. [Accessed 11 September 2018].

PharmaTimes online. 2018. Trial Success for Allergan's anti-CGRP migraine drug. Available at: http://www.pharmatimes.com/news/trial_success_for_allergans_anti-cgrp_migraine_drug_1220841 . [Accessed 11 September 2018].

ThermoFisher. Date unknown. Qubit Assays. Available at: https://www.thermofisher.com/uk/en/home/industrial/spectroscopy-elemental-isotope-analysis/molecular-spectroscopy/fluorometers/qubit/qubit-assays.html#ion. [Accessed 11 September 2018].

Appendix

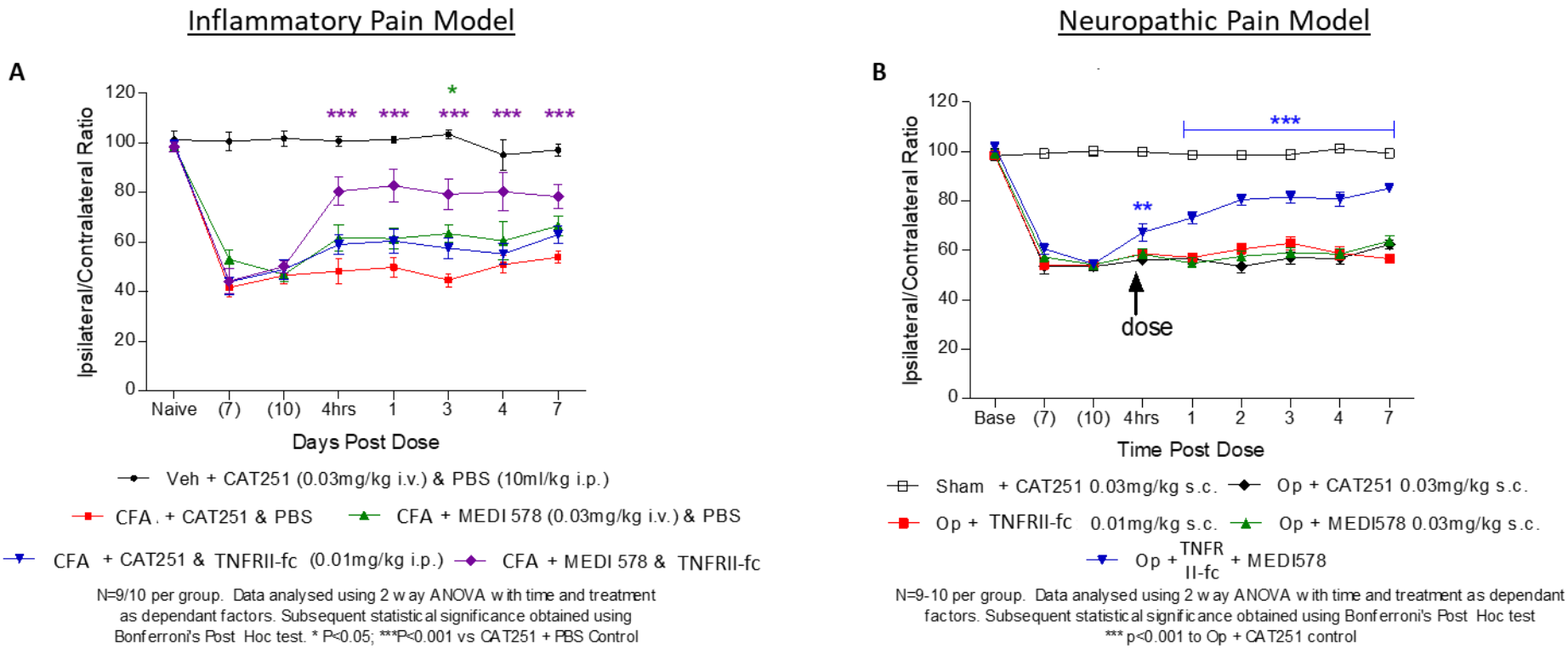

Appendix Figure 1. Historical data showing the successful reversal of mechanical hypersensitivity in A) an intra-articular CFA model of inflammatory joint pain or B) in a neuropathic pain model (PNL) when using a dual blocker against NGF and TNFα. Data displayed as Mean ± SEM, n=9-10 mice/group. Data analysed using Two-Way ANOVA followed by Bonferroni's multiple comparisons test. * P<0.05, *** P<0.001 vs CAT251 control.

Legend: CFA: complete Freund's adjuvant; PNL: partial nerve ligation; NGF: nerve growth factor; TNFα: tumour necrosis factor alpha.4

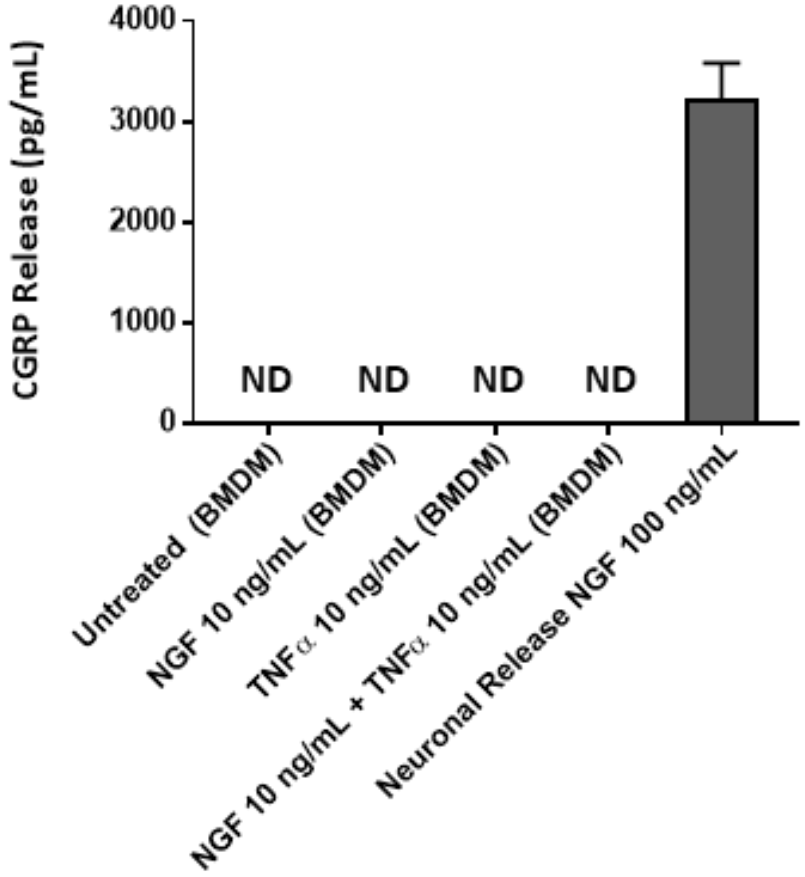

Appendix Figure 2. Potassium (25 mM)-evoked CGRP release from BMDM primed with NGF (10 ng/mL, 48 h), TNFα (10 ng/mL, 48 h) or a combination of the two (10 ng/mL, 48 h). Potassium-evoked DRG sensory neuronal CGRP release in cultures with NGF (100 ng/mL, 48 h) is included as a comparison. Lower limit of quantification in this assay is typically < 10 pg/mL.

Legend: CGRP: calcitonin gene-related peptide; BMDM: bone-marrow derived macrophages; NGF: nerve growth factor; TNFα: tumour necrosis factor alpha; ND: not detected (below limit of detection).

Appendix Table 18. DRG transcriptional changes 1-day post-vehicle or test compound administration in the mouse intra-articular CFA model. ΔΔCt values for each treatment group (CFA Only (n=4 mice), CFA + TNFRII-fc (n=4 mice), CFA + MEDI578 (n=4 mice) and CFA + TNFRII-fc + MEDI578 (n=4 mice)) relative to the sham-operated mice. Data displayed as Mean ± SEM.

Gene	Change from Sham Group (ΔΔCt) Mean ± SEM			
	CFA Only	CFA + TNFRII-fc	CFA + MEDI578	CFA + TNFRII-fc + MEDI578
P2x4	0.38 ± 0.17	0.69 ± 0.22	0.2 ± 0.41	0.89 ± 0.07
Trpv1	0.32 ± 0.30	1.7 ± 0.26	1.23 ± 0.43	1.33 ± 0.30
F2rl1	-1.21 ± 0.78	0.14 ± 0.37	-0.65 ± 0.52	0.42 ± 0.10
Calca	0.05 ± 0.44	1.48 ± 0.28	1.1 ± 0.27	0.85 ± 0.18
Scn10a	0.06 ± 0.39	1.33 ± 0.46	0.94 ± 0.55	0.47 ± 0.19
Tac1	0.1 ± 0.28	1.09 ± 0.32	0.62 ± 0.27	0.26 ± 0.09
Cd14	0.62 ± 0.31	0.65 ± 0.02	0.40 ± 0.18	0.74 ± 0.23

Appendix Table 2. DRG transcriptional changes 7-days post-vehicle or test compound administration in the mouse intra-articular CFA model. ΔΔCt values for each treatment group (CFA Only (n=3 mice), CFA + TNFRII-fc (n=5 mice), CFA + MEDI578 (n=5 mice) and CFA + TNFRII-fc + MEDI578 (n=5 mice)) relative to the sham-operated mice. Data displayed as Mean ± SEM.

Gene	Change from Sham Group (ΔΔCt) Mean ± SEM			
	CFA Only	CFA + TNFRII-fc	CFA + MEDI578	CFA + TNFRII-fc + MEDI578
P2x4	0.57 ± 0.84	0.29 ± 0.34	-0.46 ± 0.27	-0.31 ± 0.47
Trpv1	-0.45 ± 0.83	0.20 ± 0.52	-0.71 ± 0.46	-0.41 ± 0.79
F2rl1	-0.14 ± 0.50	-0.59 ± 0.50	-0.77 ± 0.42	0.10 ± 0.76
Calca	-0.15 ± 0.66	-0.01 ± 0.32	-0.37 ± 0.44	-0.12 ± 0.55
Scn10a	-0.49 ± 0.65	-0.13 ± 0.31	-0.10 ± 0.58	-0.43 ± 0.77
Tac1	-0.49 ± 0.35	0.07 ± 0.27	-0.40 ± 0.39	-0.44 ± 0.39
Cd14	-0.003 ± 0.42	0.04 ± 0.20	-0.12 ± 0.27	-0.19 ± 0.29

Appendix Table 3. Knee fat pad transcriptional changes 7-days post-vehicle or test compound administration in the mouse intra-articular CFA model. ΔΔCt values for each treatment group (CFA Only (n=2 mice), CFA + TNFRII-fc (n=5 mice), CFA + MEDI578 (n=5 mice) and CFA + TNFRII-fc + MEDI578 (n=5 mice)) relative to the sham-operated mice. Data displayed as Mean ± SEM.

Gene	Change from Sham Group (ΔΔCt) Mean ± SEM			
	CFA Only	CFA + TNFRII-fc	CFA + MEDI578	CFA + TNFRII-fc + MEDI578
Ngf	0.52 ± 0.04	0.88 ± 0.29	0.95 ± 0.39	1.14 ± 0.22
Tnf	1.50 ± 1.21	2.72 ± 0.78	2.29 ± 0.75	3.53 ± 0.35
Cxcl5	3.27 ± 0.91	4.9 ± 0.66	3. 16 ± 0.49	5.31 ± 0.17
Ccl3	0.81 ± 1.19	2.35 ± 1.15	2.13 ± 1.02	3.75 ± 0.79
Ccl1	-0.92 ± 1.15	0.66 ± 0.83	0.23 ± 0.26	1.56 ± 0.40
Itgam	1.32 ± 0.1	2.04 ± 0.54	1.34 ± 0.46	2.33 ± 0.22
Csf3	1.21 ± 0.85	3.25 ± 0.86	1.58 ± 0.77	3.98 ± 0.24
Nos2	4.23 ± 1.04	5.86 ± 1.06	4.62 ± 0.84	6.89 ± 0.45
Ccl21	-0.21 ± 0.77	-1.22 ± 0.70	-0.73 ± 0.84	-0.46 ± 1.12
Ccl5	3.54 ± 1.13	4.96 ± 0.55	3.73 ± 0.23	5.18 ± 0.30

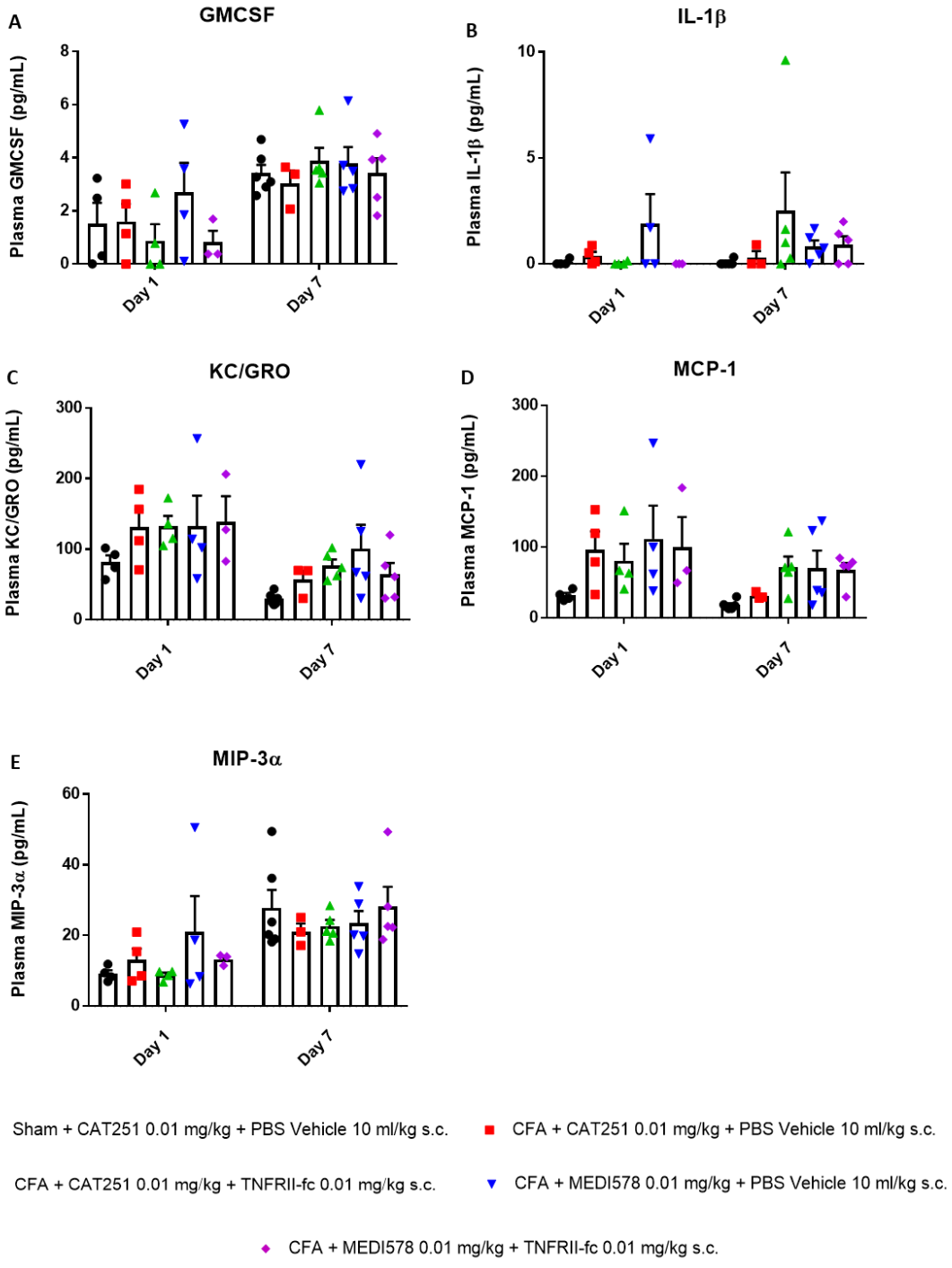

Appendix Figure 3. Levels of plasma cytokines following intra-articular CFA administration. Plasma levels of A) GMCSF (pg/mL), B) IL-1β (pg/mL), C) KC/GRO (pg/mL), D) MCP-1 (pg/mL) and E) MIP-3α in the sham group or following vehicle or test compound administration at both day 1 and day 7. Data displayed as Mean ± SEM, n=3-6 mice/group (displayed as individual data points). Data were analysed using Two-Way ANOVA with Tukey's multiple comparisons test. Lower limits of quantification (LLOQ) for these assays were 0.16 pg/mL (GMCSF), 3.1 pg/mL (IL-1β), 4.8 pg/mL (KC/GRO), 1.4 pg/mL (MCP-1) and 0.1 pg/mL (MIP-3α).

Legend: CFA: complete Freund's adjuvant; GMCSF: granulocyte-macrophage colony-stimulating factor; IL-1β: interleukin-1β; KC/GRO: keratinocyte chemoattractant/growth-regulated oncogene; MCP-1: monocyte chemoattractant protein-1; MIP-3α: macrophage inflammatory protein 3 alpha.

Appendix Table 4. DRG transcriptional changes following 1-day post-vehicle or test compound administration following PNL. ΔΔCt values for each treatment group (PNL Only (n=4 mice), PNL + TNFRII-fc (n=4 mice), PNL + MEDI578 (n=4 mice) and PNL + TNFRII-fc + MEDI578 (n=5 mice)) relative to the sham-operated mice. Data displayed as Mean ± SEM.

Gene	Change from Sham Group (ΔΔCt) Mean ± SEM			
	PNL Only	PNL + TNFRII-fc	PNL + MEDI578	PNL + TNFRII-fc + MEDI578
P2x4	0.25 ± 0.72	0.09 ± 0.38	-0.44 ± 0.22	-0.46 ± 0.27
Trpv1	0.29 ± 0.22	0.55 ± 0.23	-0.14 ± 0.39	-0.21 ± 0.54
Calca	0.02 ± 0.24	0.19 ± 0.27	-0.22 ± 0.29	-0.61 ± 0.26
Ngf	0.41 ± 0.05	0.4 ± 0.4	0.55 ± 0.38	0.54 ± 0.24
Ntrk1	-0.22 ± 0.15	0.15 ± 0.50	-0.11 ± 0.19	-0.92 ± 0.45
Ngfr	0.52 ± 0.16	0.92 ± 0.48	0.67 ± 0.39	0.04 ± 0.59
Tnf	-0.25 ± 0.59	-0.44 ± 0.28	-0.16 ± 0.24	0.26 ± 0.48
Tnfrsf1a	0.11 ± 0.10	0.09 ± 0.32	-0.19 ± 0.14	0.05 ± 0.33
Scn10a	0.04 ± 0.14	0.67 ± 0.49	-0.03 ± 0.17	-0.69 ± 0.58
Itgam	-0.43 ± 0.34	-0.12 ± 0.38	-0.34 ± 0.26	-0.46 ± 0.2
Tac1	0.14 ± 0.32	0.45 ± 0.16	-0.29 ± 0.22	-0.65 ± 0.45

Appendix Table 5. DRG transcriptional changes following 7-day post-vehicle or test compound administration following PNL. ΔΔCt values for each treatment group (PNL Only (n=5 mice), PNL + TNFRII-fc (n=5 mice), PNL + MEDI578 (n=5 mice) and PNL + TNFRII-fc + MEDI578 (n=5 mice)) relative to the sham-operated mice. Data displayed as Mean ± SEM.

Gene	Change from Sham Group (ΔΔCt) Mean ± SEM			
	PNL Only	PNL + TNFRII-fc	PNL + MEDI578	PNL + TNFRII-fc + MEDI578
P2x4	0.4 ± 0.29	0.17 ± 0.12	-0.26 ± 0.3	-0.18 ± 0.26
Trpv1	-0.19 ± 0.37	-0.11 ± 0.34	-0.40 ± 0.29	0.51 ± 0.37
Calca	-0.20 ± 0.24	-0.05 ± 0.15	-0.33 ± 0.23	0.24 ± 0.3
Ngf	0.292 ± 0.28	0.5 ± 0.13	0.21 ± 0.21	0.63 ± 0.18
Ntrk1	-0.54 ± 0.27	-0.36 ± 0.24	-0.76 ± 0.28	0.10 ± 0.37
Ngfr	0.08 ± 0.30	-0.05 ± 0.28	-0.20 ± 0.28	0.68 ± 0.43
Tnf	0.72 ± 0.27	0.46 ± 0.35	-0.92 ± 0.29	-0.22 ± 0.37
Tnfrsf1a	0.73 ± 0.15	0.40 ± 0.20	0.19 ± 0.22	0.78 ± 0.25
Scn10a	-0.87 ± 0.32	-0.63 ± 0.12	-0.98 ± 0.24	0.19 ± 0.44
Itgam	0.58 ± 0.22	0.05 ± 0.17	-0.08 ± 0.34	0.48 ± 0.28
Tac1	-0.06 ± 0.22	-0.01 ± 0.17	-0.34 ± 0.27	0.18 ± 0.19